

AD-A038 525

AEROSPACE MEDICAL RESEARCH LAB WRIGHT-PATTERSON AFB OHIO F/G 13/12
IMPACT TESTS OF A NEAR-PRODUCTION AIR CUSHION RESTRAINT.(U)

FEB 77 J W BRINKLEY, G C MOHR, H C RUSSELL DOT-HS-017-1-017-1A

UNCLASSIFIED

AMRL-TR-75-47

DOT-HS-802-248

NL

1 OF 5
AD
A038525



DOT HS-802 248

AD A 038525

IMPACT TESTS OF A NEAR-PRODUCTION AIR CUSHION RESTRAINT

Contract No. DOT-HS-017-1-017-1A
February 1977
Final Report

COPIES AVAILABLE TO DDC DOES NOT
PERMIT FULLY LESKLE PRODUCTION

DDC FILE COPY

PREPARED FOR:

U.S. DEPARTMENT OF TRANSPORTATION
NATIONAL HIGHWAY TRAFFIC SAFETY ADMINISTRATION
WASHINGTON, D.C. 20590

Document is available to the public through
the National Technical Information Service,
Springfield, Virginia 22161

DDC
RECEIVED
APR 20 1977
B

NOTICES

This document is disseminated under the sponsorship of the Department of Transportation in the interest of information exchange. The United States Government assumes no liability for its contents or use thereof.

The voluntary informed consent of the subjects used in this research was obtained in accordance with Air Force Regulation 169-8.

This report has been identified by the Aerospace Medical Research Laboratory as AMRL-TR-75-47.

DEPARTMENT OF THE AIR FORCE
6570TH AEROSPACE MEDICAL RESEARCH LABORATORY (AFSC)
WRIGHT-PATTERSON AIR FORCE BASE, OHIO 45433



REPLY TO
ATTN OF: TOP(STINFO)

18 April 1977

SUBJECT: AMRL/DOT Technical Report for Entry in DDC

TO: Defense Documentation Center
ATTN: DDC-TC
Cameron Station
Alexandria, VA 22314

The attached report, Impact Tests of a Near-Production Air Cushion Restraint, by J. W. Brinkley (AMRL); Col G. C. Mohr, MC, CFS (AMD); Major H. C. Russell, BSC; Major S. M. Cooper, MC; and Captain J. T. Shaffer; will be entered in National Technical Information Service by the Department of Transportation. Since it was written by Air Force personnel for DOT, we think that it belongs in DDC as well. As performing organization we assigned the report number AMRL-TR-75-47.

Joan C. Robinette
JOAN C. ROBINETTE
Scientific and Technical
Information Officer

Atch:
DOT HS-802 248/
AMRL-TR-75-47

NOTE: There are several printout tables in the appendices; they are barely legible, but have little interest to anyone, other than DOT.



6202F

TECHNICAL REPORT STANDARD TITLE PAGE

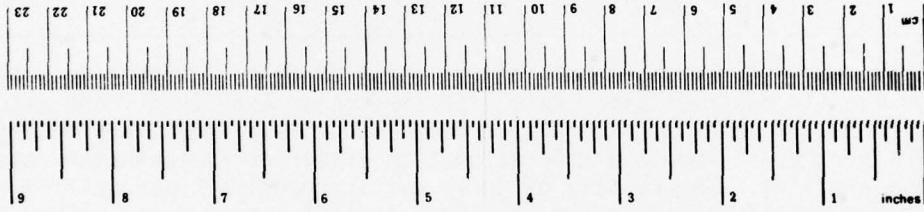
1. Report No. DOT-HS-802-248	2. Government Accession No.	3. Recipient's Catalog No.
4. Title and Subtitle Impact Tests of a Near-Production Air Cushion Restraint.	5. Report Date February 1977	6. Performing Organization Code
7. Author(s) J. W./Brinkley, Col G. C./Mohr, MC, CFS; Major H. C./Russell, BSC, Major S. M./Cooper MC; and Capt J. T./Shaffer	8. Performing Organization Report No. AMRL-TR-75-47	
9. Performing Organization Name and Address Aerospace Medical Research Laboratory Aerospace Medical Division Air Force Systems Command Wright-Patterson Air Force Base, Ohio 45433	10. Work Unit No. 021WB101	
12. Sponsoring Agency Name and Address Department of Transportation National Highway Traffic Safety Administration Office of Vehicle Structures Research, Biomechanics Div. 400 7th St., S.W., Washington, D.C. 20590	11. Contract or Grant No. DOT-HS-017-1-017-IA	
15. Supplementary Notes 7231 1746 12409p.	13. Type of Report and Period Covered Final Report. January 1972 to Sep 1975	
14. Sponsoring Agency Code		
16. Abstract A series of impact tests were accomplished to demonstrate the protection provided by an automotive air bag restraint system for the center and right front passengers. Fifteen young healthy male volunteers were impacted at velocities ranging from 14.9 to 30.8 miles per hour. Impact acceleration-time histories approximated automotive barrier crash profiles. The results of dummy tests preceding human testing are summarized and detailed test data are presented from 33 impact tests with volunteer subjects. Test data are compared with similar data collected during earlier impact tests of a prototype air bag restraint system. The restraint that was tested was a near production air cushion system designed and fabricated by the Fisher Body Division of the General Motors Corporation. The air cushion restraints that were tested were provided by the General Motors Corporation to the National Highway Traffic Safety Administration for use in this test program. An extensive series of tests of the air cushion restraint was performed with anthropometric dummies at the General Motors Proving Grounds to demonstrate the reliability of the air cushion and the test apparatus. Final tests with anthropometric dummies and volunteers were conducted on the Daisy Decelerator located at Holloman Air Force Base, New Mexico.		
17. Key Words Impact Air Bag Human Subjects Passive Restraint	18. Distribution Statement Document is available to the public through the National Technical Information Service, Springfield, Virginia 22161	
19. Security Classif. (of this report) Unclassified	20. Security Classif. (of this page) Unclassified	21. No. of Pages 407
		22. Price

METRIC CONVERSION FACTORS

Approximate Conversions to Metric Measures

Symbol	When You Know	Multiply by	To Find	Symbol
LENGTH				
in	inches	2.5	centimeters	cm
ft	feet	30	centimeters	cm
yd	yards	0.9	meters	m
mi	miles	1.6	kilometers	km
AREA				
in ²	square inches	6.5	square centimeters	cm ²
ft ²	square feet	0.09	square meters	m ²
yd ²	square yards	0.8	square meters	m ²
mi ²	square miles	2.6	square kilometers	km ²
	acres	0.4	hectares	ha
MASS (weight)				
oz	ounces	28	grams	g
lb	pounds	0.45	kilograms	kg
	short tons (2000 lb)	0.9	tonnes	t
VOLUME				
tsp	teaspoons	5	milliliters	ml
Tbsp	tablespoons	15	milliliters	ml
fl oz	fluid ounces	30	milliliters	ml
c	cups	0.24	liters	l
pt	pints	0.47	liters	l
qt	quarts	0.95	liters	l
gal	gallons	3.8	liters	l
ft ³	cubic feet	0.03	cubic meters	m ³
yd ³	cubic yards	0.76	cubic meters	m ³
TEMPERATURE (exact)				
°F	Fahrenheit temperature	5/9 (after subtracting 32)	Celsius temperature	°C

Symbol	When You Know	Multiply by	To Find	Symbol
LENGTH				
mm	millimeters	0.04	inches	in
cm	centimeters	0.4	inches	in
m	meters	3.3	feet	ft
m	meters	1.1	yards	yd
km	kilometers	0.6	miles	mi
AREA				
cm ²	square centimeters	0.16	square inches	in ²
m ²	square meters	1.2	square yards	yd ²
km ²	square kilometers	0.4	square miles	mi ²
ha	hectares (10,000 m ²)	2.5	acres	ac
MASS (weight)				
g	grams	0.035	ounces	oz
kg	kilograms	2.2	pounds	lb
t	tonnes (1000 kg)	1.1	short tons	st
VOLUME				
ml	milliliters	0.03	fluid ounces	fl oz
l	liters	2.1	pints	pt
l	liters	1.06	quarts	qt
l	liters	0.26	gallons	gal
m ³	cubic meters	35	cubic feet	ft ³
m ³	cubic meters	1.3	cubic yards	yd ³
TEMPERATURE (exact)				
°C	Celsius temperature	9/5 (then add 32)	Fahrenheit temperature	°F



*1 in = 2.54 inexact. For other exact conversions and more detailed tables, see NBS Misc. Publ. 286, Units of Weights and Measures, Price \$2.25, SO Catalog No. C13.10.286.

PREFACE

This study was conducted by the Impact Branch, Biodynamics and Bionics Division, Aerospace Medical Research Laboratory, Wright-Patterson AFB, Ohio, under Project 7231, "Biomechanics of Aerospace Operations," Task 723106, "Impact Exposure Limits and Personnel Protection Criteria." The experimental phase of the effort was accomplished at the Impact Branch Operating Location at Holloman AFB, New Mexico. The work was conducted and supported as a joint USAF-DOT program and planned to fulfill the requirements of the National Highway Traffic Safety Administration, Department of Transportation, under Interagency Agreement Number DOT-HS-017-1-017-IA. Mr. Arnold Johnson was the technical monitor for the National Highway Traffic Safety Administration during the planning stages of the work and Mr. Thomas Glenn was the technical monitor during the experimental and data analysis phases.

This report presents the experimental procedures and results of impact tests of an air bag restraint system that has been produced for evaluation by automotive fleet users.

The human tests that are reported were performed during the period of 9 August to 20 September 1972.

ACCESSION FOR		
NTIS	White Section	<input checked="checked" type="checkbox"/>
ODC	Dot Section	<input type="checkbox"/>
UNANNOUNCED		<input type="checkbox"/>
JUSTIFICATION		
BY		
DISTRIBUTION/AVAILABILITY CODES		
Dist.	AFAM. and/or SPECIAL	
A	XXXXXXXXXX	.

ACKNOWLEDGMENTS

The design, fabrication, and testing efforts of the General Motors Corporation, Fisher Body Division, were supplied to the Department of Transportation for this program. Specific acknowledgment is given to Messrs. Steve S. Hurite and Anthony M. Camilletti of the Fisher Body Division and Mr. George R. Smith of the General Motors Environmental Activities Staff for their invaluable assistance during the planning and testing phases of the program. Installation of the air cushion device into the test buck was performed by personnel of General Motors and the Allied Chemical Corporation. Onboard motion picture cameras and lighting were provided by the General Motors Proving Grounds and operated by their personnel.

Special commendation is given to the Air Force officers and airmen who volunteered to participate as subjects in the experiments and to Major Dennis L. Buschman, USAF, MC, FS, who was the medical officer on the program during the planning and dummy test data evaluation efforts prior to his departure from active duty. We wish to express our gratitude to the entire team of personnel of the Impact Branch, the Holloman AFB Hospital and the Land Air Division of the Dynalectron Corporation, under Contract DAAAD-07-69-C-0032, for their devotion and professionalism in the successful and safe accomplishment of this program. We are also indebted to the personnel of the USAF Hospital, Holloman Air Force Base for their support throughout the test series and to Dr. Alan P. Berens of the University of Dayton Research Institute for his review of the statistical analyses and his contributions to those analyses.

TABLE OF CONTENTS

	Page No.
Preface	iii
Acknowledgements	iv
List of Illustrations	vii
List of Tables	xii
I. Introduction	1
II. Technical Approach	5
III. Methods and Materials	20
A. Impact Environments	20
B. Test Apparatus	25
C. Instrumentation	48
D. Data Processing	74
E. Anthropomorphic Dummies	80
F. Volunteer Subjects	81
IV. Results	88
A. Dummy Tests Conducted at the GM Proving Grounds	88
B. Impact Tests with Dummies on the Daisy Decelerator	96
C. Development and Demonstration of a Revised Air Cushion Inflator System	110
D. Tests with Volunteers	122
E. Medical Findings	170
V. Analysis of Results and Discussion	178
A. Impact Tests Using Dummy Subjects	178
B. Tests with Volunteers	206
C. Comparison of Dummy and Volunteer Tests	229

	Page No.
VI. Summary	232
VII. References	237
Appendix A - Summary of Installation, Materials and Configuration Aspects Deviating From The Production Air Cushion System	A-1
Appendix B - TSC 4-Channel Linear/Rotational Mouthpiece Accelerometer Specifications	B-1
Appendix C - Two-Bit Displacement Measuring System	C-1
Appendix D - Photometric Data Processing Methods	D-1
Appendix E - Chronological Listing of Tests Conducted on the Daisy Decelerator During the Production Air Cushion Test Program	E-1
Appendix F - Photometric Data Processing Procedure to Determine Head Motion Trajectories	F-1
Appendix G - AD Plots of Test Data From Tests Numbers 6571, 6572, 6574 and 6575	G-1

LIST OF ILLUSTRATIONS

Figure No.	Page No.
1. Logic Model Concept	8
2. Phase I Seat and Headrest Configuration	12
3. Phase II Seat and Headrest Configuration	13
4. 30 MPH Barrier Crash Acceleration Profiles	21
5. Typical Daisy Decelerator Impact Profiles Used in the Test Program	24
6. General Layout of the Body Buck	26
7. Photograph of the Body Buck	28
8. Steel Instrument Panel Dimensions	30
9. Photograph of the Instrument Panel Installation	31
10. Seat Back Bracing and Headrest	33
11. Air Cushion Restraint Activation Switch Actuation Ramp, Brake Penetration and Velocity Measuring Device	36
12. Air Cushion Inflator Assembly	39
13. Air Cushion Restraint Initiation and Safety Interlock System Circuit	40
14. Indicator Light and Switch Panel of the Restraint Initiation and Safety Interlock System	41
15. Air Cushion Restraint System During Impact	44
16. Secondary Safety Restraint Harness	46
17. Secondary Safety Harness Actuation Circuitry	47
18. Typical Single Transducer Wiring Diagram	51
19. Typical Detonator and Squib Current Monitor	57
20. Side View of Test Subject Showing Chest and Head Accelerometers	59

Figure No.	Page No.
21. Side View of Test Subject Showing Mouthpiece Accelerometer and Velcro Harness	60
22. Accelerometer Mounting Technique and Dummy Head Displacement Measuring System with Potentiometers	64
23. Six Cord Head Displacement Measuring System Used in Dummy Tests	66
24. Head Displacement Measuring System Used With Volunteer Test Subjects	67
25. Motion Picture Camera Mounted Under the Instrument Panel	69
26. Instrument Panel Accelerometer Mount and Displacement Reference System	70
27. Photometric Data Processing Coordinate System	72
28. Magnetic Tape Data Processing Schematic	75
29. Anthropometric Dimensions	82
30. Photometric Target Disc Locations for Volunteer Subjects	85
31. Damage of Polystyrene Windshield - Test Number 6313	101
32. G_x Acceleration Measured on the Dummy's Head During Test Numbers 6338, 6340, 6355 and 6356	102
33. G_x Acceleration Measured on the Dummy's Head During Test Numbers 6354 and 6357	103
34. Air Bag Tear Found After Test Number 6381	108
35. Air Bag Tear Found After Test Number 6384	109
36. Acceleration-Time Histories From Accelerometers Mounted Externally on the Test Dummy - Test Number 6486	115
37. Acceleration-Time Histories from Accelerometers Mounted Within the Test Dummy - Test Number 6486	116
38. Composite of Dummy Head Positions Determined From Measurements During 20 Successive Tests	121

Figure No.	Page No.
39. Dye Mark on Windshield - Test Number 6514	126
40. Dye Mark on Windshield - Test Number 6556	127
41. Dye Mark on Windshield - Test Number 6569	128
42. Histogram of Remaining Head to Instrument Panel Distance for Each Test	129
43. Head Positions Determined from Cord Lengths - 15, 20 and 22 MPH Tests	130
44. Head Positions Determined from Cord Lengths - 24, 26, 28 and 30 MPH Tests	131
45. Sequence Still Photograph 1 at Instant of Air Cushion Deployment Initiation	133
46. Sequence Still Photograph 2 Showing Subject Impacting the Air Cushion	134
47. Sequence Still Photograph 3 Showing the Air Cushion Encircling the Subject	135
48. Sequence Still Photograph 4 Showing the Subject Rebounding from the Air Cushion	136
49. Sequence Still Photograph 5 Showing the Subject Returned to the Seat Backrest	137
50. Photometric Head Position Trajectory Within Sled Coordinate System - Test No. 6507	139
51. Photometric Head Position Trajectory from Test Number 6514	141
52. Photometric Head Position Trajectory from Test Number 6528	142
53. Photometric Head Position Trajectory from Test Number 6534	144
54. Photometric Head Position Trajectory from Test No. 6537	146
55. Photometric Head Position Trajectory from Test No. 6556	147
56. Photometric Head Position Trajectory from Test No. 6569	149

Figure No.		Page No.
57.	Photometric Head Position Trajectory from Test Number 6571	150
58.	Photometric Head Position Trajectory from Test Number 6572	152
59.	Photometric Head Position Trajectory from Test Number 6574	153
60.	Photometric Head Position Trajectory from Test Number 6575	154
61.	Maximum Displacements of the Head Reference Points	155
62.	Minor Laceration of Left Thumb - Test Number 6532	173
63.	Comparison of Head Impact Severity Indices for Air Cushion Tests with Paper Windshields and Polystyrene Windshields	179
64.	Comparison of Peak Chest Acceleration Values for Air Cushion Tests with Paper Windshield and Polystyrene Windshields	180
65.	Comparison of Head Impact Severity Indices from Tests with Steel and Polystyrene Instrument Panels	182
66.	Comparison of Peak Chest Acceleration from Tests with Steel and Polystyrene Instrument Panels	183
67.	Peak Resultant Acceleration Measured on the Dummies Chests During Air Cushion Tests 6321 to 6357	185
68.	Head Impact Severity Indices from Air Cushion Tests 6321 to 6357	186
69.	Head Impact Severity Indices from Air Cushion Tests 6321 to 6392	187
70.	Head Impact Severity Indices from Air Cushion Tests with Revised Gas Generator Using Dummy Subjects	190
71.	Head Impact Severity Indices from Test with Revised Gas Generator and Increased Stored Gas Pressure - Dummy Subjects	192
72.	Comparison of Peak Chest Acceleration Data From Tests at the GM Proving Grounds and the Daisy Decelerator	203

Figure No.		Page No.
73.	Comparison of Head Impact Severity Index Values From Tests at the GM Proving Grounds and the Daisy Decelerator	205
74.	Peak Chest Resultant Acceleration Values From Air Cushion Tests Using Volunteer Subjects	207
75.	Head Impact Severity Indices from Air Cushion Tests 6507-6575	208
76.	Peak G _x Acceleration Values Measured on the Head of Volunteers Using Externally Mounted Accelerometers	210
77.	Head Injury Criteria Values for Tests 6507 to 6575	212
78.	Average Remaining Head-to-Panel Distances for Impact Velocity Groups	219
79.	Distance Remaining Between Head and Instrument Panel for Each Test with Human Subjects	220
80.	Remaining Head-to-Panel Distance Data Grouped for Each Subject	221
81.	Resultant Foot Load Data Plotted as a Function of Impact Sled Acceleration	224
82.	Head Impact Severity Index Values for Prototype Air Bag and Near-Production Air Cushion Tests with Human Subjects	227
83.	Peak Chest Acceleration Data for Prototype Air Bag and Near-Production Air Cushion Tests with Human Subjects	228

LIST OF TABLES

Table No.		Page No.
I.	Component Reliability Data	9
II.	Test Condition Probabilities Computed From Component Reliability Data	10
III.	Design Data for Brake Patterns	23
IV.	Inflator Initiation Switch Activation Intervals	37
V.	Chart of Frequency Responses	53
VI.	Chart of Frequency Responses	54
VII.	Chart of Frequency Responses	55
VIII.	Foot Load Cell Blocks Used by Each Subject	62
IX.	Dummy Anthropometry	80
X.	Anthropometry of the Volunteers	82
XI.	Photometric Target Positions for Each Subject	85
XII.	Summary of Results from Air Cushion Impact Tests with Paper Windshield	90
XIII.	Summary of Results from Air Cushion Impact Tests with Polystyrene Foam Windshield	91
XIV.	Summary of Test Results from Nondeployment Tests	93
XV.	Restraint Harness Load Measurements	94
XVI.	Summary of Results from Tests to Select the Best Instrument Panel Configuration	97
XVII.	Summary of Data from the Initial Series of Impact Tests of the Air Cushion Restraint Conducted on the Daisy Decelerator	100
XVIII.	Summary of Data from Additional Low Velocity Impact Tests of the Air Cushion Restraint	107
XIX.	Summary of Data from Impact Tests of the Air Cushion System with Revised Gas Generator Charges	111

Table No.		Page No.
XX.	Summary of Data from Impact Tests of the Air Cushion System with Revised Gas Generator Charges and 2700 PSI Stored Gas Pressure	112
XXI.	Checkout Test Results	113
XXII.	Summary of Data from 20 Successive Successful Impact Tests with Dummy Subjects	114
XXIII.	Summary of HIC Data from 20 Successive Tests with Dummy Subjects	120
XXIV.	Summary of Data from Tests with Human Subjects	123
XXV.	Peak Head and Chest Impact and Rebound Accelerations	157
XXVI.	Summary of Data From Tests with Volunteers: Results Obtained from Data Processing by General Motors	158
XXVII.	Listing of Peak Accelerations Measured on the Subjects' Head and Mouth	160
XXVIII.	Peak Triaxial Foot Load Measurements	161
XXIX.	Statistical Summary of the 20 Successive Dummy Tests	162
XXX.	Statistical Summary of 15 MPH Test Results (n=4)	163
XXXI.	Statistical Summary of 20 MPH Test Results (n=4)	164
XXXII.	Statistical Summary of 22 MPH Test Results (n=4)	165
XXXIII.	Statistical Summary of 24 MPH Test Results (n=6)	166
XXXIV.	Statistical Summary of 26 MPH Test Results (n=7)	167
XXXV.	Statistical Summary of 28 MPH Test Results (n=4)	168
XXXVI.	Statistical Summary of 30 MPH Test Results (n=4)	169
XXXVII.	Comparison of Differences Between Peak Resultant Chest Acceleration Values Using Gas Generators with 20 and 25 Grams of Propellant	193
XXXVIII.	Comparison of Differences Between the Severity Indices Using Gas Generators With 20 and 25 Grams of Propellant	193

Table No.		Page No.
XXXIX.	Comparison of Differences Between the Peak Resultant Chest Acceleration Values Using Inflator Pressures of 2350 PSI and 2700 PSI	195
XL.	Comparison of Differences Between the Severity Indices Using Inflator Pressures of 2350 PSI and 2700 PSI	195
XXXVIIa.	Analysis of Variance Table for Chest Accelerations at Two Levels of Velocity and Propellant	197
XXXVIIb.	Average Chest Accelerations	197
XXXVIIIa.	Analysis of Variance Table for Severity Indices at Two Levels of Velocity and Propellant	197
XLI.	Comparison of Head Impact Severity Indices From Tests with 50th and 95th Percentile Dummies	199
XLII.	Comparison of Peak Resultant Acceleration Values From Tests with 50th and 95th Percentile Dummies	199
XLIII.	Comparison of H.I.C. Values Calculated by General Motors and the Aerospace Medical Research Laboratory	213
XLIV.	Data From Tests Where Acceleration Recordings Were Digitized To Filter Above 500 Hertz	215
XLV.	Data From Tests Where Acceleration Recordings Were Digitized To Filter Above 50 Hertz	216

I. Introduction

The objective of this program was to demonstrate the impact protection efficacy of a near-production automobile air cushion restraint under experimental conditions simulating an automotive barrier crash. The air cushion restraint that was tested was designed and fabricated by the Fisher Body Division of the General Motors Corporation to provide passive restraint for the center and right front seat passengers during frontal impact. The air cushion systems that were tested were provided by the General Motors Corporation to the National Highway Traffic Safety Administration for use in this test program.

This program is a portion of an extensive interagency research task to study the effectiveness of impact protection techniques under various impact environmental conditions. The overall program is concerned with the development of improved protection systems and the evaluation of these systems using animal, anthropometric dummy and human subjects.

The research that has been conducted by the Aerospace Medical Research Laboratory (AMRL) using animal subjects has been focused on determining the relative efficacy of specific restraint systems (ref 1,2,3). The technical approach has been one of experimentally establishing the relative acceleration levels at which each restraint will cause a similar degree of injury. The experimentation has been designed to determine the levels where the probability of lethality is 50 percent. This approach is not as straightforward as it might initially seem since each restraint configuration might, and in actual practice does, cause a unique injury pattern. For example,

when a lap belt is the only restraint, the lethal trauma might result from impact of the head upon the windshield or the instrument panel, while neck trauma might be the endpoint when a lap belt and shoulder harness is used. Therefore, the ongoing research with animal subjects within this laboratory has been redirected toward the definition of the sublethal injury mechanisms and their frequencies as a function of the restraint system design configuration.

The experimentation that has been accomplished by the AMRL with anthropometric dummies during this interagency program has been accomplished for two purposes. First, to structurally proof-test impact protection systems and other portions of the test apparatus prior to human tests. Second, to evaluate the repeatability of the dummy response (ref 4) and the impact environment. Motion picture data from dummy tests has also been used to study the kinematic responses of the dummy body segments in order to gain some insight into such factors as subject rebound, limb motion envelopes, etc. However, this application of data collected from dummy tests must be approached with considerable caution since, to date, anthropometric dummies have not been designed that adequately represent the mechanodynamic response characteristics of the human body in the $-G_x$ direction. The simulation has been inadequate in both the kinematic and the inertial response properties when the dummy data has been compared with data collected with human subjects under similar conditions (ref 5).

Tests with human subjects have been conducted to provide several different types of information (ref 6,7,8,9). This information has included measurements of inertial and kinematic response, subjective

comments, physiological responses, and pathological changes. The tests have been limited to experimentation at subinjury levels. Testing at such levels has been adequate to provide data to compare to dummy tests and to discover causes of minor trauma that have been encountered.

Tests of the deployment characteristics of an air bag restraint in a stationary test fixture (ref 8) have disclosed undesirable operating characteristics of the prototype that was tested. A series of 41 tests were completed by the AMRL with volunteer subjects at Holloman AFB. The portion of the study that was designed to evaluate the effects of the deployment of the air bag on subjects leaning forward was terminated at a thorax horizontal angle of 61 degrees due to symptoms of mild concussion. These tests also revealed varying degrees of soft tissue trauma that were attributed to specific aspects of the air bag system design. Impact tests with volunteers were also accomplished with this same prototype air bag restraint on the Daisy Decelerator at Holloman AFB (ref 9). Thirty-five tests were performed by the AMRL at impact velocities ranging up to 31.5 mph. The trauma that was observed was mild, ranging from none to various combinations of abrasion, contusion and edema. Subjective symptomatology included one incident of abdominal pain which subsided within one minute, one complaint of medial thigh pain of unknown etiology, several complaints of popliteal pain attributed to hyperextension of the knee during rebound, and several complaints of mild headaches and stiffness in the area of the cervical spine that might have been related to the rebound of the head. The head rebound that occurred after the initial impact was considered to be undesirable from an operational standpoint, although it was tolerated by the

subjects since a special large headrest was used.

The results of these two test programs have provided the impetus for revision of the design and performance characteristics of the air bag restraint. The changes, which include the use of a lighter weight outer bag material, a larger outer bag (14.5 cu ft vs. 10 cu ft), an increase of the porous area of the outer bag, a decrease of the outer bag pressure level, and lengthening of the pressure time history, have been incorporated by the General Motors Corporation into the air cushion restraint that has been used in the test program described within this report.

The air cushion restraint consists of the air bag assembly, the diffuser manifold, the inflator and the inflation initiation system. The air bag assembly is composed of a nonporous inner bag to restrain the subject's knees and a porous outer bag to restrain the subject's head and torso. The outer bag is constructed of a ripstop nylon material and is porous over its entire surface, whereas the outer bag of the prototype system that was tested in the earlier program had only porous end panels. The bags are inflated by a combination of stored gas and gas generated by two pyrotechnic devices within the gas storage container of the inflator. Only stored gas was used in the prototype system. The inflator system has two modes of operation. For low velocity (below approximately 18 mph) impact the stored gas is released and one of the pyrotechnic gas generators is ignited. When a high velocity impact occurs the second gas generator is fired to sustain the bag pressure. This system is described in more detail within the Methods and Materials Section of this report.

II. Technical Approach

Testing air bag restraint systems presents extraordinary problems when human subjects are to be used. Obviously this type of testing cannot be accomplished until every reasonable precaution against injury has been taken. The concept of deliberately exposing a human subject to high level impact without any restraint and depending upon a relatively complex series of mechanical and electrical sequences to occur to deploy the air bag, with all of these sequences required to occur after the impact has been initiated, is certainly a challenging position. The air bag restraint system may, in the long run, prove to be a very effective and reliable system in operational use, and it may represent a reasonable alternative in a life threatening situation on the highway. However, at the time of this test program, its reliability had not been adequately demonstrated for use in premeditated impact tests with human subjects. The authors concluded that measures would be required to insure a low risk of injury to the subjects.

One approach that has been used to limit the hazard to the subject is to deploy the restraint before the test. This technique was used by Bendixen (ref 6). Neither the GM prototype air bag nor the GM nearproduction air cushion restraint could be tested using this technique because of the porous construction of the outer bag. Even if this restriction could be surmounted, e.g., by maintaining the inflated bag pressure by a continuously operating pump, dummy tests of this type of restraint had shown that the motion of the bag during its deployment and the motion of the subject prior to

contacting the bag were critical factors in the overall performance of the air bag restraint.

The approach that was selected for this test program was the same as had been used in the initial series of impact tests of the GM air bag conducted by this laboratory (ref 9). First, the reliability of the restraint system was demonstrated experimentally to a level that was determined to be attainable within practical time, manpower and cost limits. Although the General Motors Corporation has designed the air cushion restraint system to have an overall system reliability of at least 0.9999 in mass use, it was clearly not practical to verify the design reliability. Just to demonstrate a reliability of 0.99 at the 90 percent confidence level would require 229 consecutive, successful tests. The reliability requirement that was ultimately established by the investigators was a demonstrated whole system reliability of 0.97 at the 90 percent confidence level. Second, other mechanisms to minimize the risk of injury were to be provided for the cases where the air bag might fail to deploy or where the air bag deployment would be incomplete, i.e., inadequate pressure within one or both portions of the air bag system. To provide protection against the first eventuality the subject was restrained to the frame of the test apparatus by a lap belt, shoulder harness, and crotch straps. This restraint was released by an electrically actuated explosive belt when four electrical wires were broken during the deployment process. Protection for the subject in the event of an incomplete deployment was provided by constructing the windshield and instrument panel of crushable materials. Additional protection was provided by

such devices as shin guards, goggles, earplugs and mouthpiece described in the Methods and Materials Section.

In order to evaluate the probability of encountering different air bag failure modes and the probability of using the restraint harness or impacting the instrument panel, the General Motors Corporation developed a reliability logic model of the test apparatus (ref 10). The logic model concept is shown in Figure 1. The actual model was much more complex and contained several hundred elements to represent the components of the entire air cushion system and their operating conditions and alternative conditions. The reliability model was programmed on a digital computer and was used by both the General Motors Corporation and this laboratory to evaluate the design of the overall test system. The component reliability test data and reliability estimates used in the model prior to the start of the whole system test program are given in Table I. The data sources that are given in Table I are specified in terms of number of unsuccessful tests/total number of tests, reliability data provided by air cushion system component vendors, or engineering judgment of the reliability of a simple component such as a battery, wire, switch or the transducer (a break wire).

The probabilities of encountering various test conditions that were computed from the component reliability data are given in Table II. The values that are cited are at the 90 percent confidence level.

As the program was originally conceived, the General Motors Corporation was to conduct a sufficient number of additional consecutively successful whole system tests at the GM Proving Grounds to

LOGIC MODEL CONCEPT

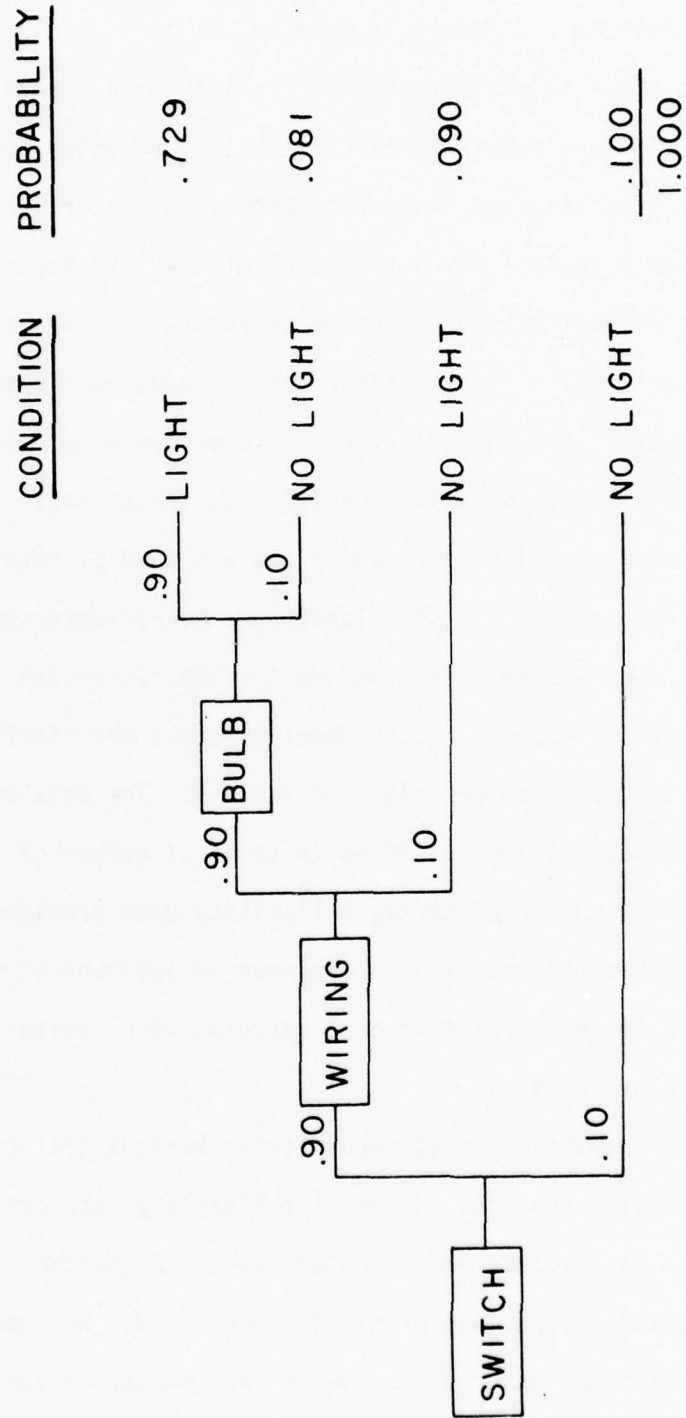


Figure 1. Logic Model Concept

TABLE I. COMPONENT RELIABILITY DATA

<u>COMPONENT</u>	<u>DATA SOURCE</u>	<u>RELIABILITY</u>
COVER	0/54	.9853
KNEE BAG	0/217	.996327
MAIN BAG	0/226	.996473
DIFFUSER	0/278	.9971
MANIFOLD	0/278	.9971
LO LEVEL PYRO	0/1352	.99941
HI LEVEL PYRO	2/1352	.998168
VESSEL	0/223	.9964
DIAPHRAGM	VENDOR DATA	.99975
SQUIBS	2/3500	.999292
DETONATORS	2/3500	.999292
RELEASE NUT	VENDOR DATA	.9999
WIRING	ENG JUDGMENT	.999
SWITCH	ENG JUDGMENT	.999
BATTERY	ENG JUDGMENT	.999
TRANSDUCER	ENG JUDGMENT	.99

TABLE II. TEST CONDITION PROBABILITIES COMPUTED
FROM COMPONENT RELIABILITY DATA

<u>CONDITION</u>	<u>PROBABILITY</u>
COMPLETE DEPLOYMENT	.942677
TORSO HARNESS NOT RELEASED	.048106
INSTRUMENT PANEL PLUS MAIN BAG	.003475
INSTRUMENT PANEL PLUS SOFT MAIN BAG	.000005
INSTRUMENT PANEL PLUS KNEE BAG	.003337
INSTRUMENT PANEL PLUS SOFT KNEE BAG	.000005
INSTRUMENT PANEL PLUS SOFT BAGS	.002239
INSTRUMENT PANEL ONLY	.000156

raise the computed system reliability for the complete deployment condition to a value of 0.95 at a confidence level of 90 percent. The tests were to be accomplished at impact velocities of 15, 20, 26 and 30 mph using 50th and 95th percentile dummy subjects. The torso harness and the crushable instrument panel were also to be demonstrated. After completion of the tests at the GM Proving Grounds, 8 to 10 additional dummy tests were planned to be accomplished at Holloman AFB to (1) demonstrate the compatibility of the test apparatus with the impact facility, (2) proof test the test buck structure, (3) provide final training for the test personnel, and (4) further elevate the demonstrated reliability of the test apparatus. The plan called for the accumulation of a sufficient number of consecutive, successful whole system deployment tests to raise the computed probability of the air cushion deployment to 0.97 at the 90 percent confidence level.

The test protocol for tests with volunteer subjects was originally designed to be accomplished in two phases. The first phase was to consist of 35 tests using the seat and headrest configuration in Figure 2. The seat back and headrest used in the Phase I test program were to be similar to the configuration used in the test program described in reference 9. The seat back and headrest were to be solidly mounted to the structure of the test buck. The second phase of the test program was a replication of the Phase I series in all aspects except the headrest design and the structural mounting of the seat back and headrest. The Phase II seat and headrest configuration are shown in Figure 3. The protocol was designed in this manner

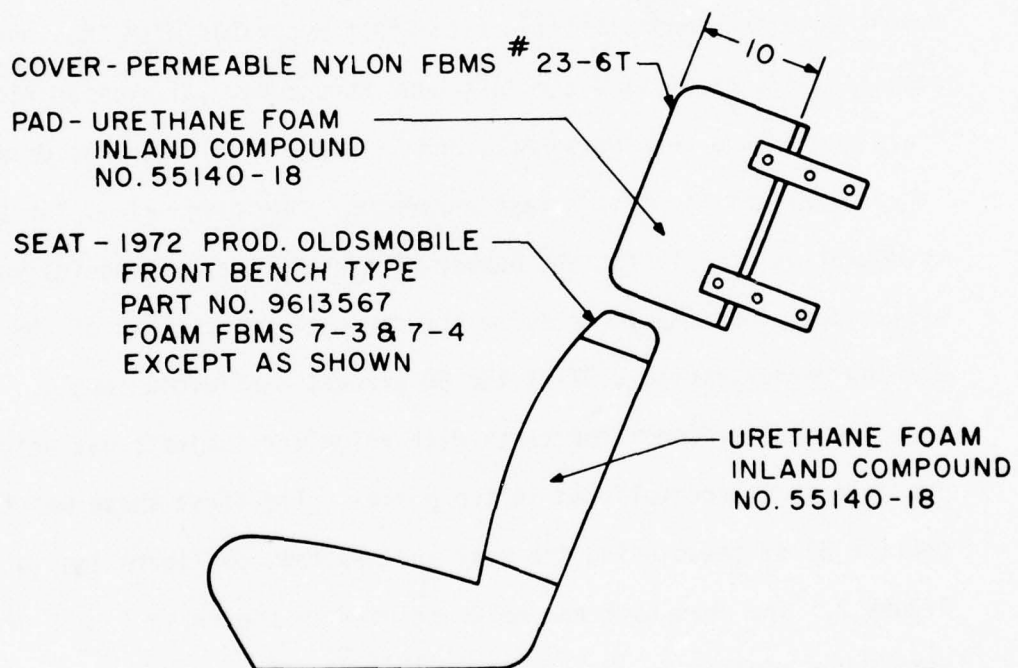


Figure 2. Phase I Seat and Headrest Configuration

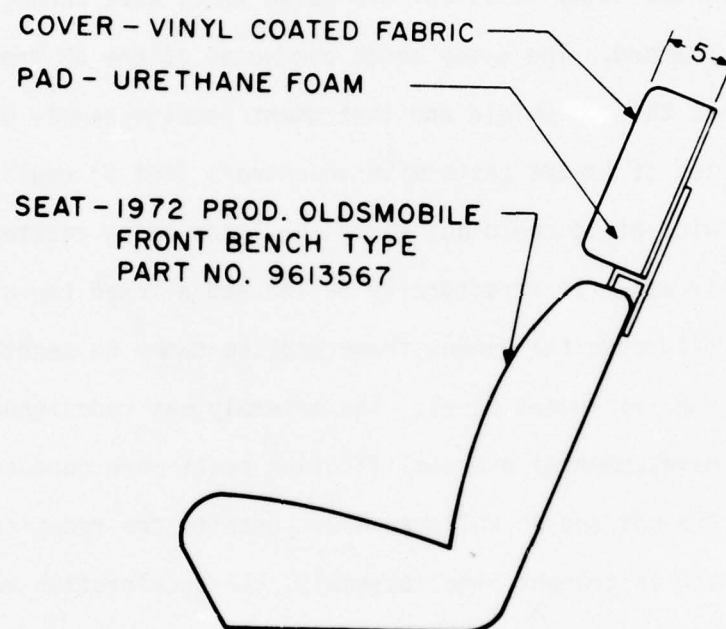


Figure 3. Phase II Seat and Headrest Configuration

to first, determine the severity of head and torso rebound in a configuration similar to the one used in the earlier test series, and second, if the rebound was not too severe, to determine the effects of head and torso rebound with a near-production seat back and headrest. If the Phase II tests were successful, it was thought that the investigators might be encouraged to conduct several demonstration tests using a production seat and headrest.

Neither the dummy tests nor the human tests were conducted as originally planned. The dummy tests conducted at the GM Proving Grounds revealed that the windshield and instrument panel assembly used in the earlier series of impact tests with volunteers (ref 9) could not be used. The windshield could not carry the loads being reacted through it by the air bag. It structurally failed and allowed the air bag to move forward through the window frame and the dummy to penetrate the air bag to the instrument panel. The assembly was redesigned and additional developmental and qualification tests were conducted at the GM Proving Grounds and at Holloman AFB. Despite the redesign of the windshield and instrument panel assembly, the acceleration measured at the dummy's head indicated to the investigators that the head was continuing to penetrate to the instrument panel. This is discussed further in the Results Section. Although the degree of penetration was not as extensive as before the redesign, evidence of the dummy's head penetration nearly to the surface of the instrument panel demonstrated a potential risk of injury to the subject. Although the actual injury that might result might not be life threatening, deliberate exposure of a human subject to an environment that the investi-

gators believed would cause injury could not be permitted. As a result of this situation the equipment manufacturer increased the amount of propellant used in the inflator gas generator, increased the pressure of the stored gas in the inflator, and additional demonstration tests were accomplished with dummy subjects. A series of 20 consecutive, replicate tests were conducted at 26 mph with a 50th percentile dummy to demonstrate the reliability and reproducibility of the air cushion restraint system after the performance of the inflator had been altered.

A summary of the dummy tests conducted prior to the initiation of testing with volunteer subjects is provided in the Results Section of this report.

The test plan was redesigned so that tests with volunteer subjects would be accomplished in increments up to 26 mph and then the human and dummy test data would be analyzed to determine if the volunteers should be exposed to impact velocities up to 30 mph. The two-phase experimental design which would change the design of the headrest and the structural mounting of the seat back and headrest was abandoned before the completion of the volunteer tests at 26 mph. The test data failed to show any significant head and torso rebound and, therefore, it was pointless to continue with the original two-phase plan.

The revised test plan specified that the tests with volunteer subjects would be accomplished at impact velocities of 15, 20, 22, 24, 26, 28 and 30 mph. As in the earlier air bag test program conducted by this laboratory (ref 9), a "stepped severity" testing approach was used in the original experimental design as well as the final design. This approach is loosely based upon a sequential sampling test technique

where the investigator may be able to evaluate statistically the risk of proceeding to the next stress level. Unfortunately, use of an actual sequential sampling approach in a test program such as this would be extremely expensive and require large numbers of subjects. In the stepped severity approach that was used, smaller numbers of subjects were used and, thus, the investigators did not have the benefits of this statistical evaluation technique. They made their decision to proceed to the next stress level or to increase the sample size at any particular level on the basis of the results of four to five tests. Motion picture films, subjective comments obtained from debriefing of the volunteers, acceleration data, indications and predictions of subject head and "riding characteristics" position, and medical examination results for each day's test, usually two tests, were available to the investigators early the following morning to facilitate the decision to continue testing. Since the tests were conducted in a sequence of increasing stress, the effects of the order of presentation of experimental conditions cannot be handled statistically as they might otherwise be if the stress levels were presented in a random fashion. Nevertheless, the approach that was used appeared to be the most practical in terms of subject safety and overall economy.

The physical measurements that were made during the program included: acceleration measured on the impact sled and the subject's head and chest; foot loads; movement of the subject with respect to the impact sled; displacement of the impact sled with respect to the water brake of the deceleration facility; velocity at the end of the acceleration of the impact sled and at the entrance of the water brake;

and specific operating sequences of the air bag restraint system. Movement of the subject was monitored by onboard as well as offboard movie cameras, but quantitative measurements were not often possible, or at least accurate, since much of the subject was obscured within the air bag during impact.

Considerable emphasis was placed upon the development of techniques to measure the position of the subject's head during impact. A large number of techniques were studied by the Impact Branch. The techniques that were considered ranged from the use of relatively simple displacement potentiometers to more sophisticated devices such as radar source tracking systems. Unfortunately, no single completely acceptable method was found that was sufficiently developed to be incorporated into the test program. A number of techniques, each of limited capability, were actually used during the experiments. They included "Met Net" developed by the General Motors Corporation, tape coated with frangible, dye filled capsules, developed by the National Cash Register Company, to determine if the subject's head had impacted the windshield or instrument panel, and several methods to measure the length of cords attached to the subject's head. These methods are described in the Methods and Materials Section and the Appendices of this report.

Physical measurements were analyzed on a "quick-look" basis immediately after each test. Motion picture films were available from each test by the next morning for semi-quantitative analysis by the investigators prior to their decision to conduct the next tests. More comprehensive data processing and analysis efforts were accomplished after completion of the entire test program. These efforts included

computation of head Severity Indices (S.I.) and Head Injury Criteria (H.I.C.) from the measurements of head acceleration (ref 11, 12).

Physiological measurements taken during the impact were limited to electrocardiographs. During the experiment planning stage of the program a number of other measurements were considered, however. These included myocardial enzymes, electroencephalograms, and measurements of innerabdominal and esophageal pressure. A study of serum myocardial enzyme levels had been made during the previous air bag restraint tests (ref 9) and no significant change had been observed. Data collected from impact tests of the air cushion using dummy subjects had shown that the acceleration environment transmitted to the subject would be considerably less severe than that measured in the previous program. Therefore, it seemed logical to conclude that the serum enzyme levels would not reflect significant change in the tests of the air cushion system. Considering this as the most likely outcome of such tests and the practical difficulties of accomplishing the tests, the investigators elected not to proceed with them. Equipment for electroencephalographic studies and measurement of abdominal and esophageal pressure was either available within the laboratory or was purchased for the program. However, this equipment was not used because the significance of such measurements in the impact environment had not been established and the equipment represented an additional risk to the subject.

The entire set of data collected during this test program has been provided to the National Highway Traffic Safety Administration for their files and for further analysis, if it is required. The

data reported within this report are those required by the Interagency Agreement (ref 12), and parameters that were of special interest to the investigators. The discussion of the test results has been limited to observations of events occurring during the test program and a comparison of findings with those of the earlier series of prototype air bag restraint tests with volunteer subjects. Extrapolations beyond the test conditions to the operational use of the air cushion restraint are not made. Interpretation of these results in terms of their application to the safety program of the National Highway Traffic Safety Administration is not within the purview of the USAF.

III. Methods and Materials

A. Impact Environments

The impact tests were conducted on the Daisy Decelerator located at Holloman AFB, New Mexico. Chandler (ref 13) has previously described the operation of this facility. It is an impact device consisting of a test sled, an accelerating device, a track, and a hydraulic brake. A pneumatic piston accelerates the test vehicle to a desired velocity on a 120 foot track. The sled then coasts along the rails into a water brake. The experiment is conducted during the deceleration of the sled into the braking device. The shape of the deceleration pulse, onset rates, and duration desired may be programmed by installing various presized orifices in the jacket of the water brake.

In this test series, composite acceleration profiles measured during actual automobile barrier crashes were used to design brake patterns to simulate the desired deceleration pulses. Figure 4 illustrates a typical barrier crash acceleration profile. Four acceleration profiles were provided by Fisher Body Division, General Motors Corporation, for this purpose. The stated nominal peak accelerations for these profiles were 10, 14, 18, and 22 G, at velocities of 15, 20, 26, and 30.5 mph respectively. All four had irregular but similar shapes which correlated with the four acceleration profiles provided for the previous test series (ref 9). The stated nominal peak accelerations for this group of profiles were 10, 14, 18 and 22 G at velocities of 15, 19, 24, and 30 mph respectively. Brake patterns for this program were designed based on these data.

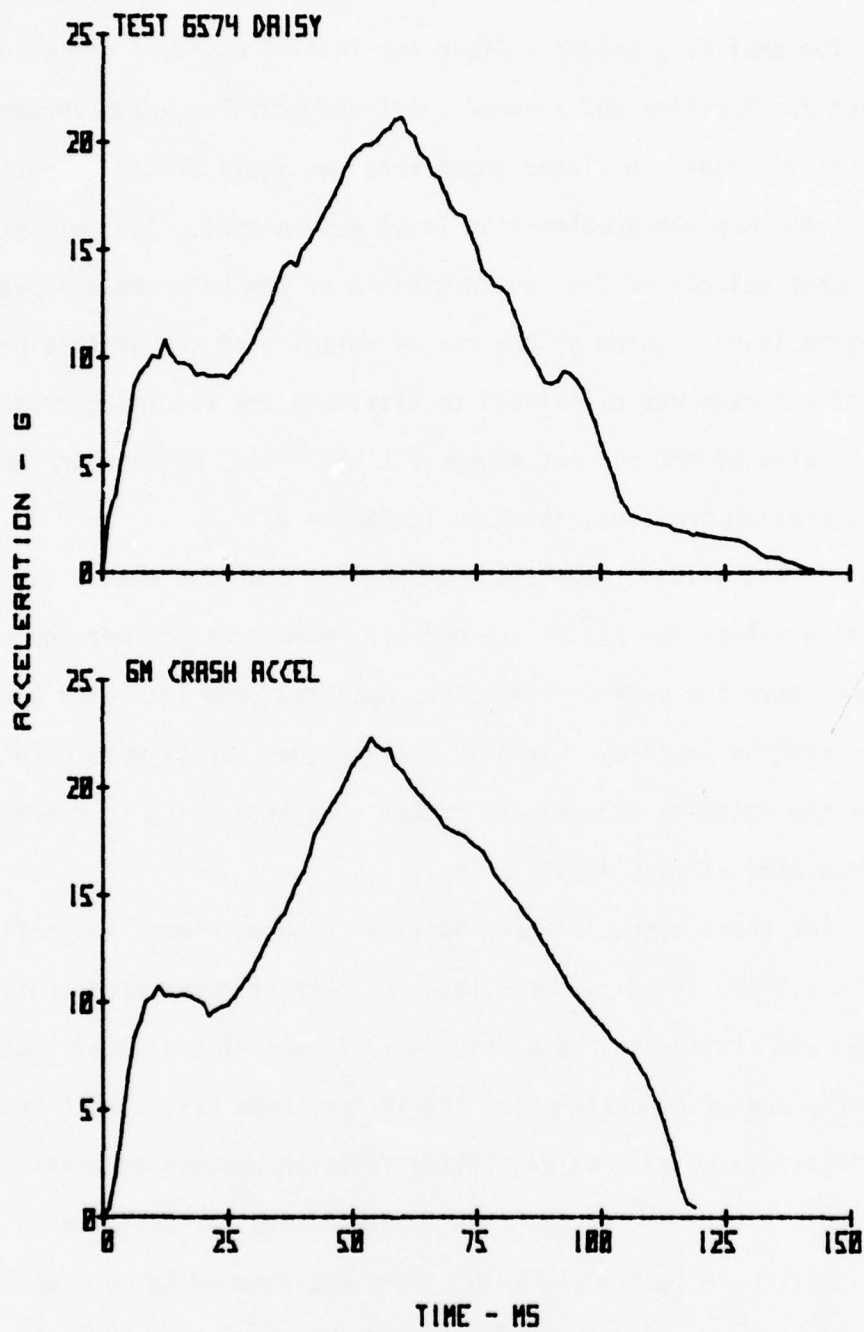


Figure 4. 30 MPH Barrier Crash Acceleration Profile and Daisy Decelerator Simulation

A linear onset was initially fitted to each barrier crash acceleration profile provided. After the initial onset, a period of constant acceleration was assumed until the profiles again showed an increased onset. A linear onset rate was again fitted to each profile until the maximum acceleration level was reached. The velocity change was then calculated from the beginning of the pulse to the peak acceleration level. Based on the stated velocity of the profile provided, an offset rate was calculated to dissipate the remaining velocity. The calculated offset did not always fit the offset of the barrier crash acceleration profiles, as shown in Figure 4.

It was evident upon close inspection that the stated nominal acceleration values for all of the barrier crash profiles were generally higher than the peak accelerations measured from the Daisy Decelerator acceleration profile. For this reason, these tests were conducted to meet the velocity requirement rather than attempting to reproduce the stated nominal peak accelerations.

For those tests in which barrier crash acceleration profiles were not provided, it was assumed that the barrier crash acceleration pulse shape was similar to those provided. It was also assumed that the anticipated peak acceleration levels for these test conditions could be interpolated as a straight-line function between adjacent acceleration profiles. The stated peak accelerations for both the 24 and 26 mph tests were identical, 18 G. This was assumed to be a unique function of structural deformation of the automotive body; therefore, the brake patterns were designed for peak accelerations of 18 G for these two test conditions. Table III tabulates design data used to

approximate the provided acceleration profiles. Figure 5 plots typical Daisy acceleration profiles recorded during this test program.

TABLE III. DESIGN DATA FOR BRAKE PATTERNS

<u>NOMINAL G</u>	<u>TYPICAL FT/SEC</u>	<u>VELOCITY MPH</u>	<u>STOPPING DISTANCE INCHES</u>
10	23.6	16.1	18.3
14	30.2	21.3	22.8
16	34.4	23.5	22.8
18	35.6	24.3	22.8
18	38.1	26.0	23.5
20	41.1	28.0	25.5
22	45.6	31.1	30.6

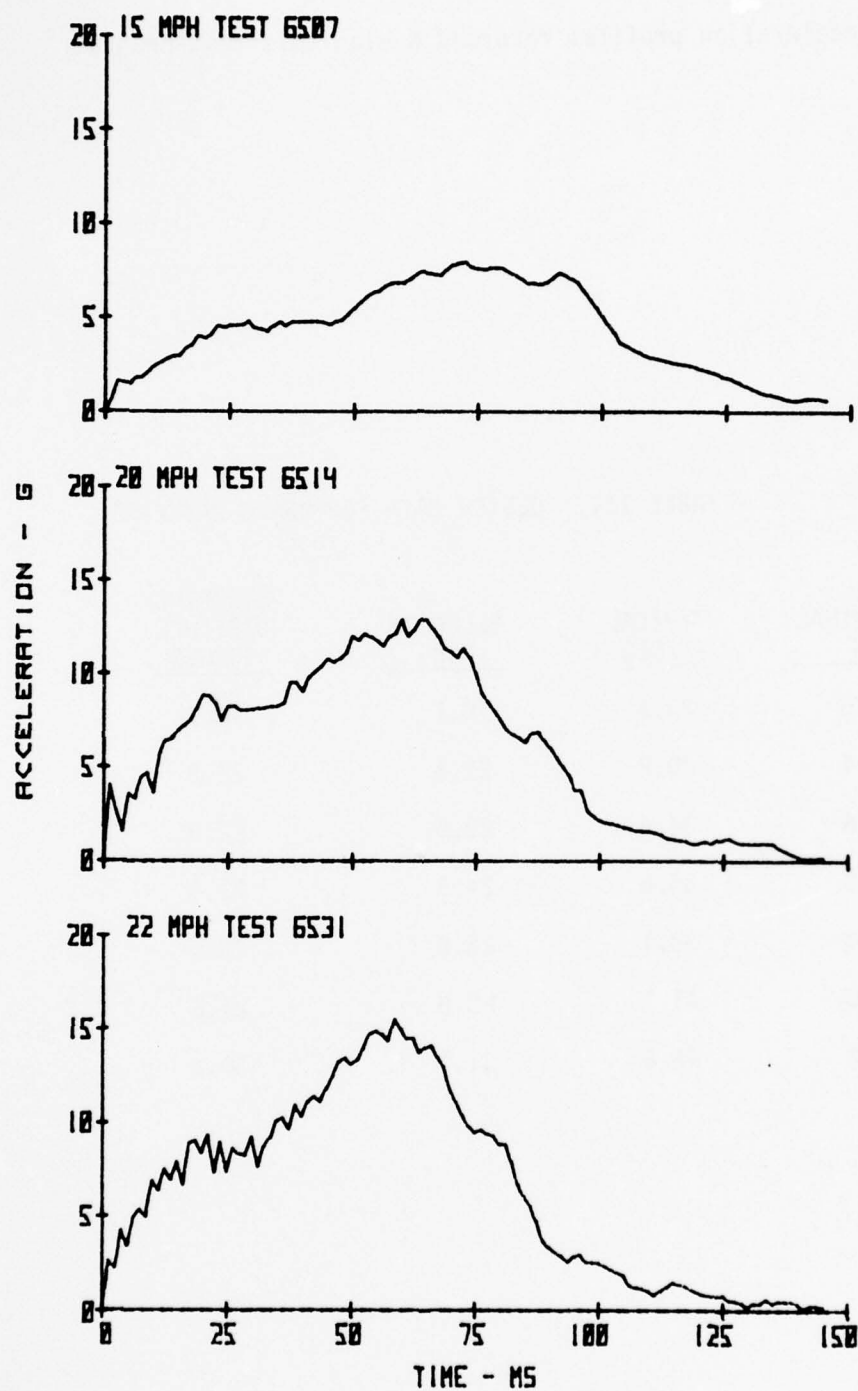


Figure 5a. Typical Daisy Decelerator Impact Profiles Used in the Test Program

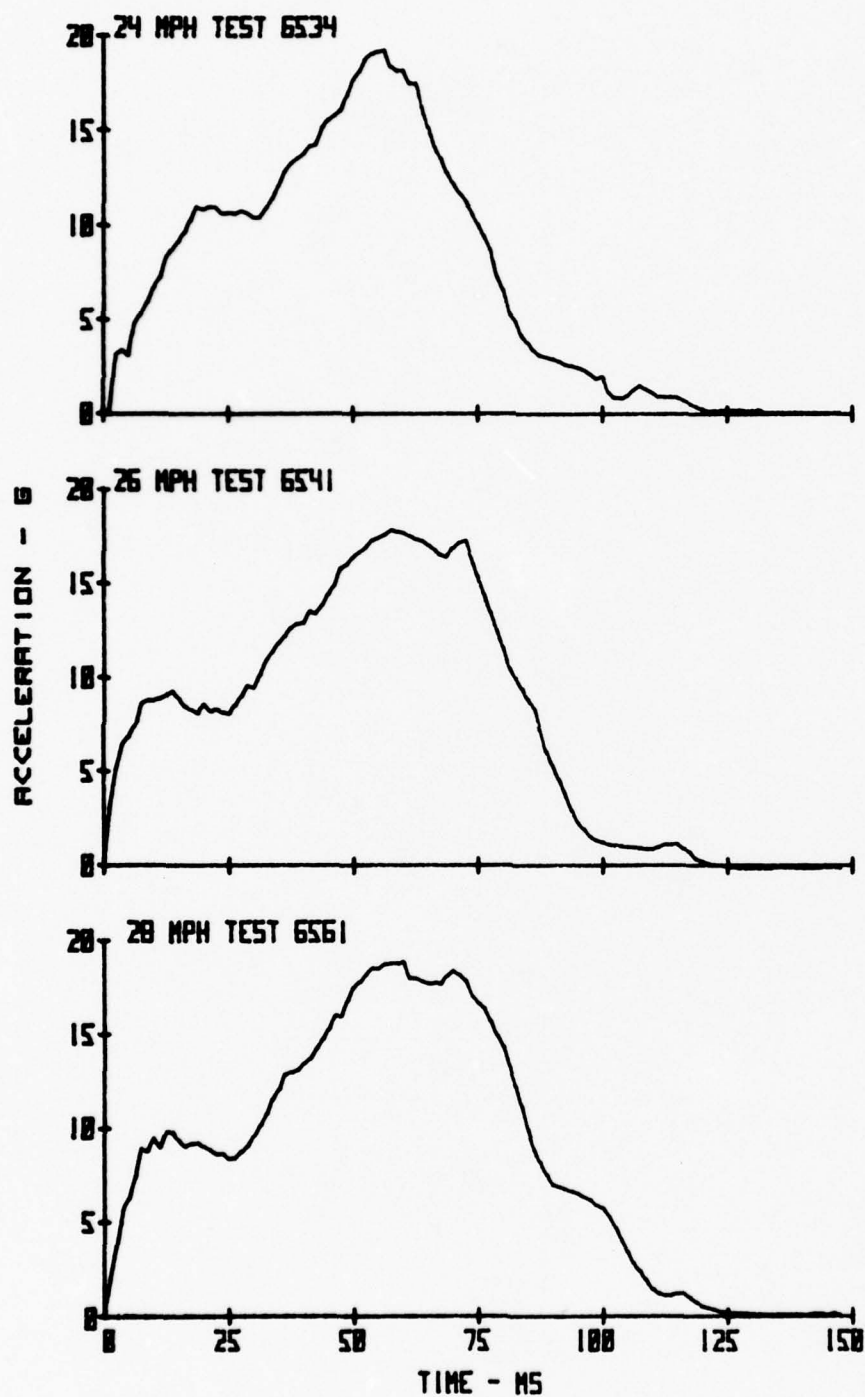


Figure 5b. Typical Daisy Decelerator Impact Profiles Used in the Test Program

B. Test Apparatus

The test vehicle used in this series of impact tests was a modified version of the device used in the previous air bag restraint test series (ref 9). The vehicle, referred to as a body buck, was designed and constructed specifically for use on the Daisy Decelerator by the Fisher Body Division, General Motors Corporation. It was furnished to the Air Force for use in this test program under the auspices of the Department of Transportation.

The body buck was constructed of structural grade rectangular steel tubing which reproduced the dimensions and clearances found in the interior front passenger compartment of a 1972 family size (B body) automobile. The body buck frame and components used to produce this interior simulation were designed to survive a 60 G test impact without structural failure. The test buck was impacted at a level of 45 G at a velocity of 60 mph without failure to demonstrate the adequacy of the structure prior to initiating human testing. The test vehicle when fully assembled, wired, and mounted on the test sled weighed 4460 pounds compared to a weight of 5200 pounds in the previous series.

Every effort was made to use production equipment and hardware manufactured for automotive sales to outfit the test buck without adversely affecting safety. The major components of the test buck included: the windshield surface simulation, the instrument panel simulation, the bench seat, the headrest, the air cushion restraint system, photometric camera and lighting system, firing actuation and safety interlock panel, and the back-up safety harness restraint. Figure 6 illustrates the general layout of the test apparatus and its components.

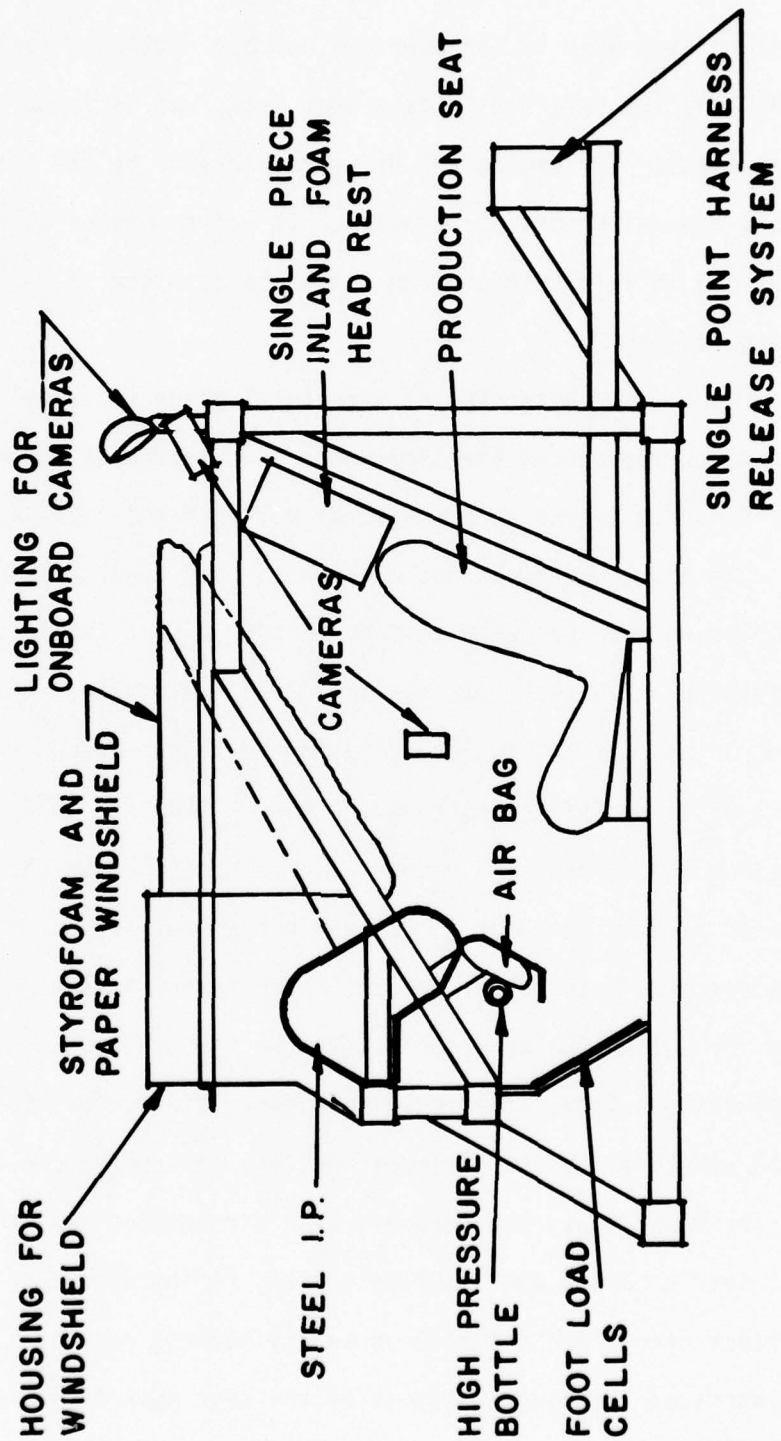


Figure 6. General Layout of the Body Buck

The windshield surface simulation was constructed from a solid block of styrofoam which was shaped to conform to the interior curvature of a 1972 Buick B body style windshield. The block was perforated throughout with 1 inch diameter holes cored from the block on 1 1/2 inch centers. These horizontal holes were cut from the styrofoam block to enhance its crushability. The shaped interior contour of the windshield simulation was covered with kraft paper and painted white. The windshield simulation was suspended in an aluminum cover by two rods mounted on the body buck frame as shown in Figure 7. During the test program, a vertical, 1/8 inch wide, black stripe was painted on the contoured portion of the windshield simulation at the 15 inch line. The 15 inch line describes the right front passenger's position for testing according to FMVSS (ref 12). This stripe aided in positioning the subjects prior to testing as well as determining whether the motion of the subject's head was restricted to a single x-z plane, the mid-sagittal plane, during impact.

The instrument panel simulation selected for use was a modified model of one of the two simulations developed for the previous test series (ref 9). The instrument panel simulation was constructed of crushable 20-gauge cold rolled sheet metal steel. The sheet metal was formed to follow the contour of a 1972 Oldsmobile B-body style instrument panel to its crest, but from that point it entered the windshield simulation on a 45 degree angle. This provided a large bearing surface on which the volunteer's head and chest would impact in the event both the air bag and back-up safety harness restraints failed simultaneously. The purpose of this design was to minimize

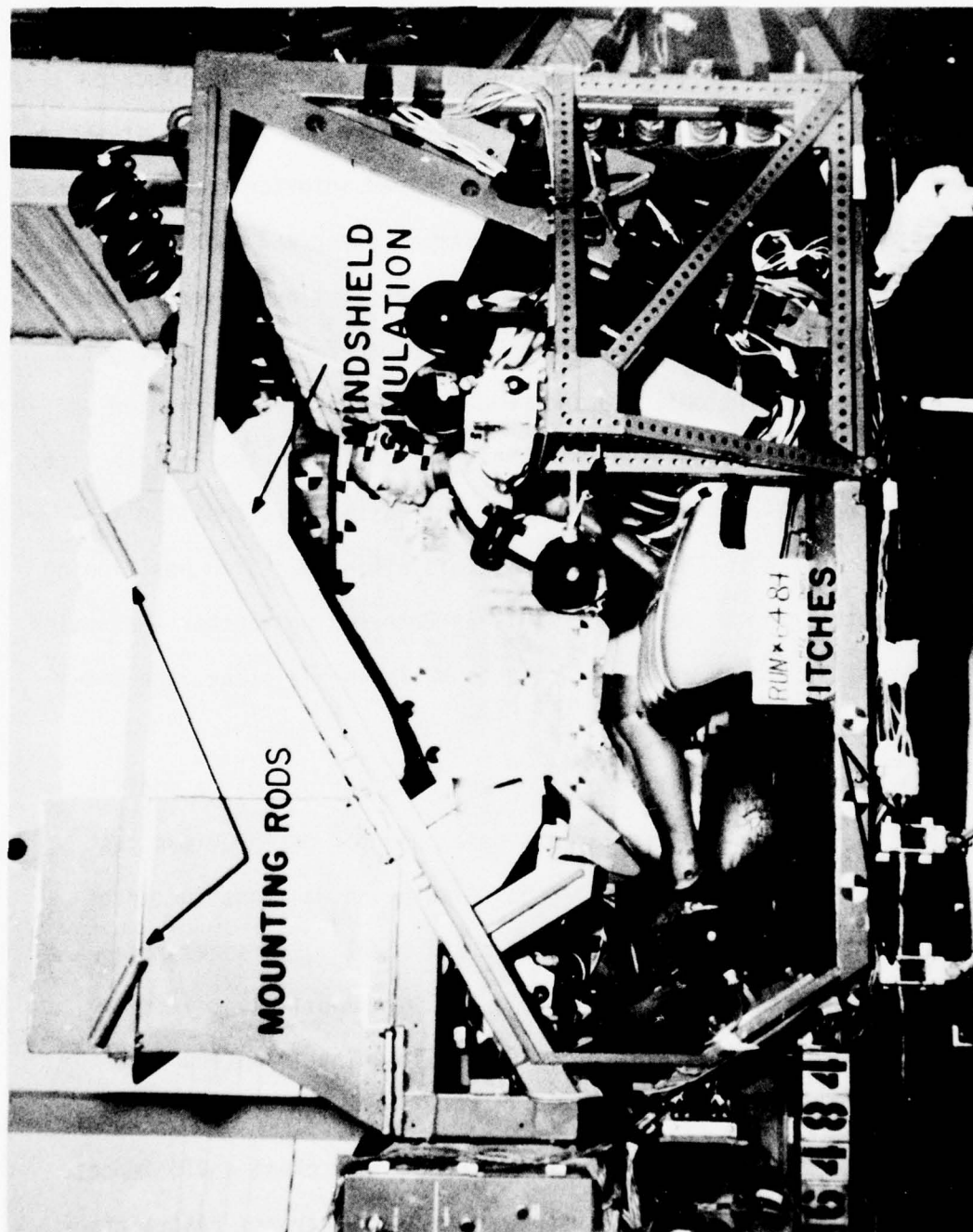
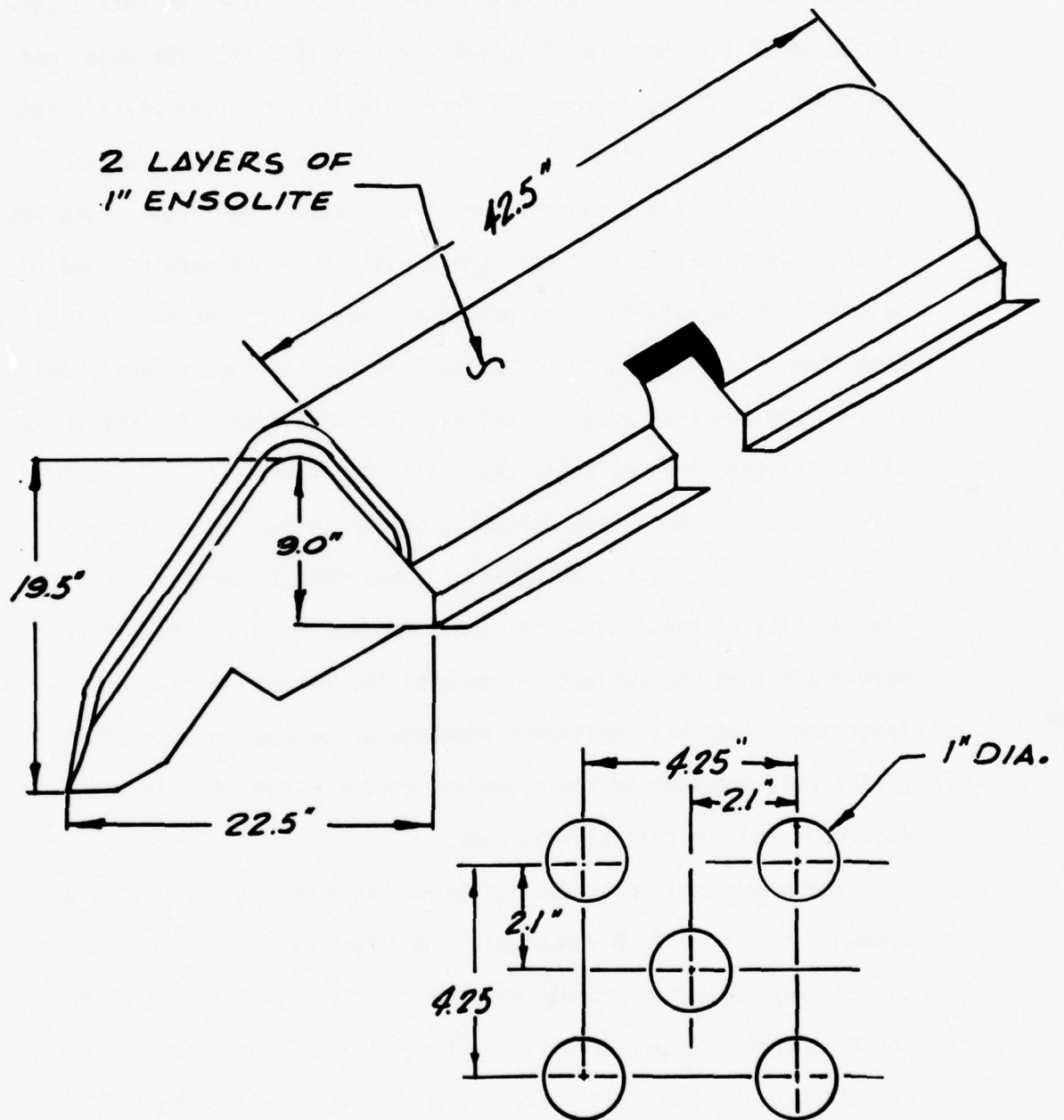


Figure 7. Photograph of the Body Buck

injuries in the event of such a double catastrophic failure. One inch diameter holes were drilled on staggered centers over the entire surface area of the sheet metal to enhance crushability. The sheet metal was covered with two layers of 1 inch polyvinyl chloride plastic foam conforming to MIL-F-81134A(AS) Grade 1. Figure 8 illustrates the instrument panel and provides dimensional data. The actual installation is shown in Figure 9; note that the plastic foam has been removed to reveal the hole pattern. The design did not provide as much energy absorbing capability as that reported for the instrument panel used in the previous test program (ref 9). The side panels and the front of the instrument panel below the crest were materially reduced in size to install the airbag restraint system in the space normally reserved for the glove compartment. These modifications reduced the crushability of the instrument panel, thereby reducing the safety margin afforded the subject. Even with the reduced safety margin, the instrument panel was considered adequate protection because of the reliability provided by the redundant protection of the air bag restraint and the restraint harness.

The bench seats provided for these tests were a production model commonly used in 1972 Oldsmobiles. Each seat was covered with a coated vinyl material and was mounted rigidly bolted to the floor of the test buck in the rear-most position allowed by the normal seat adjusters (which were not used). The seat was attached to the body buck by floor brackets to the test vehicle frame. The back of the bench seat was reinforced by a structural member which held the seat back upright and prevented forward flexure of the seat back at impact.



PANEL PERFERATIONS

Figure 8. Steel Instrument Panel Dimensions



Figure 9. Photograph of the Instrument Panel Installation

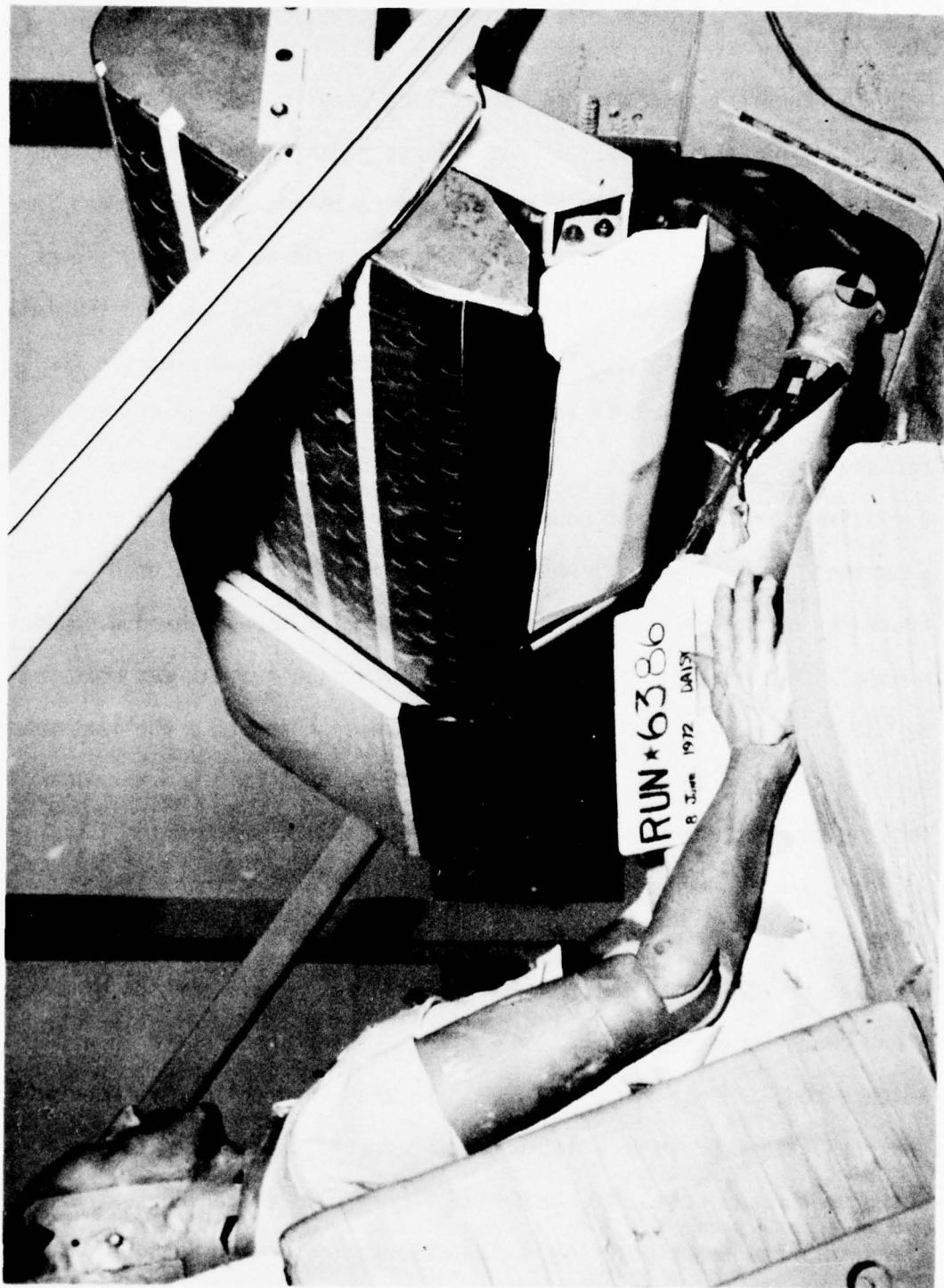


Figure 9. Photograph of the Instrument Panel Installation

This bracing member ran the full width of the seat back and was bolted to the body buck frame. The seat back brace is illustrated in Figure 10.

The headrest used was the same device used in the previous air bag restraint test series. It was a large pad of a polyurethane foam material covered with nylon material mounted immediately above and in line with the top of the seat back. Rigidly mounted to the body buck frame, it extended upward 18 inches from the seat back and ran the full width of the seat. Originally, the experimental plan called for the removal of the headrest if it was determined that the head did not rebound into the headrest. This plan was abandoned even though excessive rebound did not occur. The headrest was used for a more important function. The foam material of the headrest was used as a brake for a string measuring device to determine forward head displacement of the subject's head during impact since this event was obscured by the air bag. The position of the head with respect to the instrument panel-windshield during impact was considered critical in determining if testing could continue safely at the next velocity increment.

The floor board of the test buck was made of 3/4 inch plywood which ran the full width of the test vehicle. No attempt was made to simulate the drive shaft tunnel. The inclined forward portion of the floor board conformed to the angle formed by the floor board in a 1972 Buick B-body style automobile. Two, triaxial load cells were mounted under the floor board to measure bracing forces transmitted to the foot board by the subject's feet (refer to Figure 6). Since the seat was fixed in the aftmost position, wooden blocks (described in detail later

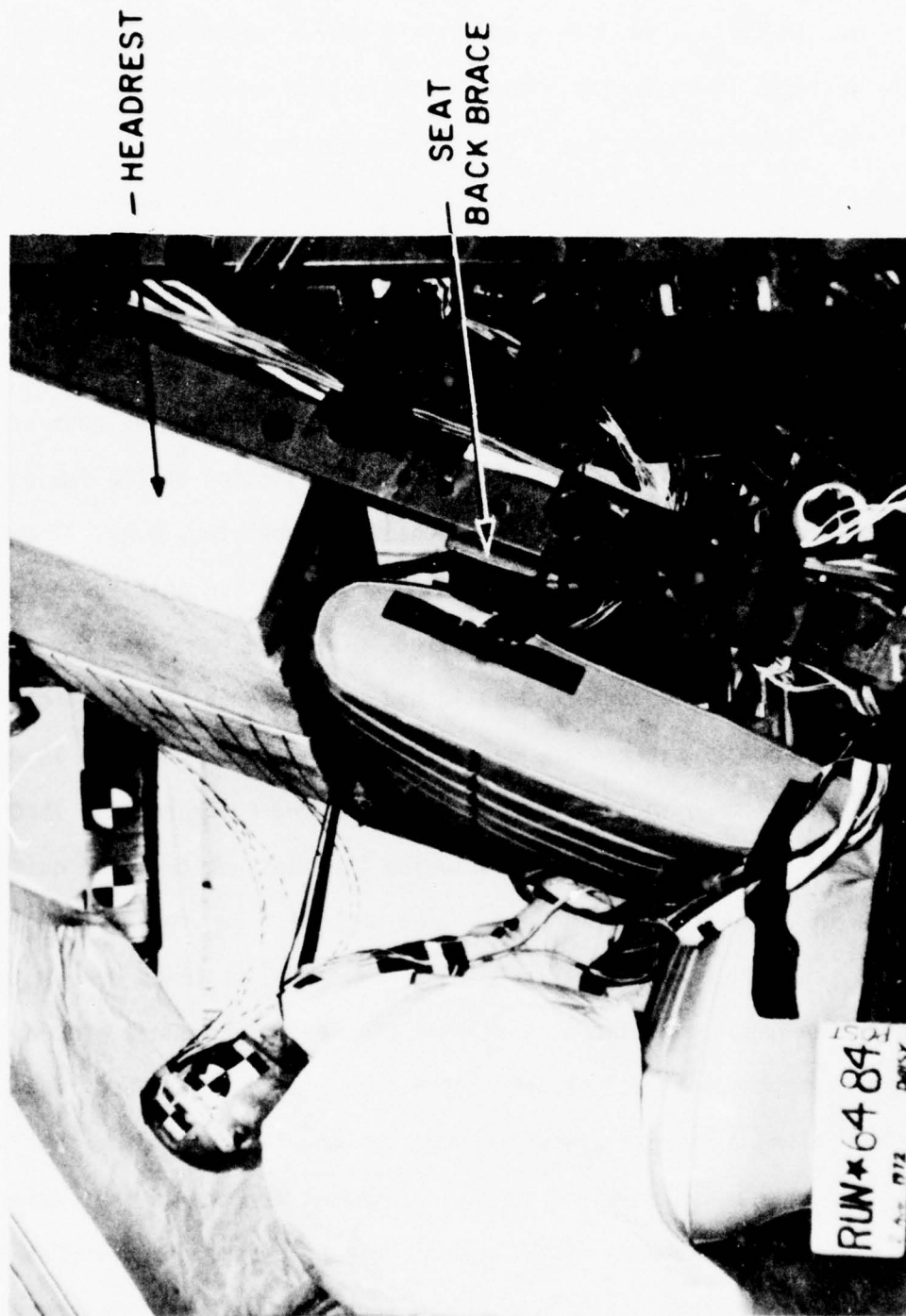


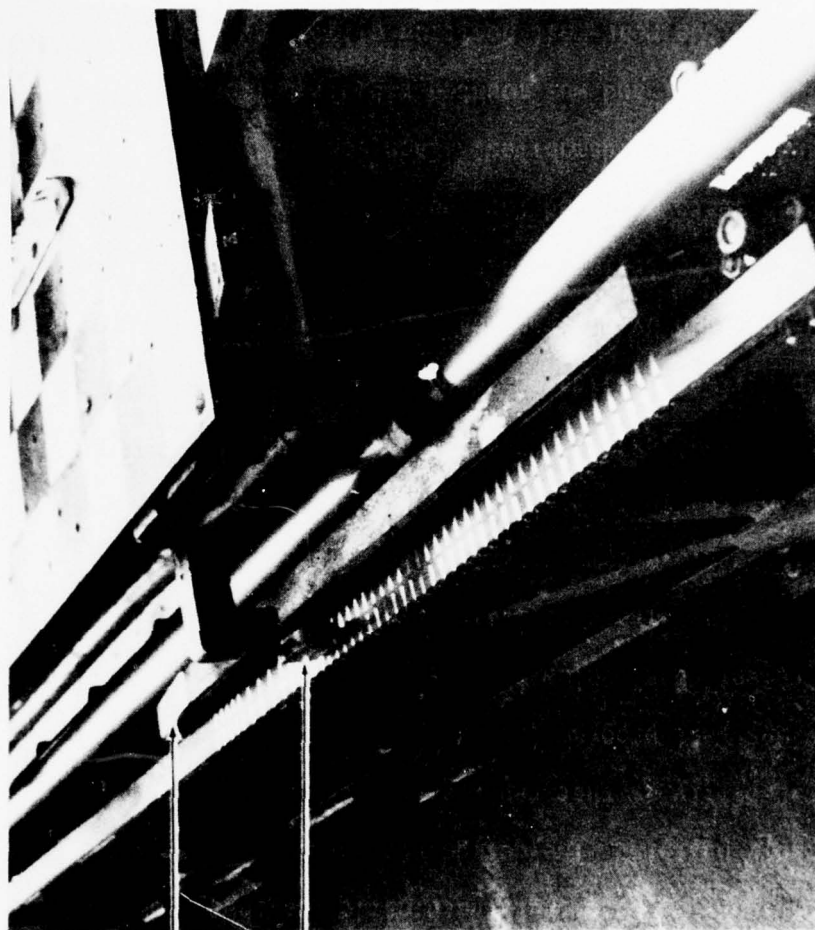
Figure 10. Seat Back Bracing and Headrest

in the text) were added to the load cells to assure that the subject's feet were in contact with them and that a normal thigh-leg popliteal angle would be formed. The load cells were also centered about the 15 inch line describing the right front passenger position. Each load cell measured the forces transmitted to the foot pan in three orthogonal axes corresponding to down, forward, and lateral forces.

A removable transparent panel that allowed access to the subject during the pretest preparations and continuous observation of the volunteer during the impact was used to roughly simulate the door of an automobile. The side panel also prevented ejection of the subject in the event of a partial failure of the test apparatus, e.g., if the air bag deployment was not completed and the explosive bolt fastening the torso harness to the test buck fired. The side panel was constructed from a sheet of polycarbonate plastic and was designed to slide into mounting brackets on the passenger's side of the test vehicle. It was secured in the mounting brackets by a bar and two quick release latches at the rear of the vehicle. Following the test, it could be quickly removed to allow immediate access to the subject. During the test series that was conducted with dummy subjects small metal brackets were attached to the side panel and used as part of a physical measurement procedure to assure that the dummy was seated in the same position for each test. Steel pointing rods were passed through the metal brackets and the dummy's position was adjusted so that alignment markers on the dummy were adjacent to the ends of the rods. This procedure assured that the dummy was in the same position prior to each test within an accuracy of $\pm 1/4$ inch.

The passive air bag restraint system (referred to herein as the air cushion restraint) evaluated in this series of tests for the Department of Transportation was a near-production model of a system proposed for manufacture in 1973. This second generation air bag restraint system was designed to protect front passengers in frontal accidents (± 30 degrees from head on) at speeds in excess of 11 mph. Consisting of four major subassemblies, this restraint system was developed for two operational modes. One mode was to be effective in accidents at speeds of 11 to 18 mph, while the other mode was to be effective for speeds above 18 mph. The four major subassemblies include the sensor assembly, the inflator assembly, the air bag assembly, and the cover assembly.

The sensor assembly, which initiates the operation of the restraint system in the automotive installation, was not used in this study. The function of this device was simulated by two sets of two electromechanical cam switches. Each set, mounted on opposite sides of the test buck was positioned to be operated by ramps mounted on the test track at specific time intervals during impact. One set of switches is shown in Figure 7 and the ramp can be seen in Figure 11. The time intervals for operating these switches were specified by Fisher Body to conform with actual sensor assembly activation times. The time intervals are given in Table IV. The forward switch in each switch set initiates the operation of the inflator assembly. When this switch is closed, two separate signals are generated. One signal explodes an electrically activated pyrotechnic initiator (a squib) which ruptures a 0.75 inch diameter diaphragm that seals the inflator bottle. The



SWITCH RAMP

PENETRATION AND
VELOCITY MEASUREMENT
DEVICE

Figure 11. Air Cushion Restraint Actuation Switch Actuation Ramp, Brake Penetration and Velocity Measuring Device

TABLE IV. INFLATOR INITIATION SWITCH ACTIVATION INTERVALS

SPEED (MPH)	FIRST SWITCH TIME (SECONDS)	SECOND SWITCH TIME (SECONDS)
10	N.T.	N.T.
11	0.0200	N.T.
12	0.0180	N.T.
13	0.0160	N.T.
14	0.0145	N.T.
15	0.0135	N.T.
16	0.0120	N.T.
17	0.0110	N.T.
18	0.0105	0.0600
19	0.0100	0.0560
20	0.0090	0.0525
21	0.0085	0.0485
22	0.0085	0.0450
23	0.0085	0.0415
24	0.0080	0.0385
25	0.0080	0.0355
26	0.0080	0.0330
27	0.0075	0.0315
28	0.0075	0.0295
29	0.0075	0.0280
30	0.0070	0.0270

N.T. = NO TRIGGER

other signal electrically initiates a pyrotechnic gas generator which heats and augments the volume of gas stored in the inflator bottle. Figure 12 shows the general configuration and indicates the positions of the pyrotechnic devices. The restraint initiation and safety interlock circuit is shown in Figure 13. This circuit also contains electrical networks used to activate the explosive nut anchoring the safety restraint harness, monitor the inflator activation, conduct system checks before the tests, and to arm the system during the final stages of the pretest countdown. Individual functions of this circuit are described elsewhere in this section of the report (see page 49). The safety interlock circuit was housed in the box shown in Figure 14. The box was mounted to the driver's side of the test buck and can be seen in Figure 7. The switches and the lights on the cover panel of the box were within the view of the motion picture cameras at the track side. The switch positions and the light emitted from each light lens could be monitored by the cameras.

The production version of the inflator uses argon gas pressurized at 2350 psig stored in the 100 cubic inch bottle. In the first mode of operation, that used when the impact velocity is within the range of 11 to 18 mph, the first gas generator (referred to as the lo-level pyro), containing 20 grams of propellant, is ignited to augment the stored gas. Above 18 mph, the automotive sensor assembly generates a second signal which initiates a 25 gram pyrotechnic gas generator (referred to as the hi-level pyro). This signal was generated by the rear switch of each initiation switch set. The operation of this second gas generator extends the pressure-time history of the gas to allow the air bag

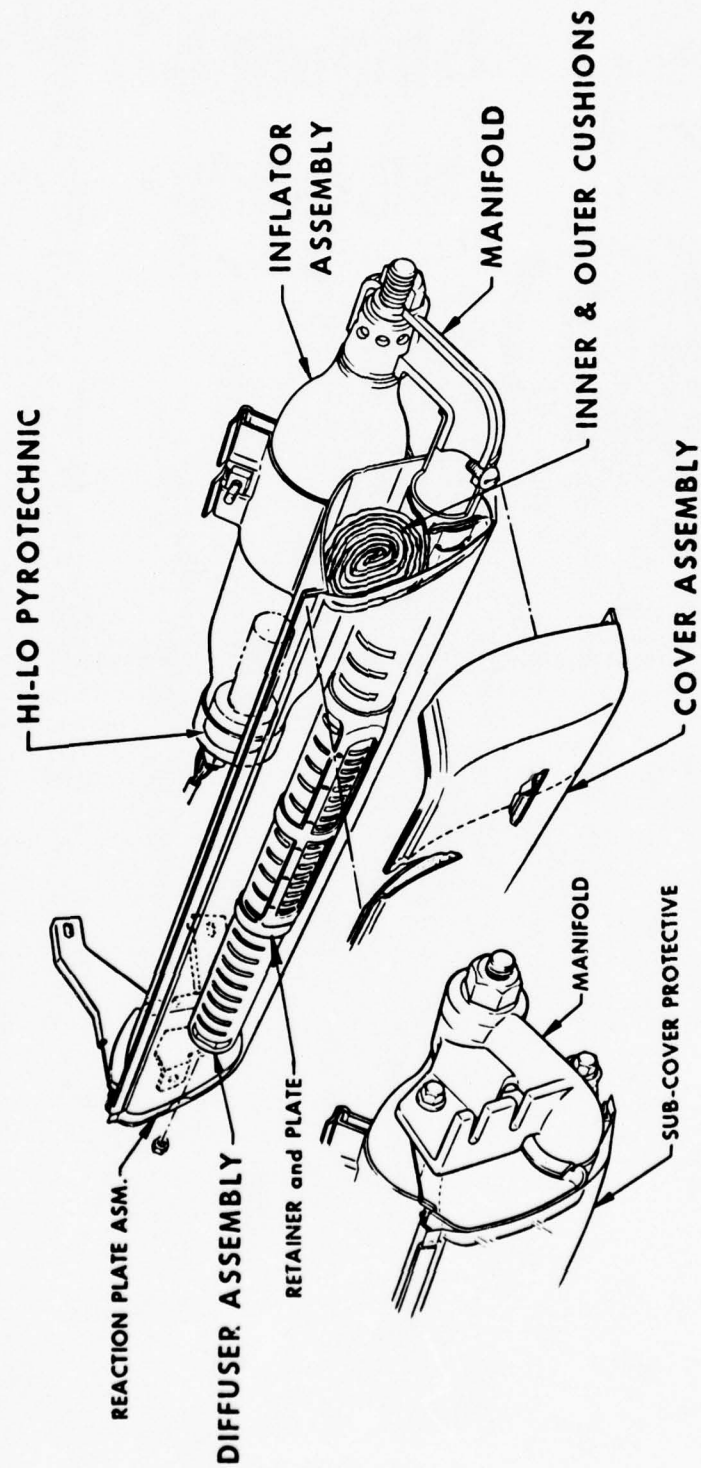


Figure 12. Air Cushion Inflator Assembly
(Illustration by GM)

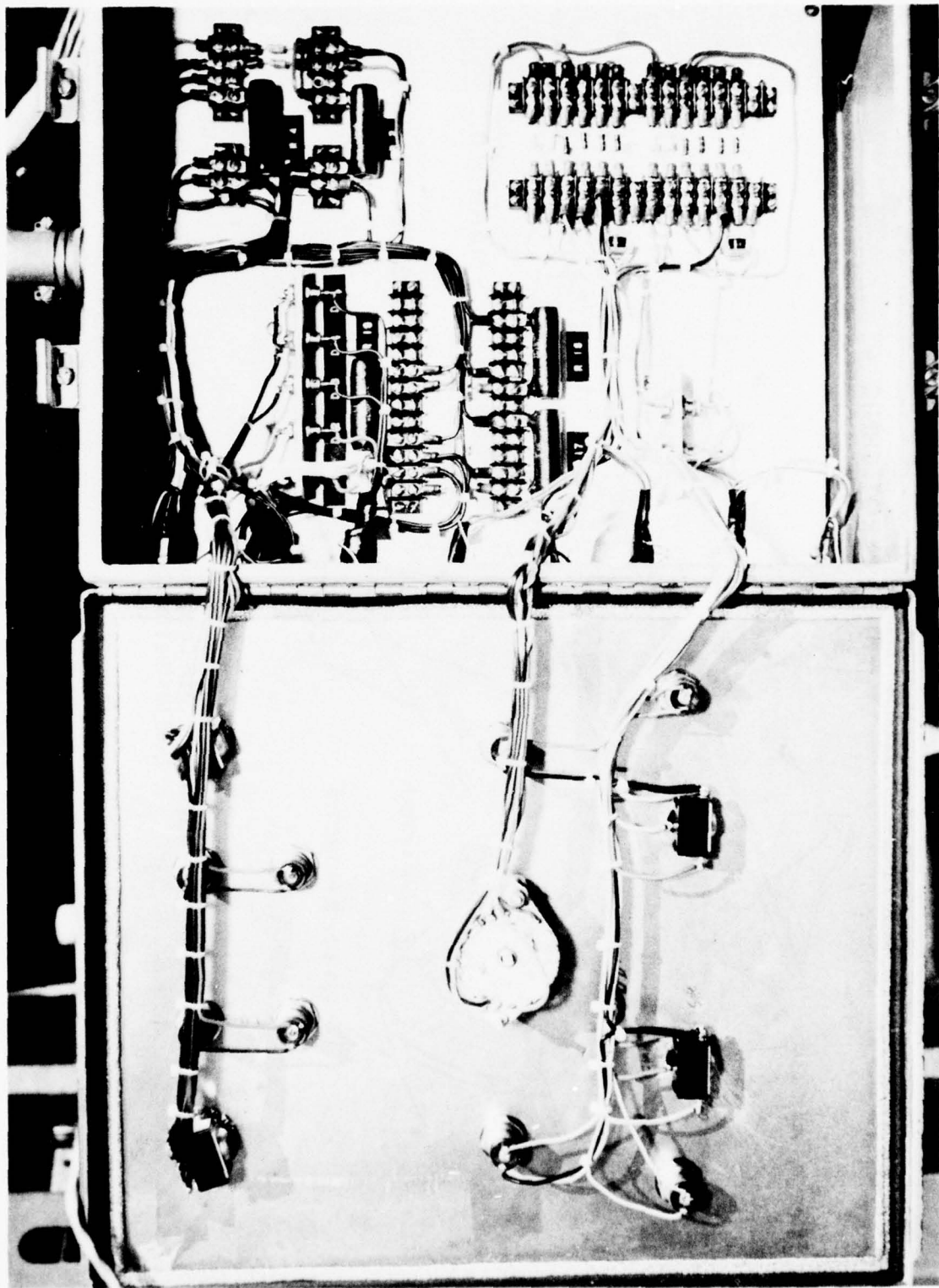


Figure 13. Air Cushion Restraint Initiation and Safety Interlock System Circuit

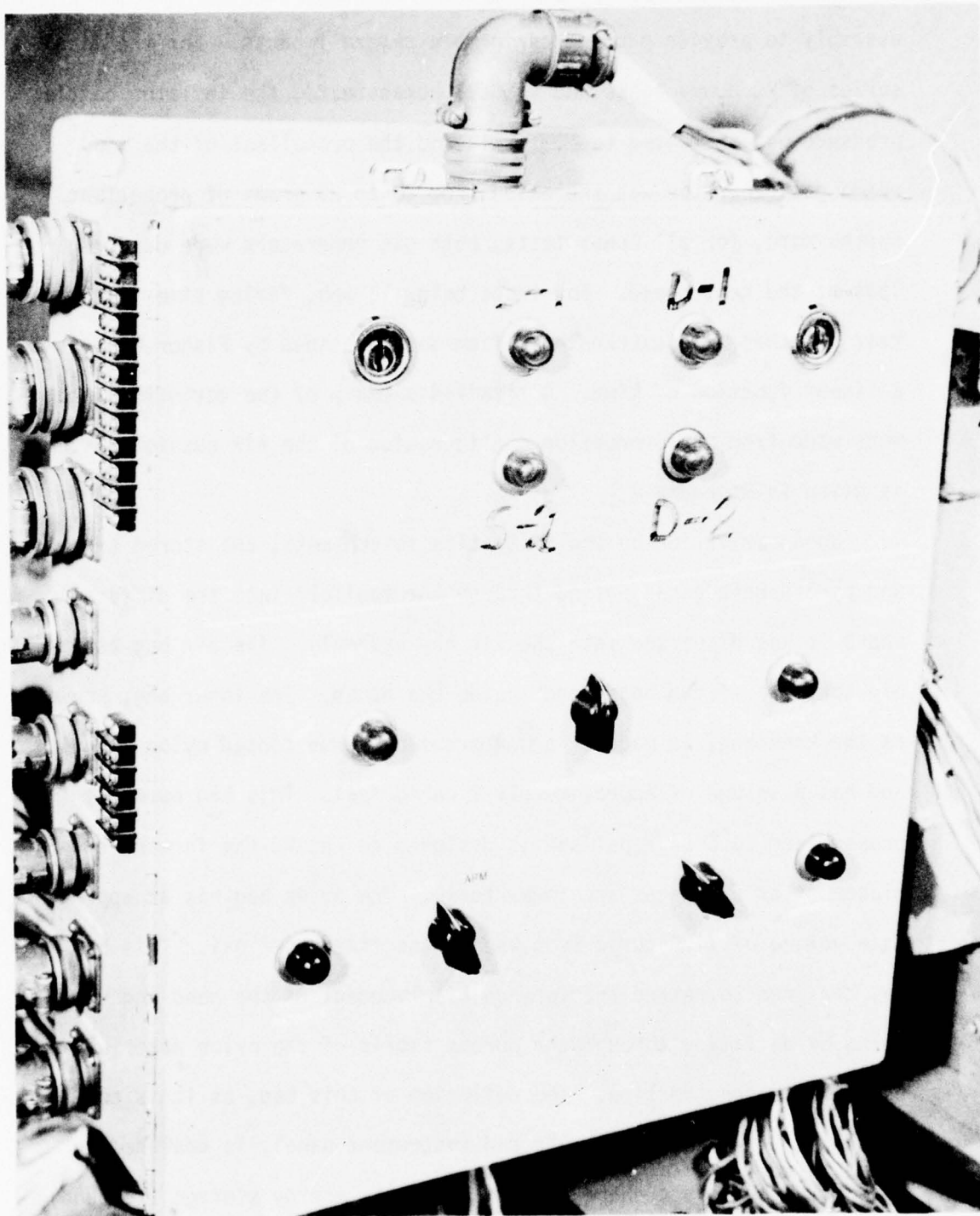


Figure 14. Indicator Light and Switch Panel of the
Restraint Initiation and Safety
Interlock System

assembly to provide protection in more severe impacts. For the final series of 20 dummy tests and for all human tests, the inflator bottle pressure was increased to 2700 psig and the propellant of the low speed gas generator was increased from 20 to 25 grams of propellant. Furthermore, for all human tests, both gas generators were used regardless of the test speed. For tests below 18 mph, firing times for the rear switches were extrapolated from data provided by Fisher Body as a linear function of time. A detailed summary of the deviations that were made from the production configuration of the air cushion system is given in Appendix A.

Upon activation by the initiation switch sets, the stored argon and pyrotechnic gases passed through the manifold into the diffuser where it was dispersed into the air bag assembly. The air bag assembly consists of two bags, one inside the other. The inner bag, known as the knee bag, is made of a nonporous neoprene coated nylon material and has a volume of approximately 2 cubic feet. This bag normally is pressurized to 6 or 7 psi and is designed to retard the forward displacement of the knees and lower torso. The outer bag has an approximate volume of 14.5 cubic feet when pressurized to 2 psi. This bag was designed to retard the forward displacement of the head and upper torso by deflating through the porous fabric of the nylon material used in its construction. The deflation of this bag, as it is compressed against the windshield and instrument panel, is designed to dissipate the impact energy and minimize the energy storage (rebound) characteristics of earlier prototypes.

The inner knee bag is bolted directly to the diffuser manifold

assembly. The outer torso bag slides over the diffuser manifold and knee bag assembly and is clamped to the manifold diffuser assembly at its elbow. The diffuser manifold assembly inlet is then attached to the inflator outlet with a clamp flange. The cover assembly is then clamped to the inflator diffuser manifold subassemblies, thus unifying the air bag assembly into a single system.

The air bag system assemblies were attached to the test buck by reaction plates mounted on the simulated firewall and the right main vertical forward pillar post of the test buck. Similar reaction plates are required to connect the system to the firewall and the A-pillar of an automobile. The upper portion of the air bag system is also bolted to the lower portion of the instrument panel simulation to complete the installation of the air cushion restraint.

The cover assembly of the air cushion restraint system is the device that protects the restraint prior to use. It is attached to the bottom of the instrument panel and the bottom of the inflator assembly. Constructed of a steel-reinforced, formed polyurethane foam material, it provides a decor compatible with the automotive interior. The cover assembly is covered with an ABS plastic material and scored around the edge of the air bag assembly. During the deployment process the cover assembly tears open along scored lines to allow the air bags to be deployed and positioned between the subject and the instrument panel and windshield. Figure 15 illustrates the air cushion restraint system in use during this study.

To simulate exposure to the deployment of the air cushion restraints as realistically as possible, the subjects were restrained only by the

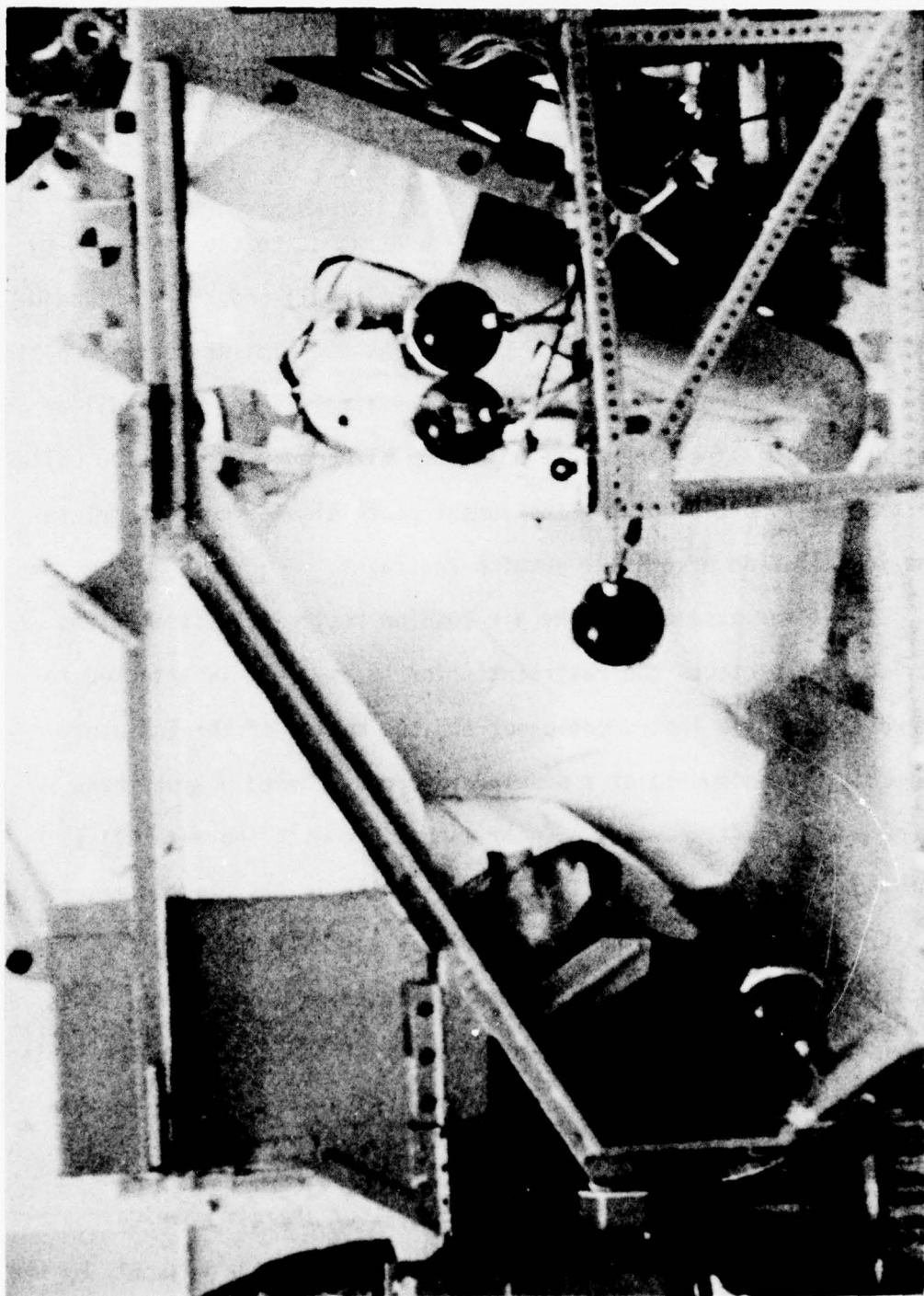


Figure 15. Air Cushion Restraint System During Impact

air cushion during impact. To achieve this objective and provide maximum safety for the subject, a secondary restraint harness with a single point explosive release system was designed, as illustrated in Figure 16. The harness was designed to act as backup restraint, should the air bag fail. The harness was connected to the explosive bolt. The explosive bolt was fired if three wires wrapped around the folded air bags were broken and an inflation detection wire within the pyrotechnic inflator assembly was severed by the firing of the inflators. The actuation circuitry is shown in Figure 17. Following the release of the secondary safety harness, the subject was then restrained only by the air cushion during impact.

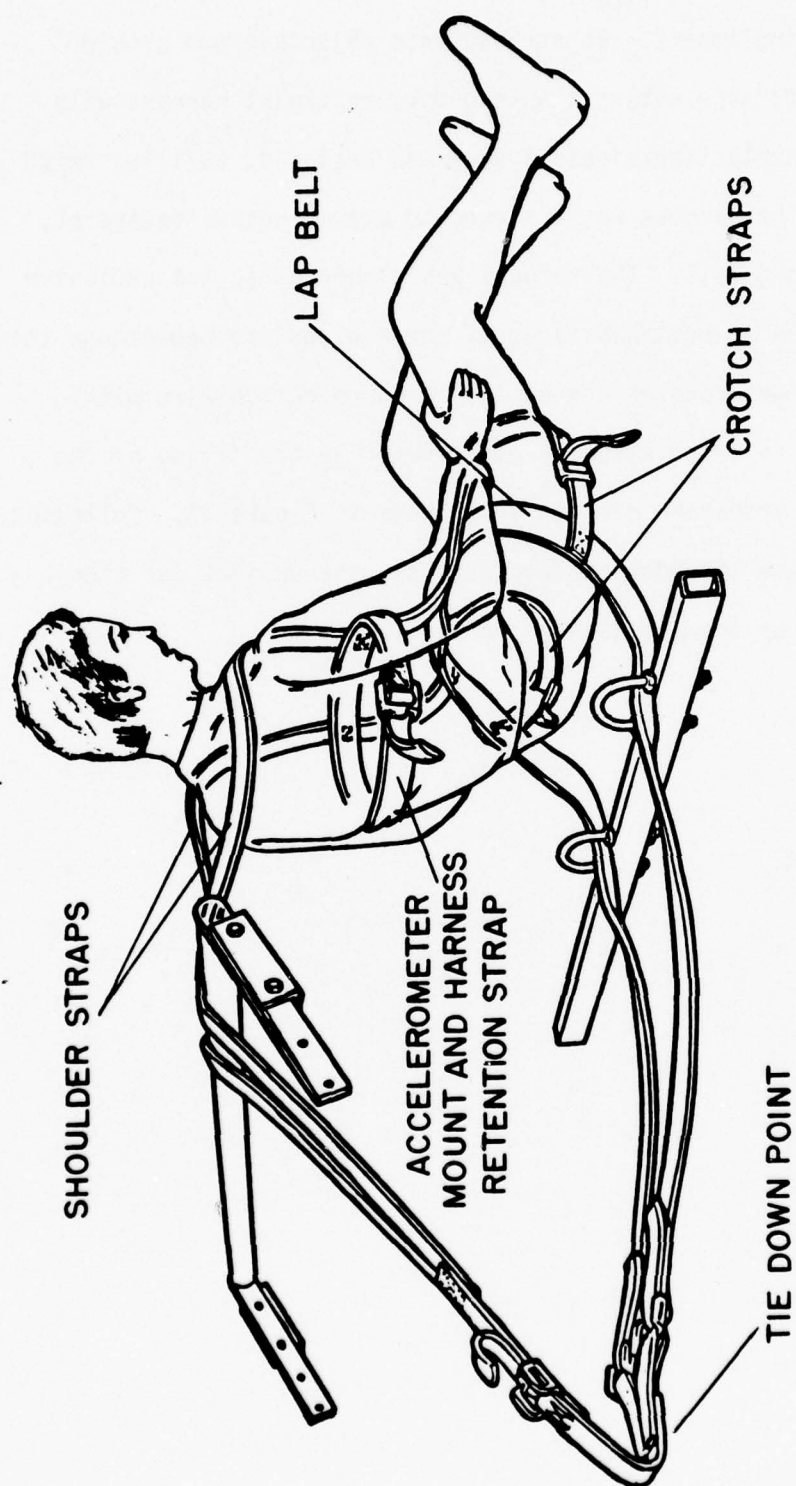


Figure 16. Secondary Safety Restraint Harness (Illustration by GM)

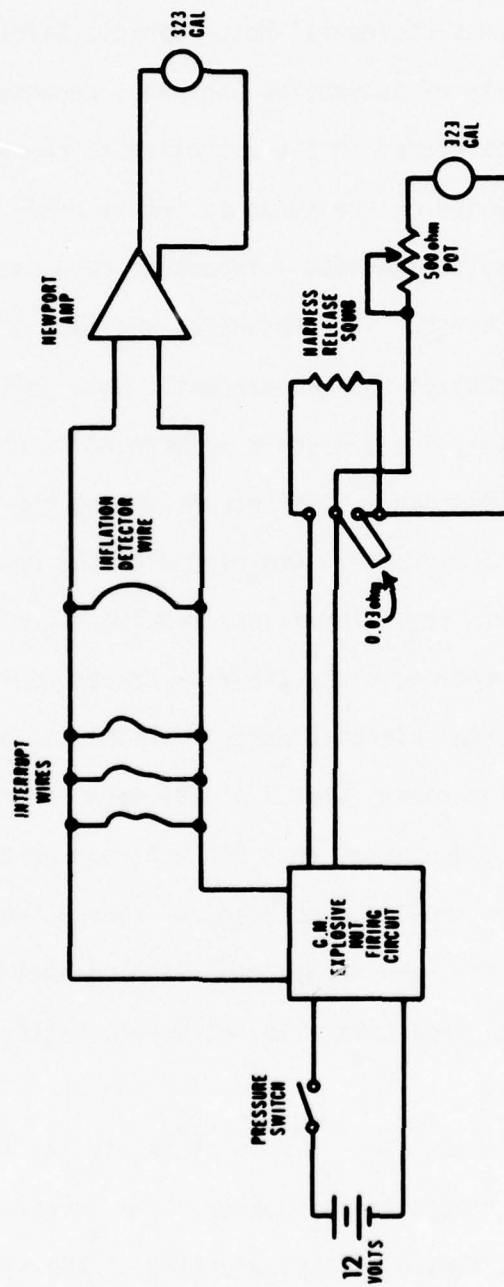


Figure 17. Secondary Safety Harness Actuation Circuitry

C. Instrumentation

The instrumentation system that was developed for this test program met the requirements of Federal Motor Vehicle Safety Standard No. 208 (ref 12) and Society of Automotive Engineers recommended practice (ref 14) in all aspects except in the selection of channel class for the accelerometers mounted on the human subject's head. The accelerometers that were selected provided a frequency response that was flat within $\pm 1/2$ dB to 800 Hertz. This deviation was made in the interest of improving the accuracy of the measurement. Data collected with dummy subjects completely met the above referenced documents.

An electrostatic discharge¹ that occurs during the air bag deployment saturated the amplifiers that are used with the Daisy Decelerator instrumentation system. These amplifiers require 150 milliseconds to recover following saturation; thus, the data traces would be unusable during this period. Data collected during earlier air bag test programs accomplished by this laboratory (ref 8 and 9) were recorded on photo oscillographs using galvanometers that did not require amplifiers. FM magnetic tape recorders could not be used, of course, due to the need for signal amplification. New signal conditioning amplifiers, purchased for use at an Air Force impact facility at Wright-Patterson Air Force

¹Photographs taken during a night firing of an air bag system identified the anomaly as an electrostatic phenomenon. The investigators theorize that the phenomenon is caused by the unfurling of the nylon bag material in a dry climate and/or charged ions developed within the gas flow from the inflator.

Base, were temporarily installed into the data collection system of the Daisy Decelerator for this test program. The new amplifiers that were installed have a recovery time of 75 microseconds. They did not entirely eliminate the spurious signals generated by the static discharges; however, the data traces that were produced were readable during the impact sequence. Use of these amplifiers permitted the use of FM magnetic tape recorders to satisfy the requirement for high frequency channels.

The sled velocity immediately prior to impact was determined by timing the interval required for the sled to travel one foot. This is accomplished by a contact bar mounted on the test sled which triggers two open contacts mounted on a plate attached to the side of the track immediately in front of the water brake. This device is shown in Figure 11. The open contacts on the plate are positioned exactly to correspond to the location of the leading edge of the sled probe. The first contact was positioned to locate the leading edge of the sled probe one foot from the brake entrance. The second contact positioned the sled probe at the entrance to the water brake. When the contact bar closes the first open contact, a voltage is applied to a circuit which starts two digital electronic counters, Hewlett-Packard Model 5233C. Similarly, when the contact bar closes the second open contact, the voltage applied to the circuit stops the counter. This recorded time interval is converted to velocity by a 1/T converter, Dynallectron Model 2701-801, and presented digitally after each test. This method is capable of measuring the sled velocity within ± 0.5 ft/sec.

The contact bar and plate mechanism is also used to measure the penetration of the probe into the water brake and trigger a photometric timing reference strobe light. Additional open contacts are positioned on the ramp which corresponds to station locations (stopping distance) within the water brake. The applied circuit voltage resulting from the contact bar closing these open contacts is recorded as a voltage change on magnetic tape or recording oscillographs. This recorded voltage change is used to relate penetration with time. Thus, one can determine stopping distance as well as the instantaneous velocity or velocity changes as a function of time.

All other information from this test series is transmitted from the sled through a 130 foot shielded cable to amplifiers and recording equipment in the instrumentation blockhouse. Figure 18 illustrates a typical single transducer wiring diagram used in this data collection system. Data channels were calibrated just prior to each test using a resistive shunt technique. During the test, transducers were excited and their outputs balanced and amplified with high impedance amplifiers. Filters that were used exceeded the frequency response class requirements. The conditioned signals were then recorded on magnetic tape for storage prior to data reduction. Three tape recorders, Ampex CP100, Ampex FR600, and a Honeywell 7600 were used. These recorders operated at 60 inches per second and were numbered Tape 1, 2, and 3 respectively. Recordings were made from 5 seconds prefire to 10 seconds post impact.

Three high speed recording oscillographs, Consolidated Electrodynamics Corporation Model 5-119, numbered CEC 1, 2, and 3, were operated in conjunction with each tape recorder for quick-look data

BEST AVAILABLE COPY

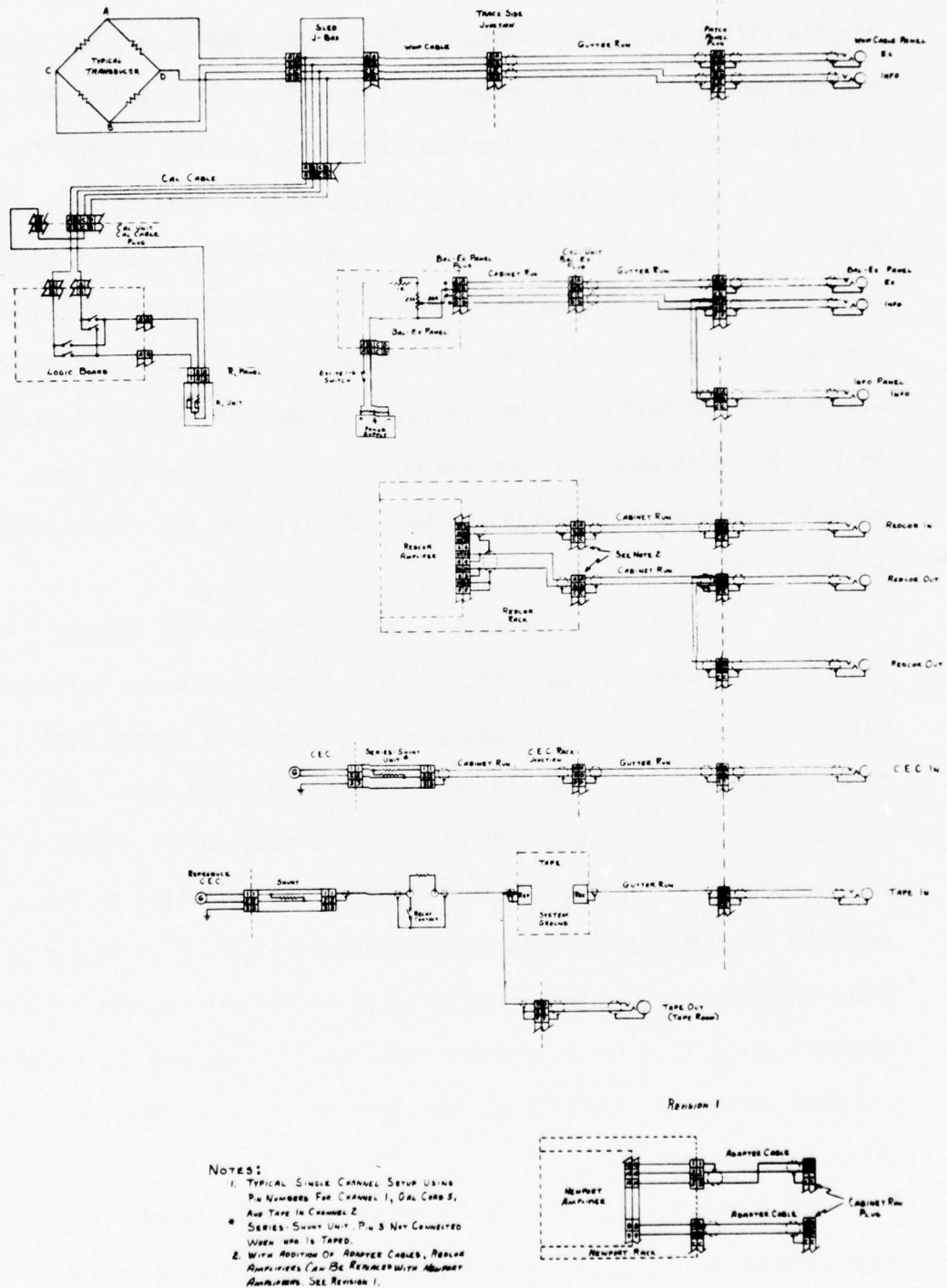


Figure 18. Typical Single Transducer Wiring Diagram

and data that was directly comparable with earlier air bag tests. These oscillographs were operated at 6.3 inches per second for calibration and 63 inches per second for the test. Tables V, VI, and VII list each transducer used, shunt calibrations, and the natural frequencies of the galvanometers for each tape recorder - oscillograph combination. The external damping resistance of the galvanometers of the oscillographs was 120 ohms to provide a damping coefficient of 0.64. For the data collected by the oscillographs, the galvanometer, which was flat to 125 Hertz, was the limiting factor in frequency response. An IRIG B timing code was recorded on all oscillographs and tape recorders to provide simultaneous identification of all events with respect to time.

For all tests seven parameters associated with the operation of the air bag system were monitored. These parameters were: inflator bottle pressure, pyrotechnic gas generator pressure, system firing times, bag deployment time and safety harness release time. The pressure measurements were made with two CEC transducers, Model 4-326. The transducer for inflator bottle pressure was installed on the high pressure hose of the 100 cubic inch inflator bottle. The second pyrotechnic gas generator chamber to be fired in the air cushion inflation sequence was ported for a pressure transducer to measure the pressure produced during its operation. This transducer was mounted on a high pressure hose from this port.

The system firing times for initiation of the air bag inflation, bag deployment time and safety harness release time were measured by circuits fabricated by the Fisher Body Division of the General Motors

TABLE V. CHART OF FREQUENCY RESPONSES

CEC #1 and TAPE #1**

INFORMATION	TRANSDUCER TYPE	GAL (units/in)	TRANSDUCER NATURAL FREQ. (Hertz)	AMP BANDWIDTH (Hertz)	GAL TYPE	GAL* RESPONSE (Hertz)	COMMENTS
Sled X-1	Statham A-6	10 g 20 g	300	100	7-338	0-125	Mounted on plate behind probe
#Bag Interrupt	Current Monitor				7-323	0-600	Monitor points furnished by G. M.
#Harness Release Current I	Current Monitor	20 amps***			7-323	0-600	Voltage drop across .03 ohm resistor monitored as current by galvanometer circuit
#Harness Release Current II	Current Monitor	20 amps***			7-323	0-600	Voltage drop across .03 ohm resistor monitored as current by galvanometer circuit
Shoulder	3" Strain Gage Buckle	1,000 lbs		1K	7-338	0-125	Mounted on subject shoulder strap****
Left Lap	3" Strain Gage Buckle	1,000 lbs		1K	7-338	0-125	Mounted on subject left lap strap****
Right Lap	3" Strain Gage Buckle	1,000 lbs		1K	7-338	0-125	Mounted on subject right lap strap****
Left Foot Down	NBS Foot Load Cell	500 lbs		1K	7-338	0-125	Integral part of foot load cell mounted in floor board of body buck****
Right Foot Down	NBS Foot Load Cell	500 lbs		1K	7-338	0-125	Integral part of foot load cell mounted in floor board of body buck****
Left Foot Forward	AF Strain Gage Beam	250 lbs		1K	7-338	0-125	Integral part of foot load cell****
Right Foot Forward	AF Strain Gage Beam	250 lbs		1K	7-338	0-125	Integral part of foot load cell****
Left Foot Lateral	AF Strain Gage Beam	50 lbs		1K	7-338	0-125	Integral part of foot load cell****
Right Foot Lateral	AF Strain Gage Beam	50 lbs		1K	7-338	0-125	Integral part of foot load cell****
Upper Head Displacement	Photo Interrupter Module	5 pulses			7-326	0-3000	Mounted above and flush with head rest****
Lower Head Displacement	Photo Interrupter Module	5 pulses			7-326	0-3000	Mounted behind seat approximately level with top of seat****

Not on Tape

* Stated from Galvanometer Specifications by C.E.C.

** Tape Response specified by Manufacturer - 20 KC

*** Calibrated by Voltage Sub.

**** Human runs only

TABLE VI. CHART OF FREQUENCY RESPONSES

CEC #2 and TAPE #2**

INFORMATION	TRANSDUCER TYPE	GAL (units/in)	TRANSDUCER NATURAL FREQ. (Hertz)	AMP BANDWIDTH (Hertz)	GAL TYPE	GAL* RESPONSE (Hertz)	COMMENTS
Sled X-2	Endevco 2264-150	10 g	3,400	1,000	7-338	0-125	Mounted on plate behind probe
#Detonator	Current Monitor	20 g					
		2 amps***			7-326	0-3000	Monitor points furnished by G. M.
#Low Squib I	Current Monitor	2 amps***			7-326	0-3000	Monitor points furnished by G. M.
#Low Squib II	Current Monitor	2 amps***			7-326	0-3000	Monitor points furnished by G. M.
#High Squib I	Current Monitor	2 amps***			7-326	0-3000	Monitor points furnished by G. M.
#High Squib II	Current Monitor	2 amps***			7-326	0-3000	Monitor points furnished by G. M.
#Bottle Pressure	CEC 4-326	2000 psi	10,000	1,000	7-338	0-125	Installed on high pressure hose at bottle
#High Pyro Pressure	CEC 4-326	4000 psi	10,000	1,000	7-338	0-125	Installed on high pressure hose at bottle
External Head X	Endevco 2264-150	50 g	3,400	3,000	7-338	0-125	Mounted on head strap in back of head
External Head Y	Endevco 2264-150	50 g	3,400	3,000	7-338	0-125	Mounted on head strap in back of head
External Head Z	Endevco 2264-150	50 g	3,400	3,000	7-338	0-125	Mounted on head strap in back of head
External Chest X	Endevco 2264-150	50 g	3,400	3,000	7-338	0-125	Mounted on harness in front of sub.
External Chest Y	Endevco 2264-150	50 g	3,400	3,000	7-338	0-125	Mounted on harness in front of sub.
External Chest Z	Endevco 2264-150	50 g	3,400	3,000	7-338	0-125	Mounted on harness in front of sub.
Mouthpiece X	Endevco 2264-150	50 g	3,400	3,000	7-338	0-125	Mounted in subjects mouthpiece
Mouthpiece Y	Endevco 2264-150	50 g	3,400	3,000	7-338	0-125	Mounted in subjects mouthpiece
Mouthpiece Z	Endevco 2264-150	50 g	3,400	3,000	7-338	0-125	Mounted in subjects mouthpiece

Not on Tape

* Stated from Galvanometer Specifications by C.E.C.

** Tape Response specified by Manufacturer - 10 KC

*** Calibrated by Voltage Sub.

TABLE VII. CHART OF FREQUENCY RESPONSES

CEC #3 and TAPE #3**
(Run on Dummy Runs only)

INFORMATION	TRANSDUCER TYPE	CAL (units/in)	TRANSDUCER NATURAL FREQ. (Hertz)	AMP BANDWIDTH (Hertz)	CAL TYPE	GAL* RESPONSE (Hertz)	COMMENTS
Sled X-3	Endevco 2264-150	10 g 20 g	3,400	1,000	7-338	0-125	Mounted on plate behind probe of sled
Internal Head X	Endevco 2260C	50 g	14,000	3,000	7-338	0-125	Mounted on block on rear head plate
Internal Head Y	Endevco 2260C	50 g	14,000	3,000	7-338	0-125	Mounted on block on rear head plate
Internal Head Z	Endevco 2260C	50 g	14,000	3,000	7-338	0-125	Mounted on block on rear head plate
Internal Chest X	Endevco 2260C	50 g	14,000	3,000	7-338	0-125	Mounted on block on anterior side of spine
Internal Chest Y	Endevco 2260C	50 g	14,000	3,000	7-338	0-125	Mounted on block on anterior side of spine
Internal Chest Z	Endevco 2260C	50 g	14,000	3,000	7-338	0-125	Mounted on block on anterior side of spine
Internal Left Femur	G. M.	1,000 lbs		3,000	7-338	0-125	Mounted as a dummy modification between the knee joint and thigh box, primarily sensitive to compression
Internal Right Femur	G. M.	1,000 lbs		3,000	7-338	0-125	Mounted as a dummy modification between the knee joint and thigh box, primarily sensitive to compression

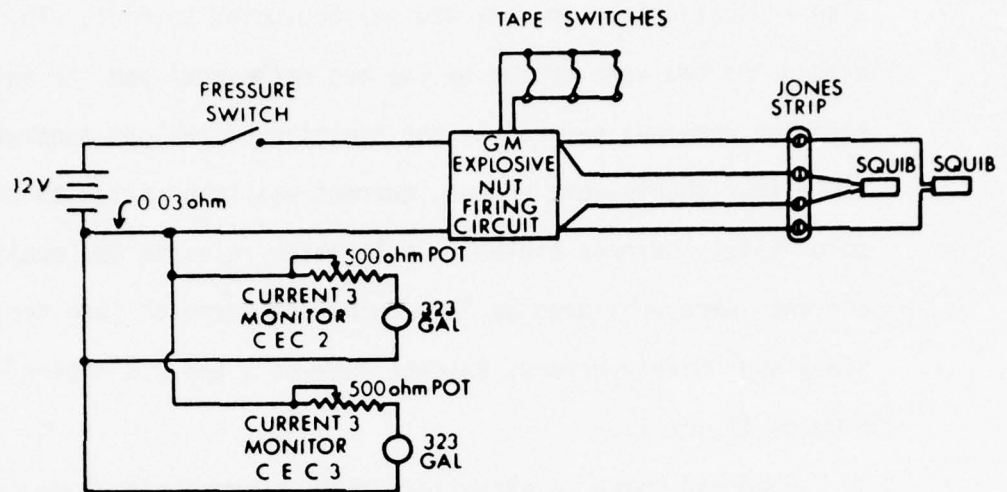
* Stated from Galvanometer Specification by C.E.C.

** Tape Response specified by Manufacturer - 10 KC

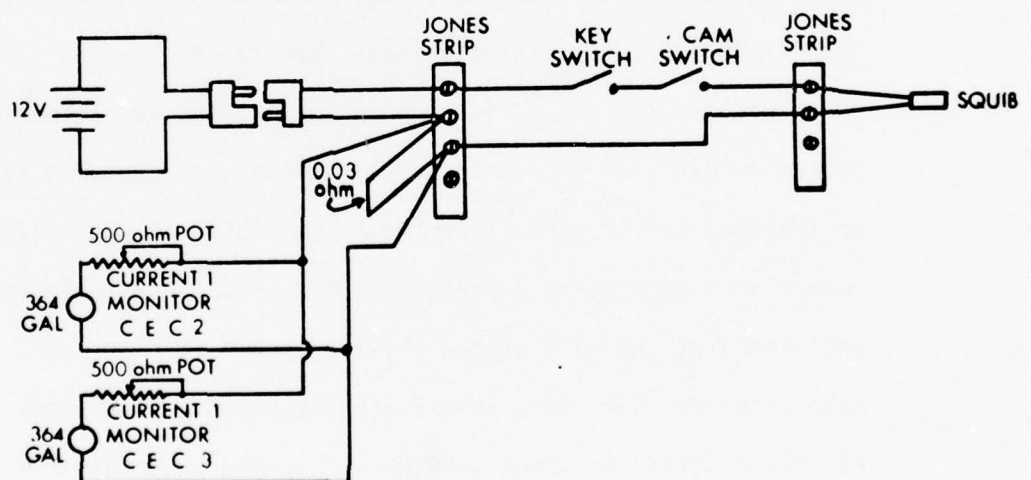
Corporation. These circuits were contained in the restraint initiation and safety interlock control box, shown in Figures 13 and 14. Figures 17 and 19 illustrate typical circuits used to actuate system components and measure component firing times. The voltage changes in these circuits signaled the time at which the current was transmitted to the various electrically activated pyrotechnic initiators used to inflate the air bag system and release the secondary safety harness. Just prior to testing, the key switches were placed in the "armed" position leaving only the cam switches open in the circuit. The cam switches were operated by two ramps attached to the test track. The ramps were positioned to trigger the cam switches during the impact sequence (see pages 37 and 49).

Four electromechanical cam switches were used to initiate the air cushion system. Two switches were mounted on both the driver's and passenger's sides of the test vehicle, thereby providing redundant circuit systems to assure reliability of operation of the air cushion system. The two most forward cam switches provided current to the inflator bottle detonator and the first pyrotechnic gas generator to be actuated in the inflation sequence. These were monitored as "Detonator Current" and "Lo Pyro Currents 1 and 2." The two rear switches provided current to the second pyrotechnic gas generator to be actuated and were monitored as "Hi Pyro Current 1 and 2."

The bag deployment time was measured by monitoring the detonator circuit signal that released the backup safety harness. The interruption of three shunt wires around the folded air bag and the inflation detector wire in the lo-level pyrotechnic gas generator



Harness Release System, and Current 3 Monitor



Bottle Squib Firing Circuit Showing Current 1 Monitor Circuit
Current 2 Monitor Identical to Current 1 Monitor

Figure 19. Typical Detonator and Squib Current Monitor

initiated the circuit to release the safety restraint harness. It also indicated that the air bag was beginning to fill. The wire shunts around the bag were broken by the bag deployment and the inflation detector wire was severed by the ignition of the gas generator. When these four shunts were broken, current was transmitted to the single point safety harness explosive bolt which released the subject. These currents were monitored as "Bag Interrupt Current" (bag deployment time) and "Safety Harness Release Current 1 and 2." Refer back to Figures 17 and 19.

Head and chest accelerations were measured with Endevco Model 2264 piezoresistive accelerometers with a range of 0-150 g. Shunt calibrations were 50 g per inch. The accelerometers were oriented triaxially for both head and chest measurements. The chest accelerometers were attached to a metal plate which was mounted on a chest strap that was part of the torso restraint harness shown in Figure 16. This chest strap was tightly fitted to each subject so the accelerometer package rested on his sternum. Head accelerations were measured externally on the head and internally in the mouth. The external head accelerometers were mounted on a plate attached to an adjustable webbing and positioned at the base of the skull as shown in Figure 20. The external head accelerometers were then further secured by a harness constructed of Velcro straps as shown in Figure 21. The internal accelerometers were mounted on a plate covered with silicone rubber sealant and mounted in the subject's mouthpiece. This technique has been previously described in reference 9. Measurements in the X, Y, and Z axes were obtained from these nine transducers.

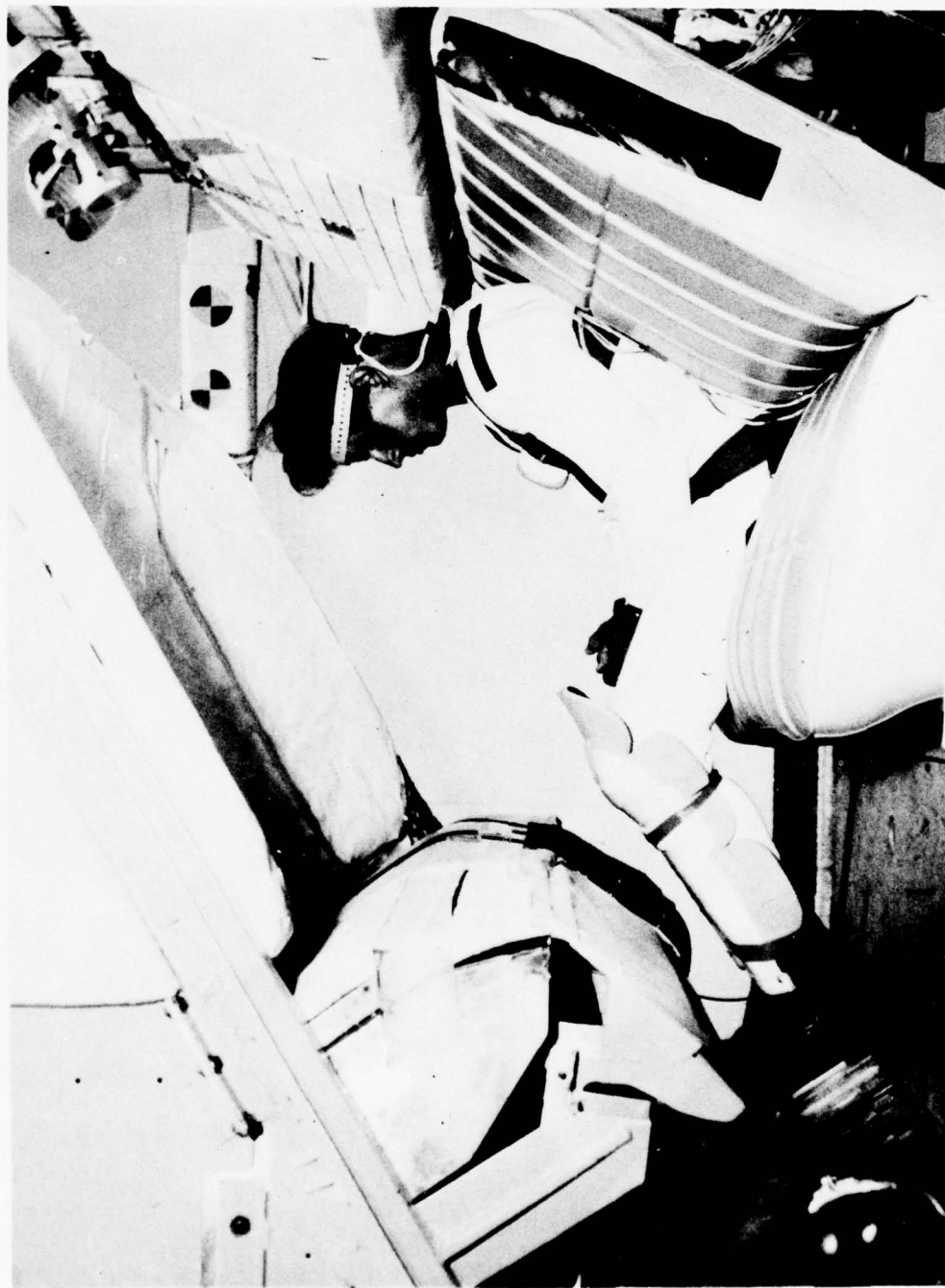


Figure 20. Side View of Test Subject Showing Chest and Head Accelerometers



Figure 21. Side View of Test Subject Showing Mouthpiece Accelerometer and Velcro Harness

In three tests, run numbers 6556, 6557, and 6559, the internal head acceleration package was replaced with an accelerometer package constructed by the Department of Transportation, Transportation Systems Center. This device used four Endevco Model 2264 accelerometers. Three were oriented triaxially for conventional linear acceleration measurements. The fourth accelerometer was mounted parallel to and a known distance from the Z-axis accelerometer of the triaxial group. The two Z-axis acceleration measurements were used to determine the rotational acceleration of the subject's head (ref 15 and 16). This device was covered with silicone rubber sealant and mounted within the subject's mouthpiece. Calibrations used for this device were 20 g per inch. Measurements recorded from this device are reported and discussed in reference 16. The specifications for the device are provided within Appendix B.

Shoulder harness and lap belt loads were measured prior to the safety harness release. The measurements were made using strain gauged buckles fabricated by Land-Air. These devices have a range of 0-4000 pounds. They were mounted on the shoulder harness yoke and on each side of the lap belt. Shunt calibrations were for 1000 pounds per inch. (The results of these measurements are not reported since they were negligible.)

The forces reacted through the subject's legs and feet during impact were measured by two foot load cells mounted below the inclined portion of the floor of the test vehicle. These devices were mounted so that the surface of foot contact was flush with the floor and centered about the 15 inch line which describes the right front passenger's

position. The load cells measured forces in three orthogonal axes; down, forward, and laterally for each foot. Refer to Figures 6 and 20. Shunt calibrations were 500 pounds down, 250 pounds forward, and 50 pounds laterally. After the initial human test, the medical investigator required that plywood blocks be attached to the foot load cells if necessary so that the subject's feet would be in contact with the load cells prior to impact (refer to Figure 20). This procedure was developed because the first subject's feet did not contact the inclined portion of the floor prior to impact and he complained of ankle pain following testing. Motion picture films indicated that his feet struck the floor during impact. These blocks provided each subject an optimal knee angle of approximately 132 degrees prior to testing, regardless of their leg length. Table VIII lists numbers of 3/4 inch plywood blocks used by each subject.

TABLE VIII

FOOT LOAD CELL BLOCKS USED BY EACH SUBJECT

SUBJECT	A	B	C	D	E	F	G	H	I	J	K	L	M
NO. BLOCKS	0	0	3	0	1	0	3	3	5	5	5	4	0

For dummy testing, eight channels of additional information were collected. The data included internal head and chest accelerations in the X, Y, and Z axes as well as right and left femur loads. Endevco 2260C accelerometers with a range of 0-250 g were used for acceleration measurements. These accelerometers, oriented triaxially, were mounted to mounting blocks on the head plate and the anterior spine of the dummy. Shunt calibrations were 50 g per inch. The internal mouth accelerometer for human testing was also mounted to the head plate mounting block for these tests to operationally check these transducers (good correlation was demonstrated). Externally mounted head accelerometers were attached to the head by straps, as shown in Figures 21 and 22, to compare the accelerations measured in this manner with those measured within the head. The transducers for femur load measurements, fabricated by General Motors Corporation, were mounted between the knee joint and the thigh box of the dummy. These transducers were designed to measure compression loads and had a range of 0-3000 pounds. Shunt calibrations were for 1000 pounds per inch.

Several methods were used in attempts to measure the position of the dummy's head with respect to the positions of the windshield and instrument panel during impact. The first method involved the use of four fiberglass cords attached to the dummy's head. Two cords were attached to a point on each side of the dummy's head; one cord on each side passed through the upper portion of the headrest while the other cord on each side passed through the midsection of the headrest. The plastic foam material of the headrest acted as a friction brake to stop the cord at the point of its maximum extension. This method was

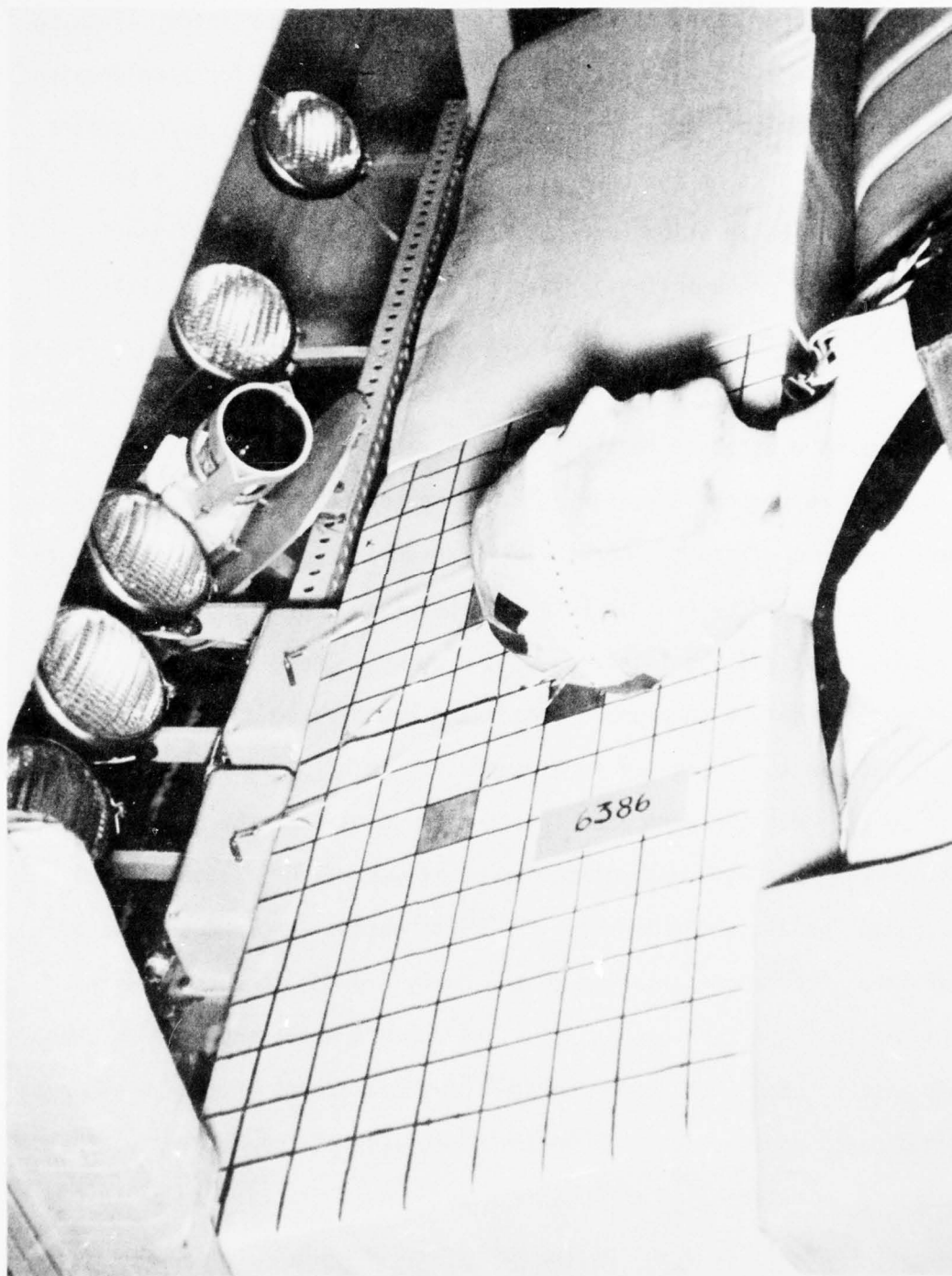


Figure 22. Accelerometer Mounting Technique and Dummy Head Displacement Measuring System with Potentiometers

used in the final series of tests conducted at the General Motors Proving Grounds (test numbers 2795 to 2845) and the initial dummy tests conducted on the Daisy Decelerator. The system used in intermediate dummy tests of the air cushion restraint also used cords attached to two potentiometers mounted at the top of the headrest. This system is shown in Figure 22. The system was used in test numbers 6386 to 6469. The investigators found that this system was unacceptable due to the inertial characteristics of the potentiometers. The potentiometers required a small force to start their rotation and appeared to overshoot the point of maximum deflection due to the rotational inertia. The final series of dummy tests conducted on the Daisy Decelerator used the six cord system shown in Figure 23. This system was used to determine the head positions reported in the Results Section.

The maximum forward displacement of the volunteer subject's head during impact was determined by the length of fiberglass cords that were attached to the subject's head with straps made of Velcro material. These cords were arranged to define the position of three points at the back of the subject's head. This system is shown in Figure 24. The cords were marked and then measured immediately after impact to determine the maximum head displacement. For data reduction purposes it was assumed that each cord reached its maximum extension simultaneously with the subject's most forward head position. These data were then transferred to an engineering drawing of the body buck to provide an immediate assessment of the relationship of a 50th percentile headform with the instrument panel. These data were analyzed more precisely after the completion of the test program.



Figure 23. Six Cord Head Displacement Measuring System Used in Dummy Tests

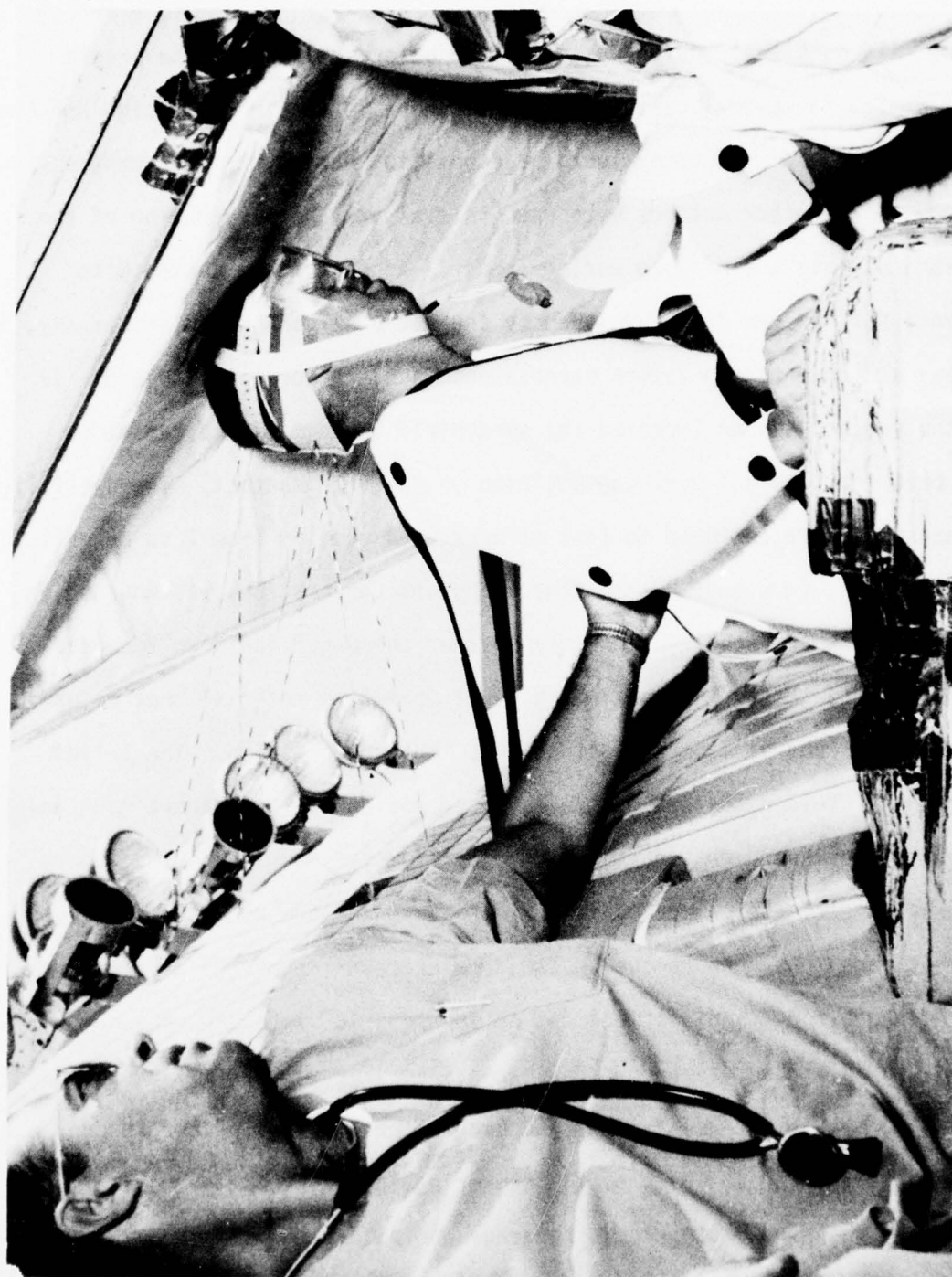


Figure 24. Head Displacement Measuring System Used with Volunteer Test Subjects

An experimental device was developed parallel to this program to more easily and accurately determine the head displacement. This device, known as the Two-Bit System, is described in detail in Appendix C. Although this device was completed before the end of the program and used in several tests, these tests were to verify the design and the data were not used to evaluate head position during the test program.

Three other methods were used to evaluate the penetration of the subject into the air bag during impact. Adhesive tape coated with encapsulated red dye, furnished by the National Cash Register Company, was attached to the Velcro harness each subject wore on his head. If the subject's head impacted the windshield the dye-filled capsules would fracture and mark the position of the head contact. The dye-filled capsules were designed to fail at pressures ranging from 7 to 28 psi. "Met Net", furnished by the General Motors Corporation, was mounted on the instrument panel to indicate whether the panel had been impacted during the test. "Met Net" is a metal foam-like material that deforms on impact and permanently retains the impact depression. The third method involved the use of a high speed motion picture camera mounted under the instrument panel and an accelerometer mounted to the instrument panel. The camera position is shown in Figure 25 where the instrument panel has been removed. The accelerometer mount, displacement reference rods, and displacement reference grid system are shown in Figure 26. The reference rods were nails. Every other nail was bonded to the metal instrument panel and each alternate nail passed through the two-inch thick layer of foam covering the instrument panel.

High speed photographic coverage was obtained with seven 16 mm cameras. Six of the camera locations are shown in Figure 27. Four

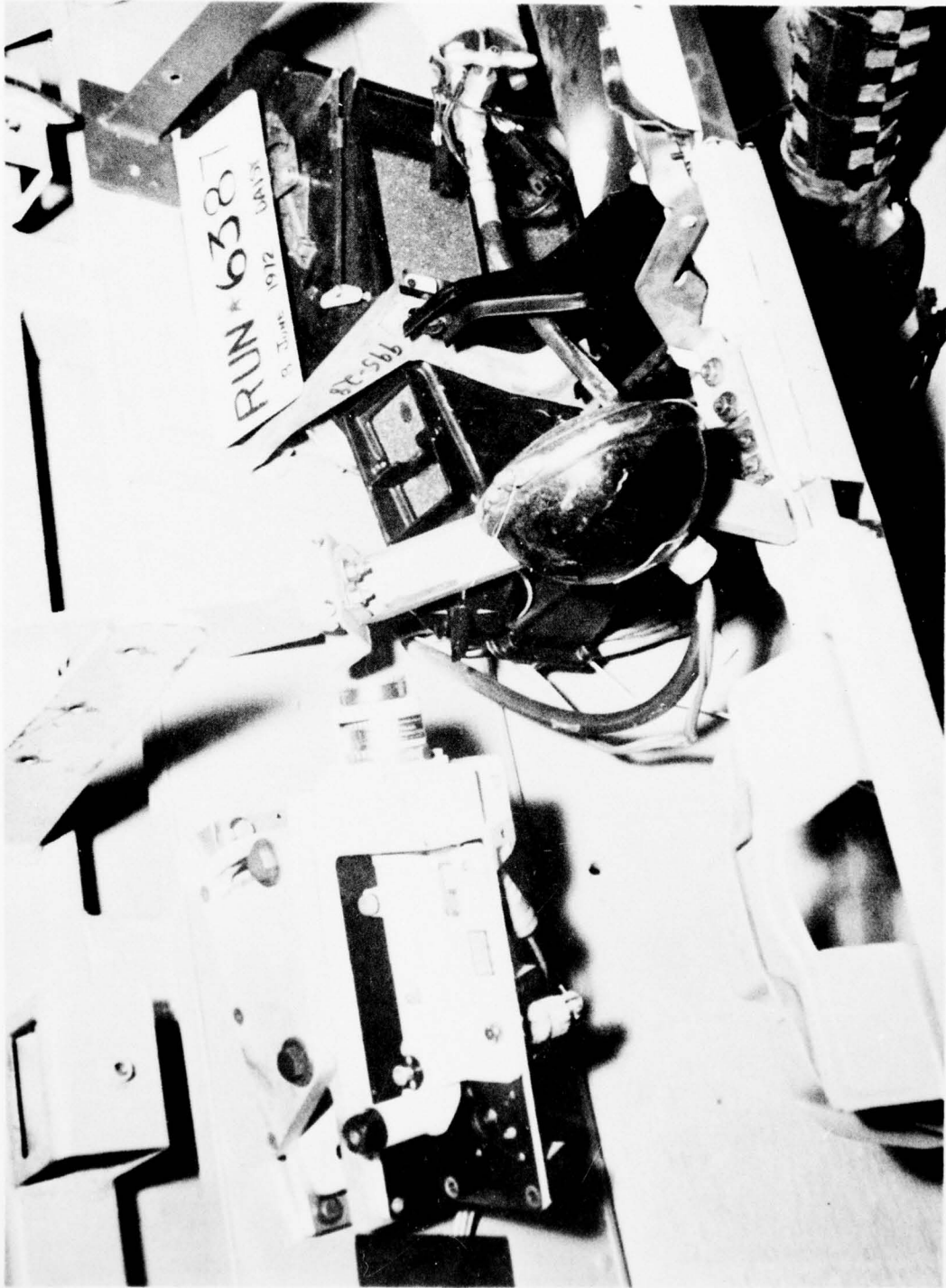


Figure 25. Motion Picture Camera Mounted under the Instrument Panel

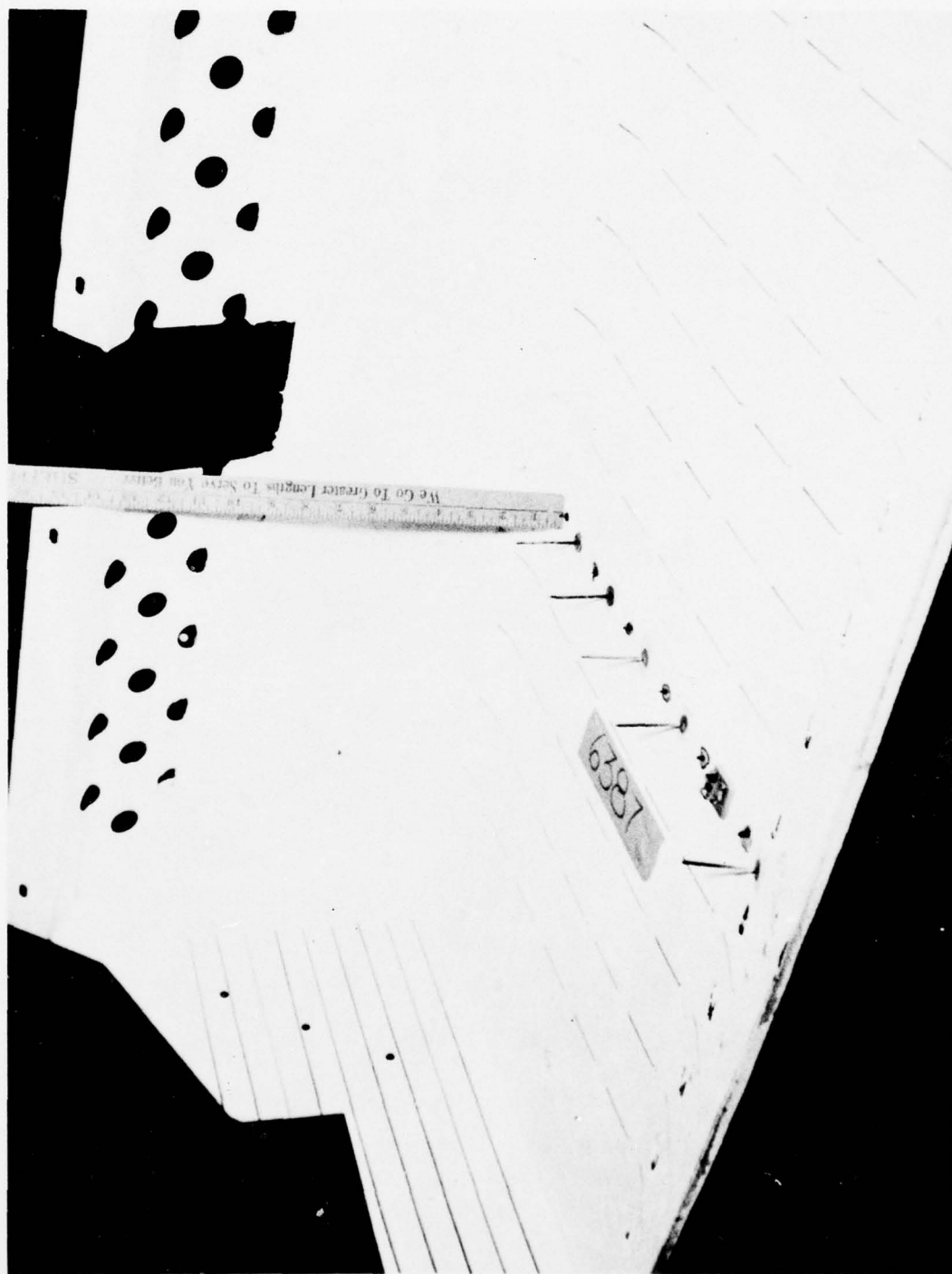


Figure 26. Instrument Panel Accelerometer Mount and Displacement Reference System

onboard cameras were mounted on the test vehicle. Two cameras provided an over-the-shoulder view. Onboard camera number one was mounted directly behind the subject's head and in line with the 15 inch line to show motion forward as well as laterally. Onboard camera number two was mounted behind the subject's head to give an oblique view of motion during impact. This camera was mounted to the left of the subject on an angle of 15 degrees with the plane of his forward vertical motion as can be seen in Figures 22 and 27. Onboard camera number three was mounted on a 90 degree angle to view the subject's motion forward and vertically. Onboard camera number four, which is not shown in Figure 27, was mounted beneath the instrument panel to show motion of the instrument panel to determine if contact with instrument panel was made. The installation of this camera is shown in Figure 25. The three offboard cameras were positioned 90 and 270 degrees relative to longitudinal axis of the track and the acceleration vector. Two cameras, offboard cameras numbers one and two, positioned at 270 degrees provided both a long range view of the impact event and a closeup view of the hip, knee, and ankle complex movements. Offboard camera number three was positioned at 90 degrees to the track to provide a long range view of the impact event. All data cameras were operated at 1000 frames per second.

An electrically independent strobe flash unit was activated by a shorting bar to mark the start of the sled deceleration profile for both onboard and offboard cameras. Coded timing pulses and event marks were recorded on all magnetic tape and oscillographic instrumentation as well as the high speed film records for correlation of events with

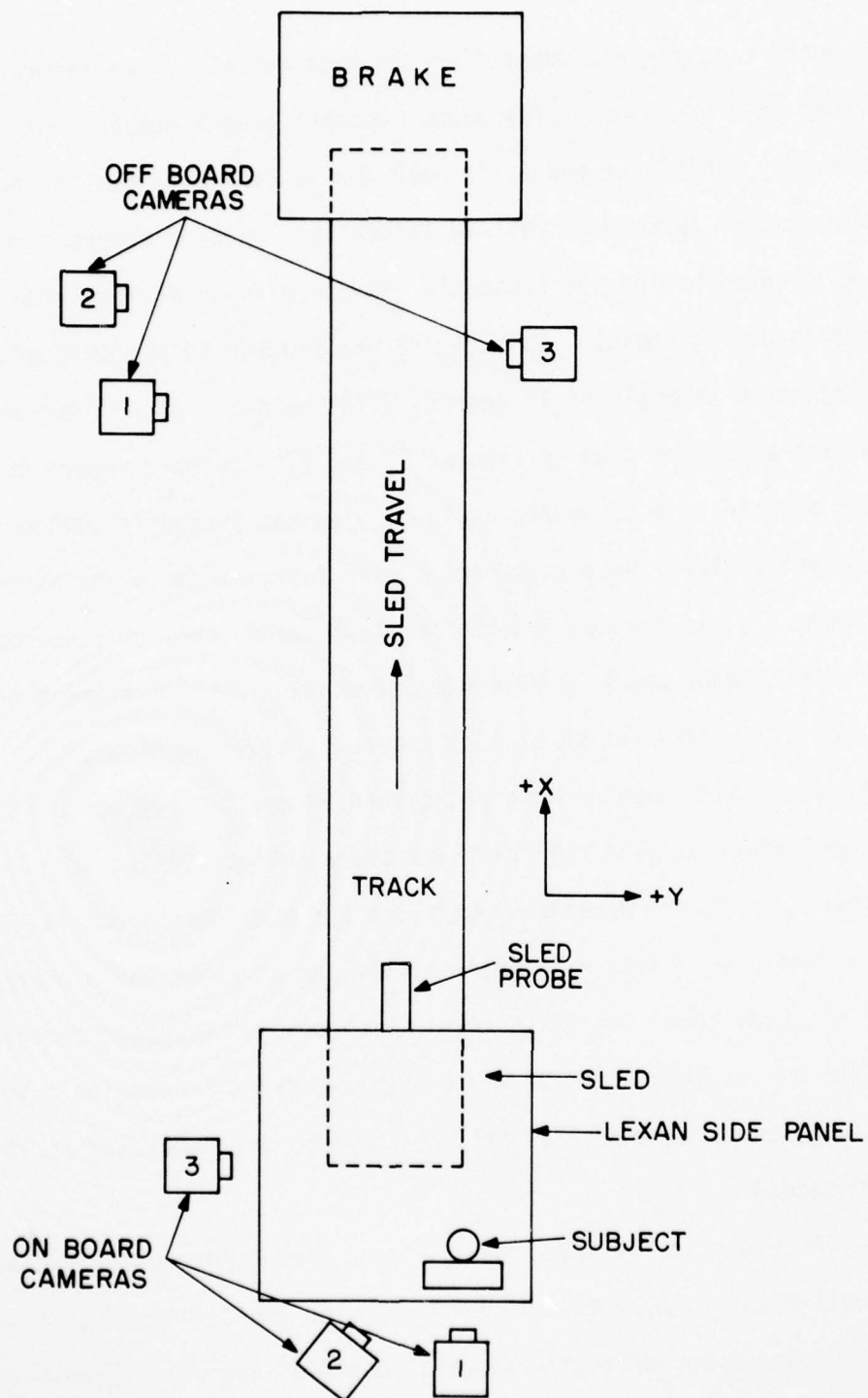


Figure 27. Photometric Data Processing Coordinate System

time. The IRIG B code was used on the offboard cameras while a 1000 Hertz pulse was recorded on the edge of the onboard camera films. In addition, extensive documentary photographic coverage of all operations of the test program was obtained. Documentary motion picture film coverage was obtained with 16 mm cameras operating at 24 frames per second. On selected tests 70 mm camera coverage obtained time sequenced still photos of higher quality.

For all human tests, four channels of electrocardiographic data were collected. This information was transmitted via shielded cable to a Hewlett-Packard ink pen recorder. This recorder documented brake penetration; I, II, and III standard lead electrocardiograph traces as well as cardiometer traces. The cardiometer was triggered electrically by standard lead II and, thus, its response lags other data traces by a few milliseconds. An internally generated time code of one pulse per second was used for time correlation. The chart speed of the recorder was maintained as 25 millimeters per second. Recordings were made from 20 seconds prefire to 60 seconds post impact.

D. Data Processing

Oscillograph data reduction included the determination of the various air bag system firing times, harness release time, safety harness loadings prior to release, maximum bracing foot loads, time to maximum values, pulse duration, and maximum sled, head, mouth, and chest accelerations. Data curve readings and calibration step displacements from the reference line were measured directly from the oscillograph traces. Data curve readings were converted to function values by linear interpolation between calibration steps. Function values for data curves that exceeded calibration limits were computed as linear extrapolations of the calibration steps. Time zero for this data reduction was taken as the leading edge of the 6th interruption record on the Daisy brake penetration trace.

Data was processed from the magnetic tapes to produce the head and mouth resultant acceleration-time histories. These acceleration-time histories were then used to calculate Severity Indices (S.I.). Head Injury Criteria (H.I.C.) values were also calculated on one portion of the data. Fig 28 illustrates the magnetic tape data processing procedure. Two channels of data were processed simultaneously, one channel serving as a source of time correlation for vector summing of X, Y, and Z axes accelerations. The Sled acceleration was used in this capacity.

Step 1 in the processing procedure was to bandlimit the data to the desired analysis bandwidth by passing the analog signal through a low-pass anti-biasing filter. The filter type used was an 8 pole Tchebycheff. As both channels were passed through this type filter simultaneously, changes in phase were identical and their relationships not altered.

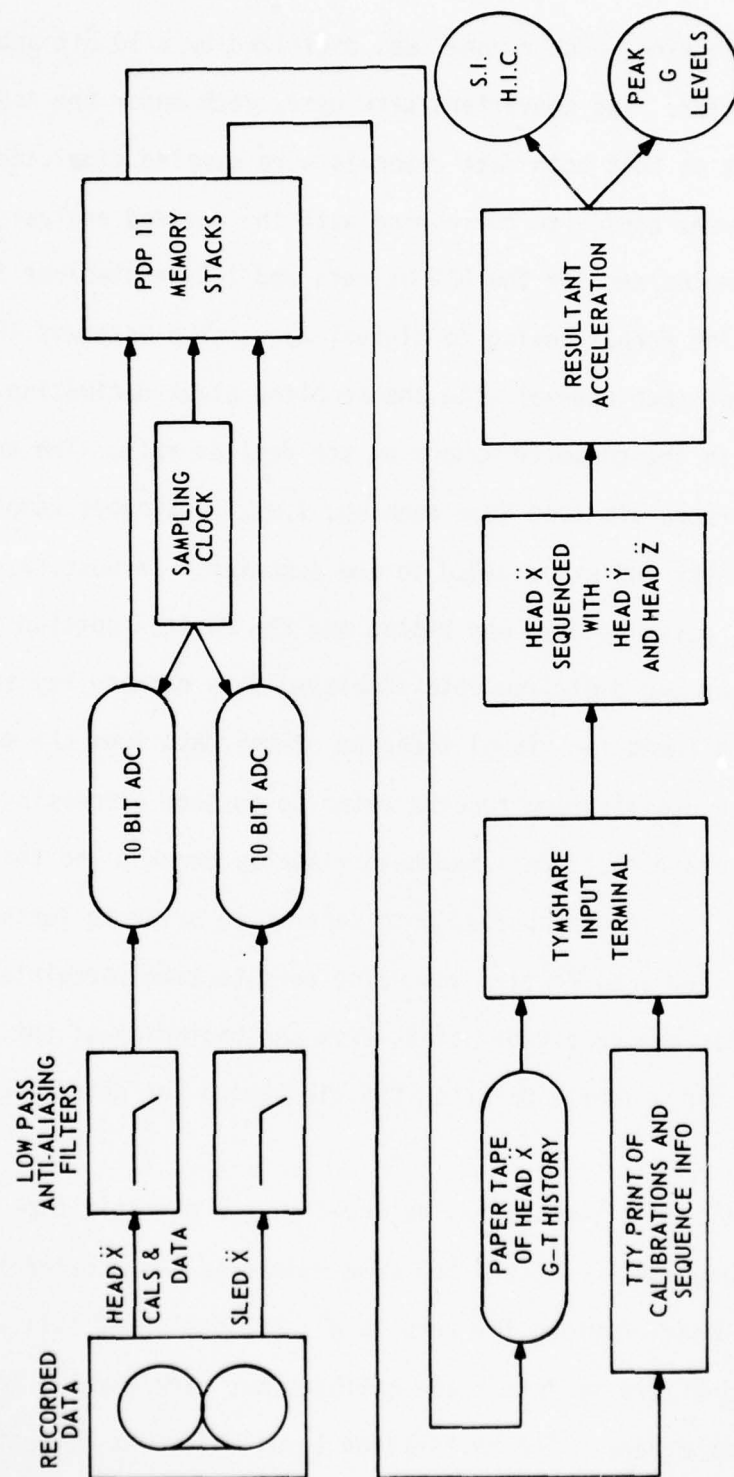


Figure 28. Magnetic Tape Data Processing Schematic

After filtering, each channel was digitized by a 10 bit analog to digital converter. Two converters were used, each under the control of the same clock so that both data channels were sampled simultaneously. Sample rates were chosen to correspond with the desired analysis range, i.e., 2000 samples/sec for the 500 Hz data and 200 samples/sec for the 50 Hz data. The actual analog to digital conversion rate was 100,000 samples/sec for each channel with the sampling clock decimating and transferring data to the computer memory at the desired rate. The analog to digital converters are also free running, i.e., continuous sampling, with data input starts and stops gated to the computer. In most cases more data than was actually used was stored and the desired portion selected after examining the digitized data displayed on a cathode ray tube. The process also allowed for visual checking of the data from the magnetic tapes with the oscillograph records prior to further processing.

After the digitized data had been visually checked and the required portion selected, it was punched onto paper tape prior to further processing. As the sled acceleration was being used to time correlate the X, Y, and Z channels, the number of points from the beginning of the punched data to a distinguishable point on the sled trace was determined and recorded.

Calibration data, which was recorded on the magnetic tape before each test, was processed in exactly the same manner as the acceleration data. Calibrations were provided for zero level, 1/2 scale and full scale. Zero to 1/2 and zero to full scale calibrations were checked to verify linearity on the tape. The calibration level which was closest to the

peak of the test acceleration measurement was used to convert the digitized data to G-values later.

When digitized acceleration-time histories, calibration data, and time correlation information were available for the X, Y and Z components of the head or mouth accelerometers on a particular test, they were read into the TYMSHARE² system. Programs in this computer system converted the digitized data files, using the calibration information, into acceleration-time histories and calculated the resultant accelerations using the time correlation information. After this, the Severity Indices were calculated and peak levels recorded for both the X-axis alone and the resultant acceleration.

Photometric data processing methods are described in Appendices D and E as mentioned previously. Time zero for the photometric data reduction was taken from a flash initiated by an independently operated fiber optical system. The optic system was actuated by the closing of an electrical circuit at the moment the position of the sled on the track corresponded to the initiation of the acceleration pulse. This is represented when the sled brake plunger reached station five in the water brake or the 6th interruption of the brake penetration trace on the photo oscillographs.

Offboard camera data reduction techniques were one camera position solutions. The X and Z component data are computed parallel to the film plane using the relationship between the subject target movement and reference markers located on the sled. Appendix D of this report provides a complete description of the data reduction techniques that were used to process the offboard data.

²The TYMSHARE system is a commercially available digital computer terminal.

AD-A038 525

AEROSPACE MEDICAL RESEARCH LAB WRIGHT-PATTERSON AFB OHIO F/G 13/12
IMPACT TESTS OF A NEAR-PRODUCTION AIR CUSHION RESTRAINT.(U)

FEB 77 J W BRINKLEY, G C MOHR, H C RUSSELL DOT-HS-017-1-017-1A

UNCLASSIFIED

AMRL-TR-75-47

DOT-HS-802-248

NL

2 OF 5

AD
A038525



Reduction of onboard camera data was accomplished through position computation based on line of sight camera readings. Line of sight readings were correlated with surveyed grid orientation readings to determine a direction cosine from the camera to the specified target. In the event that only one camera was used to compute position, a trigonometric solution was used which computes X and Z component positions. It was assumed there is no lateral Y-axis movement. This assumption was verified by an overhead camera in the evaluation of head position data. The computed position is the point where the line of sight intersects the vertical plane assumed to contain the test target.

The photometric data processing to determine head position was first accomplished using semiautomatic data reduction methods and the computer program described in Appendix D. While there is nothing inherently wrong with these methods (the Appendix is, in fact, provided for reference by future users), the results that were obtained using the method were unsatisfactory for several reasons. First, the data processing method assumed that data would be available from three cameras used to view the subject's head motion. Only two cameras could actually view the motion of the head throughout the entire test. Only one of these two cameras could be used to solve for the position of the subject's head. Second, the accuracy of the method, as it was used, was no better than \pm one inch. Third, the organization that used this data processing method did not understand the experimental setup, the purpose of the experiment, the required accuracy, etc.

A second photometric data processing procedure was developed to improve the accuracy of the head motion trajectory data. This procedure, described in Appendix E, was developed to meet the unique aspects of the experimental setup and the difficulties associated with viewing the subject encircled by the air bag. A single individual was responsible for the development of the data handling procedures, the preparation of the computer program, the assessment of the accuracy of the method, and evaluation of the processed data. This procedure provides the head motion trajectory data in terms of displacement points within a Sled Coordinate System within a reference plane which was coincident with the midsagittal plane of the test subjects. Each data point was derived from a sliding three-point average. Five point averaging was also studied but found unnecessary. Velocity indices are also given with the data plots. These plots are described in more detail in Appendix D and in the Results Section of this report.

All of the motion picture films collected during this program have been provided to the National Highway Traffic Safety Administration for further analysis.

E. Anthropometric Dummies

The anthropometric dummies that were used in this program were 50th and 95th percentile dummies, Sierra Engineering Company Model numbers 292-850 and 292-895. These dummies were furnished by the General Motors Corporation. Table IX lists the dummy anthropometry.

TABLE IX
DUMMY ANTHROPOMETRY

MODEL NO.	292-850	292-895
WEIGHT (LB)	161 1/2	215
HEIGHT (IN)	68 1/2	73 1/4
SITTING HEIGHT, NORMAL (IN)	35	35 1/4
SITTING HEIGHT, ERECT (IN)	36 1/2	38 1/2
KNEE HEIGHT (IN)	21 1/8	23 1/4
BUTTOCK-KNEE LENGTH (IN)	24	25 3/8

Prior to each test, each dummy was completely disassembled, inspected and all joints were adjusted to provide an equivalent of a 1 g load in accordance with the requirements of reference 12. The 1 g load is defined as the degree of joint tightness that just allows movement of the limb under a torque equivalent to that exerted by the normal weight of the limb. Neck flexion was measured before each test by allowing the head and neck to be cantilevered off the end of a platform. Photometric target locations on the dummies were established in accordance with the recommended practice of reference 12.

F. Volunteer Subjects

All subjects for the air bag test program conducted on the Daisy Decelerator were young male officers and airmen who were members of the Air Force Hazardous Duty Impact Panel at Holloman AFB. Table X provides a summary of anthropometric data for the test subjects. Examinations performed to qualify subjects for this panel included: (1) a modified Flying Class II physical examination and medical history, (2) AP and lateral x-rays of the skull and complete spine, (3) 12 lead electrocardiogram, and (4) electroencephalograms. If the results of the above tests were judged acceptable by hospital physicians and the panel physician, the individual was recommended for certification for hazardous duty. The original panel consisted of 13 members, only two members had had prior exposure to deceleration studies. The entire panel was briefed on the approved experimental plan, the objectives, and the potential hazards of the program. Written voluntary informed consent was obtained from each subject for each exposure. All inexperienced panel members (11 out of 13) received an indoctrination exposure on the Daisy Decelerator at 6 mph using a lap and shoulder belt restraint.

Subject selection for the initial runs at 15, 20, and 22 mph impact velocities was random (with one exception for the 20 mph series). Subjects were selected for the 24, 26, 28 and 30 mph tests on the basis of the following criteria. First, bag penetration toward the instrument panel and windshield - at the higher velocities subjects were selected who appeared to penetrate the bag to a lesser degree and, therefore, were considered to be less likely to contact the instrument panel or the windshield. Although the measurement of separation from the instru-

Figure 29. Anthropometric Dimensions

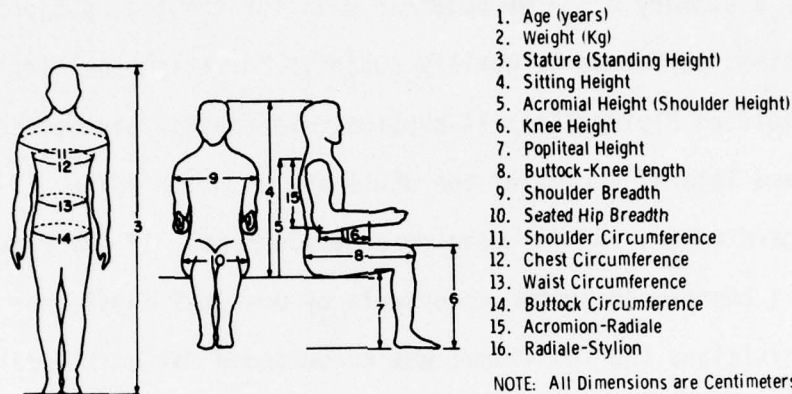


TABLE X. ANTHROPOMETRY OF THE VOLUNTEERS

	A	B	C	D	E	F	G	H	I	J	K	L	M
1	20	29	19	24	32	19	20	20	31	23	22	22	29
2	76.2	74.2	54.7	82.6	76.0	75.3	83.2	58.7	63.0	66.5	82.1	91.6	74.8
3	170.2	177.0	169.8	178.6	177.0	181.2	174.3	174.8	164.5	171.3	166.2	174.0	176.6
4	89.8	91.7	89.4	89.6	93.3	93.3	90.8	88.7	88.8	90.4	88.3	90.0	93.7
5	N.D.	59.7	58.8	58.4	59.5	62.2	58.6	57.0	55.5	62.3	55.8	58.1	65.8
6	N.D.	52.7	50.5	57.7	53.8	54.8	53.5	53.8	50.0	52.0	49.0	53.0	53.5
7	N.D.	41.5	41.7	44.3	42.8	43.3	41.8	43.4	40.0	40.5	38.7	41.6	41.9
8	N.D.	59.2	59.0	64.6	62.0	64.0	62.5	59.3	54.7	59.2	58.8	64.0	59.4
9	N.D.	46.8	41.7	46.7	47.8	46.8	48.7	41.6	45.4	47.5	50.0	51.3	48.0
10	N.D.	36.8	32.0	37.5	86.5	33.3	38.5	32.0	33.4	33.7	37.8	39.0	35.8
11	N.D.	118.0	103.0	115.0	117.5	117.0	112.0	104.0	116.0	112.5	120.5	132.0	112.0
12	N.D.	98.0	83.0	95.0	96.0	94.0	100.0	89.5	93.0	93.5	95.0	107.5	94.0
13	N.D.	84.0	71.0	89.0	84.7	79.0	92.0	73.5	80.0	80.5	93.0	95.5	83.0
14	N.D.	96.5	86.0	103.0	97.5	94.0	106.0	85.0	91.3	92.0	103.0	107.5	95.0
15	N.D.	33.5	32.3	35.3	34.3	36.0	33.8	33.4	30.4	33.8	32.4	34.0	34.1
16	N.D.	27.5	26.5	29.9	26.8	28.3	28.7	27.6	26.0	27.2	27.0	28.0	28.1

ment panel during bag penetration was not precise, and it was possible that different subjects exhibited varying degrees of reproducibility, subjects were, nevertheless, selected for the higher velocity exposures partly on this basis. Second, questionable post exposure findings--one subject was eliminated as a result of persistent muscle spasm--another for arrhythmia and a third because of anxiety. A minimum of a five-day interval (an exception was made in one case) was required between exposures for any subject. For those individuals eliminated from the panel for any reason, i.e., transfer to another base, etc., a thorough termination physical examination was performed prior to separation.³

The standard subject-handling procedures for the test series were as follows. The subjects presented themselves for a pre-exposure briefing and medical examination approximately one-half hour prior to the scheduled tests. The medical monitor performed a physical examination consisting of blood pressure and pulse rate measurement, examination of the skin, auscultation of the chest and heart, and neurologic evaluation, including pupillary responses and deep tendon reflexes. The subject was questioned about recent health history and asked to complete a form which detailed his sleep, meals, and state of mind during the prior 12 hours. The subject was asked to void as necessary. The subject was briefed by the medical monitor about the specific impact velocity and expected level of acceleration programmed for that day.

³The Operating Location of the Impact Branch has been deactivated since the completion of this test program and all of the subjects have received termination physicals.

Prior subject experiences and potential hazards were reviewed. For each test the subject signed a voluntary consent form detailing the specific conditions of the exposure.

The subjects wore long white cotton underwear and shoes of their own choice. Silver-silver chloride EKG leads were attached to the subject's chest and the cardiogram signal was checked for acceptable quality and regularity of rhythm before escorting the subject to the test sled. A continuous EKG tracing was recorded and monitored during the test. At the sled the subjects were instructed on proper positioning. They were asked to sit with their heads and backs firmly against the seat back and headrest. Arms were placed at their sides with elbows and forearms along their thighs and hands closed into fists. Appropriate floor board spacers, as shown in Table VIII, were placed under the feet of short-legged subjects so that the knees of all subjects were flexed to an angle of approximately 132 degrees. Shin guards extending from knees to ankles were strapped into place. Ear plugs were installed prior to each run. Goggles were taped over the eyes and a Velcro webbing head harness and adhesive tape coated with encapsulated dye were secured to the head. Photometric target discs were placed at selected locations on the limbs, head, and torso as shown in Figure 30.

For tests 6507 through 6515, 1-inch diameter black target dots were placed at the wrists, elbows, shoulder, ankle, knee, mid thigh 10 inches above the knee, and the H-point. The H-point is defined as the most lateral part of the greater trochanter of the femur which was manually identified to give reference to the hip joint. The displacement

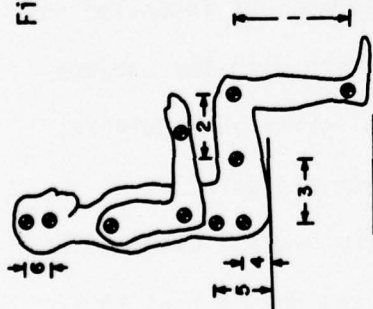


Figure 30. Photometric Target Disc Locations for Volunteer Subjects

1. Ankle Knee Length
2. Knee Mid-Thigh
3. Mid-Thigh H-point
4. H-point Height
5. Iliac Crest Height
6. Head Targets

Note: All dimensions are given in inches.

TABLE XI. TARGET POSITIONS FOR EACH SUBJECT

	A	B	C	D	E	F	G	H	I	J	K	L	M
1	N.D.	17	16	17 3/4	16 1/4	16 1/2	16 1/8	16 1/4	15 1/4	15 1/4	14 3/4		16 1/4
2	10	10	10	10	10	10	10	10	10	10	10	10	10
3	N.D.	7	6	7 3/4	10	7	9	7 7/8	6	7	8		8 1/8
4	N.D.	4 1/8	23/4	33/4	4 5/8	23/4	31/8	33/8	3	3	4		4
5	N.D.	8 1/2	8	8	7 7/8	8	8 3/8	8 1/4	8	9	10		
6	4	4	4	4	4	4	4	4	4	4	4	4	4

of these target dots as shown on high speed film provide data to evaluate interaction of the subject with the deploying bag. These target dots were also placed on the subject's head at the mandible joint and 4 inches upward perpendicular to the Frankfort Plane. After test 6515 at the request of the DOT Contract Monitor, 2-inch diameter black and white targets were used for body kinematic studies in place of the 1-inch diameter black targets. The distances between selected targets and the height of the H-point and iliac crest target with respect to a flat seat surface are given for each subject in Table XI.

Each subject wore his own individually fitted plastic mouthpiece which was placed in position prior to the run. The mouthpiece contained an accelerometer imbedded in the plastic with the wire lead emerging from the mouth and taped to the left cheek. Subjects were in voice communication with the operating personnel at all times and could abort the test up to the moment of initial sled motion by indicating a desire to do so. A removable, transparent plexiglass panel was installed on the right side of the sled to assure visual contact with the subject throughout the test. A medical monitor, medical orderly, ambulance, and resuscitation equipment were on hand for each exposure.

After each test the subject was taken to the medical examination room where he was questioned about his experiences during that test. He provided comments regarding the sensations experienced in a time sequence and, if possible, relative comments on the nature and level of discomfort and willingness to participate in further tests, etc. A post-exposure physical examination was performed and all abnormalities noted and recorded in narrative form and on a "body-region diagram".

Photographs of visible skin markings, if any, were taken. As part of this debriefing and examination the subject was instructed to fill out a post-run questionnaire on which he reported immediate post-exposure physical symptoms as well as those perceived 24 hours and 72 hours post-exposure. The pre-run and post-run questionnaires that were used are described in reference 9.

IV. Results

A. Dummy Tests Conducted at the GM Proving Grounds

The initial series of impact tests using dummy subjects were accomplished at the General Motors Proving Grounds. A total of 73 tests were conducted in this series. Fifty impact tests were accomplished to determine the normal operating performance of the air cushion restraint and to demonstrate its reliability to insure the safety of the volunteers in the later stages of testing. Nineteen tests were completed where deployment of the air cushion was deliberately not initiated. Thirteen of the nineteen tests were done to determine the subject hazards associated with impacting the instrument panel and windshield if the air cushion restraint did not inflate and the torso harness was inadvertently released. Seven of the nondeployment tests were done to determine the restraint harness loads that would be experienced and two tests were accomplished at a 75 mph impact velocity to proof test the test buck. Three additional tests were accomplished to evaluate the air cushion cover deployment and one test was done to evaluate the effect of not using the high level gas generator at an impact velocity of 30.5 mph.

The first 21 impact tests of the air cushion restraint were accomplished using the same crushable steel instrument panel and windshield constructed of paper reinforced with foamed polystyrene ribs which had been used in the earlier series of prototype air bag restraint impact tests (ref 9). Although the air cushion deployed and inflated properly in all of these tests, the polystyrene ribs and paper of the windshield frequently failed, allowing the outer air bag to move beyond the limits

of the windshield. As a result the dummy's head would penetrate through the air bag to the instrument panel. This condition added to the overall variability of the test results and clearly did not simulate conditions that would normally occur during operational use of the air cushion restraint. The data collected during these tests are summarized in Table XII.

The tests during this stage in the dummy test program were conducted at high velocities to demonstrate the performance characteristics of the air cushion system under extreme conditions. Thus, these tests were conducted at velocities of 30, 34.5, 37.5 and 40 mph. Moreover, there were discussions between the Department of Transportation, the General Motors Corporation and the Air Force investigators concerning the advisability of conducting tests beyond the goal of 30 mph originally established for the test program with volunteer subjects.

The remaining 29 impact tests of the air cushion accomplished in this series were done using a crushable polystyrene foam windshield. The foam contained hollow cores to improve its crushability. In test numbers 2361, 2363, 2364, 2367, and 2369 the cores were filled with popcorn. The data from these tests are summarized in Table XIII.

The results of the nineteen impact tests in which the air cushion restraint was not used are summarized in Table XIV. These tests were referred to as nondeployment tests during the program and will be referred to in that manner within this report. The purposes of the nondeployment tests were (1) to determine the impact environment that would be encountered in the event the air cushion restraint system failed to deploy and the subject reacted into the torso harness, (2)

TABLE XII. SUMMARY OF RESULTS FROM AIR CUSHION IMPACT TESTS
WITH PAPER WINDSHIELD

TEST NO.	DUMMY SIZE PERCENTILE	SLED VELOCITY (MPH)	SEVERITY INDEX (S.I.)	CHEST ACCEL. (G)	FEMUR LOADS LEFT (LBS)	RIGHT (LBS)
2267	50	30	490	42	740	720
2268	50	30	450	48	670	760
2269	50	34.5	490	52	1120	910
2270	50	34.5	710	48	860	830
2272	50	40	750	62	1230	1260
2274	50	40	850	72	1120	1270
2283	95	40	1300	66	1800	1300
2284	95	40	1550	56	780	1350
2285	95	40	1350	52	2310	2040
2289	95	37.5	1570	63	940	1850
2290	95	37.5	1890	63	860	2040
2292	50	37.5	1530	65	1650	2330
2293	95	34.5	1260	58	700	1120
2294	95	34.5	1100	41	650	940
2295	50	37.5	1930	82	1470	850
2344	50	30	990	44	830	690
2345	50	30	1460	43	810	740
2346	50	30	ND	ND	ND	ND
2347	95	50	1060	42	830	740
2348	95	30	930	41	580	750
2349	50	30	890	47	810	660

TABLE XIII. SUMMARY OF RESULTS FROM AIR CUSHION IMPACT TESTS
WITH POLYSTYRENE FOAM WINDSHIELD

TEST NO.	DUMMY SIZE PERCENTILE	SLED VELOCITY (MPH)	SEVERITY INDEX (S.I.)	CHEST ACCEL. (G)	FEMUR LOADS	
					LEFT (LBS)	RIGHT (LBS)
2350	50	26	470	33	650	690
2351	50	26	540	34	660	660
2352	50	26	290	35	600	550
2353	95	26	440	35	950	800
2354	95	30.5	840	40	680	750
2361*	50	30.5	930	46	800	830
2362	50	20	220	25	800	680
2363*	50	20	220	22	690	620
2364*	95	20	180	25	720	ND
2365	95	20	130	29	520	580
2366	95	15	160	17	820	920
2367*	50	15	70	13	360	330
2368	95	40	2000	72	1200	1100
2369*	50	40	2350	98	1280	1080
2370	50	75	4470	137	1360	1340
2373	95	30.5	870	53	860	1090
2378	50	30.5	550	43	850	600
2379	95	30.5	670	39	610	810
2401	50	30.5	620	51	710	680
2408	95	30.5	700	40	900	1100
2409	50	40	1600	80	1260	1180
2410	50	34.5	800	60	1100	900
2411	50	15	100	15	300	340
2412	95	15	200	10	800	800
2413	50	37.5	1750	80	1000	1000
2416	95	34.5	1100	55	1050	1250
2426	95	34.5	1200	62	1100	1300
2427	95	30	750	45	1200	750
2428	95	40	1800	70	1050	1500

*Polystyrene foam cores filled with popcorn

to determine the impact environment in the event that the air cushion restraint system failed and the torso harness was released, and (3) to measure the loads in the torso harness during impact. The test data within Table XIV are arranged in the order of increasing impact velocity and the type of instrument panel that was used. The initial tests (numbers 2286, 2287 and 2288) were done with the instrument panel and windshield design that had been used in the earlier series of impact tests of the prototype air bag restraint system (ref 9). Windshields constructed of cored polystyrene foam filled with popcorn were then evaluated in test numbers 2359 and 2360. The final configuration that was evaluated was a combination of a cored polystyrene windshield and a crushable steel instrument panel. This configuration was used in tests 2371 through 2421.

The secondary safety restraint harness was not used in the majority of dummy tests conducted at the General Motors Proving Grounds since its reliability had been demonstrated in the earlier tests of the prototype air bag restraint. However, it was used in test numbers 2376, 2377, 2429, 2430, 2419, 2420 and 2421. The fact that the restraint prevented severe impact with the windshield and instrument panel can clearly be seen in the lower Severity Indices calculated from the accelerations measured on the dummies' heads in test numbers 2376, 2377, 2429 and 2430. The improvement is not evident in tests 2419, 2420 and 2421 in the 34.5 to 40 mph range since the restraint harness was less effective at these higher velocities. Table XV provides the load measurements from the tests where the safety restraint harness was used.

TABLE XIV. SUMMARY OF TEST RESULTS FROM NONDEPLOYMENT TESTS

TEST NO.	DUMMY SIZE PERCENTILE	SLED VELOCITY (MPH)	INSTRUMENT PANEL	WINDSHIELD TYPE	SEVERITY INDEX (S.I.)	CHEST ACCEL. (G)	FEMUR LEFT RIGHT (LBS) (LBS)	
2286	50	20	PC	P	400	55	1310	970
2287	95	20	PC	P	610	43	760	970
2288	95	30	PC	P	1690	71	990	1160
2359	95	30.5	PC	PP	2220	94	1440	1670
2360	50	30.5	PC	PP	2450	119	1560	2150
2417	50	15	S	CP	100	ND	600	1100
2418	95	15	S	CP	100	10	700	850
2357	95	30.5	S	CP	2120	92	1490	1600
2358	50	30.5	S	CP	1990	139	1750	1850
2376	50	30.5	S	CP	320	27	290	260
2377	95	30.5	S	CP	950	33	980	1380
2400	50	30.5	S	CP	2070	123	1820	1630
2407	50	30.5	S	CP	1750	120	1800	2500
2429	50	30.0	S	CP	225	25	300	350
2430	95	15	S	CP	50	10	50	50
2419	95	34.5	S	CP	2000	55	2000	2000
2420	50	37.5	S	CP	2000	140	1700	1800
2421	95	40	S	CP	3300	60	2000	2000
2371	50	75	S	CP	ND	ND	--	--

PC = Polystyrene foam instrument panel filled with popcorn. PP = Polystyrene foam windshield filled

S = Crushable steel instrument panel. popcorn.

P = Paper windshield reinforced with styrofoam ribs. CP = Cored polystyrene windshield.

TABLE XV. RESTRAINT HARNESS LOAD MEASUREMENTS

TEST NO.	DUMMY SIZE PERCENTILE	SLED VELOCITY (MPH)	LEFT SHOULDER (LBS)	RIGHT SHOULDER (LBS)	LEFT LAP BELT (LBS)	RIGHT LAP BELT (LBS)
2376	50	30.5	620	810	620	770
2377	95	30.5	1220	1050	545	840
2419	95	34.5	650	750	125	75
2420	50	37.5	900	450	100	300
2421	95	40	850	725	100	225
2429	50	30	875	675	400	750
2430	95	15	450	450	250	400

Tests of the air cushion cover were conducted to (1) evaluate the effects of different scoring patterns on the cover of the air cushion, (2) demonstrate the cover had no significant effect on the deployment sequence, and (3) determine if the cover flap motion created by the air cushion deployment represented a hazard to the subject's legs. Early during the development of the air cushion cover there had been concern about the impact (slap) of the cover flap striking the volunteer's shins with sufficient force to create a hazard. Further, there had been concern that the flap might prevent proper deployment of the inner knee cushion, thereby causing the subject to submarine under the air cushion restraint. These tests showed that these concerns were unfounded. The cover flap in all cases was driven below the knee level prior to the subject beginning to translate forward. The inner knee bag was deployed normally, thus preventing the postulated submarining action. These tests also showed that the scoring pattern providing

the best deployment was one in which the cover flap was scored vertically to the connecting seam of the upper and lower instrument panel. The connecting seam was then ripped loose. Where the covers scored on three sides were used, the deployment of the air cushion was less effective and slower in reaching desired positions.

A total of 50 successive, successful air cushion deployments under impact conditions were accomplished at the General Motors Proving Grounds prior to shipment of the test apparatus to Holloman AFB. These whole system tests demonstrated a reliability of 0.95 at the ninety percent lower confidence level.

B. Impact Tests with Dummies on the Daisy Decelerator

The test apparatus was then shipped to Holloman AFB, New Mexico, and installed on an impact carriage on the Daisy Decelerator. A series of 28 impact tests of the air cushion restraint were conducted using dummy subjects and 14 impact tests were accomplished to select the instrument panel configuration that was to be used in the tests with volunteer subjects. The entire chronology of tests conducted on the Daisy Decelerator is given in Appendix E. The dummy tests that are discussed here occurred during the period of 23 March 1972 to 14 June 1972.

Two instrument panel configurations were evaluated. One configuration constructed of crushable steel covered with a 2-inch thickness of polyvinylchloride foam has been described in detail in the Methods and Materials Section of this report. The second configuration had the same outward contours of the crushable steel configuration but it was constructed of crushable polystyrene plastic foam. The foam contained hollow cores that were filled with popcorn. The tests were accomplished at four impact velocities. The tests were designed to indicate which of the two instrument panel configurations were superior in terms of minimizing the hazards to the volunteer subjects, or if one was superior in a specific speed range. The results of the tests are summarized in Table XVI. The results of test numbers 2417 and 2418 are included in Table XVI since they were considered to be part of the experimental design to evaluate the two instrument panel configurations. These two tests were performed at the General Motors Proving Grounds but were similar in all respects to the tests conducted on the Daisy Decelerator.

TABLE XVI. SUMMARY OF RESULTS FROM TESTS TO SELECT THE
BEST INSTRUMENT PANEL CONFIGURATION

TEST NO.	DUMMY SIZE PERCENTILE	SLED VEL. (MPH)	SLED ACCEL. (G)	INSTR. PANEL	SEVERITY INDEX	CHEST ACCEL. (G)	FEMUR LEFT (LBS)	LDS RIGHT (LBS)
2417*	50	17.3	9.8	S	100	--	600	1100
2418*	95	17.0	9.8	S	100	10	700	850
6329	50	22.4	13.0	S	67	32	1091	1020
6327	95	22.4	13.0	S	345	45	1040	1030
6331	50	26.1	18.0	S	317	66	1110	1316
6325	95	26.1	18.9	S	1321	74	1440	1640
6318	50	31.3	22.4	S	474	114	1338	1270
6322	95	31.3	21.4	S	1639	77	1628	1130
6337	50	16.0	9.4	PC	28	11	692	852
6339	95	16.6	9.4	PC	ND	ND	ND	ND
6330	50	22.8	13.4	PC	162	51	1370	1960
6328	95	22.8	13.4	PC	570	57	1246	1300
6332	50	26.2	17.9	PC	529	86	1210	1367
6326	95	25.6	18.3	PC	937	81	1353	1423
6319	50	31.3	22.4	PC	634	144	1645	1560
6323	95	31.8	22.2	PC	1063	81	1635	1380

*Accomplished at the GM Proving Grounds

ND = No data due to malfunction

S = Crushable steel instrument panel

PC = Cored polystyrene foam instrument panel filled with popcorn

Note that the Severity Index values reported in Table XVI are calculated from the -Gx acceleration-time history measured in the dummy's head rather than from the resultant acceleration computed from the three accelerations measured in the dummy's head. This procedure was used for expediency in the instrument panel comparison only.

An analysis of variance performed on the nondeployment test revealed no statistically significant difference in the results between the polystyrene instrument panels filled with popcorn and the steel instrument panels. Although the tests of the steel instrument panel gave higher S.I. values with the small number of the samples conducted, one could not reject the hypothesis that the tests come from the same population at the 95% confidence level. Therefore, the steel instrument panel was selected since it more nearly represents the construction of an automobile instrument panel.

The series of impact tests conducted during the March to June period included two structural tests. One test (number 6341) was conducted at 60 mph (29.6 g) to prove the adequacy of the test buck mounting to the Daisy Decelerator carriage. The second proof test (number 6345) was accomplished at 27 mph to qualify the torso restraint harness and check out the restraint harness loads measuring instrumentation system.

A sequence of 18 impact tests of the air cushion restraint system were accomplished. The purpose of these tests was to complete the reliability demonstration test sequence and to provide final training for the test personnel. The original test plan called for a series of 16 tests. Two tests were to be accomplished at each impact velocity.

The impact velocities were to be 15, 22, 24, 26, 28, 30 and 32 mph. A 50th percentile and a 95th percentile dummy were to be used at each velocity. The data from the resulting series of tests are given in Table XVII.

Two problems occurred during this series of impact tests. First, the data and physical evidence indicated that the dummy's head was penetrating through the outer air bag. The polystyrene windshield was deformed on test numbers 6313 and 6320 as shown in Figure 31. Furthermore, localized deformation of the metal instrument panel provided evidence that the dummy's head might be bottoming out on the instrument panel. Indentations of the instrument panel were found after test numbers 6320, 6338 and 6340 and also later after test numbers 6355 and 6356. Test numbers 6355 and 6356 were previously unplanned but were accomplished to replicate test numbers 6338 and 6340 in view of the evidence of head bottoming. Second, a problem was discovered in the initiator system of the second gas generator (hi-pyro level) during a routine safety procedure check after a test at 15 mph (test number 6356).

The acceleration waveforms shown in Figure 32 are tracings of the G_x accelerations measured on the dummy's head during test numbers 6338, 6340, 6355 and 6356, accomplished at velocities ranging from 15.2 mph to 15.8 mph. These waveforms are dissimilar to the waveform of the G_x head acceleration measured on other tests in this series. Figure 33 shows tracings of the G_x head accelerations measured on test numbers 6354 and 6357 with impact velocities of 18.1 and 18.7 respectively. Some dissimilarity can also be seen in the time from the start of

TABLE XVII. SUMMARY OF DATA FROM THE INITIAL SERIES OF
IMPACT TESTS OF THE AIR CUSHION RESTRAINT
CONDUCTED ON THE DAISY DECELERATOR

TEST NO.	DUMMY PERCENTILE	SLED VEL. (MPH)	SLED ACCEL. (G)	SEVERITY INDEX	CHEST ACCEL. (G)	FEMUR LDS LEFT (LBS)	RIGHT (LBS)
6312	50	31.1	18.7	ND	48	500	600
6313	50	30.7	20.0	ND	68	600	625
6320*p	50	31.8	20.4	ND	82	ND	ND
6321	50	30.3	18.8	415	38	907	715
6338*	50	15.8	8.8	161	12	200	196
6340*	95	15.8	9.1	159	11	483	208
6343	95	31.8	21.0	626	53	735	604
6344	95	30.3	19.2	442	39	828	670
6346	95	27.5	19.1	389	42	660	446
6347	95	25.6	16.1	250	32	768	580
6348	50	25.6	16.4	232	33	697	680
6349	50	27.5	19.2	328	40	720	690
6351	50	22.6	15.3	157	20	660	610
6352	95	21.8	13.6	174	25	598	550
6354	95	18.1	11.6	110	18	561	470
6355*	95	15.5	8.6	230	8	286	210
6356*	50	15.2	8.4	99	8	290	366
6357	50	18.7	12.2	104	12	630	643

p = polystyrene foam instrument panel used

* = depression in the instrument panel

ND = No Data recorded



Figure 31. Damage of Polystyrene Windshield - Test Number 6313

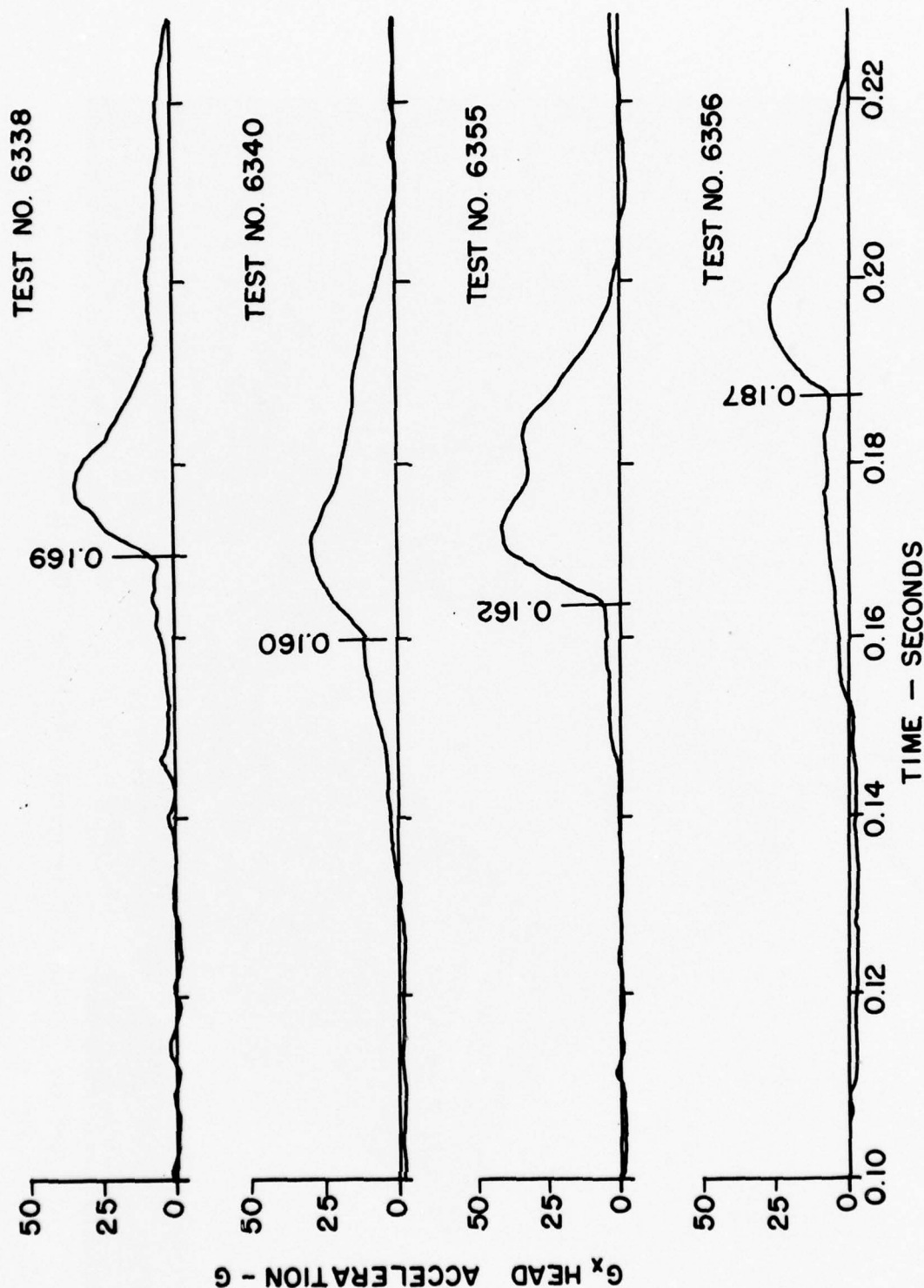


Figure 32. G_x Acceleration Measured on the Dummy's Head During Test Numbers 6338, 6340, 6355 and 6356

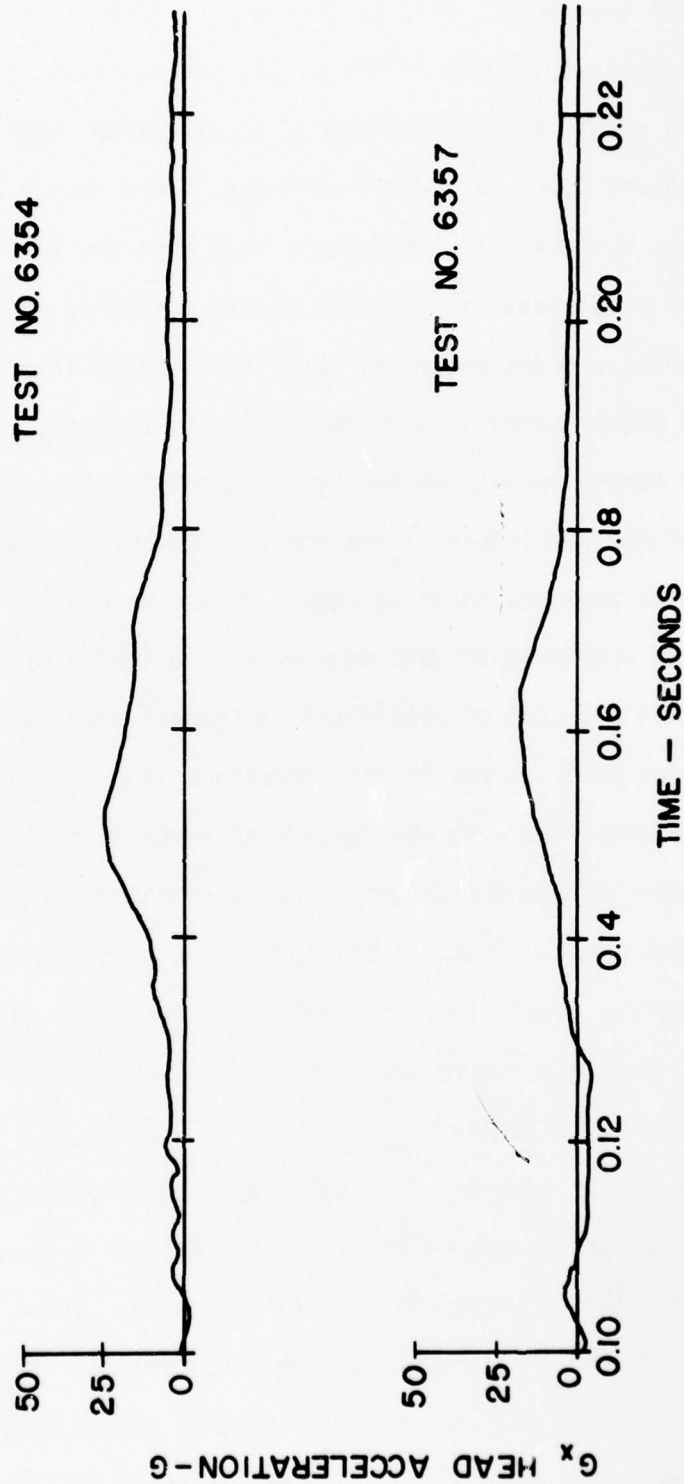


Figure 33. G_x Acceleration Measured on the Dummy's Head During Test Numbers 6354 and 6357

impact to the peak G_x head acceleration. Moreover, the waveforms of the accelerations shown in Figure 32, particularly test numbers 6338 and 6355 reveal a marked change of acceleration, almost a discontinuity, at 0.169 and 0.162 second respectively. This change was suspected to be caused by impact of the dummy's head into the instrument panel. The deformed steel instrument panels provided further evidence as they were indented at a point where the head impact would have occurred.

To acquire more data on the nature of the head impact problem, the onboard camera setup provided by the General Motors Corporation was modified. A motion picture camera and a light were installed under the instrument panel as shown in Figure 24 and were used in all tests after 6386. An accelerometer was mounted on the inside of the instrument panels and a system of photometric reference rods were attached to the instrument panel at the 15 inch reference line as shown in Figure 25. The reference rods were alternately attached to the instrument panel and driven through the 2-inch thick polyvinylchloride foam covering the instrument panel. Thus, if the foam was compressed but the metal was not deformed, every other rod would move inward to record the degree that the foam was compressed. This setup was used on test number 6386 and all tests thereafter.

The motion picture films obtained from the camera mounted under the instrument panel revealed deformations that would routinely occur at the time the inflator pyrotechnics were initiated. These deformations were typical of high frequency shock waves transmitted through sheet metal structures. The motion picture films also showed gross deformation inward on test number 6355. The deflection of the instrument panel was

estimated to be 3 inches. This deformation created an indentation that was typical of the indentations seen on the earlier test numbers 6338 and 6340. Test number 6355 was, in fact, a replicate of test 6340. Cords attached to the dummy's head to measure the displacement of the head also verified the head impact. Two additional tests were conducted to complete the tests that had been planned. Test number 6356 was a replicate of test number 6338. The results of this test were the same as those of test number 6355. Test number 6357, accomplished at a velocity of 18.7 mph, completed the series without revealing any further evidence of head impact.

After test number 6356, current was applied to the high level gas generator to fire the pyrotechnics that were not used in the low velocity tests (a routine safety precaution). The high level gas generator failed to fire. A very complete investigation of the incident was accomplished by the Allied Chemical Corporation, the manufacturer of the pyrotechnics used in the air cushion restraint system. It was theorized that the relatively long delay between functioning of the air cushion inflator system and the attempt to fire the high level gas generator allowed the pressure differential between the inside of the electrically actuated pyrotechnic initiator and the gas storage bottle to blow off the initiator cover. This, in turn, would dump the pyrotechnic material surrounding the electrical bridge wire resulting in the inability to ignite the gas generator propellant. The initiator failure was duplicated under laboratory conditions confirming the above mentioned theory of failure. The tests indicated that the initiator covers were separating between 2 seconds to 15 minutes after inflator

bottle venting. Such time delays were considerably longer than the normal delay of 0.059 sec. (at 15 mph) to 0.020 sec (at 30 mph) between inflator orifice opening and the firing of the hi-level gas generator. Initiator cover crimp strength was also investigated and related to the occurrence of the problem.

The proposed corrective action was to change the initiator assembly and inspection procedure. A hydrostatic test for crimp strength was also added to the initiator lot acceptance test requirements. After implementation of the corrective actions a series of 105 tests at pressure differentials up to 3500 psi were conducted by Allied Chemical to evaluate the effectiveness of the changes. No cover separation occurred.

Since the impact tests of the air cushion that had been accomplished had indicated evidence of head impact with the instrument panel at the first velocity level that was to be used in the testing with volunteers, an additional series of 10 tests were accomplished in an attempt to find a safer starting point for the volunteer tests. The results of these tests are given in Table XVIII. The first six tests of this series were conducted at 15 mph (nominal). Head displacement measurements made using four cords attached to the dummy's head indicated contact with the instrument panel on test numbers 6381, 6383, 6384, 6387, 6391 and 6392. The position of the dummy's head with respect to the padded surface of the instrument panel is given in the column labeled head/panel distance. The negative values indicate the depth of penetration into the instrument panel. The polyvinylchloride foam padding was removed from the instrument panel in test number 6386.

In view of the evidence of head penetration at 15 mph, test numbers 6388 and 6389 were conducted at 11 mph (nominal) to explore the feasibility of starting the tests at this level. Test 6391 was then accomplished at 15 mph and both gas generators were fired simultaneously. The final test of this series, number 6392, was conducted at 12.4 mph and resulted in head penetration of 4.0 inches.

After test numbers 6381 and 6384, tears 5 inches and 7 inches in length respectively were found at the connection of the nylon bag and the initial portion of the bag attachment to the diffuser manifold tube. Figures 34 and 35 show the tears that were found. This problem was corrected by a minor modification to the method of bag manifold attachment.

TABLE XVIII. SUMMARY OF DATA FROM ADDITIONAL LOW VELOCITY IMPACT TESTS OF THE AIR CUSHION RESTRAINT

TEST NO.	DUMMY SIZE PERCENTILE	SLED VEL. (MPH)	SLED ACCEL. (G)	SEVER. INDEX	CHEST ACCEL. (G)	FEMUR LEFT (LBS)	LDS RIGHT (LBS)	HEAD/PANEL DISTANCE (IN)
6380	50	14.9	8.1	24	8	370	420	0.9
6381	50	14.6	8.5	61	9	480	420	-3.0
6383	95	14.8	8.4	52	13	400	380	-1.0
6384	95	14.6	8.0	91	8	375	350	-4.0
6386	95	14.2	7.0	59	8	440	480	0.6*
6387	95	14.9	8.2	49	11.5	440	ND	-0.2
6388	95	10.5	4.4	16	4	280	340	0.5
6389	50	11.2	4.6	16	3	220	280	1.4
6391+	50	15.0	8.4	55	7	300	360	-0.2
6392	50	12.4	5.6	61	9	180	180	-4.0

*2.0" thick polyvinylchloride foam pad removed from instrument panel. Distance is to surface of steel panel.

+ Both high and low level gas generators fired simultaneously.



Figure 34. Air Bag Tear Found After Test Number 6381



Figure 35. Air Bag Tear Found After Test Number 6384

C. Development and Demonstration of a Revised Air Cushion Inflator System

Testing was resumed at the General Motors Proving Grounds using an identical test buck to develop an air cushion test procedure that would assure that the volunteer subjects would not impact the instrument panel during a normal air cushion deployment. The General Motors Corporation studied the feasibility of several approaches. Two types of inflator system modifications were developed to increase the margin of safety to a level that was considered by the investigators to be adequate for volunteer testing. First, the amount of pyrotechnic material used in the gas generators was increased as explained in the next paragraph. Second, the pressure of the stored gas was increased from 2350 psi to 2700 psi. The results of these tests are provided in Tables XIX and XX. Measurement of the position of the dummy's head was made with the four cord system described within the Methods and Materials Section of this report. The instrument panel clearance determination is specified in terms of contact or no contact. These determinations were generally considered to be conservative.

In test number 2735 the lo-level gas generator contained a charge of 20 grams and the hi-level gas generator contained 25 grams. On all of the following tests described in Tables XIX and XX, 25 grams was used in both gas generators. The stored gas pressure was increased to 2700 psi after test number 2829. This modification eliminated further head contacts.

At the completion of this series of tests and the analysis of the test data that had been collected, an agreement was reached to proceed with human testing if a series of 20 successively successful tests could

TABLE XIX. SUMMARY OF DATA FROM IMPACT TESTS OF THE AIR CUSHION SYSTEM WITH REVISED GAS GENERATOR CHARGES

TEST NO.	DUMMY SIZE PERCENTILE	SLED VEL. (MPH)	SEVER. INDEX	CHEST ACCEL. (G)	FEMUR LOADS		PANEL CONTACT
					LEFT (LBS)	RIGHT (LBS)	
2735*	95	15	100	21	630	720	-
2737	95	15	110	22	600	600	-
2795	95	31.4	650	47	990	920	No
2796	50	31.5	790	45	790	630	Yes
2800	50	31.5	610	45	790	600	Yes
2803	50	27	430	35	600	690	Yes
2807	50	29	460	38	700	630	Yes
2808	50	27	410	38	670	590	-
2810	50	27	350	35	680	590	-
2811	95	27	450	37	780	780	-
2812	50	25	270	32	580	470	-
2813	50	25	230	27	640	570	Yes
2815	50	25	300	27	730	660	No
2820	50	15	30	12	460	430	No
2821	95	15	80	16	620	710	Yes
2822	50	25	320	32	690	620	No
2823	50	25	250	33	690	650	No
2824	95	25	260	36	770	870	No
2825	95	25	350	38	790	820	Yes
2827	95	25	190	35	670	680	No
2828	95	15	30	15	520	560	No
2829	95	22	210	38	830	840	No

*20 grams of propellant in the lo-level gas generator and 25 grams of propellant in the hi-level gas generator. Twenty-five grams were used in both generators for all other tests.

TABLE XX. SUMMARY OF DATA FROM IMPACT TESTS OF THE AIR CUSHION SYSTEM WITH REVISED GAS GENERATOR CHARGES AND 2700 PSI STORED GAS PRESSURE

TEST NO.	DUMMY SIZE PERCENTILE	SLED VEL. (MPH)	SEVER. INDEX	CHEST ACCEL. (G)	FEMUR LOADS		PANEL CONTACT
					LEFT (LBS)	RIGHT (LBS)	
2830	95	25	310	32	870	850	No
2831	50	25	250	32	660	630	No
2832	95	15	60	15	620	640	No
2833	50	15	40	14	500	520	No
2834	50	25	210	32	710	570	No
2835	95	25	300	38	770	890	No
2840	95	15	60	17	670	760	No
2841	50	15	40	13	560	560	No
2842	50	25	290	33	700	760	No
2843	50	25	220	31	690	630	No
2844	50	22	210	27	760	840	No
2845	95	22	230	37	900	920	No

be conducted on the Daisy Decelerator with 50th percentile dummy subjects at an impact velocity of 25 mph (nominal). A successful test was simply defined as one in which the dummy's head did not contact the instrument panel. The maximum displacement of the dummy's head was measured with the six cord system. The dummy was removed from the test buck and the limbs were readjusted after each test. Prior to each test the dummy was positioned in the test buck using the positioning apparatus described in the Methods and Materials Section.

Before initiation of the series of 20 dummy tests at Holloman AFB a group of five tests were accomplished on the Daisy Decelerator to check out the overall test procedures and instrumentation. The results of these tests are listed in Table XXI. There was no evidence of contact with either the instrument panel or the windshield in any of these tests.

TABLE XXI. CHECKOUT TEST RESULTS

TEST NO.	DUMMY SIZE PERCENTILE	SLED VEL. (MPH)	SLED ACCEL. (G)	HEAD ACCEL. (G)		SEVERITY INDEX		CHEST ACCEL.	
				EXT.	INT.	EXT.	INT.	EXT.	INT.
6470	95	15.9	9.8	19	20	40	80	17	ND
6471	50	15.3	9.2	ND	18	ND	40	15	16
6472	50	20.9	13.9	32	28	160	130	31	28
6473	95	21.6	15.3	ND	ND	ND	ND	ND	ND
6474	95	25.2	16.9	ND	32	ND	220	42	ND

ND = No Data

TABLE XXII. SUMMARY OF DATA FROM 20 SUCCESSIVE SUCCESSFUL IMPACT TESTS WITH DUMMY SUBJECTS

TEST NO.	SLED VEL. (MPH)	SLED ACCEL. (G)	HEAD ACCEL. (G)		SEVERITY INDEX		CHEST ACCEL (G)		FEMUR LOAD (LBS)		DISTANCE TO INSTR PANEL (IN)
			EXT	INT.	EXT	INT	EXT	INT	LEFT	RIGHT	
6475	24.9	16.5	43	33	350	230	33	30	660	750	3.2
6476	26.0	18.0	47	36	260	220	59	38	850	750	1.6
6477	25.0	16.9	58	35	260	220	32	34	780	720	3.1
6478	25.5	16.9	37	31	230	160	34	34	790	1020	2.5
6479	25.6	17.3	32	28	260	170	41	34	870	1230	1.0
6480	25.0	16.8	48	34	220	190	32	34	700	650	4.3
6481	25.5	17.2	47	35	490	190	31	33	710	600	4.0
6482	25.7	17.5	62	32	600	170	38	32	960	860	4.4
6483	25.3	16.9	42	33	180	190	38	32	820	810	4.4
6484	25.3	16.6	36	34	170	200	31	32	740	750	1.8
6485	25.6	17.2	30	33	140	190	31	33	740	960	2.4
6486	25.7	17.6	29	27	140	160	32	30	810	900	1.5
6487	25.6	17.2	38	34	190	180	37	34	80	780	2.4
6488	24.7	16.2	39	31	220	200	38	29	800	875	0.8
6489	25.5	17.0	36	34	200	210	33	34	80	1110	6.5
6490	25.7	17.4	50	37	310	240	38	35	80	900	4.1
6491	25.2	16.8	46	37	260	220	35	31	80	680	5.3
6492	25.7	17.5	41	32	250	180	31	34	80	920	0.9
6493	25.1	16.6	52	36	300	200	32	30	650	650	4.0
6494	25.7	17.4	48	37	320	210	33	31	80	640	3.3

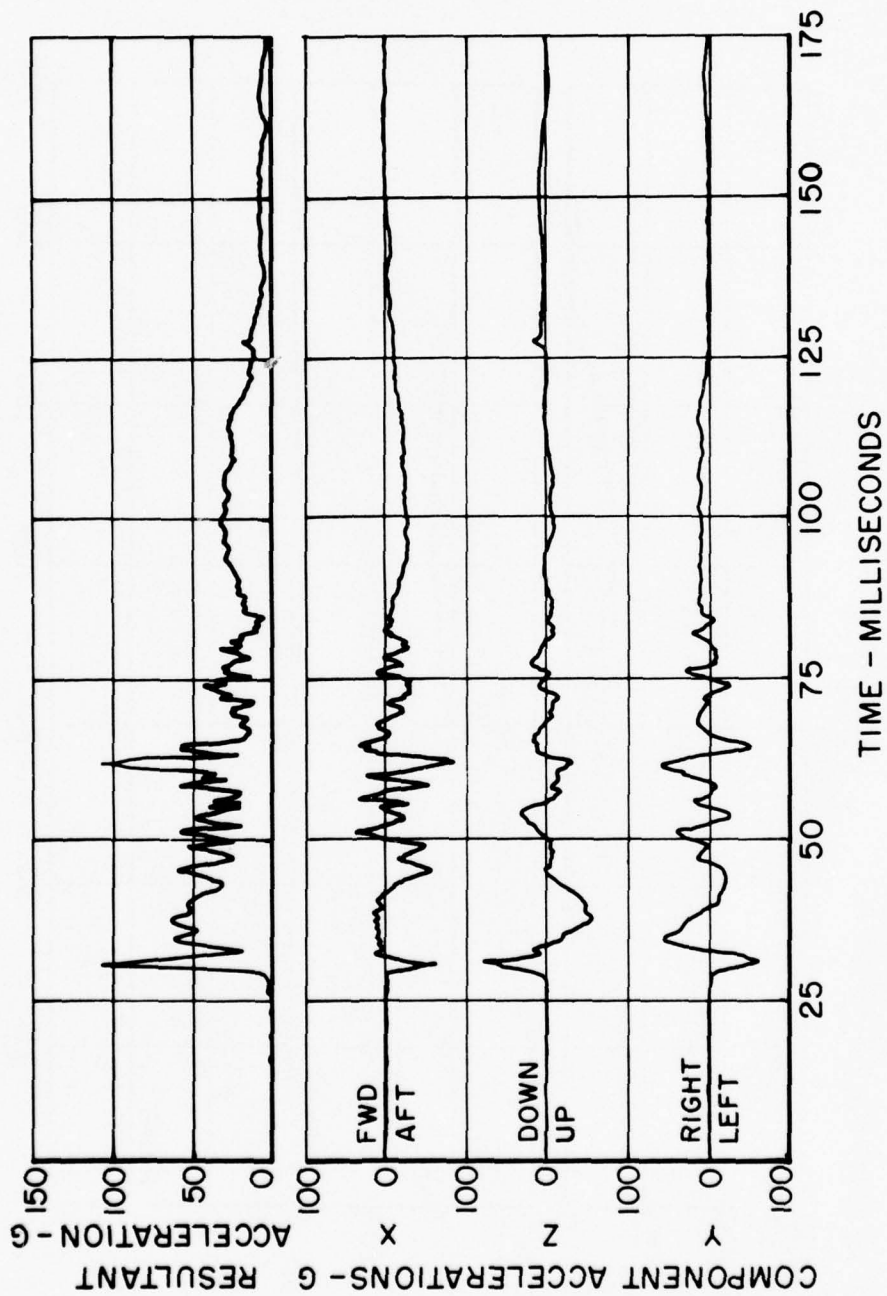


Figure 36. Acceleration-time Histories From Accelerometers Mounted Externally on the Test Dummy - Test No. 6486

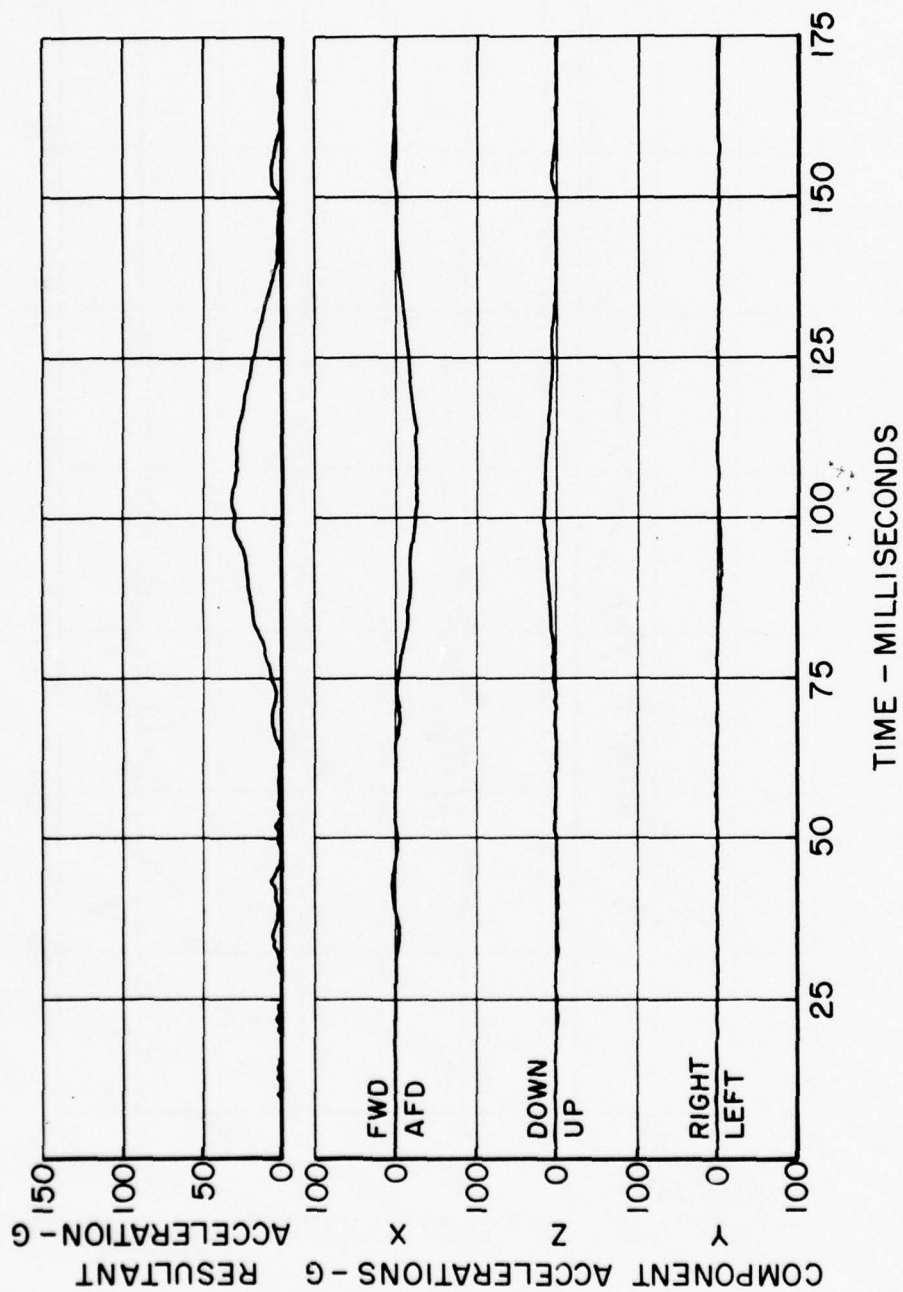


Figure 37. Acceleration-time Histories From Accelerometers Mounted Within the Test Dummy - Test No. 6486

The results of the 20 successive tests are summarized in Table XXII. The Severity Index values that are reported are calculated from two triaxial accelerometer packages, one mounted externally on the dummy's head, the second within the dummy's head. Corresponding peak resultant accelerations are also given for externally and internally mounted head accelerometer measurements. Likewise, peak resultant acceleration values measured within the dummy's chest and from a triaxial accelerometer held to the dummy's chest by a strap are also given.

In each test the acceleration measured on the dummy's chest was obscured by high frequency, large amplitude anomalous signals that occurred during the period of 0.031 (\pm 0.002) second to approximately 0.085 second. The accelerometers mounted within the dummy's chest did not record this anomaly. Typical acceleration traces from the externally and internally mounted chest accelerometers are shown in Figures 36 and 37. The investigators initially thought that this signal occurred as a result of the unfurling bag contacting the chest accelerometers. However, placement of a layer of polyvinylchloride foam over the transducers did not alter the signal. Furthermore, later study of the high speed motion picture films revealed that the bag did not contact the transducers until approximately 0.01 second after the start of the anomalous signal. After the completion of the test program, during the more extensive analysis of the 20 sequential dummy tests, the investigators found that the start of the anomaly corresponded to the time of the firing of the second gas generator. This event occurred at 0.031 (\pm 0.001) second for these tests. This correlation was checked at other impact velocities to determine if the firing of the gas

generator was acoustically driving the accelerometers. If the firing of the second gas generator was, in fact, the source of the anomaly, the start of the anomaly would change as a function of the impact velocity since the firing time was varied with impact velocity. The start of the anomaly was not found to relate to the firing times of the second gas generator at other impact velocities.

Additional attempts to determine the cause of the anomalous signal were not conclusive. The most plausible theory was that the anomaly was an acoustical phenomenon associated with the high speed unfurling of the air bag material. Its initiation could not be clearly related to the unfurling; however, it did cease when the bag was completely unfurled. To evaluate this theory tests were conducted to determine the acoustical sensitivity of accelerometers. A 38 caliber pistol loaded with blanks was fired in close proximity to triaxial accelerometers mounted on the chest of a subject. The accelerometers proved to be insensitive to this type of acoustical excitation.

Since the photometric data showed that the anomaly started before the bag contacted either the dummy or human subjects, the investigators chose to ignore the anomaly during the manual data reduction. However, it did influence the values obtained from the automatic data analysis in instances where the data sampling rate was too high to filter the high frequency peaks of the anomaly.

The distance between the instrument panel and the maximum forward position of the dummy's head ranged from 5.3 to 0.9 inches. The maximum position of the dummy's head in each of these tests has been determined from the lengths of the six cords and plotted in Figure 38. The headforms

are representative of the 95th percentile head size to illustrate the worst case. Since there was no evidence of the head contacting the instrument panel in any of these tests, the entire series was judged to be successful. Although these data showed that there was contact with the windshield, during tests numbers 6490, 6491, and 6493, the investigators placed little credence in the vertical position data since the geometry of the cords significantly limited the accuracy of the data in this axis. Furthermore, there was no corroborative evidence of windshield impact.

Table XXIII provides a summary of the Head Injury Criteria (H.I.C.) values that resulted from these 20 successive tests. These values were provided by the General Motors Corporation.

TABLE XXIII. SUMMARY OF H.I.C. DATA FROM 20 SUCCESSIVE TESTS WITH DUMMY SUBJECTS

TEST NO.	EXTERNAL HEAD ACCELEROMETERS			INTERNAL HEAD ACCELEROMETERS		
	H.I.C.	G	t (ms)	H.I.C.	G	t (ms)
6475	163	28.5	90-128	135	25.1	89-135
6476	322	22.9	88-215	165	28.5	87-125
6477	255	37.5	91-121	161	27.4	88-129
6478	148	29.6	98-124	120	23.4	88-131
6479	217	19.6	98-206	105	21.5	87-136
6480	208	33.9	95-126	142	26.2	88-128
6481	470	46.0	86-119	156	28.0	91-128
6482	608	55.2	98-120	136	21.6	88-149
6483	121	29.0	96-122	145	26.8	92-131
6484	116	27.3	95-125	146	22.9	89-147
6485	88	18.6	77-207	140	25.2	88-132
6486	108	14.6	79-211	114	22.9	88-134
6487	120	28.2	95-124	141	26.5	91-130
6488	162	31.1	98-128	145	25.6	87-131
6489	131	28.6	94-124	157	27.7	90-129
6490	219	37.2	93-119	186	29.9	92-130
6491	185	35.4	97-122	173	27.7	91-134
6492	157	18.0	90-204	128	21.3	89-150
6493	221	37.6	100-125	154	27.2	90-130
6494	233	37.6	96-122	173	27.9	90-132

BEST AVAILABLE COPY

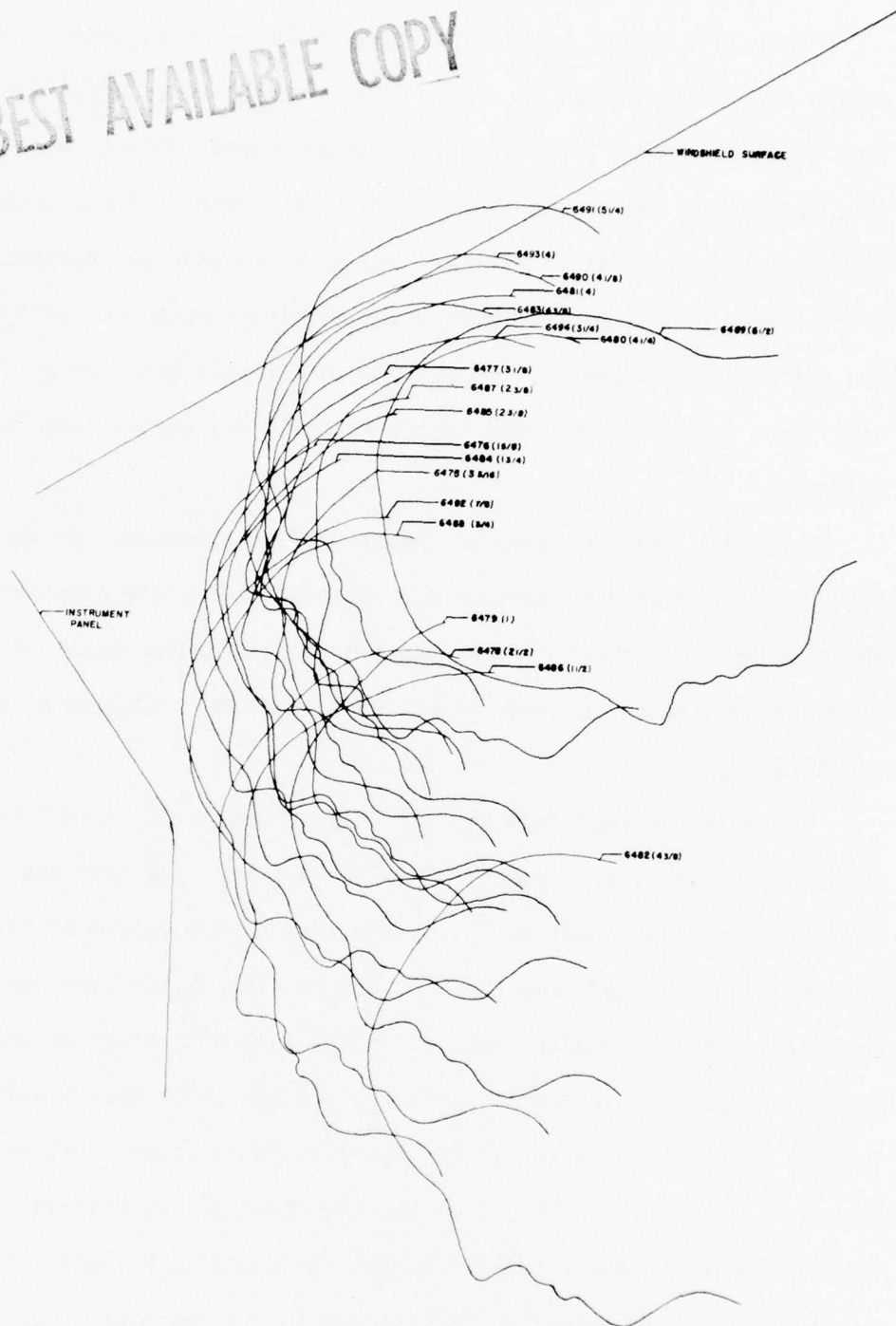


Figure 38. Composite of Dummy Head Positions Determined From Measurements During 20 Successive Tests

D. Tests With Volunteers

Forty-five impact tests were accomplished with volunteer subjects during the course of the program. Twelve of the tests were indoctrination tests conducted to familiarize inexperienced subjects with impact test procedures and expose them to low level impact. These tests were done using a conventional military lap belt and shoulder harness. Thirty-three of the impact tests with volunteers were accomplished using the air cushion restraint. Impact exposure levels were varied incrementally from 8.3 to 21.1G. The impact velocity was varied from 14.9 to 30.8 mph.

Subject L received only an indoctrination exposure. He was unexpectedly transferred to another duty station before the experimental phase began. Subject B did not require indoctrination exposure because of prior experience in other impact test programs conducted on the Daisy Decelerator.

The data obtained from the air cushion restraint systems tests with volunteer subjects are summarized in Table XXIV. The head and chest acceleration values that are given are the maximum values of the resultant acceleration computed from the x, y and z acceleration components measured by triaxial accelerometers mounted on the subject's head and chest. (The computed resultant acceleration values for the chest were provided by the General Motors Corporation.) The Severity Index values that are tabulated were calculated by the AMRL from the resultant of the triaxial accelerations measured on the subject's head. The mounting harness for the accelerometers was found to have shifted in its position by about 1 inch after test numbers 6535 and 6537. This may account for the slightly

TABLE XXIV. SUMMARY OF DATA FROM TESTS WITH HUMAN SUBJECTS

TEST NO.	SUBJECT NO.	SLED ACCEL. (G _x)	SLED VEL. (mph)	HEAD ACCEL. (G _r)	SEVERITY INDEX (S.I.)	CHEST ACCEL. (G _r)	FOOT LOADS LEFT (LBS)	FOOT LOADS RIGHT (LBS)	HEAD/PANEL DISTANCE (IN)	WINDSHIELD CONTACT (CORD)	(DYE)
6507	A	9.3	16.0	17.7	31	11	353	715	11.1	Yes	--
6508	B	9.1	15.6	12.6	19	13	705	737	12.9		
6510	C	8.3	14.9	14.9	18	12	615	490	12.8		
6511	D	8.9	15.5	17.3	35	20	810	810	10.0		
6514	E	13.0	20.5	26.8	89	22	815	835	9.8	Yes	Yes
6515	F	13.4	20.9	32.4	158	32	915	930	6.6		
6524	C	13.4	20.9	30.2	97	19	750	698	6.6		
6525	G	12.9	20.5	31.0	135	33	850	910	11.3		
6528	H	15.4	22.0	56.3	298	32	630	690	7.1	Yes	No
6529	I	16.3	22.3	44.9	155	32	600	600	8.8		
6531	K	15.2	21.5	47.5	216	27	610	720	ND		
6532	J	15.0	21.5	31.7	133	32	730	740	4.0		
6534	M	20.0	24.0	87.0	359	28	840	981	6.5	Yes	No
6535	B	19.4	23.7	99.0	521	22	840	1001	7.2*		
6537	E	19.2	24.1	43.1	160	31	745	846	3.5*	Poss.	Yes
6538	J	19.9	24.3	47.8	183	44	673	700	4.5		
6556	B	19.0	24.2	23.7	94	27	900	940	8.5	Poss.	Yes
6557	C	19.4	24.3	24.2	108	27	850	820	8.4		

NOTE: Chest acceleration (G_r) peak values obtained by manual data reduction.

* = Instrumentation Harness on Subject's Head Displaced

TABLE XXIV. SUMMARY OF DATA FROM TESTS WITH HUMAN SUBJECTS

TEST NO.	SUBJECT NO.	SLED ACCEL. (G _x)	SLED VEL. (mph)	HEAD ACCEL. (G _r)	SEVERITY INDEX (S.I.)	CHEST ACCEL. (G _r)	FOOT LOADS LEFT (LBS)	FOOT LOADS RIGHT (LBS)	HEAD/PANEL DISTANCE (IN)	WINDSHIELD CONTACT (CORD) (DYE)
6540	G	18.1	25.9	43.5	297	35	610	680	10.3	
6541	H	18.2	26.0	31.0	240	43	703	817	7.0	
6543	I	18.7	26.5	30.0	216	33	763	794	6.6	
6544	K	18.5	26.2	49.0	339	47	700	704	4.9	
6559	E	17.6	25.5	34.1	200	33	850	800	7.6	
6563	D	18.3	26.2	38.3	166	45	951	871	10.0	
6564	F	18.2	26.2	46.2	168	31	981	871	6.6	
6561	G	18.8	28.1	58.0	373	47	740	775	7.3	
6566	I	19.2	28.2	91.2	420	35	920	890	8.1	
6567	M	18.6	27.7	40.9	229	36	974	823	5.4	
6569	B	19.5	28.0	34.1	127	34	1020	860	5.8	No
6571	G	19.4	29.7	45.6	282	46	760	744	9.0	
6572	C	18.7	29.8	42.2	150	30	715	660	4.3	
6574	H	21.1	30.8	36.8	256	33	785	820	8.1	
6575	M	20.3	30.1	50.4	297	35	900	998	6.5	

NOTE: Chest acceleration (G_r) peak values obtained by manual data reduction.

higher peak acceleration and significantly higher Severity Index associated with test number 6535.

Dye released from the indicator tape (coated with encapsulated red dye) attached to the head accelerometers mounting harness was found on the paper cover of the polystyrene windshield after tests numbers 6514, 6537, 6556 and 6569. The dye marks are shown in Figures 39, 40 and 41. The dye mark that was detected after test number 6537 occurred on the black 15-inch reference line that had been adhered to the windshield and cannot be reproduced by black and white printing. The width of the reference line was reduced prior to the next test to eliminate the recurrence of this problem.

The distances between the subject's head and the instrument panel were computed from the six cord lengths attached between the subject's head and the headrest. These distances ranged from 4.0 to 12.9 inches as reported in Table XXIV and shown in Figure 42. Figures 43 and 44 show the maximum positions of the subjects' heads with respect to the instrument panel and the polystyrene windshield as they were determined from the cord lengths. The error in the head position data obtained from the cord lengths is greatest in the vertical axis due to its dependence upon the geometry of the cord arrangement. Since the angles between the cords were necessarily small this error is large and the investigators have elected not to report the vertical positions in a quantitative manner. However, Figures 43 and 44 show that these data do indicate impact with the windshield. The last columns of Table XXIV show in a nonquantitative manner where the cord measurements indicated where windshield contact was possible or where it apparently occurred compared to the dye indications of impact.

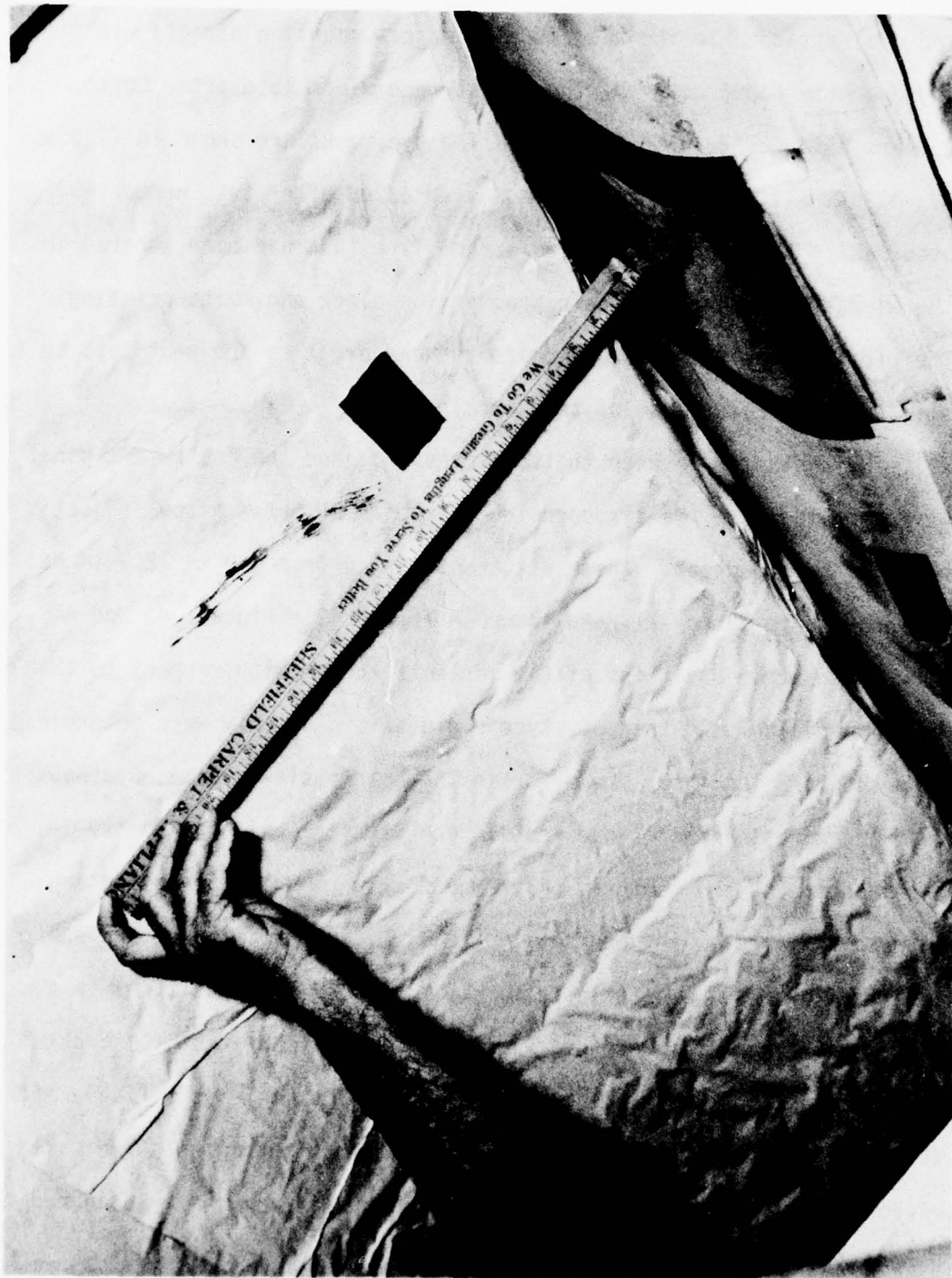


Figure 39. Dye Mark on Windshield - Test No. 6514



Figure 40. Dye Mark on Windshield - Test No. 6556

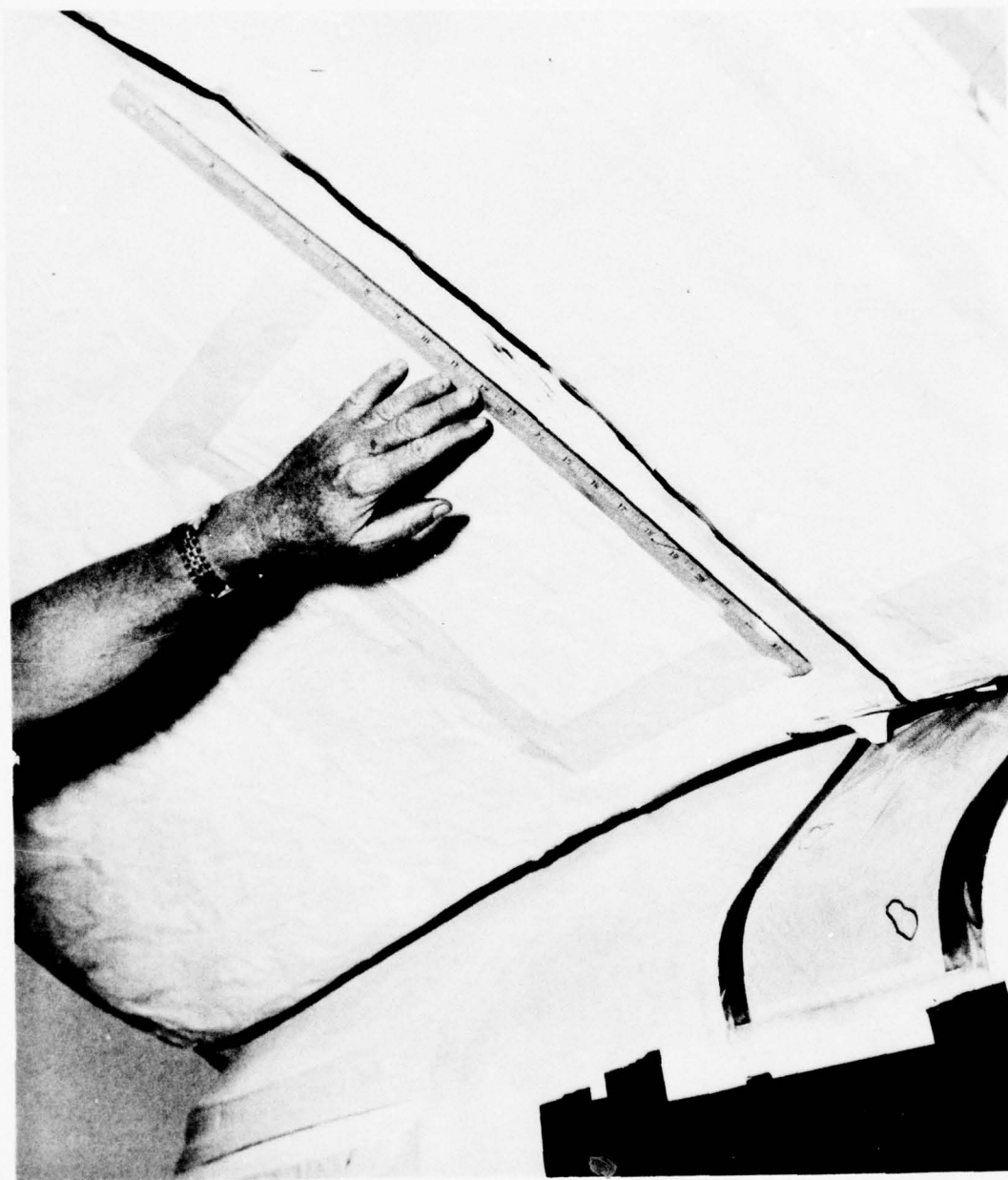


Figure 41. Dye Mark on Windshield - Test No. 6569

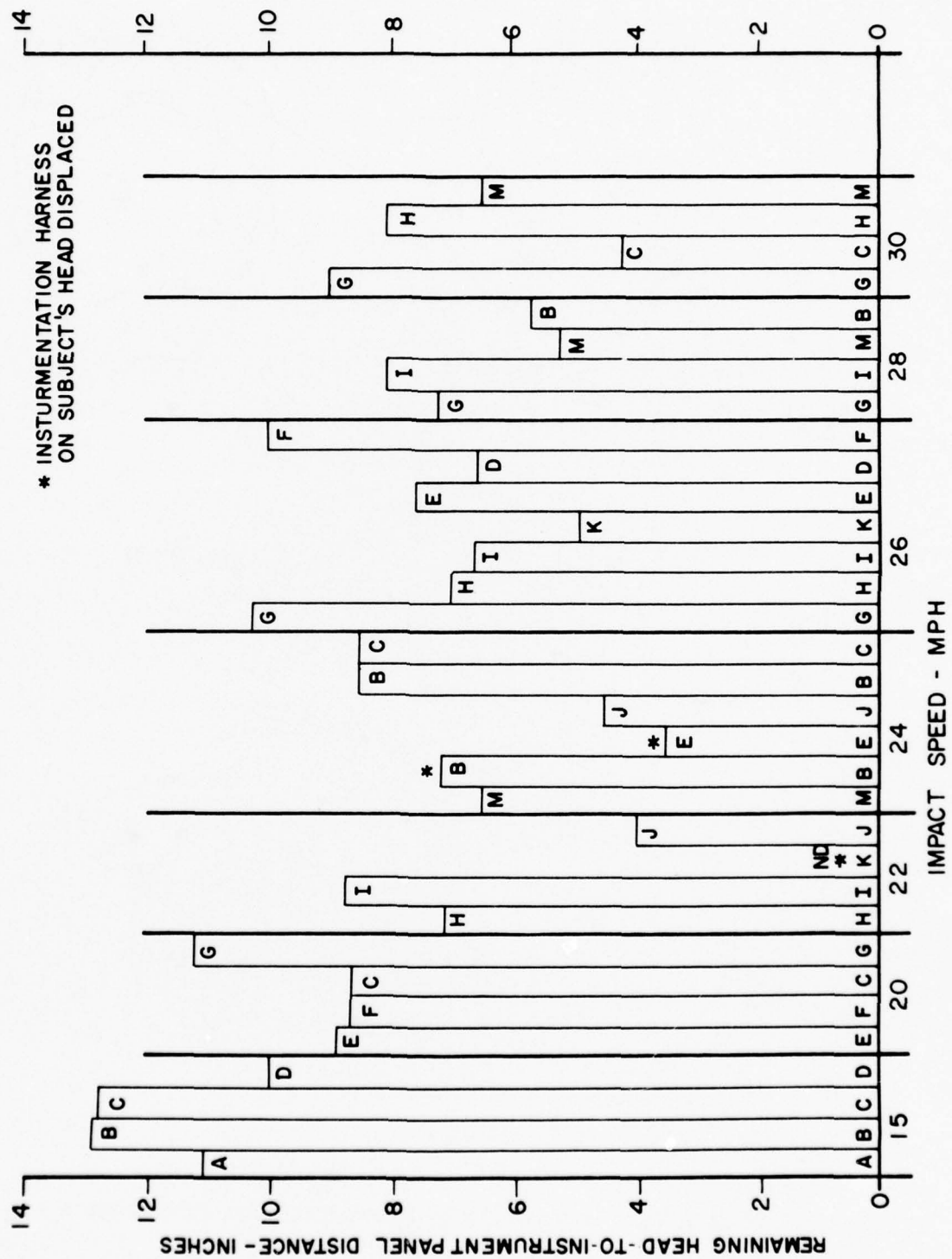


Figure 42. Histogram of Remaining Head-to-Instrument Panel distance for Each Test

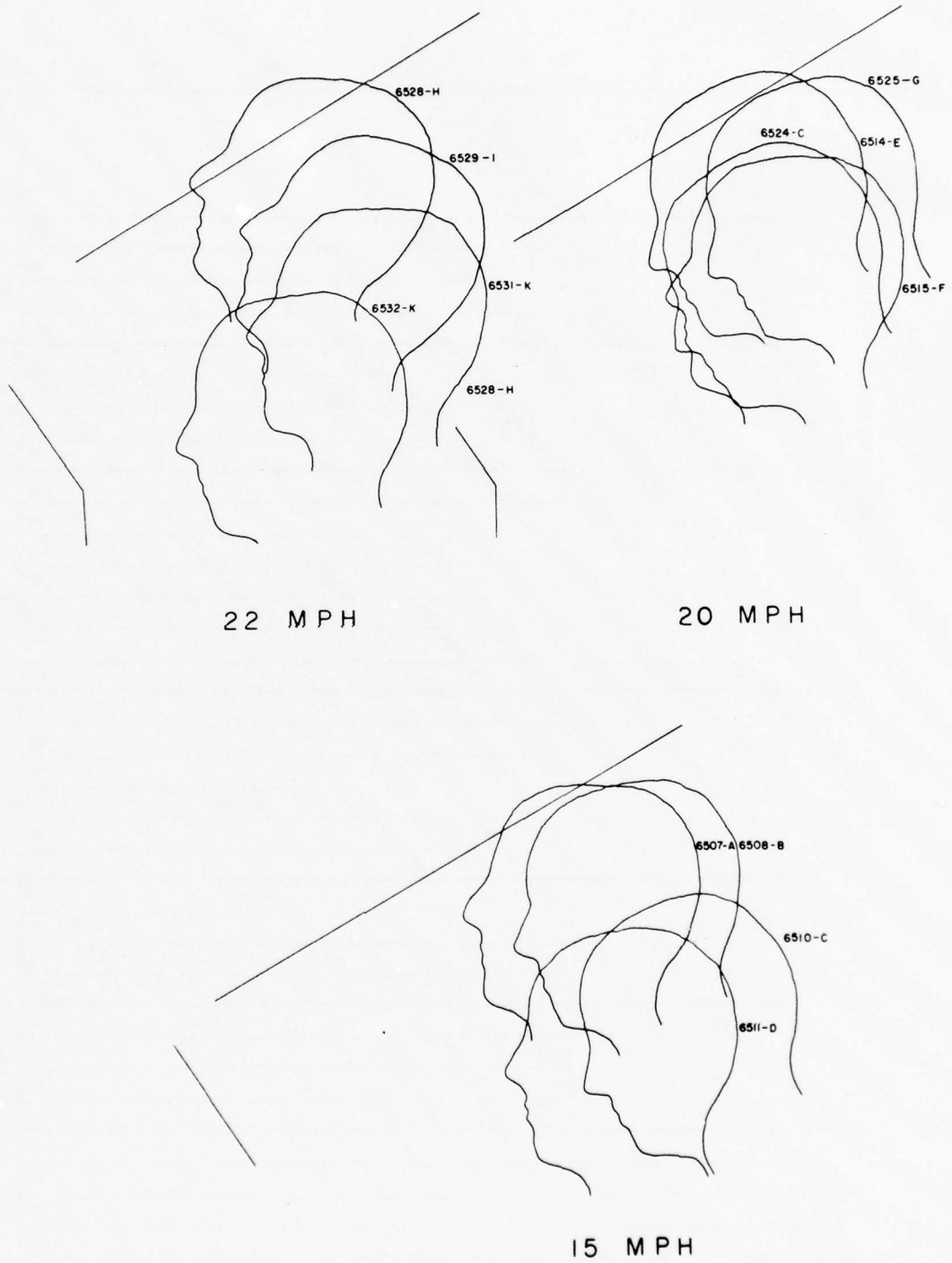


Figure 43. Head Positions Determined from Cord Lengths - 15, 20 and 22 MPH Tests

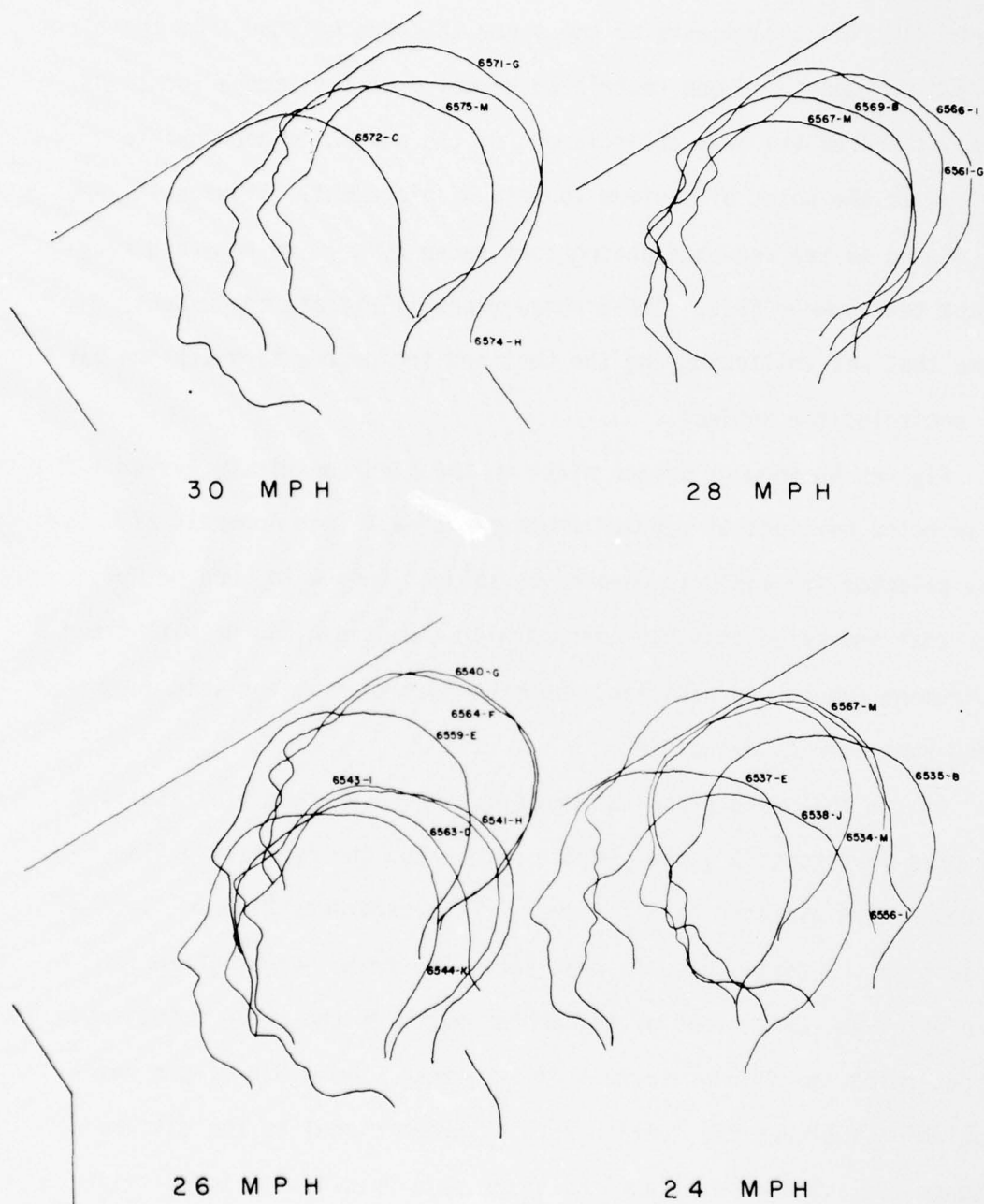


Figure 44. Head Positions Determined from Cord Lengths - 24, 26, 28 and 30 MPH Tests

Determining the positions of the subjects' heads from photometric data was quite difficult and time consuming. The quality of the photometric data is poor because of the smoke that was emitted from the air bag during impact and the restricted geometry of the camera locations necessitated by the near encirclement of the subject's head by the air bag at the point of maximum forward displacement. Figures 45, 46, 47, 48 and 49 are sequence photographs taken by a 70 mm camera during impact test number 6575. These photographs illustrate the amount of smoke that was emitted during the test and the degree to which the air bag encircled the subject.

Figures 50 through 60 are plots in the Sled Coordinate System (SCS) of selected portions of reduced photometric data (see Appendix F). The runs selected for analysis were human subject runs with cord or dye data that indicated possible contact with the windshield or with the instrument panel. In addition, photometric data from the last four high speed runs were also included.

In the following graphical presentation of photometric results (Figures 50 through 60) the plotted points and the connecting lines represent the averaged path followed by the reference fiducial located closest to the test subject's left ear. The frame number given for each point was the number of the center point of the three points used to determine the sliding three point average. The width of the envelope which includes the average path is proportional to the difference between the average point and the three data points used to calculate average point location. The plotted value is the component of the total difference perpendicular to the direction of travel as described in

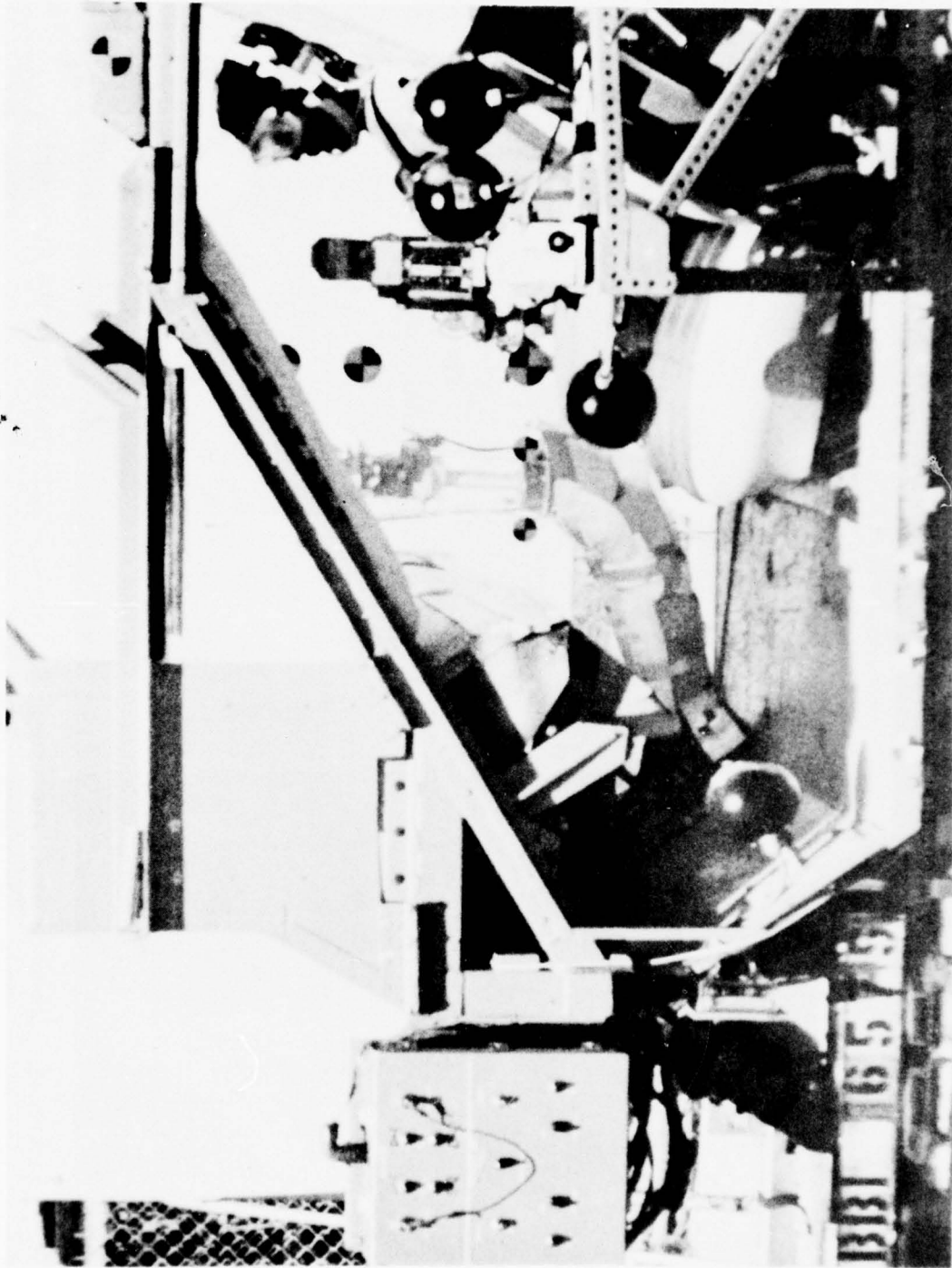


Figure 45. Sequence Still Photograph 1 at Instant of Air Cushion Deployment Initiation

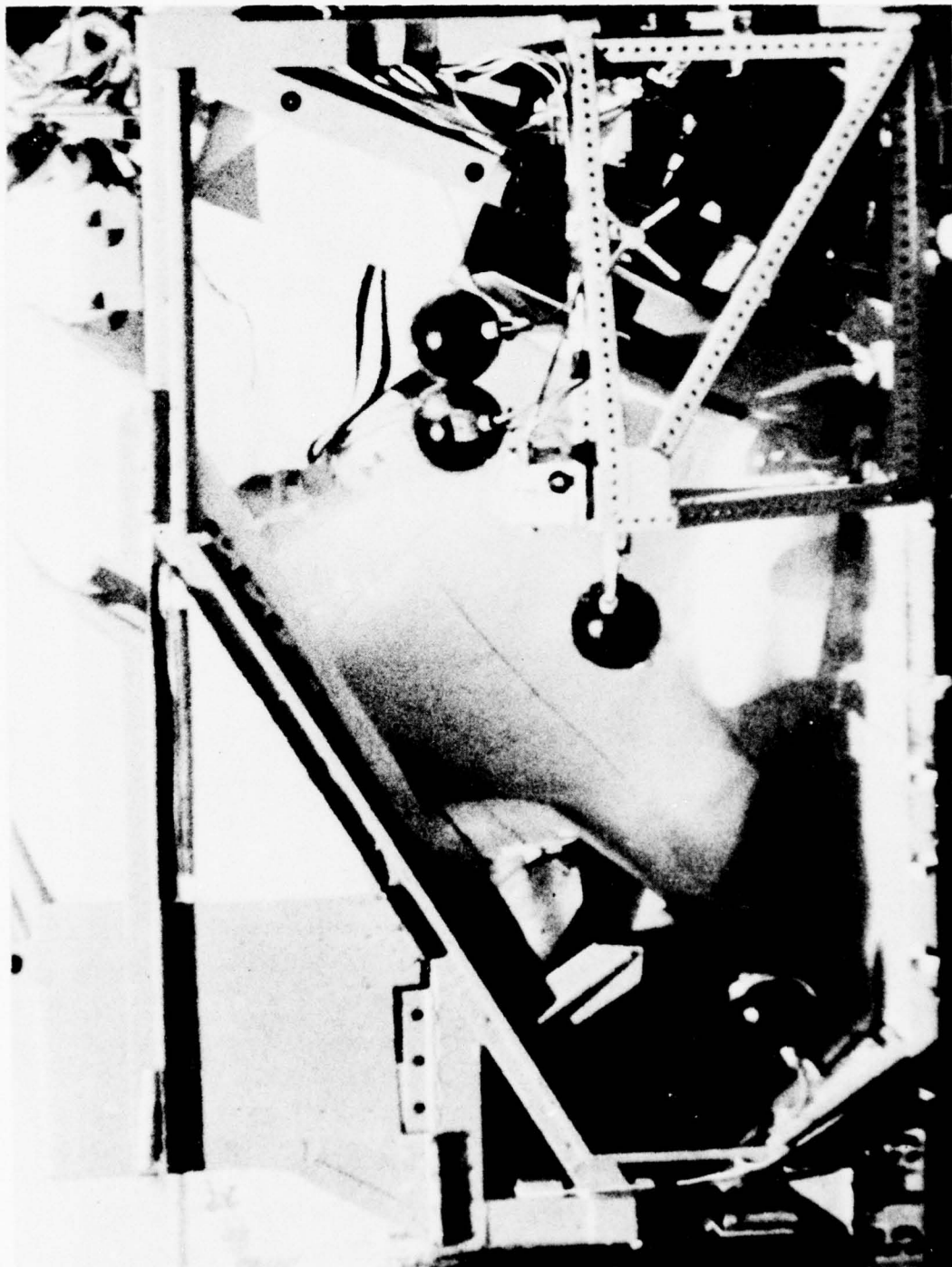


Figure 46. Sequence Still Photograph 2 Showing Subject Impacting the Air Cushion

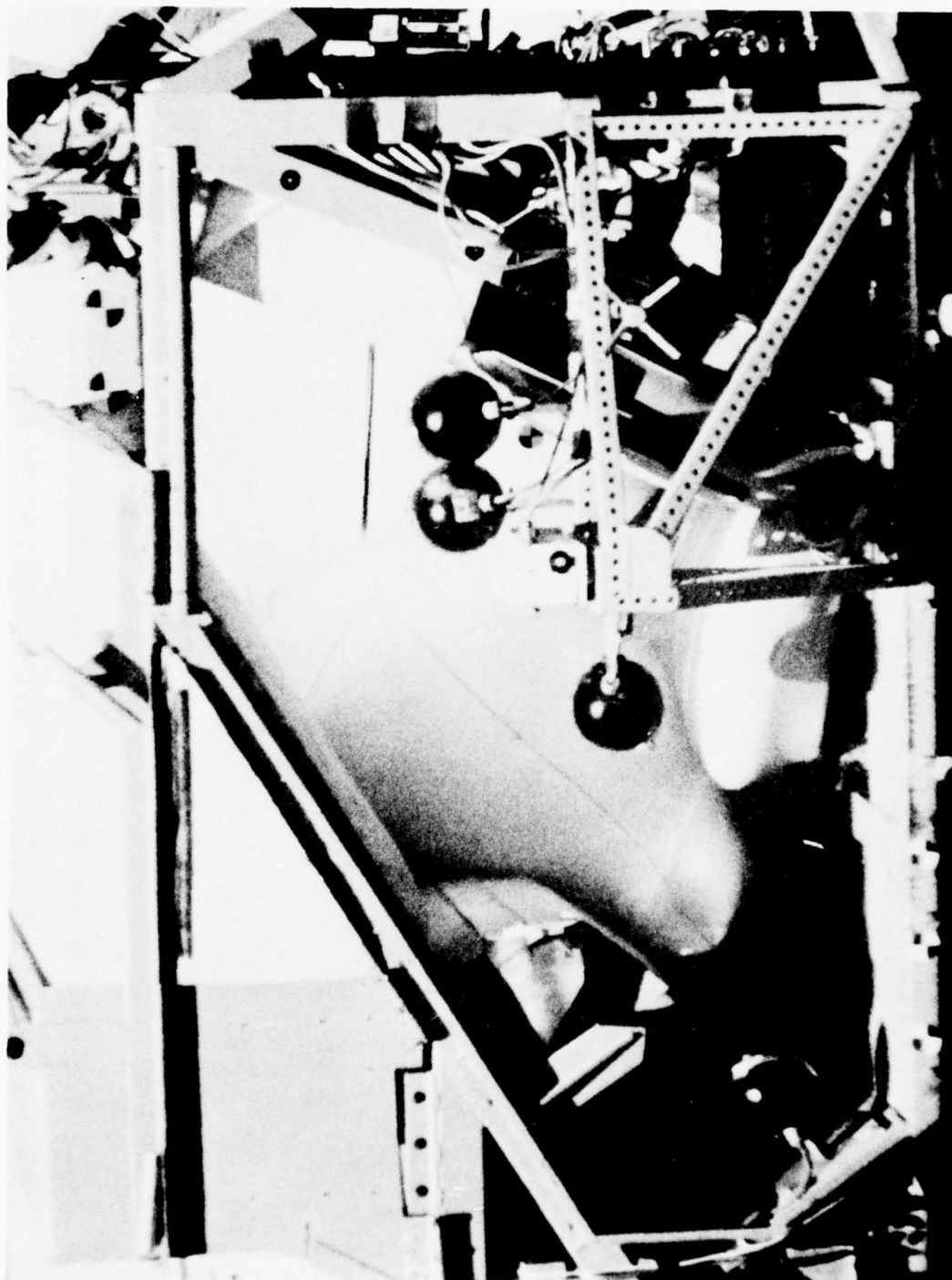


Figure 47. Sequence Still Photograph 3 Showing the Air Cushion Encircling the Subject

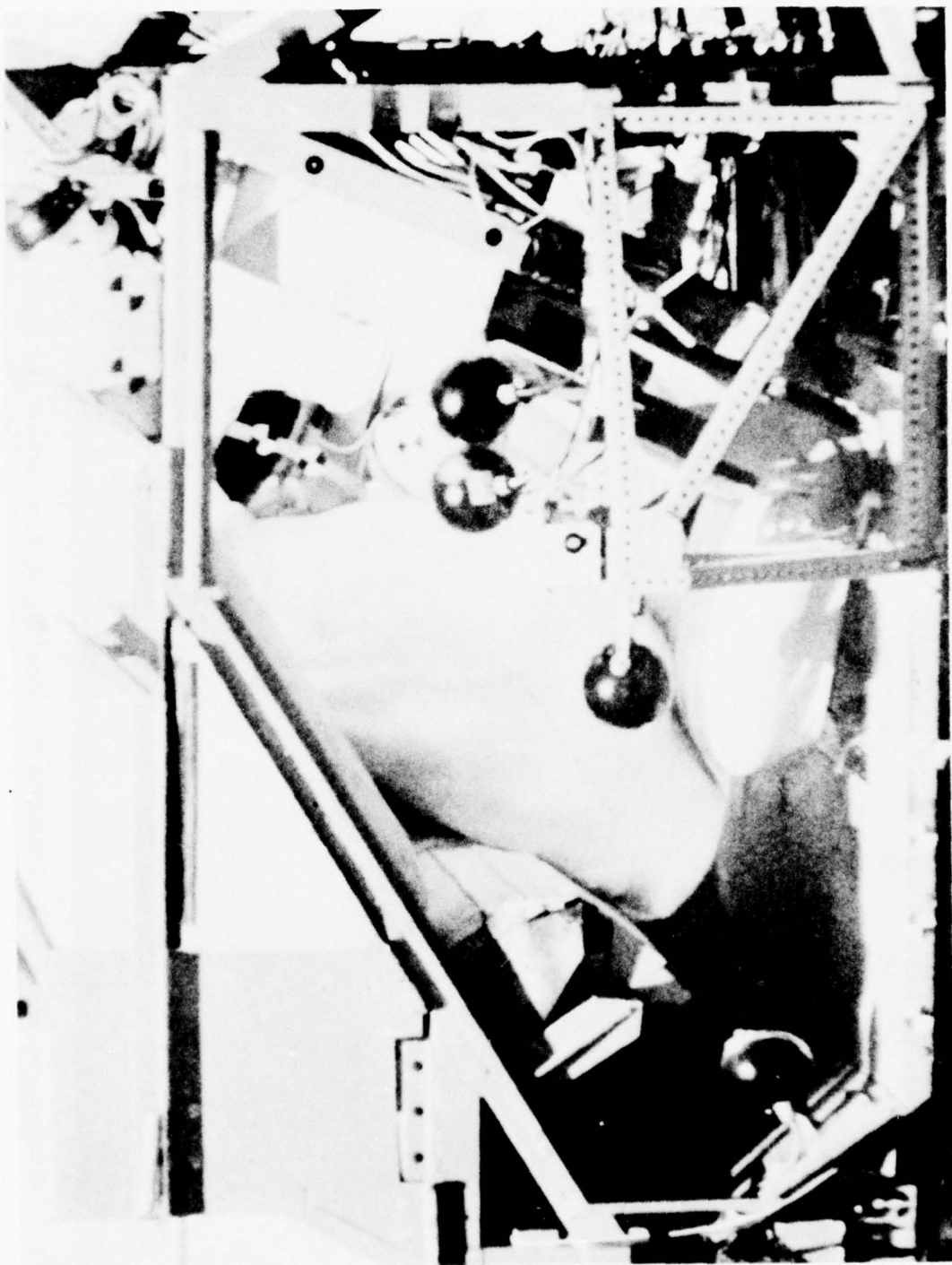


Figure 48. Sequence Still Photograph 4 Showing the Subject Rebounding from the Air Cushion

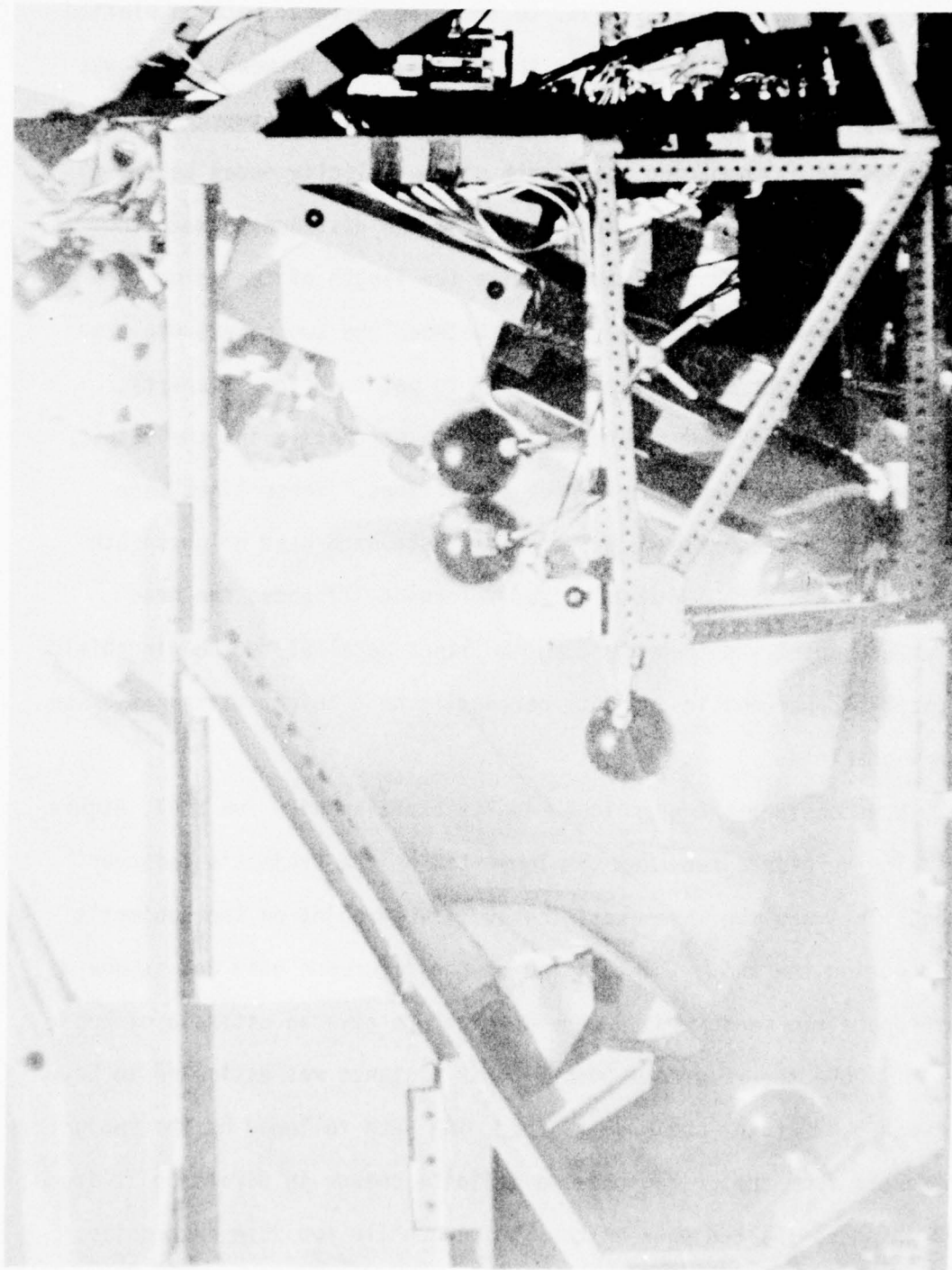


Figure 49. Sequence Still Photograph 5 Showing the Subject Returned to the Seat Backrest

Appendix F. The velocity indices given on each figure represent the distance which would be covered at an average velocity of 10 feet per second for an elapsed time equal to the time interval between plotted points. For most of the figures the elapsed time between points was approximately 2 milliseconds. The average velocity between points can be estimated by comparing the length of the velocity index to the distance between points. For example, if the distance between two plotted points was approximately twice the length of the velocity index line then the average velocity between the two points would be about 20 feet per second (applies only to points 2 frames apart). Plotted on most of the figures are the 5th percentile and the 95th percentile windshield interference limit lines. These lines were determined for each figure by estimating standard head heights (5th percentile and 95th percentile from reference 17) above the head reference point and then plotting two lines parallel to the windshield located 5th percentile and 95th percentile head height distances below the windshield.

Now consider the graphical results starting with run 6507, Figure 50. The reference read was the lower tip of the subject's left ear lobe. This was the most consistently visible point on the subject's head during the run. The location of the reference used and standard anthropometric measurements were combined to give an estimate of head height above the reference point. This distance was estimated to be between 5.82" (5th) and 6.98 (95th). The path followed by the subject on recoil from the airbag shows a definite change in direction at frame 170 which is located between the 5th percentile and 95th percentile

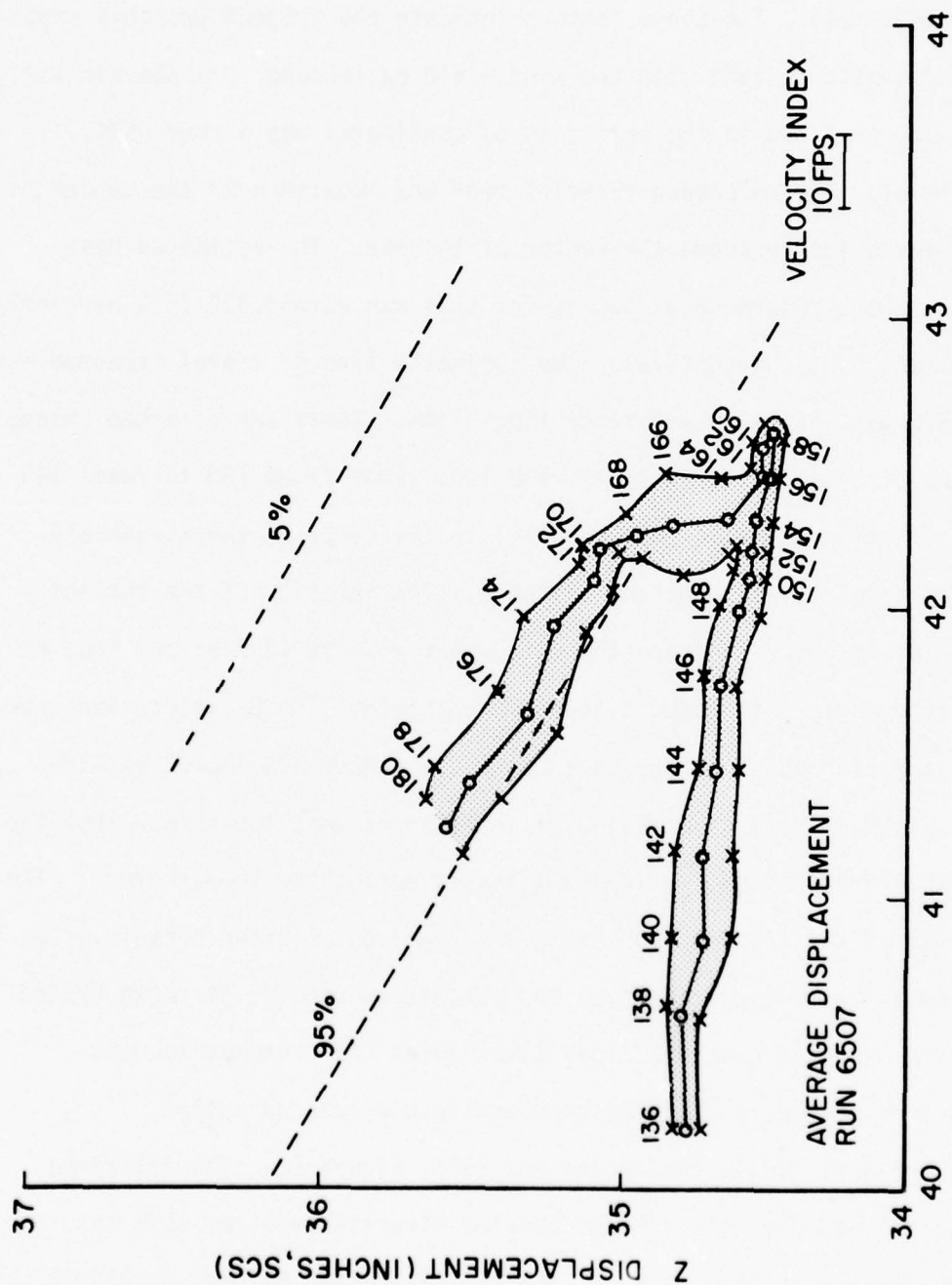


Figure 50. Photometric Head Position Trajectory Within Sled Coordinate System - Test No. 6507

interference limit lines. After frame 170, the rebound path assumes a track parallel to the limit lines. Subject velocity immediately prior to frame 170 was relatively low and at an acute angle with respect to the windshield. The above factors indicate the subject probably experienced a mild contact with the windshield on rebound from the air bag.

The next run in the series to be considered was number 6514, Figure 51. The reference fiducial read was located over the subject's left ear slightly above the center of the ear. The estimated head height above reference distances for this run were 4.35" (5th percentile) and 5.35" (95th percentile). The subject's line of travel exceeded even the 5th percentile interference limit line. There was a marked change in the direction of travel at frame 130. From frame 130 to frame 140 the direction of travel was parallel to the slope of the windshield and at a relatively constant distance. The velocity of the subject immediately prior to frame 130 was probably 10 to 15 feet per sec. at an acute angle with respect to the windshield. These factors indicate the subject probably experienced at least a moderate impact with the windshield. In fact, a review of the film of this run showed that the windshield was actually displaced upward during the impact event. The rebound of the subject from the air bag was not plotted because of a marked lateral displacement of the subject on rebound as shown by the onboard overhead cameras. This invalidates the photometric data reduction procedure which assumed negligible lateral motion.

The next run in the series was 6528, Figure 52. The reference fiducial read for this run was located directly over the left ear approximately at the tragon. The estimated head heights above the

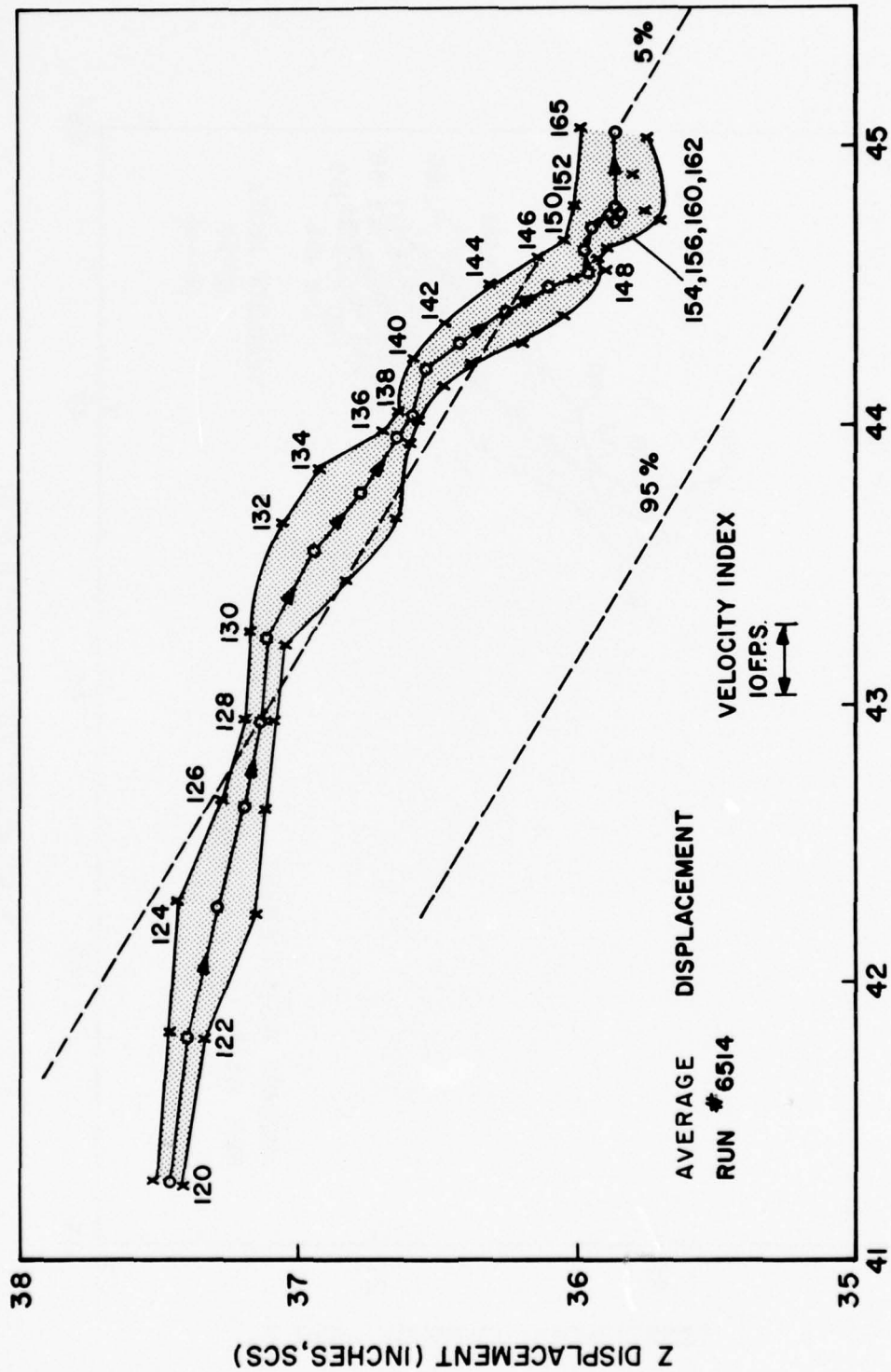
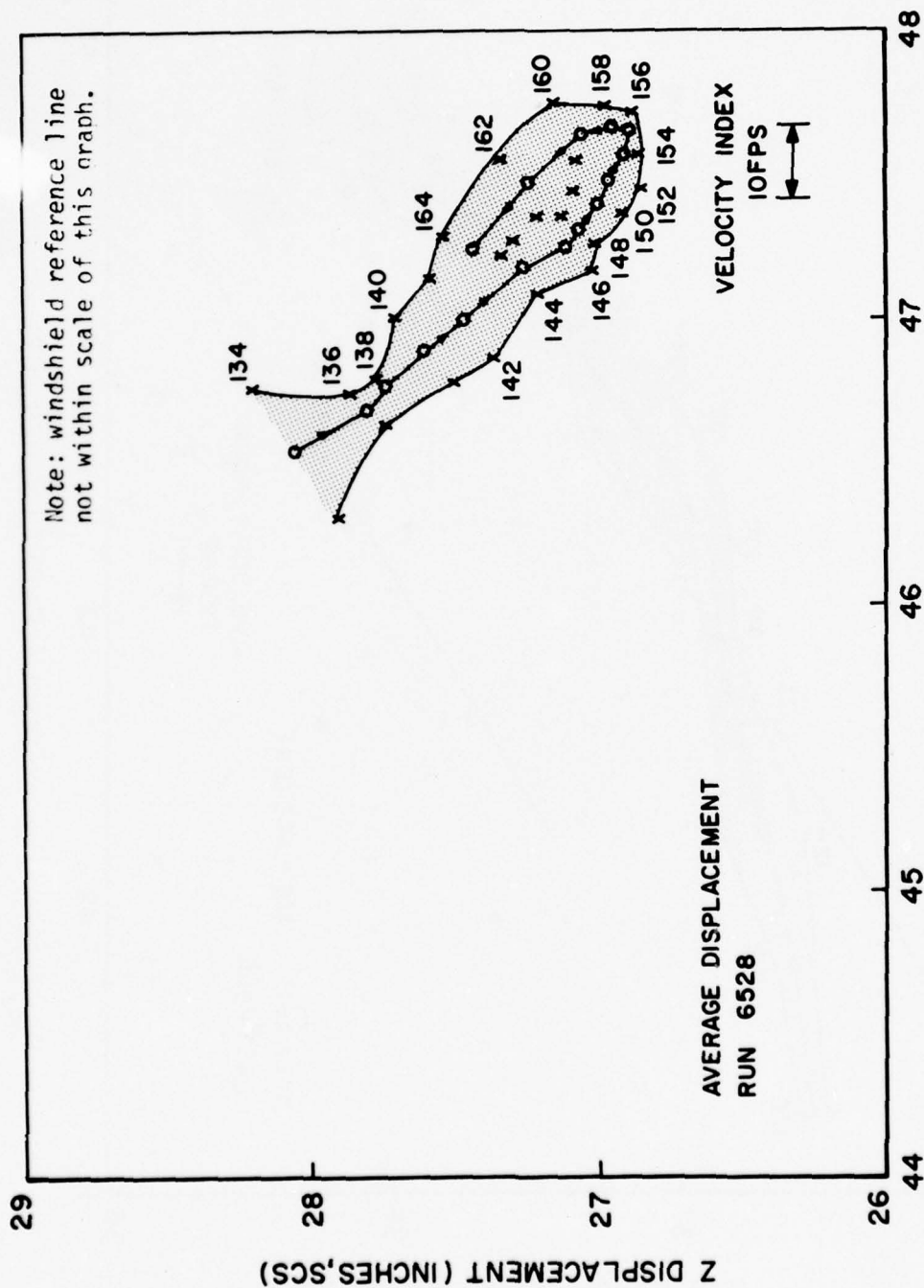


Figure 51. Photometric Head Position Trajectory from Test No. 6514



X DISPLACEMENT (INCHES, SCS)

Figure 52. Photometric Head Position Trajectory from Test No. 6528

reference fiducial for this run were 4.6" (5th percentile) and 5.6" (95th percentile). The path followed by the subject and the spacing between points indicates a smoothly decreasing velocity up to the point of inflection followed by a mild velocity increase probably due to recoil from the air bag. Clearance between the subject's head and the windshield was sufficient to prevent plotting, at this scale, of the inflection point and the interference limit lines on the same graph.

Compared to run 6528, run number 6534, Figure 53 had much larger variations in both velocity and displacement indicating what was probably a much rougher ride for the subject. The reference fiducial read was located slightly above and slightly in front of the ear center. In the vertical direction, the reference was located at about the level of the tragon. This location of the reference fiducial led to the standard head heights above the reference of 4.6" (5th percentile) and 5.6" (95th percentile). There did not appear to be any head-windshield contact in the plotted portion of the data; however, the unsmoothed data available for frames prior to 124 indicates head contact with the windshield may have occurred prior to frame 124. The estimated velocities of 10 to 15 feet per second just prior to the inflection point were as high or higher than those measured in any of the other runs. In addition, the X displacement was greater for this run than for any of the other runs, including those with a higher sled velocity. If there was an instrument panel impact during the human tests it would have been in this run because the reference fiducial to instrument panel clearance was a minimum during this test.

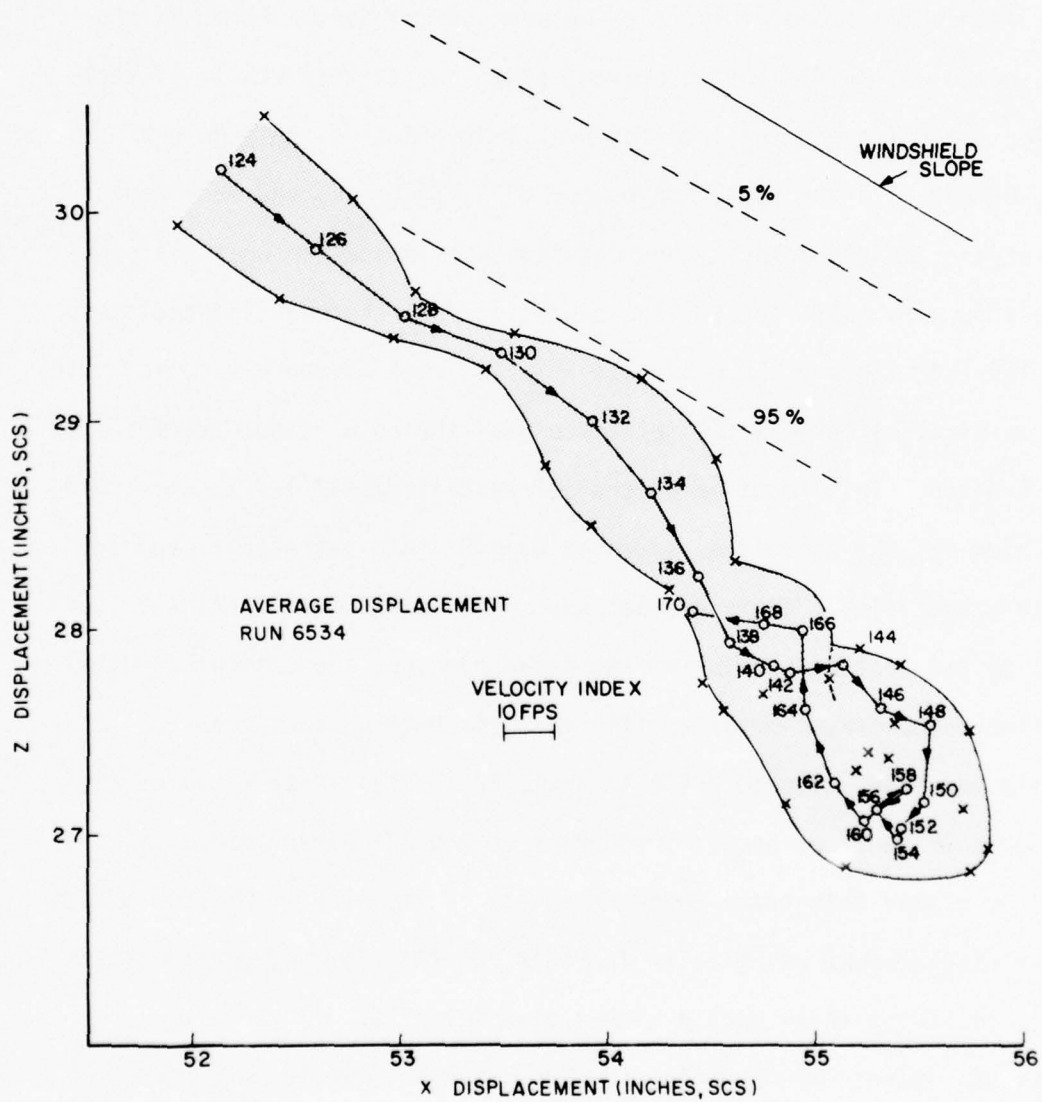


Figure 53. Photometric Head Position Trajectory from Test No. 6534

The reference fiducial read for run number 6537, Figure 54, was located directly over the left ear (tragion). With the reference in this location the two head height values become 4.6" (5th percentile) and 5.6" (95th percentile). There were no indications of head contact with either the windshield or the instrument panel in the plotted segment of the data; however, unsmoothed data from frames 96 to 110 indicate head-windshield contact probably occurred (see Appendix F). The path followed by the subject was reasonably smooth with a steady decrease in velocity indicated up to the point of inflection after which a slight increase in velocity was noted probably due to recoil from the air bag.

The next run considered was number 6556, Figure 55. The reference read in this case was located just below the head band intersection and slightly above the ear center. The head height above the reference fiducial was estimated to be between 4.35" (5th percentile) and 5.35" (95th percentile). There was a definite indication of head contact with the windshield during this run. The plot of the subject's head motion path indicates the possibility of head contact with the windshield up to frame 126 at which point a moderate change in the direction of travel did occur. The estimated velocity of the subject's head was low throughout the plotted portion of the data ranging from near 0 to about 8 feet per second.

The reference fiducial read for run number 6569, Figure 56 covered the left ear. The head height above the reference fiducial was estimated to be between 4.6" (5th percentile) and 5.6" (95th percentile). The subject's head rotated approximately 45° or more counterclockwise after

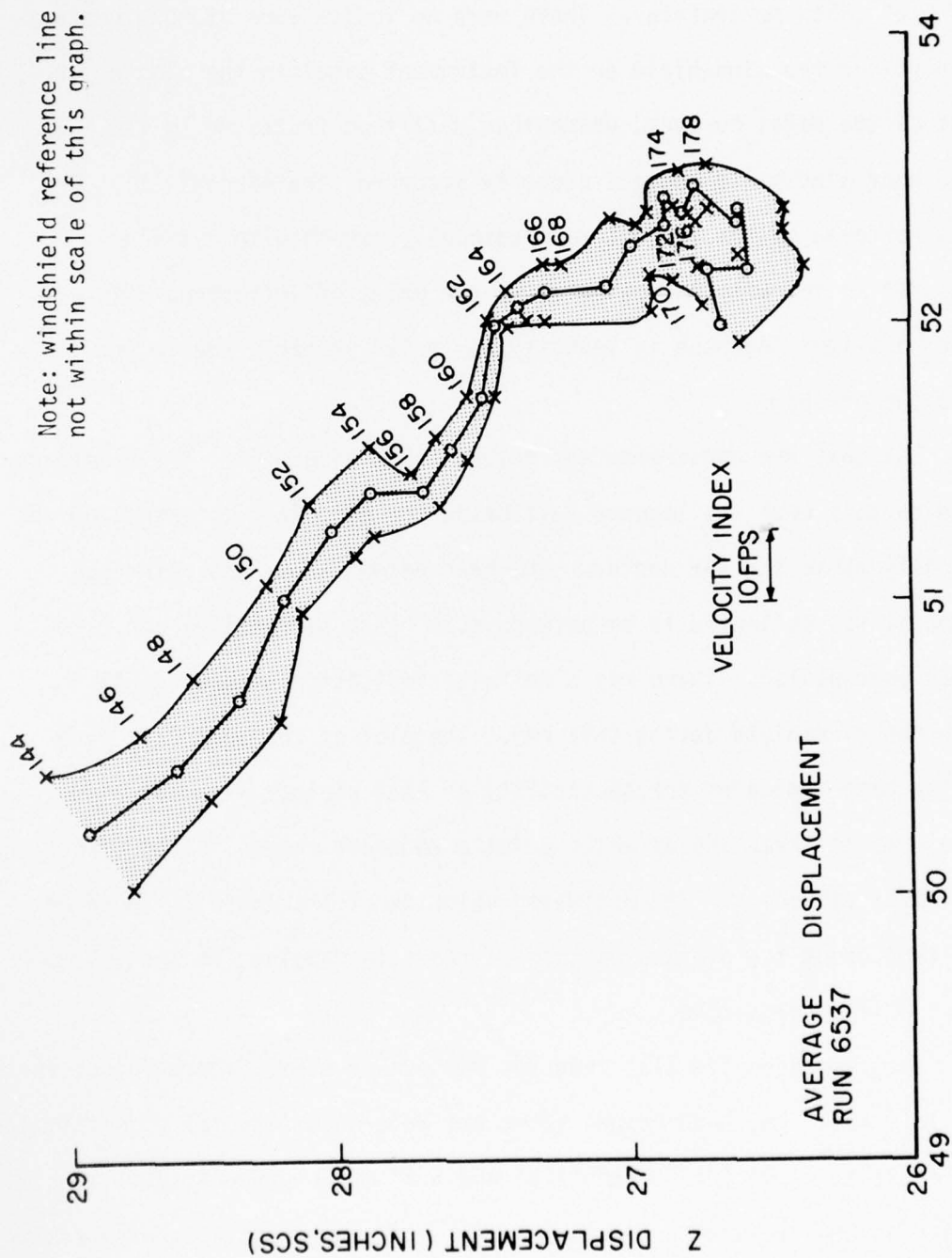


Figure 54. Photometric Head Position Trajectory from Test No. 6537

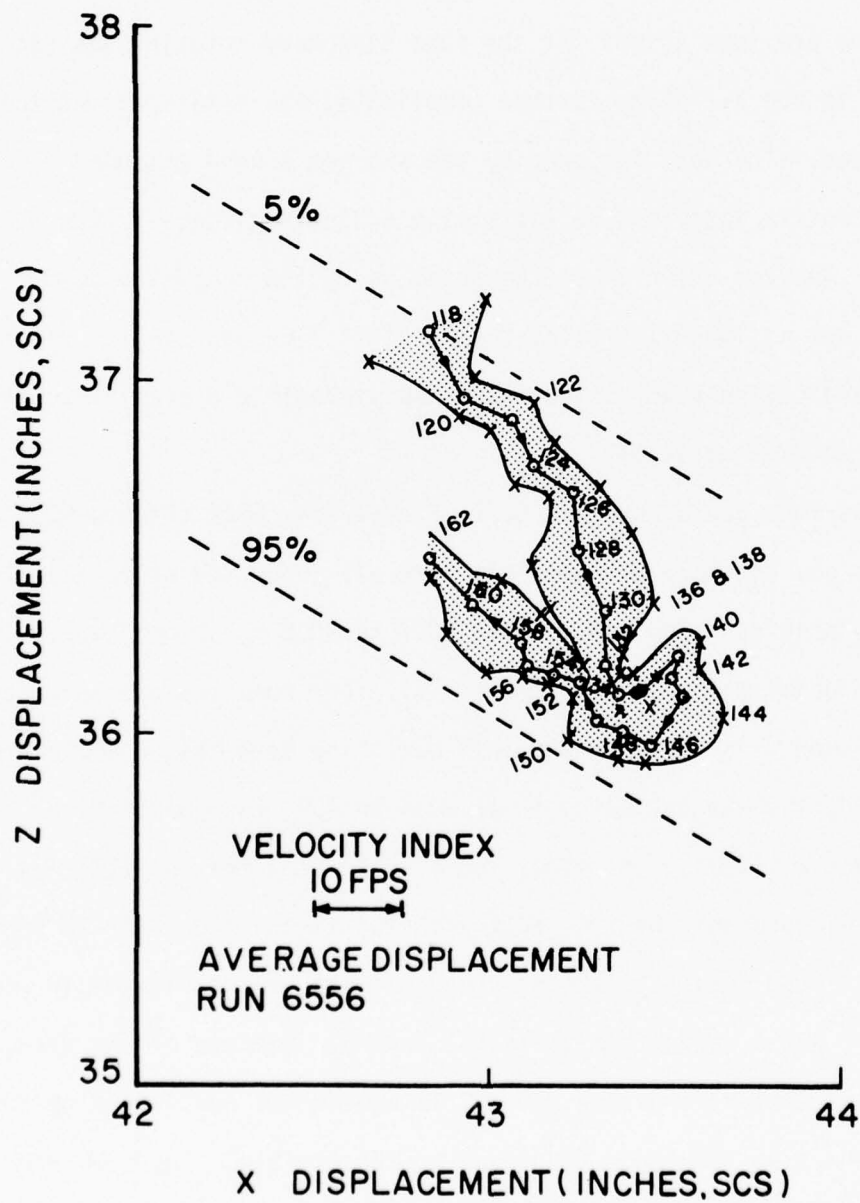


Figure 55. Photometric Head Position Trajectory from Test No. 6556

contact with the air bag which could account to some extent for the "S" shape of the plotted path. As the individual's head rotated counter-clockwise the reference fiducial located at the left ear would tend to travel in the negative "X" direction. Conversely, on rebound from the air bag, the subject's head returned to a forward looking position thus reversing the previous trend. At the same time head rotation was occurring, motion in the X-Z plane further complicated the trajectory of the subject's head. The path followed by the subject's head exceeded even the 5th percentile interference limit line indicating contact with the windshield. Average velocity at the point where the subject's head motion path was no longer parallel to the limit line was still 10 feet per second indicating head contact with the windshield probably occurred at moderate to high velocity.

The last four tests, numbers 6571 (Figure 57), 6572 (Figure 58), 6574 (Figure 59) and 6575 (Figure 60), were all conducted at relatively high sled velocities which ranged from 29.7 to 30.8 miles per hour. The reference fiducial read was the same for all four runs and was located on the head band directly over the left ear. The head height above the reference fiducial was estimated to be between 4.6" (5th percentile) and 5.6" (95th percentile) for all four tests. The plot for run 6571 indicated there was probably head contact with the windshield prior to frame 111. Subject head velocity leaving the proximity of the windshield was probably high but a good estimate is not possible because of the irregular interval between frame readings. This unevenness was caused by the masking of the sled reference fiducials by the air bag. The same air bag interference with the film reading process occurred during run 6572

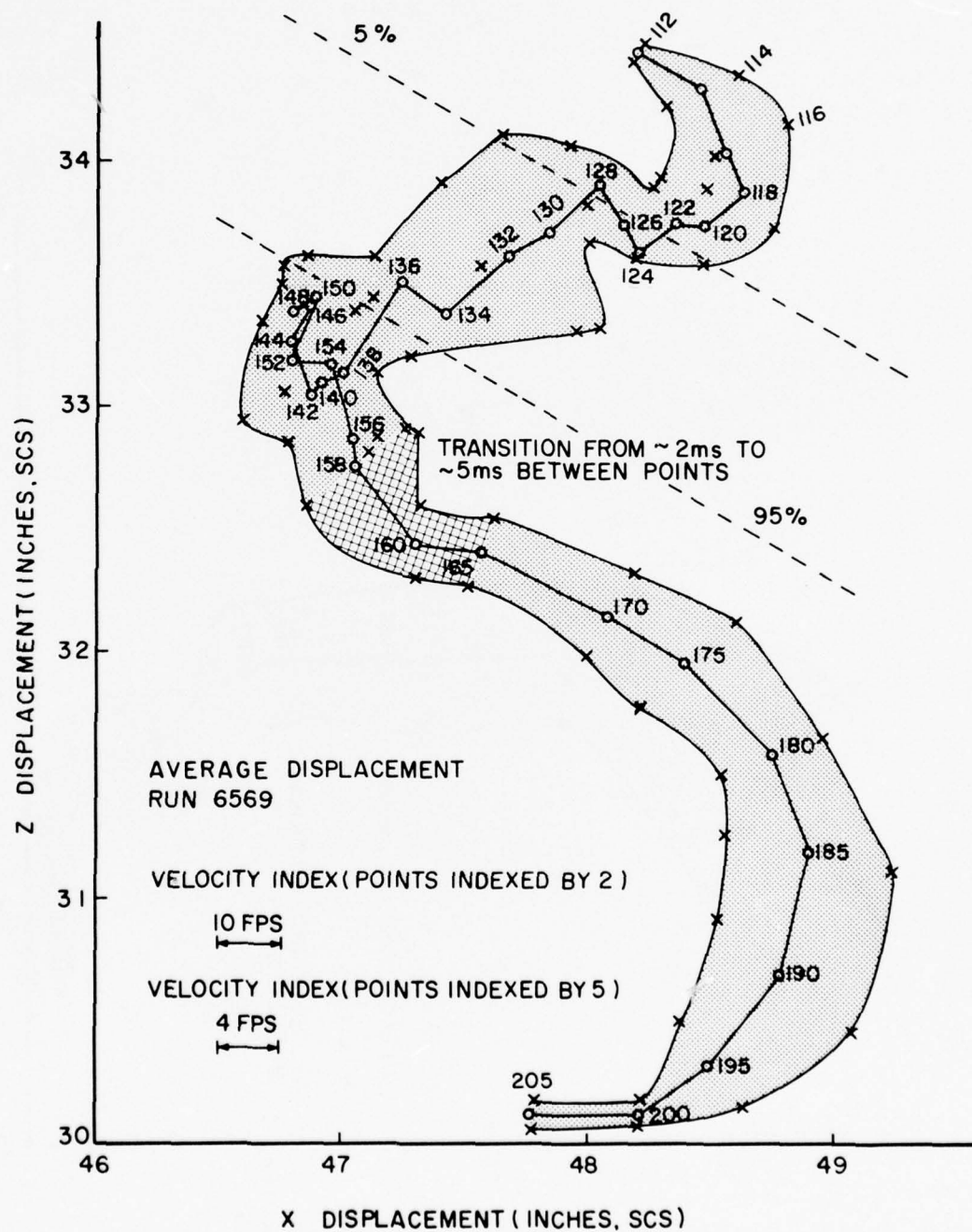


Figure 56. Photometric Head Position Trajectory from Test No. 6569

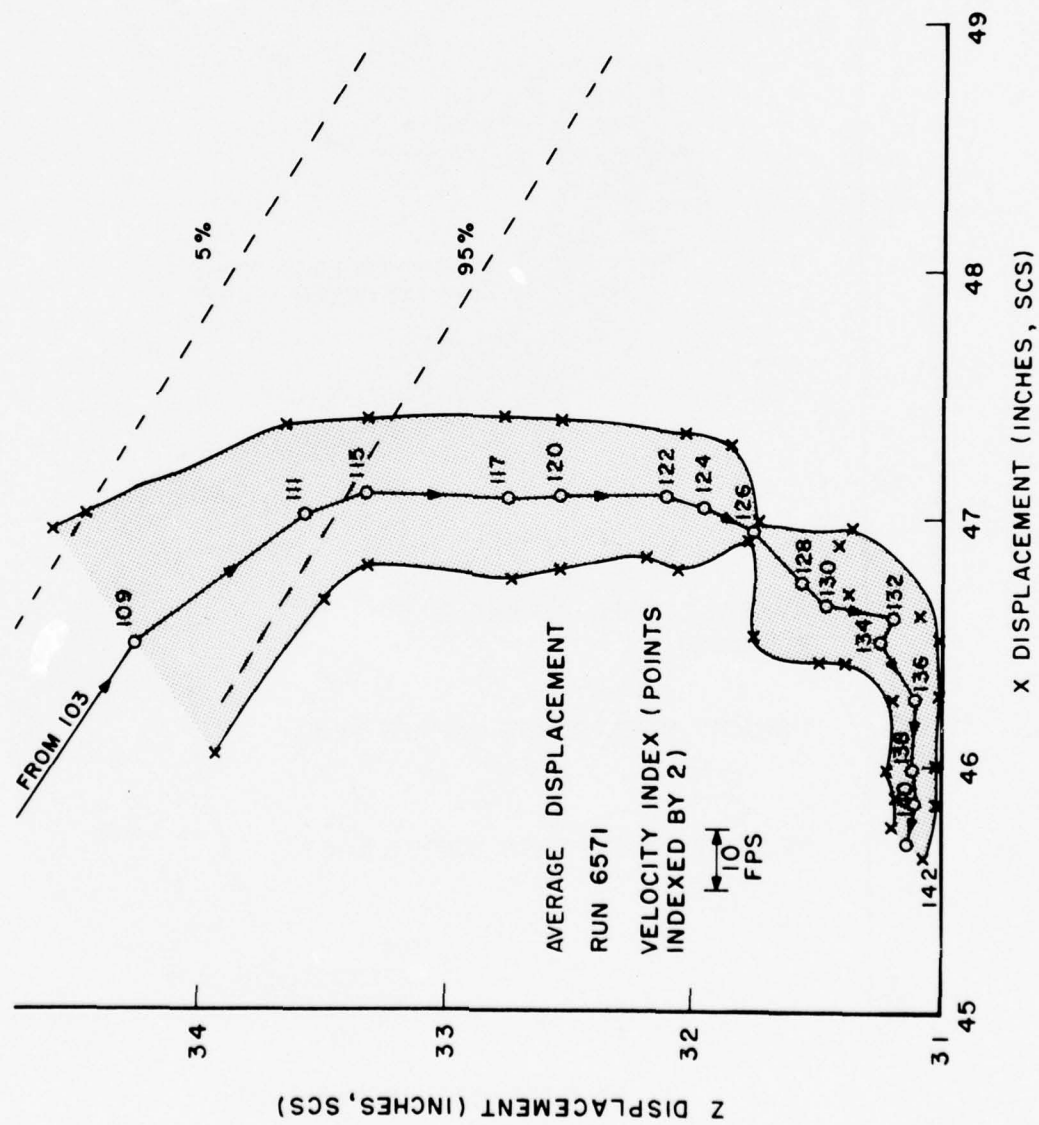


Figure 57. Photometric Head Position Trajectory from Test No. 6571

(Figure 58) making it impossible to track the subject into the point of inflection. There was no photometric evidence of head contact with the windshield in tests 6572, 6574 and 6575. The approach to the inflection point in test numbers 6574 and 6575 was at a relatively high velocity; however, the change in direction was accomplished with more than adequate clearance between the subject's head and the instrument panel or windshield.

The final graph to be considered is Figure 61 which depicts the maximum "X" displacement of the head reference points for each of the runs for which photometric data was analyzed. A consideration of the previously discussed figures will show that the maximum "X" and maximum "Z" displacements do not always occur at the same time, thus this figure does not represent windshield clearance but rather the maximum displacement of the subject from the starting point.

A time-based consideration of the inflection points of the various runs indicates the turn-around occurs quicker for the high speed runs. For example, the average time to the inflection point in the last four runs was about 130 milliseconds while for the three slowest runs (6507, 6514, and 6528 this same point occurred at about 165 millisecond after the impact event.

Table XXV provides a tabulation of the sled acceleration and a comparison of peak accelerations measured during impact and rebound of the chest and head. The acceleration values that are reported here are the maximum accelerations measured by the x axis accelerometers.

The maximum values of the chest and head resultant acceleration, the head impact Severity Index, and the Head Injury Criteria computed

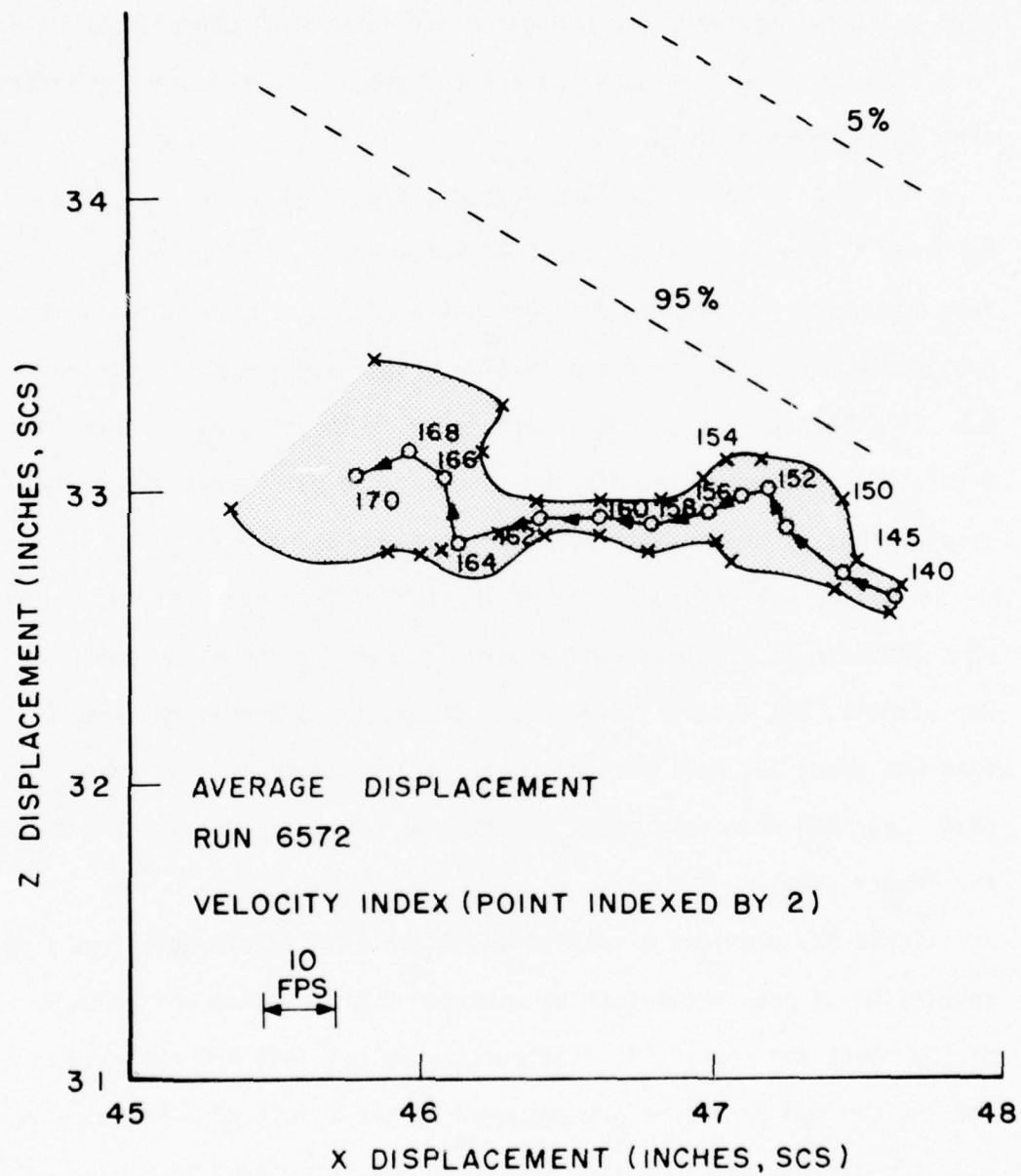


Figure 58. Photometric Head Position Trajectory from Test No. 6572

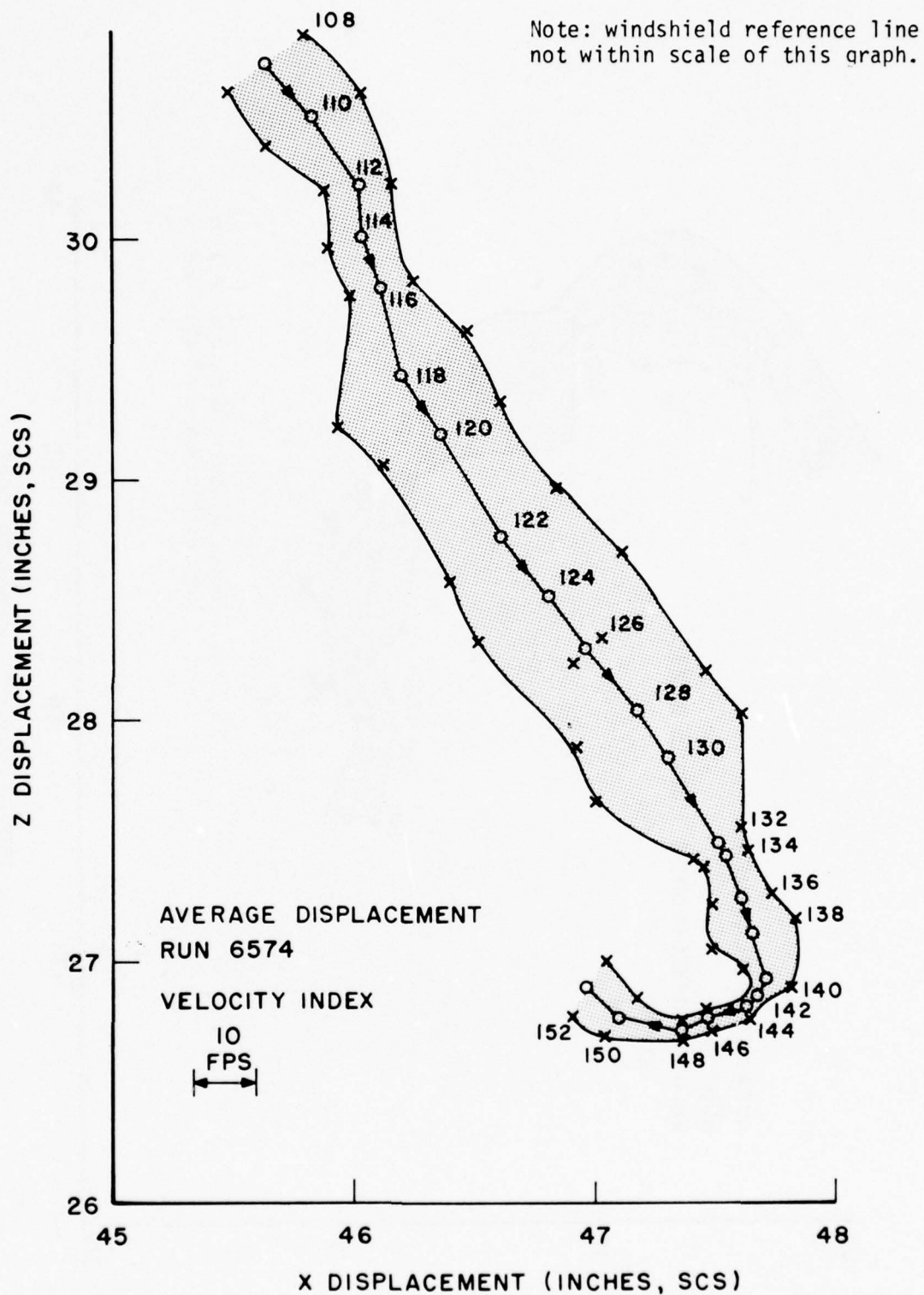


Figure 59. Photometric Head Position Trajectory from Test No. 6574

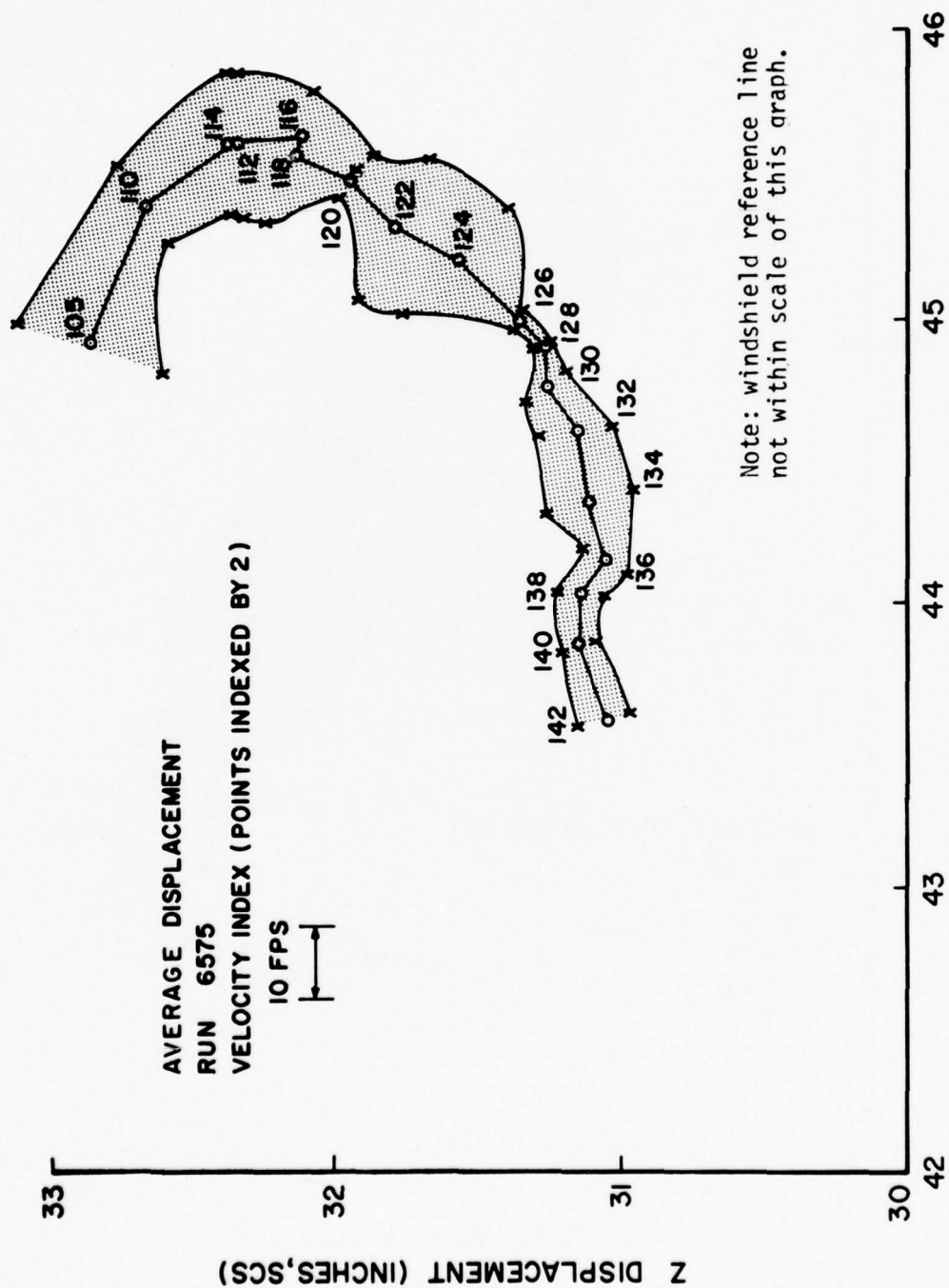


Figure 60. Photometric Head Position Trajectory from Test No. 6575

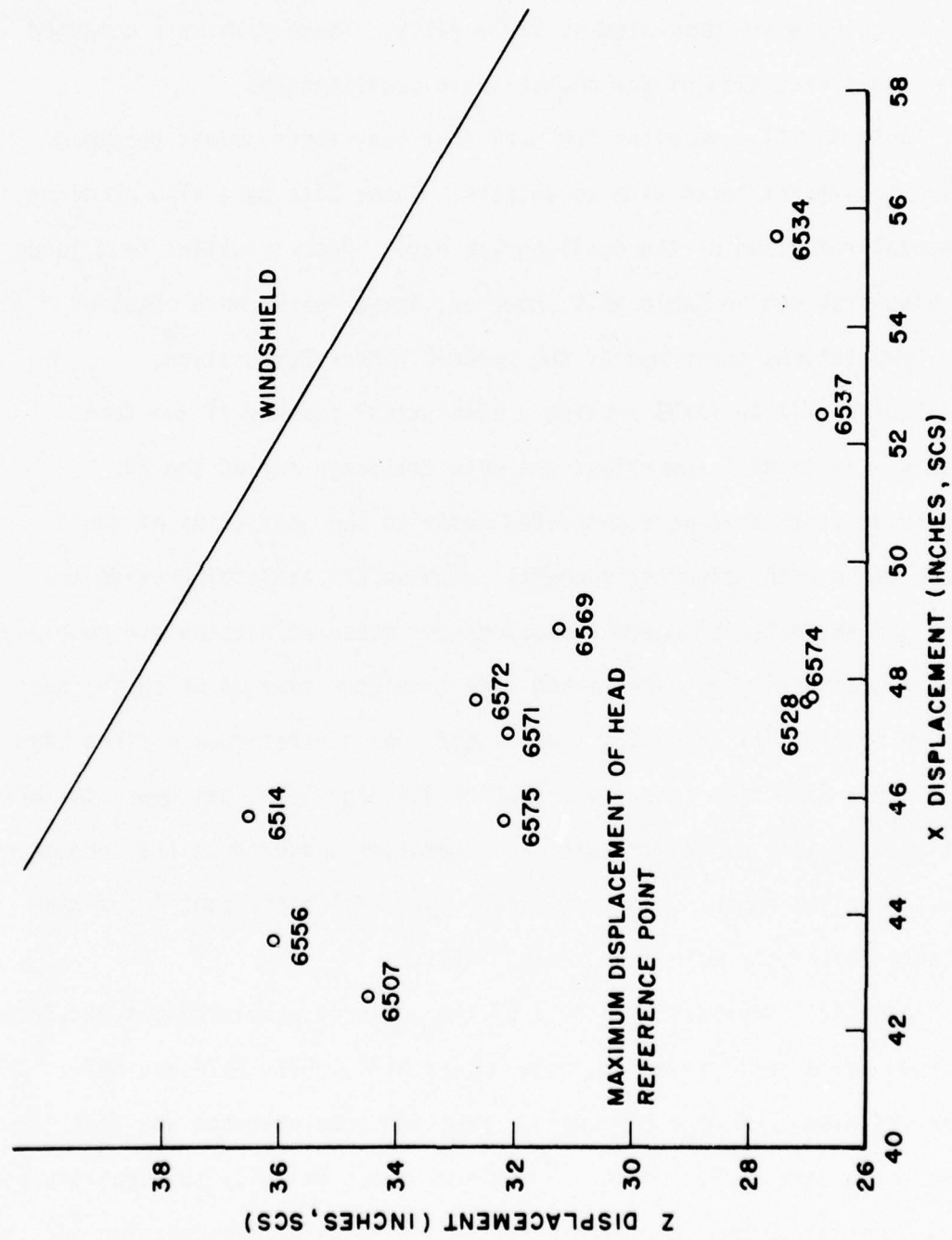


Figure 61. Maximum Displacements of the Head Reference Points

by the General Motors Corporation are provided in Table XXVI. The acceleration level (designated G) and computation interval (designated t) where the maximum H.I.C. occurred are also listed.

Peak x, y and z axis accelerations measured in the subject's mouth and on the head are presented in Table XXVII. These data were obtained from manual reduction of the photographic oscillographs.

Table XXVIII summarizes the peak foot load measurements recorded during the impact tests with volunteers. These data were also obtained by manual reduction of the oscillograph data. Peak resultant foot loads are also provided in Table XXIV; however, these values were obtained from computations performed by the General Motors Corporation.

Tables XXIX to XXXVI provide a statistical summary of the test results. Table XXIX summarizes the data collected during the 20 successive tests that were completed prior to the initiation of the impact tests with volunteer subjects. Tables XXX to XXXVI provide the means and estimated standard deviations for measured data on air cushion performance parameters such as bag fire time (the time at which the gas storage bottle seal detonator and lo-level gas generator were fired) and the hi-pyro fire time (the time at which the high level gas generator was initiated as well as the triaxial accelerations measured on the subject's head, chest and mouth. The statistical analysis of the foot loads was conducted using the data from Table XXVIII.

Appendix G provides printouts of the measured accelerations and forces recorded on magnetic tape for test numbers 6571, 6572, 6574 and 6575. The printouts also include the computed resultant accelerations and foot loads. These tests were conducted at the maximum impact velocity that was investigated (nominal 30 mph) and were selected for detailed presentation for this reason.

TABLE XXV. PEAK HEAD AND CHEST IMPACT AND REBOUND ACCELERATIONS

TEST NO.	SUBJECT NO.	SLED VEL. G_x	PEAK HEAD IMPACT	ACCEL. (G_x) REBOUND	PEAK CHEST IMPACT	ACCEL. (G_x) REBOUND
6507	A	16.0	15.0	4	12.5	5
6508	B	15.6	11.5	4	11.0	6
6510	C	14.9	13.5	3	14.0	3
6511	D	15.5	14.0	3	28.1	0
6514	E	20.5	22.3	9	14.0	5
6515	F	20.9	15.1	4	28.4	0
6524	C	20.9	15.2	6	15.0	3
6525	G	20.5	18.3	5	29.1	3
6528	H	22.0	22.0	3	30.0	3
6529	I	22.5	22.4	4	26.1	3
6531	K	21.5	20.7	3	15.1	-
6532	J	21.5	21.2	6	33.8	2
6534	M	24.0	19.1	11	24.9	5
6535	B	23.7	23.4	4	20.3	4
6537	E	24.1	19.2	3	29.6	3
6538	J	24.3	19.9	3	44.2	2
6556	B	24.2	19.0	9	24.5	3
6557	C	24.3	19.4	7	20.0	3
6540	G	25.9	32.7	3	38.0	2
6541	H	26.0	30.1	8	29.4	3
6543	I	26.5	26.9	10	27.4	6
6544	K	26.2	32.7	4	45.4	3
6559	E	25.5	24.4	1	31.9	3
6563	D	26.2	34.4	2	46.2	2
6564	F	26.2	37.1	3	22.5	2
6561	G	28.1	35.1	3	47.2	2
6566	I	28.2	34.3	12	26.0	9
6567	M	27.7	32.8	4	34.7	3
6569	B	28.0	26.6	1	31.7	1
6571	G	29.7	38.6	4	50.5	2
6572	C	29.8	28.6	-	35.0	3
6574	H	30.8	33.9	4	29.7	3
6575	M	30.1	34.1	4	32.6	3

TEST XXVI. SUMMARY OF DATA FROM TESTS WITH VOLUNTEERS:
RESULTS OBTAINED FROM DATA PROCESSING BY
GENERAL MOTORS

TEST NO.	CHEST ACCEL. (G)	HEAD ACCEL. (G)	S.I.	H.I.C.	G	Δt (ms)
6507	26	16	30	27	12	136-192
6508	30	12	20	17	9.3	141-204
6510	30	13	20	17	8.2	115-200
6511	35	14	30	23	8.3	93-207
6514	59	23	70	50	11.8	104-209
6515	32	22	100	78	13.4	74-191
6524	NA	NA	NA	NA	NA	NA
6525	NA	NA	NA	NA	NA	NA
6528	32	38	230	163	21.2	84-163
6529	32	30	150	110	14.9	83-211
6531	52	33	170	123	23.1	89-137
6532	32	26	120	92	18.3	95-160
6534	28	--	310	179	22.3	68-165
6535	33	69	430	232	52.0	93-105
6537	31	--	150	105	18.1	72-148
6538	44	35	180	122	20.1	70-137
6556	27	--	90	70	14.9	82-167
6557	27	20	110	90	15.1	75-180

NA = Not Available

TABLE XXVI. (CONT'D) SUMMARY OF DATA FROM TESTS WITH
VOLUNTEERS: RESULTS OBTAINED FROM DATA
PROCESSING BY GENERAL MOTORS

TEST NO.	CHEST ACCEL. (G)	HEAD ACCEL. (G)	S.I.	H.I.C.	G	Δt (ms)
6540	35	--	340	155	19.4	87-181
6541	43	31	220	172	21.2	66-149
6543	--	30	180	150	22.6	84-185
6544	47	49	310	227	30.5	83-127
6559	33	31	180	270	31.0	62-132
6564	38	67	700	320	21.9	47-190
6561	47	40	330	270	27.9	82-147
6566	56	--	380	260	26.6	77-149
6567	36	35	230	170	26.2	65-136
6569	34	31	120	90	17.2	87-160
6571	46	40	280	220	26.3	86-148
6572	33	26	140	110	17.2	79-170
6574	50	34	250	200	24.3	79-150
6575	--	38	270	220	26.2	85-146

TABLE XXVII. LISTING OF PEAK ACCELERATIONS MEASURED
ON THE SUBJECTS' HEAD AND MOUTH

TEST NO.	SLED G _x	HEAD ACCELERATIONS			MOUTH ACCELERATIONS		
		G _x	G _y	G _z	G _x	G _y	G _z
6507	9.3	15.0	2.0	6.5	12.0	7.5	7.5
6508	9.1	11.5	3.1	4.1	9.0	6.0	6.5
6510	8.3	13.5	2.0	8.5	11.8	8.8	5.9
6511	8.9	14.0	3.6	8.9	19.0	10.7	8.9
6514	13.0	22.3	10.6	8.3	17.5	8.0	9.0
6515	13.4	15.1	10.7	7.0	17.7	13.9	12.9
6524	13.4	15.2	12.3	12.2	16.5	11.0	10.0
6525	12.9	18.3	9.7	15.4	15.3	6.8	14.5
6528	15.4	22.0	14.5	30.0	23.5	13.0	11.0
6529	16.3	22.4	15.6	14.7	20.0	11.7	20.1
6531	15.2	20.8	12.8	36.2	27.5	21.8	19.7
6532	15.0	21.2	10.0	20.3	23.0	18.9	11.6
6534	20.0	19.1	10.5	11.5	17.7	6.5	14.9
6535	19.4	23.4	29.6	23.5	19.9	10.8	13.5
6537	19.2	20.9	18.0	14.1	20.0	19.7	19.1
6538	19.9	23.7	24.6	31.1	23.7	17.0	17.0
6556	19.0	21.7	12.4	15.3	23.5	21.1	14.3
6557	19.4	19.6	10.4	4.4	18.1	16.7	20.0
6540	18.1	32.7	13.8	25.3	30.8	12.6	18.2
6541	18.2	30.1	13.5	20.8	26.2	4.9	22.0
6543	18.7	26.9	20.5	15.6	22.0	16.0	16.5
6544	18.5	32.7	20.1	50.3	28.5	15.2	16.3
6559	17.6	24.4	12.7	28.5	23.0	24.9	25.1
6563	18.3	34.4	12.5	50.6	31.5	13.7	23.3
6564	18.2	37.1	8.4	26.4	27.0	16.4	14.6
6561	18.8	35.1	43.2	25.8	33.8	13.7	20.5
6566	19.2	34.3	16.1	22.1	25.9	16.6	17.8
6567	18.6	32.8	14.7	21.9	26.9	16.0	17.6
6569	19.5	26.7	16.0	17.5	28.9	16.3	17.7
6571	19.4	38.6	12.8	23.9	30.9	14.9	16.8
6572	18.7	28.6	8.1	9.8	18.0	14.3	19.0
6574	21.1	33.9	9.9	24.9	25.4	10.4	20.6
6575	20.3	34.1	18.4	33.0	24.4	20.6	18.1

TABLE XXVIII. PEAK TRIAXIAL FOOT LOAD MEASUREMENTS

TEST NO.	SLED (G _x)	LEFT FOOT LOADS - LBS			RIGHT FOOT LOADS - LBS		
		DOWN	FORWARD	LATERAL	DOWN	FORWARD	LATERAL
6507	9.3	353	249	131	715	297	88
6508	9.1	705	206	34	737	225	57
6510	8.3	617	193	66.4	490	160	55
6511	8.9	810	155	26	810	175	30
6514	13.0	815	275	47	835	305	32
6515	13.4	915	202	18	930	225	37
6524	13.4	750	263	38	698	320	48
6525	12.9	850	249	64	910	362	68
6528	15.4	631	210	72	690	277	62
6529	16.3	600	300	53	600	300	53
6531	15.2	610	230	46	720	225	65
6532	15.0	730	250	39	740	239	46
6534	20.0	840	242	57	981	393	49
6535	19.4	840	325	41	1001	336	28
6537	19.2	745	241	27	846	285	63
6538	19.9	673	253	31	700	222	54
6556	19.0	900	330	14	940	360	39
6557	19.4	850	335	56	820	365	59
6540	18.1	610	180	5	680	385	72
6541	18.2	703	222	31	817	298	54
6543	18.7	763	275	30	794	568	66
6544	18.5	700	255	75	704	419	108
6559	17.6	850	285	22	800	250	60
6563	18.3	951	300	28	871	325	35
6564	18.2	981	226	15	871	266	16
6561	18.8	740	225	59	775	230	73
6566	19.2	920	370	60	890	400	75
6567	18.6	974	272	32	823	390	45
6569	19.5	1020	341	37	860	185	52
6571	19.4	760	198	35	744	200	58
6572	18.7	715	345	102	660	365	92
6574	21.1	785	240	31	820	255	58
6575	20.3	900	266	27	998	420	60

TABLE XXIX. STATISTICAL SUMMARY OF 20 SUCCESSIVE DUMMY TESTS

	MEAN VALUE	STANDARD DEVIATION	VARIANCE	COEFFICIENT OF VARIATION
Test Speed (MPH)	25.42	0.33	0.11	0.013
Test Velocity (FPS)	37.26	0.49	0.24	0.013
Sled Accel. (G_x)	17.08	0.42	0.18	0.025
Head Accel. (G_x)	27.45	2.65	7.05	0.097
Head Acceleration Interval (G_r)	33.55	2.54	6.47	0.076
Head Acceleration External (G_r)	43.05	8.81	77.53	0.205
Chest Accel. G_x	29.75	1.92	3.69	0.065
Chest Acceleration Internal (G_r)	32.70	2.16	4.64	0.066
Chest Acceleration External (G_r)	35.45	6.33	40.06	0.179
Remaining Head-to- Panel Distance (in)	3.08	1.56	2.43	0.097

TABLE XXX. STATISTICAL SUMMARY OF 15 MPH TEST RESULTS (n=4)

TEST VARIABLES	MEAN VALUES	STANDARD DEVIATIONS
Test Speed (mph)	15.50	0.39
Test Velocity (fps)	22.73	0.53
Sled Acceleration (G)	8.99	0.48
Bag Fire Times (ms)	11.50	0.24
Harness Release (ms)	17.35	0.23
Hi-Pyro Fire (ms)	68.30	1.85
Peak Accelerations (G)		
Head X Axis	13.52	1.26
Head Y Axis	2.68	0.69
Head Z Axis	7.01	1.92
Chest X Axis	16.39	6.81
Chest Y Axis	7.08	4.08
Chest Z Axis	13.17	5.51
Mouth X Axis	12.95	3.71
Mouth Y Axis	8.26	1.37
Mouth Z Axis	7.18	1.15
Peak Foot Loads (lbs)		
Left Foot Down	621.40	169.15
Left Foot Forward	200.55	33.50
Left Foot Lateral	57.63	30.68
Right Foot Down	688.00	119.79
Right Foot Forward	214.08	53.54
Right Foot Lateral	57.56	20.45

TABLE XXXI. STATISTICAL SUMMARY OF 20 MPH TEST RESULTS (n=24)

TEST VARIABLES	MEAN VALUES	STANDARD DEVIATIONS
Test Speed (mph)	20.70	0.20
Test Velocity (fps)	30.38	0.28
Sled Acceleration (G)	13.25	0.29
Bag Fire Times (ms)	8.75	0.21
Harness Release (ms)	15.35	0.61
Hi-Pyro Fire (ms)	49.63	0.78
Peak Accelerations (G)		
Head X Axis	17.74	2.94
Head Y Axis	10.82	0.94
Head Z Axis	10.72	3.31
Chest X Axis	21.62	7.13
Chest Y Axis	7.30	2.94
Chest Z Axis	12.91	3.65
Mouth X Axis	16.75	0.95
Mouth Y Axis	9.93	2.76
Mouth Z Axis	11.60	2.20
Peak Foot Loads (lbs)		
Left Foot Down	832.55	59.62
Left Foot Forward	247.08	27.58
Left Foot Lateral	41.73	16.58
Right Foot Down	843.25	91.03
Right Foot Forward	303.00	49.64
Right Foot Lateral	46.15	13.93

TABLE XXXII. STATISTICAL SUMMARY OF 22 MPH TEST RESULTS (n=4)

TEST VARIABLES	MEAN VALUES	STANDARD DEVIATIONS
Test Speed (mph)	21.83	0.34
Test Velocity (fps)	31.98	0.51
Sled Acceleration (G)	15.68	0.53
Bag Fire Times (ms)	8.58	0.26
Harness Release (ms)	14.98	0.59
Hi-Pyro Fire (ms)	47.55	1.17
Peak Accelerations (G)		
Head X Axis	21.59	0.65
Head Y Axis	13.21	2.12
Head Z Axis	25.30	8.39
Chest X Axis	26.24	6.98
Chest Y Axis	7.03	3.04
Chest Z Axis	17.24	2.17
Mouth X Axis	23.50	2.67
Mouth Y Axis	16.35	4.16
Mouth Z Axis	15.59	4.32
Peak Foot Loads (lbs)		
Left Foot Down	642.68	51.62
Left Foot Forward	247.50	33.45
Left Foot Lateral	52.53	12.34
Right Foot Down	687.50	53.56
Right Foot Forward	260.28	29.82
Right Foot Lateral	56.48	7.48

TABLE XXXIII. STATISTICAL SUMMARY OF 24 MPH TEST RESULTS (n=6)

TEST VARIABLES	MEAN VALUES	STANDARD DEVIATIONS
Test Speed (mph)	24.10	0.21
Test Velocity (fps)	35.33	0.32
Sled Acceleration (G)	19.82	0.27
Bag Fire Times (ms)	7.77	0.24
Harness Release (ms)	13.75	0.77
Hi-Pyro Fire (ms)	39.88	0.40
Peak Accelerations (G)		
Head X Axis	21.40	1.75
Head Y Axis	17.59	7.35
Head Z Axis	16.66	8.57
Chest X Axis	27.26	8.23
Chest Y Axis	8.61	1.79
Chest Z Axis	15.97	5.22
Mouth X Axis	20.48	2.37
Mouth Y Axis	15.28	5.08
Mouth Z Axis	16.47	2.94
Peak Foot Loads (lbs)		
Left Foot Down	807.92	75.76
Left Foot Forward	287.60	42.68
Left Foot Lateral	37.72	15.55
Right Foot Down	881.35	104.57
Right Foot Forward	326.75	57.29
Right Foot Lateral	48.65	11.92

TABLE XXXIV. STATISTICAL SUMMARY OF 26 MPH TEST RESULTS (n=7)

TEST VARIABLES	MEAN VALUES	STANDARD DEVIATIONS
Test Speed (mph)	26.07	0.19
Test Velocity (fps)	38.21	0.42
Sled Acceleration (G)	18.39	0.31
Bag Fire Times (ms)	7.01	0.33
Harness Release (ms)	13.51	0.96
Hi-Pyro Fire (ms)	31.34	0.40
Peak Accelerations (G)		
Head X Axis	31.18	4.06
Head Y Axis	14.49	4.01
Head Z Axis	31.06	12.86
Chest X Axis	34.39	8.40
Chest Y Axis	12.27	4.63
Chest Z Axis	26.89	7.27
Mouth X Axis	26.99	3.35
Mouth Y Axis	14.80	5.48
Mouth Z Axis	19.40	3.71
Peak Foot Loads (lbs)		
Left Foot Down	793.86	127.81
Left Foot Forward	248.93	39.01
Left Foot Lateral	29.49	20.63
Right Foot Down	790.94	69.00
Right Foot Forward	358.60	102.46
Right Foot Lateral	58.74	26.91

TABLE XXXV. STATISTICAL SUMMARY OF 28 MPH TEST RESULTS (n=4)

TEST VARIABLES	MEAN VALUES	STANDARD DEVIATIONS
Test Speed (mph)	28.00	0.19
Test Velocity (fps)	41.13	0.31
Sled Acceleration (G)	19.41	0.39
Bag Fire Times (ms)	6.68	0.70
Harness Release (ms)	12.93	0.74
Hi-Pyro Fire (ms)	28.60	0.29
Peak Accelerations (G)		
Head X Axis	32.22	3.31
Head Y Axis	22.49	11.99
Head Z Axis	21.81	2.93
Chest X Axis	34.90	7.73
Chest Y Axis	5.93	2.90
Chest Z Axis	14.57	4.52
Mouth X Axis	28.88	3.01
Mouth Y Axis	15.65	1.14
Mouth Z Axis	18.40	1.19
Peak Foot Loads (lbs)		
Left Foot Down	913.50	106.24
Left Foot Forward	302.00	56.95
Left Foot Lateral	47.05	12.59
Right Foot Down	837.00	42.95
Right Foot Forward	301.25	95.16
Right Foot Lateral	61.03	12.79

TABLE XXXVI. STATISTICAL SUMMARY OF 30 MPH TEST RESULTS (n=4)

TEST VARIABLES	MEAN VALUES	STANDARD DEVIATIONS
Test Speed (mph)	30.10	0.43
Test Velocity (fps)	44.13	0.66
Sled Acceleration (G)	20.60	0.64
Bag Fire Times (ms)	6.93	0.29
Harness Release (ms)	12.70	0.51
Hi-Pyro Fire (ms)	25.75	0.66
Peak Accelerations (G)		
Head X Axis	33.80	3.53
Head Y Axis	12.28	3.90
Head Z Axis	22.87	8.33
Chest X Axis	36.94	8.06
Chest Y Axis	20.46	14.02
Chest Z Axis	27.37	6.26
Mouth X Axis	24.67	4.60
Mouth Y Axis	15.28	3.98
Mouth Z Axis	18.61	1.39
Peak Foot Loads (lbs)		
Left Foot Down	790.00	68.28
Left Foot Forward	259.75	53.58
Left Foot Lateral	48.80	30.85
Right Foot Down	805.50	124.72
Right Foot Forward	310.00	86.96
Right Foot Lateral	67.00	14.46

E. Medical Findings

The specific findings of the medical investigators are provided in impact velocity groups as follows:

15 mph (Tests 6507, 6508, 6510, 6511)

Test 6507, Subject A -- Immediately upon impact the subject felt a sharp pain between the toes of his left foot. The pain radiated up to the anterior peroneal area. Ten minutes post-impact there was only slight tenderness to deep pressure between the 3rd and 4th toes. There were no residual findings after 24 hours. The subject reported a scraping sensation as the bag contacted his chin. Although this subject may have struck the windshield he did not make any comment that might indicate that he was aware of such a contact. This subject's feet could not reach the floor board prior to impact. After this run wooden blocks were added to the test apparatus, when required, to assure that the subject's feet were in contact with the floor board prior to impact.

Test 6508, Subject B -- This subject had been a panel member during tests with an earlier prototype air bag. He felt that the near-production air bag felt "softer." He experienced a stinging slap over his left hemithorax and arm and there was slight erythema over this area after the run.

Test 6510, Subject C -- This subject felt pressure on his shins from the bag leading to hyperextension of the knees. He also felt the bag slap his chin.

20 mph (Tests 6514, 6515, 6524, 6525)

Test 6514, Subject E -- Stinging pressure was reported over the left hemithorax and left arm after impact. There was mild erythema

correlating well with the distribution of the pressure. Perceptible pain in upper left arm lasted for about 72 hours. The subject was dis-oriented momentarily on impact and had a mild residual headache which persisted for approximately 60 hours. Photometric data, cord lengths, and a dye smear on the windshield indicated that the subject struck the polystyrene windshield.

Test 6515, Subject F -- "Wind was knocked out" sensation was experienced on impact. The subject felt the bag scrape his chin. He experienced mild soreness over the lower sternum for about 5 days post-impact.

Test 6524, Subject C -- The bag was felt brushing his lip on impact. There was less pressure over shins than on the 15 mph test.

Test 6525, Subject G -- The subject felt the bag hit his face and the pit of his stomach. However, there was no discomfort from this blow. He also experienced an instantaneous, minor pain in both ankles.

22 mph (Tests 6528, 6529, 6531, 6532)

Test 6528, Subject H -- The subject felt pressure over his face and shins but there was no discomfort.

Test 6529, Subject I -- The subject felt numbing pressure on his lips, epigastrium and ankles. This was followed by a tingling sensation 10 minutes after impact. Mild pressure and pain over the epigastric area occurred on bag contact. The subject felt this ride was easier than the indoctrination ride at 6 mph with a lap belt and shoulder harness.

Test 6531, Subject K -- The subject reported that there was a mild blow to the pit of the stomach and a momentary sensation of breathlessness. There was also a slight burning sensation over his lower lip secondary to scraping of the bag on impact.

Test 6532, Subject J -- The subject felt sudden pain in his back starting at T3 and radiating to L3. This pain was fleeting and there was no residual soreness. He also felt a blow to the xiphoid area and had his wind knocked out. There was a 3 mm incisive wound on the lateral-dorsal surface of the right thumb (probably produced by the right thumb sliding over the shin guard or perhaps the edge of the air cushion cover). This incision is shown in Figure 60 to illustrate the minor nature of it.

24 mph (Tests 6534, 6535, 6537, 6538, 6556, 6557)

Test 6534, Subject M -- The subject felt a stinging blow to his mouth. A small area of petechial rash was noted on the left anterior upper arm.

Test 6535, Subject B -- The subject felt a stinging slap to his mouth. Again, the air cushion restraint felt softer than the earlier prototype used in the previous test series. There was some slight pressure on the lower legs. A three-inch area of erythema was noted on the left upper arm.

Test 6537, Subject E -- This subject felt that this ride was easier than the 20 mph ride. He felt the bag hit his lips and also noted a cramping sensation in the popliteal area after impact. The subject thought he struck his right thumb on the right shin guard. Dye found on the windshield and photometric data indicated that this subject contacted the windshield. The subject was not aware of the contact.

Test 6538, Subject J -- This subject again felt instantaneous pain from T4 to L3 on impact. He also felt that his wind was knocked out and that he received a blow to his face. Two weeks after the impact the



Figure 62. Minor Laceration of Left Thumb - Test No. 6532

AD-A038 525

AEROSPACE MEDICAL RESEARCH LAB WRIGHT-PATTERSON AFB OHIO F/G 13/12

IMPACT TESTS OF A NEAR-PRODUCTION AIR CUSHION RESTRAINT.(U)

FEB 77 J W BRINKLEY, G C MOHR, H C RUSSELL

DOT-HS-017-1-017-1A

UNCLASSIFIED

AMRL-TR-75-47

DOT-HS-802-248

NL

3 OF 5
AD
A038525



subject had residual low back pain. There were no physical findings and x-rays of the spine were negative. Due to the stringent requirements governing the use of human subjects, this subject was not used in any further air cushion restraint system tests because of the unexplained low back pain.

Test 6556, Subject B -- This subject felt a pressure sensation to face and knees during impact. He had his knees in full extension prior to impact. The encapsulated dyes of the indicator tape revealed that the subject brushed the windshield on impact, but he was not aware of this contact.

Test 6557, Subject C -- The subject felt a slight stinging across his mouth. His right earplug was almost out and he stated that the impact sounded like a shotgun blast. He felt that he really didn't need the earplugs.

26 mph (Tests 6540, 6541, 6543, 6544, 6559, 6563, 6564)

Test 6540, Subject G -- The subject reported an instantaneous, sharp pain in right ankle which lasted about 3 minutes after the impact. He also reported a stinging sensation to his mouth. The subject stated that this ride seemed easier than the 20 mph ride that he had previously experienced.

Test 6541, Subject A -- A scraping sensation in the mouth area was felt during the impact.

Test 6543, Subject I -- The subject complained of a sharp pain in the region of his right sacroiliac joint radiating to the right greater trochanter. The pain persisted for more than 30 minutes after the impact exposure. The subject also noted pain in the left sacrospinalis

muscle on impact. This back pain was gone before subject's next run, approximately three weeks later.

Test 6544, Subject K -- The subject reported that he experienced mild pressure on mouth and epigastric area during impact. An erythematous streak was noted on left upper arm during the post-test examination.

Test 6559, Subject E -- A sharp, instantaneous pain, localized to C7 was noted. This pain soon disappeared and was replaced by a dull ache in the left suprascapular area which lasted for approximately one week. The only physical finding was spasm of the left trapezius muscle. The cervical mobility of this subject was within normal limits, but pain was accentuated when the right ear was touched to the right shoulder. The examining physician believed that this injury resulted when the subject entered the bag with his neck flexed at about a 45" angle, rather than keeping his head firmly against the headrest as he had been instructed (this subject had contacted the windshield on an earlier test). This forward flexion of the head resulted in extreme rotation of the head to the left upon impact with the bag, and further allowed for more extreme lateral displacement of the head to the right. It is not hard to envision how extreme tension would be developed in the left trapezius under these circumstances. The persistent pain from this minor injury effectively eliminated this subject from participating in the tests that were still to be conducted.

Test 6563, Subject D -- This subject felt a blow to his chest during impact and felt that his wind was knocked out. The EKG recorded during this test revealed a 1.70 second R-R interval immediately post-impact, followed by a normal complex, one PVC and then normal sinus rhythm at

about 70/minute. Complete cardiac reevaluation after this incident revealed no pathologic basis for this transient arrhythmia, but the monitoring physician eliminated this subject from the panel pending further consultation.

Test 6564, Subject F -- The subject reported that he experienced a blow to his left leg followed by short period of numbness. He also complained of a scraping sensation on the face. The subject was very apprehensive and could hardly talk for several minutes after completing the test. The medical monitor felt that it would be unwise to use this subject again because of this exhibition of extreme anxiety.

28 mph (Tests 6561, 6566, 6567, 6569)

Test 6561, Subject G -- The subject stated that his wind was knocked out from impact on his chest. He also reported moderate pressure on his knees. He estimated that the force of the impact was definitely greater than he had experienced in prior tests at 20 and 26 mph.

Test 6566, Subject I -- He reported a stinging sensation in his upper lip. There was slight pressure in the right sacroiliac region, but much less than that encountered at 26 mph (Test 6543).

Test 6567, Subject M -- The subject commented on a mild stinging sensation in his upper lip. Mild erythema was noted in left axilla and upper lip. He reported that the ride was easier than previous tests he had experienced.

Test 6569, Subject B -- He felt pressure and strain in the right wrist. He also reported a stinging sensation to his mouth and a sensation of being tapped on his head (this subject contacted the

windshield during impact).

30 mph (Tests 6571, 6572, 6574, 6565)

Test 6571, Subject G -- The subject stated that he felt less impact to his chest than he had in tests at 28 and 26 mph. He commented on a sensation of pressure on both shins. He felt that the test was a "very easy ride".

Test 6572, Subject C -- The subject reported a great amount of pressure on his lower body, from the waist down. He also reported some pain in back of his knees and ankles. This subject felt he took a greater percentage of the force of the impact on his legs, without any significant discomfort.

Test 6574, Subject H -- The subject felt more pressure from the bag on his shins but he stated that this test was easier overall than those at 26 and 22 mph.

Test 6575, Subject M -- The subject reported mild pressure to both of his knees. The subject felt that this was the easiest ride of all.

V. Analysis of Results and Discussion

A. Impact Tests Using Dummy Subjects

Figure 63 is a plot of head impact Severity Index as a function of impact velocity for the tests conducted at the General Motors Proving Grounds using the paper windshield (reinforced with polystyrene ribs) and the polystyrene windshield. This plot shows several important points. First, the range of head impact Severity Index values is larger for any given impact velocity where the paper windshield was used. Second, the size of the dummy has no apparent effect upon the resulting Severity Index value associated with the tests of the polystyrene windshield. The scatter of data points in cases where the paper windshield was used and the limited number of tests prevent speculation on this point. Note that an S.I. of 1000 is the limit in accordance with reference 12.

Figure 64 plots the peak chest acceleration values from Tables XII and XIII as a function of impact velocity. This plot shows, as one might suspect, that the acceleration measured on the dummy's chest did not appear to be influenced by the type of windshield that was used. At the highest velocity the chest acceleration tends to be higher where the polystyrene windshield was used. Note that 60 G is considered to be a limit value in reference 12. As in the comparison of Severity Index values, the size of the dummy does not appear to have a consistent effect upon the value of the dependent variable.

The earlier dummy impact studies conducted prior to the air bag restraint system test program conducted by Greer et al (ref 9) had shown that the paper windshield configuration was less likely to cause hyper-

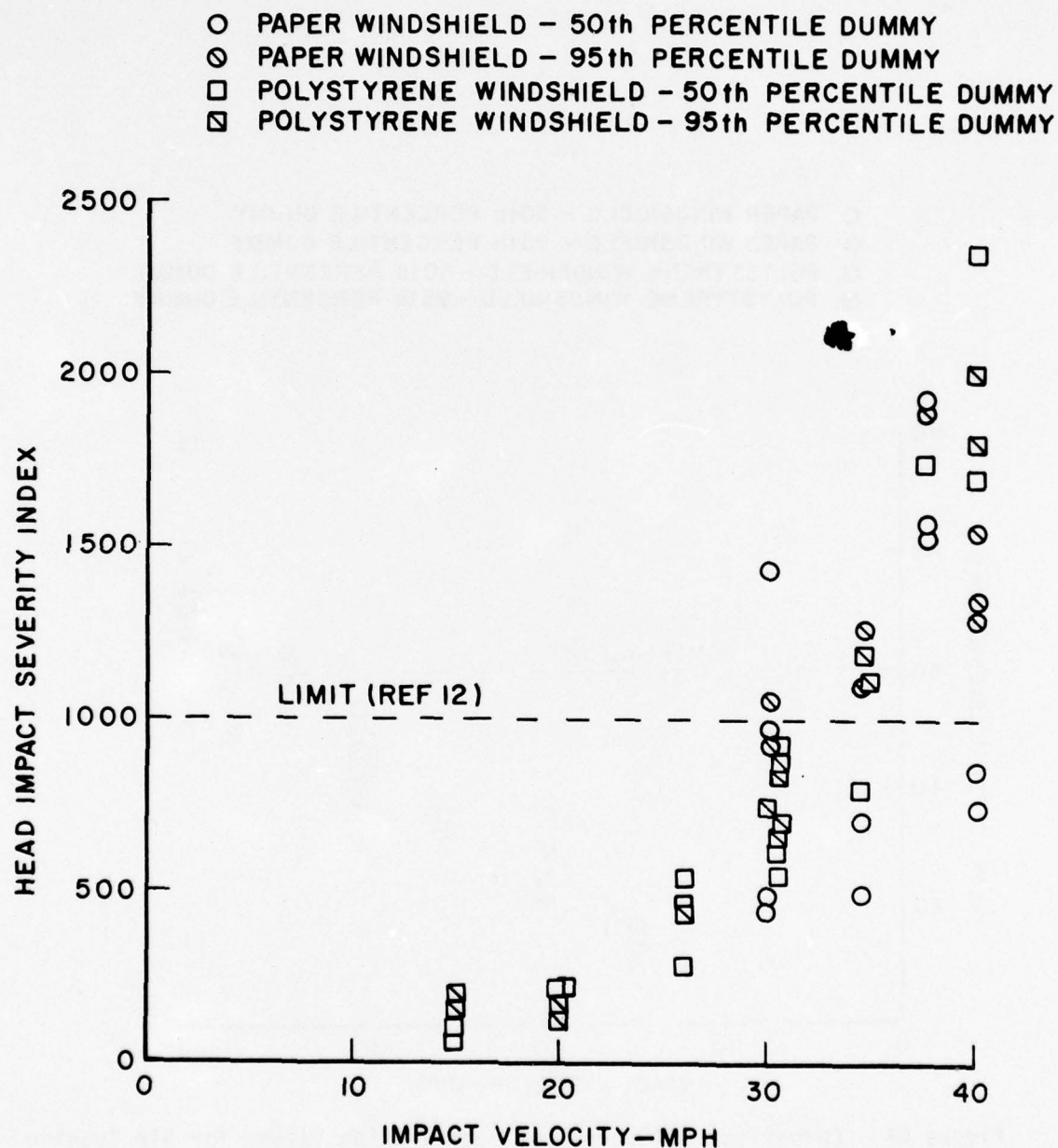


Figure 63. Comparison of Head Impact Severity Indices for Air Cushion Tests with Paper Windshields and Polystyrene Windshields

- PAPER WINDSHIELD - 50th PERCENTILE DUMMY
- ◊ PAPER WINDSHIELD - 95th PERCENTILE DUMMY
- POLYSTYRENE WINDSHIELD - 50th PERCENTILE DUMMY
- ◻ POLYSTYRENE WINDSHIELD - 95th PERCENTILE DUMMY

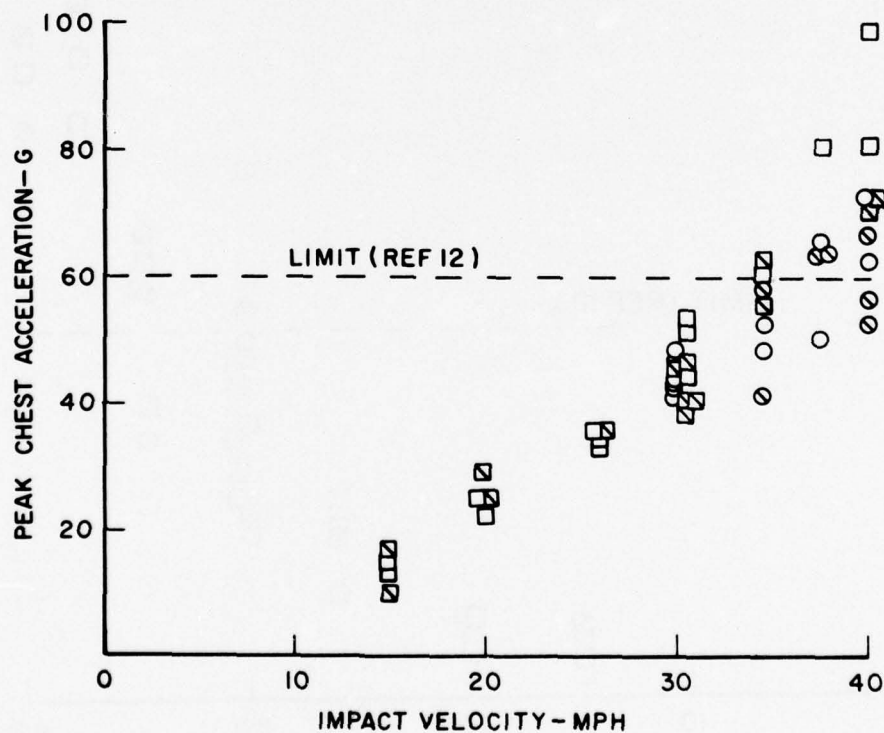


Figure 64. Comparison of Peak Chest Acceleration Values for Air Cushion Tests with Paper Windshield and Polystyrene Windshields

extension of the cervical spine if the head were to impact the windshield configuration. If this situation occurred, the paper and polystyrene rib construction would break out and allow the chest and head to impact together on an upper extension of the instrument panel.

The investigators elected to use the polystyrene windshield in the tests with human subjects described in this report as has been mentioned earlier. The selection was based upon consideration of the consistency of the air cushion performance with the polystyrene windshield versus the lower head impact Severity Index and lesser chance of hyperextension injury to the neck associated with the paper windshield configuration. The selection was based upon the rationale that the consistent performance under normal impact conditions was the most important consideration since a normal impact was the most probable outcome of any test.

Figures 65 and 66 show comparisons of head impact Severity Index calculated from the G_x acceleration measured on the dummy's head, and the peak G_x acceleration measured on the dummy's chest with the impact velocity. These plots were developed from the data provided in Table XVI to show the relative efficacy of the crushable steel and polystyrene instrument panels. Figure 65 shows that the range of Severity Indices increased greatly as the impact velocity increased and that the range was greater when the crushable steel panel was used. Statistical analysis of the two sets of data, which was done immediately after completion of these tests, revealed no significant difference. Figure 66 also shows little difference between the two instrument panel configurations in terms of peak chest acceleration -- probably the most important objective parameter for the selection of the instrument panel configuration.

- STEEL INSTRUMENT PANEL-5th PERCENTILE DUMMY
- ⊙ STEEL INSTRUMENT PANEL-95th PERCENTILE DUMMY
- POLYSTYRENE INSTRUMENT PANEL-5th PERCENTILE DUMMY
- ▣ POLYSTYRENE INSTRUMENT PANEL-95th PERCENTILE DUMMY

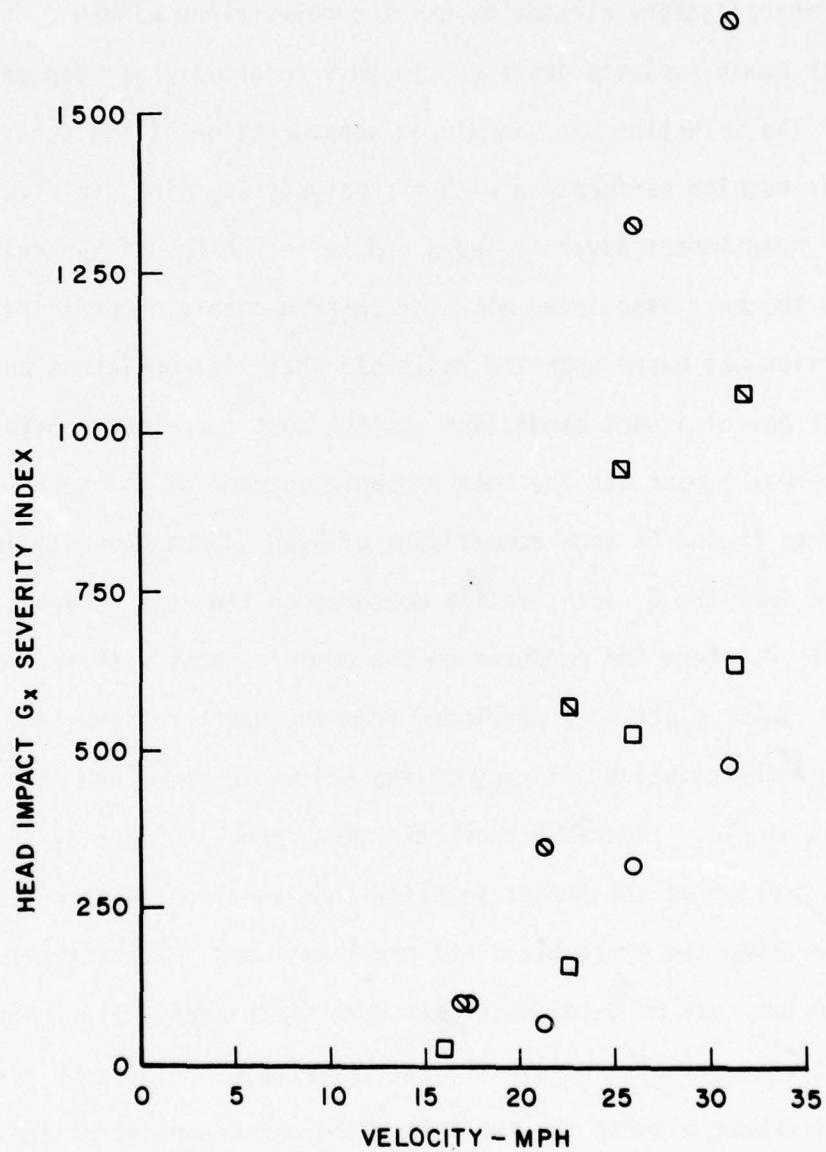


Figure 65. Comparison of Head Impact Severity Indices From Tests With Steel and Polystyrene Instrument Panels

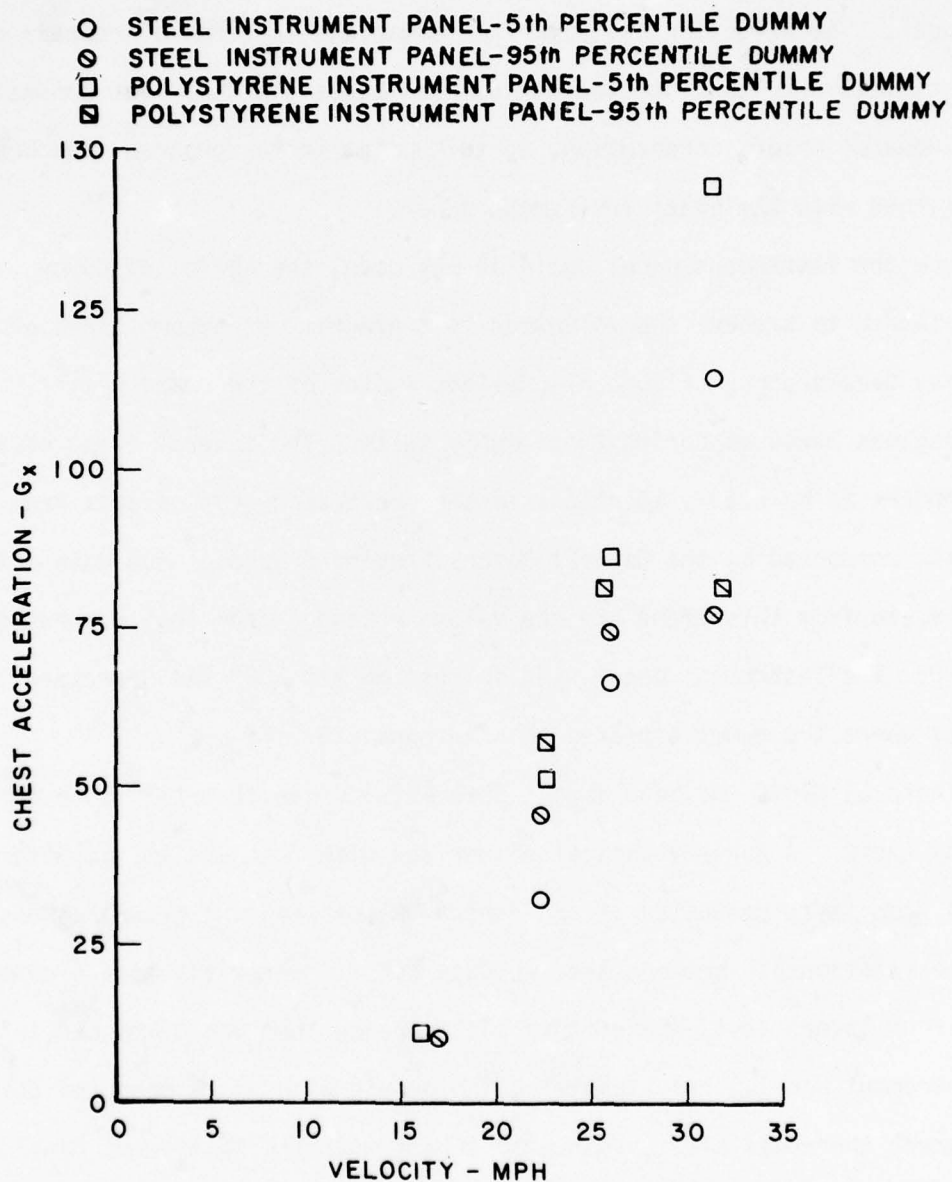


Figure 66. Comparison of Peak Chest Acceleration From Tests With Steel and Polystyrene Instrument Panels

As mentioned earlier in this report, the steel instrument panel was selected for use in the tests with volunteer subjects. The primary reason for this selection was the better simulation of the automotive instrument panel. The selection had a further advantage in terms of comparability of test results since the air cushion tests that had been conducted by the General Motors Corporation, to this point in the program, had been accomplished with the steel instrument panel.

Once the instrument panel decision was made, the series of dummy tests planned to precede the volunteer test program was accomplished on the Daisy Decelerator. Figure 67 provides a plot of the peak chest accelerations measured during these dummy tests. The general trend of the data appears to be nearly identical to the chest acceleration data from the tests conducted at the General Motors Proving Grounds. The data points that deviate from this trend are the values obtained from test numbers 6313 and 6320. The instrument panel used in test number 6320 was depressed in the area where the dummy appeared to have contacted it.

Figure 68 plots the head impact Severity Indices from this same series of dummy tests. A non-statistical comparison with the head impact Severity Indices from tests conducted at the General Motors Proving Grounds shows that the relationship between the two data sets is generally good except in the four 15 mph tests where there was evidence that the dummy had impacted the instrument panel. Unfortunately, the acceleration data measured during 6320, where there was also evidence of impact with the instrument panel, were not adequate for computation of the head impact Severity Index.

Figure 69 shows the results of ten additional dummy tests plotted with the initial series of dummy tests on the Daisy Decelerator. The first six

RUNS 6321 TO 6357

- O - 50TH PERCENTILE DUMMY
- ⊙ - 95TH PERCENTILE DUMMY
- ⊙ - DEPRESSION IN THE INSTRUMENT PANEL

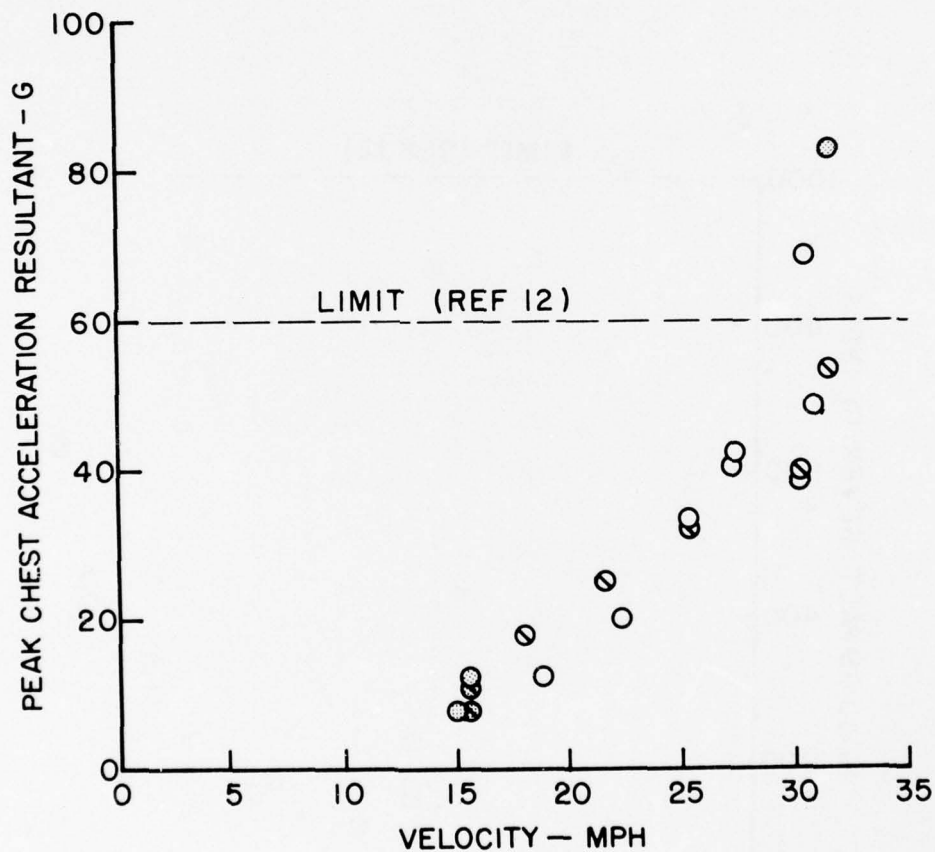


Figure 67. Peak Resultant Acceleration Measured on the Dummies Chests During Air Cushion Tests 6321 to 6357

TEST NUMBERS 6321-6357

○ - 50TH PERCENTILE DUMMY
⊙ - 95TH PERCENTILE DUMMY
⊗ - DEPRESSION IN THE INSTRUMENT PANEL

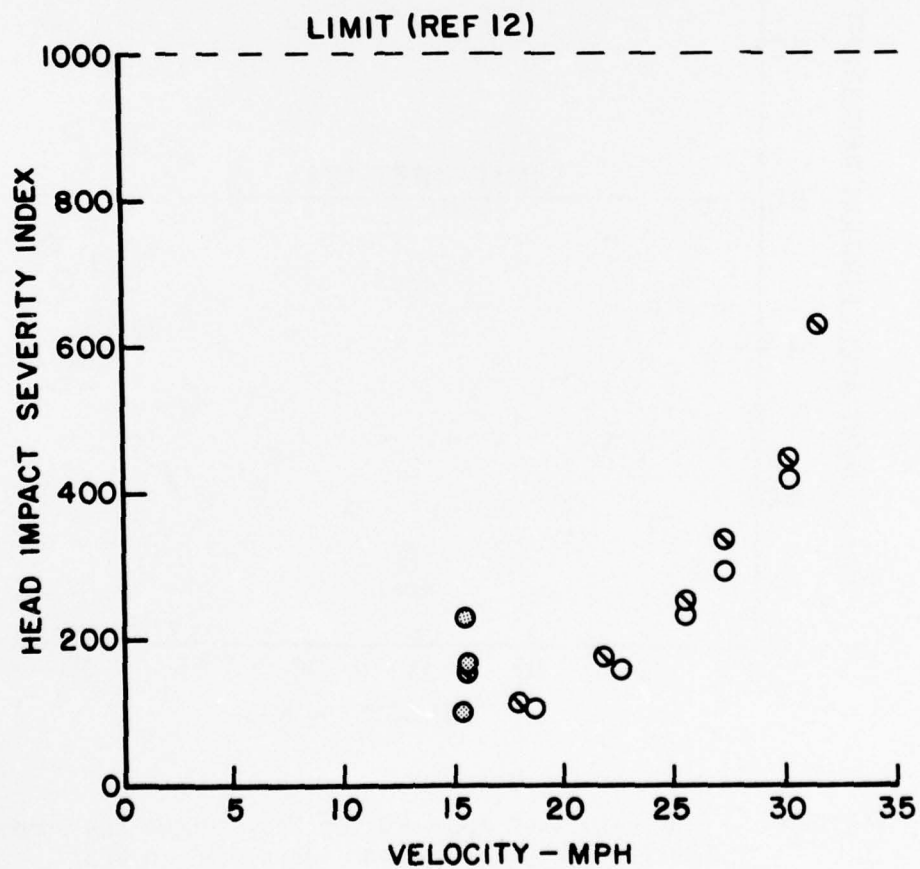


Figure 68. Head Impact Severity Indices from Air Cushion Tests 6321 to 6357

TEST NUMBERS 6321-6392

- - 50TH PERCENTILE DUMMY
- ⊙ - 95TH PERCENTILE DUMMY
- ⊗ - DEPRESSION IN THE INSTRUMENT PANEL

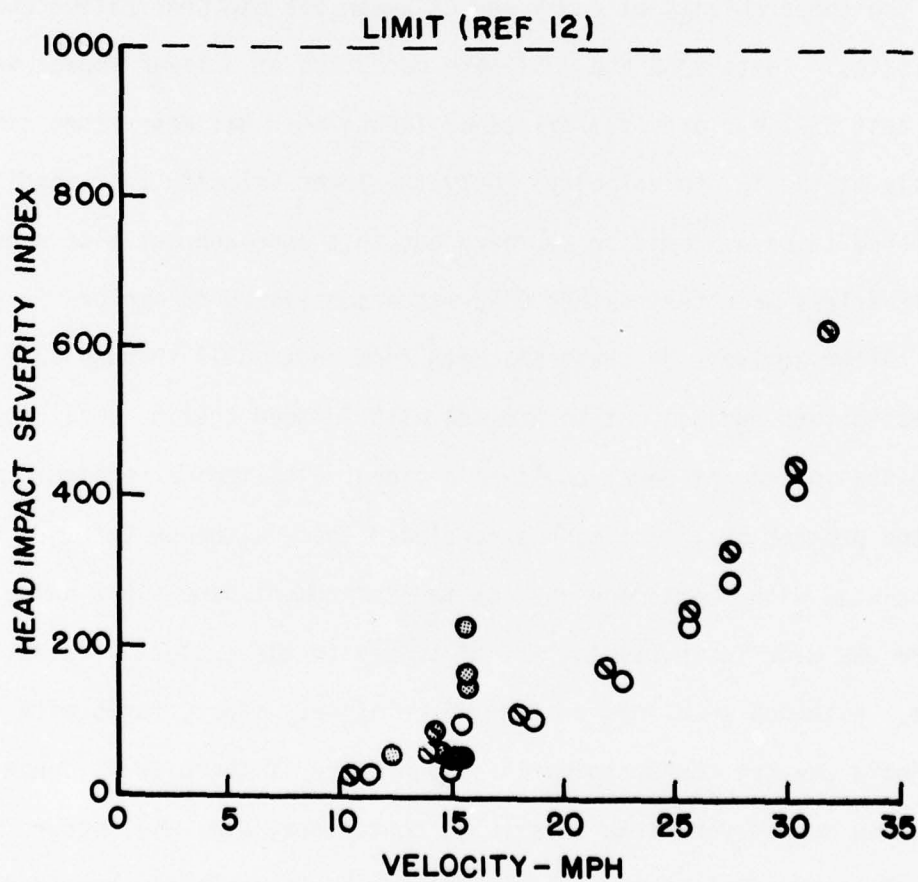


Figure 69. Head Impact Severity Indices from Air Cushion Tests 6321 to 6392

of these tests, test numbers 6380, 6381, 6383, 6384, 6386 and 6387, were conducted to provide further evidence to determine probability and severity of impact between the dummy and the instrument panel. Panel impact was demonstrated in four of the six tests. Furthermore, the dummies' heads appeared to be within one inch of the instrument panel in the two tests where impact did not occur. Tests 6388, 6389, 6391 and 6392 were then conducted to determine if a safe test condition could be demonstrated. The strategy was to find a set of conditions where human tests could be initiated which would also answer fundamental questions regarding the comparability of dummy versus human air bag penetration characteristics. Tests 6388 and 6389 were conducted at a lower impact velocity and test 6391 explored the effect of firing both gas generators simultaneously at the 15 mph velocity. Only the lower velocity test condition appeared to be a promising approach but this approach was also shown to be fruitless when test number 6392 was accomplished to explore it further.

After analysis of the tests data from tests 6312 through 6392, the investigators decided not to proceed with further testing until impact with the instrument panel could be avoided. The medical officer assigned to the program at this time had concluded that, although the impact levels associated with "bottoming out" on the instrument panel were quite low, there was a definite possibility of injury to the subject's facial structure. Although such injury might be relatively minor, tests with volunteer subjects are not conducted by this laboratory if there is evidence that injuries more severe than abrasions, contusions, etc. will occur.

The use of a hockey goalie's face mask was seriously considered as an approach for proceeding. It was thought that the use of the mask might

eliminate the possibility of facial injury and thereby allow commencement of testing with volunteers. This approach was rejected, however, since it might unduly compromise the basic objectives of the test program. With the exceptions of the ear plugs and goggles, the protective equipment that was used throughout the volunteer test program was used to provide protection for cases where the air cushion restraint might fail. For example, the shin guards were worn by the subjects to reduce the probability of permanent damage to the knee joint since the knee would probably impact the relatively unyielding air cushion supporting structure if the air bag failed to deploy and the secondary safety harness was also released or if only a partial air bag inflation occurred. (The type of knee injury that the investigators thought more probable during a normal air cushion deployment sequence would have been due to hyperextension of the knee joint. This injury mechanism did not occur during the volunteer test program.)

Impact tests of the air cushion restraint system were resumed at the General Motors Proving Grounds to evaluate changes to the test configuration that would improve subject safety. In the first test the amount of propellant in the high level gas generators was increased from 20 to 25 grams. The next 21 tests were accomplished with 25 grams of propellant in both gas generators. The test results have been given in Table XIX. The instrument panel was contacted in six instances which upset the previous trend of panel impact at low velocity only. Figure 70 plots the head impact Severity Index values obtained from these tests. These data reveal another tendency; the tests where contact was recorded did not yield higher Severity Indices than those tests where contact was indeterminate. One could conclude from this data that the stiffness of the air bag, as the dummy's head

TESTS OF THE REVISED AIR CUSHION GAS GENERATOR

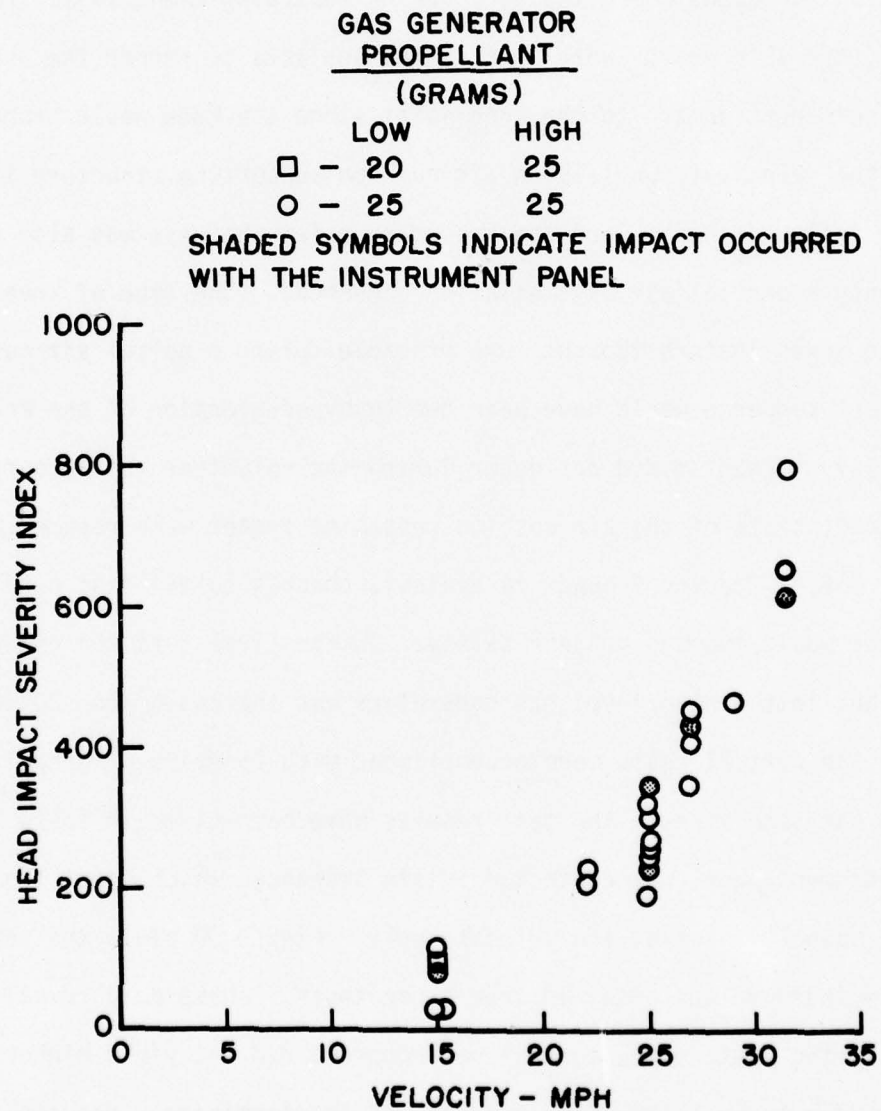


Figure 70. Head Impact Severity Indices From Air Cushion Tests With Revised Gas Generator Using Dummy Subjects

approached from the instrument panel, had been increased by the gas generator change to a point where it approximated that of the instrument panel. Therefore, the "bottoming" effects that had been observed would not be apparent.

The decision to increase the pressure of the stored gas within the air cushion inflator assembly to 2700 psi had a more positive effect upon the problem of instrument panel contact. Twelve impact tests were conducted in the range of 15 to 25 mph without contact. Figure 71 shows the head impact Severity Index data computed from the entire series of tests conducted to verify the performance of the modified air cushion restraint system.

Study of the chest acceleration data as well as the head impact Severity Indices did not reveal a significant difference in the performance of the inflator revisions. The study was accomplished in two stages. First, by comparing matched sets of data from the series conducted with an inflator pressure of 2350 psi where the size of the pyrotechnic charge within the gas generator was changed, and second, by making a comparison of sets of data where the gas stored within the inflator was increased from 2350 psi to 2700 psi. The comparisons were done by evaluating the differences between the means using a t-test to evaluate the null hypothesis that the difference between the means is zero (ref 18).

Tables XXXVII and XXXVIII provide a listing of the matched pairs of data that were used to evaluate the differences between the head impact Severity Indices and peak resultant chest acceleration from tests where the amount of propellant in the low level gas generator was 20 grams versus those where 25 grams was used. The sets were matched in terms of all other test variables including impact velocity, stored gas pressure (2350 psi) and the size of the dummy.

COMPARISON OF TESTS WITH STORED GAS
PRESSURES OF 2350 psi AND 2700 psi

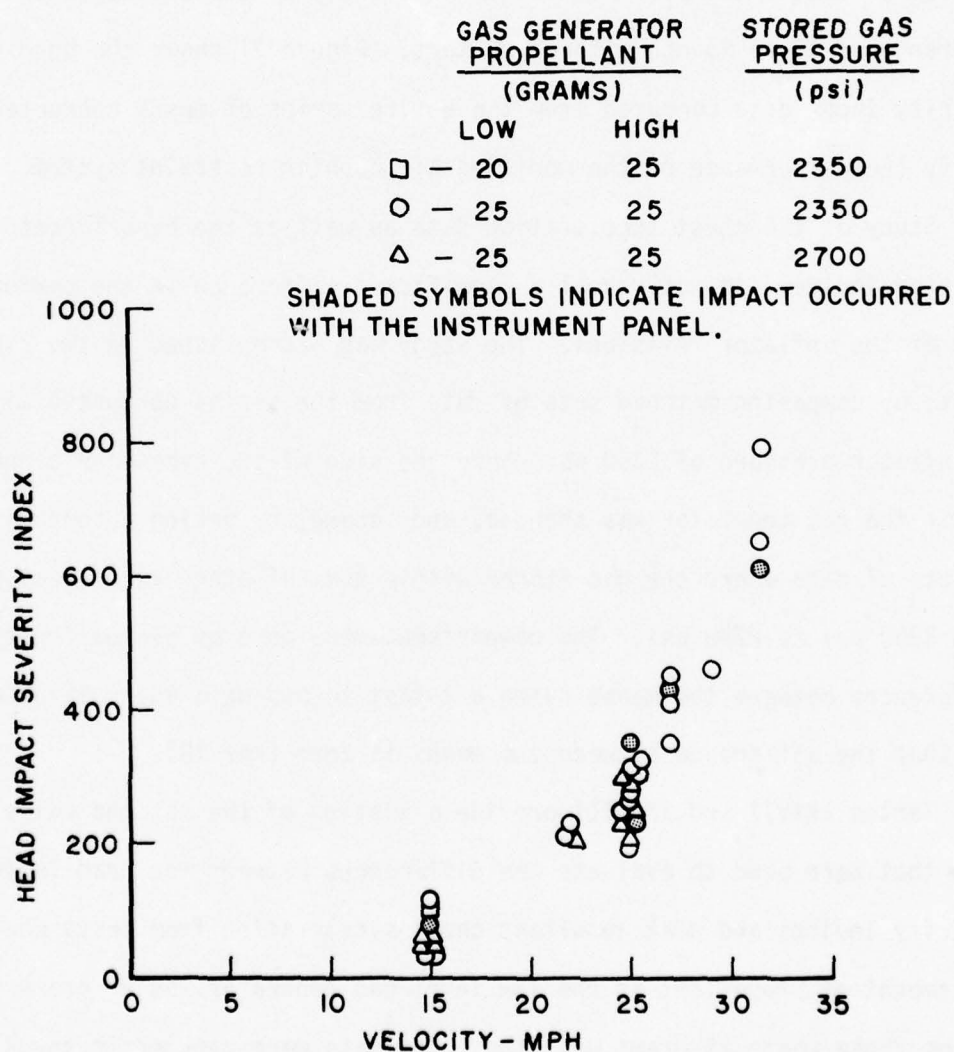


Figure 71. Head Impact Severity Indices from Tests with Revised Gas
Generator and Increased Stored Gas Pressure - Dummy Subjects

TABLE XXXVII. COMPARISON OF DIFFERENCES BETWEEN THE PEAK RESULTANT CHEST ACCELERATION VALUES USING GAS GENERATORS WITH 20 AND 25 GRAMS OF PROPELLANT

NOMINAL VELOCITY (MPH)	TEST NO. 20 GRAMS	CHEST ACCEL. (G ₁)	TEST NO. 25 GRAMS	CHEST ACCEL. (G ₂)	DIFFERENCE (G ₁ - G ₂)
15	2366	17	2735	21	-4
15	2367	13	2820	12	1
15	2411	15	2737	22	-7
15	2412	10	2821	16	-6
25	2350	33	2812	32	1
25	2351	34	2813	27	7
25	2352	35	2815	27	8
25	2353	35	2824-7*	36	-1

TABLE XXXVIII. COMPARISON OF DIFFERENCES BETWEEN THE SEVERITY INDICES USING GAS GENERATORS WITH 20 AND 25 GRAMS OF PROPELLANT

NOMINAL VELOCITY (MPH)	TEST NO. 20 GRAMS	SEVERITY INDEX (S.I. ₁)	TEST NO. 25 GRAMS	SEVERITY INDEX (S.I. ₂)	DIFFERENCE (S.I. ₁ - S.I. ₂)
15	2366	160	2735	100	60
15	2367	70	2820	30	40
15	2411	100	2737	110	10
15	2412	200	2821	80	120
25	2350	470	2812	270	200
25	2351	540	2813	230	310
25	2352	290	2815	300	-10
25	2353	440	2824-7*	267	173

*Average of data from tests 2824, 2825 and 2827

Both comparisons were accomplished using a t-test to evaluate the null hypothesis that the mean difference is zero. The mean difference between the peak resultant chest accelerations given in Table XXXVII is -0.125 G with an estimated standard deviation of the mean difference of 1.98. The computed value of t was 0.064. The mean difference between the Severity Indices in Table XXXVIII is 110 with an estimated standard deviation of the mean difference of 39.7. The computed t value is 2.77. A t value of 2.365 or larger is required to reject the null hypothesis with no more than a 0.05 probability of rejecting it when it is true.

The t-test was also used to determine if these same parameters were significantly altered when the gas pressure within the inflator was increased from 2350 psi to 2700 psi. The matched pairs of data used in this analysis are given in Tables XXXIX and XL. Both sets of data are from tests with 25 grams of propellant in both gas generators.

The analysis of the pairs of chest acceleration data shows that the mean difference between tests conducted with inflator pressure of 2350 psi and those with the 2700 psi is 0.64 G with an estimated standard deviation of the mean difference of 1.16. The t value is 0.55 (for 10 degrees of freedom the t value to reject the null hypothesis with 0.05 probability of rejecting a true hypothesis is 2.228). The analysis of the differences between the Severity Indices yielded a t value of 2.13. The mean difference of the pairs of S.I. data is 30 with an estimated standard deviation of the mean difference of 14.1.

Therefore, using the t-test it is possible to show that increasing the pyrotechnic charge in the gas generators had a significant influence upon the head impact S.I. values but not the peak chest accelerations.

TABLE XXXIX. COMPARISON OF DIFFERENCES BETWEEN THE PEAK
RESULTANT CHEST ACCELERATION VALUES USING
INFLATOR PRESSURES OF 2350 PSI AND 2700 PSI

NOMINAL VELOCITY (MPH)	TEST NO. 2350 PSI	CHEST ACCEL. (G ₁)	TEST NO. 2700 PSI	CHEST ACCEL. (G ₂)	DIFFERENCE (G ₁ - G ₂)
15	2735	21	2832	15	6
15	2737	22	2840	17	5
15	2820	12	2833	14	-2
15	2821	16	2841	13	3
22	2829	38	2845	37	1
25	2812	32	2831	32	0
25	2813	27	2834	32	-5
25	2815	27	2842	33	-6
25	2822	32	2843	31	1
25	2824	36	2830	32	4
25	2825	38	2835	38	0

TABLE XL. COMPARISON OF DIFFERENCES BETWEEN THE SEVERITY
INDICES USING INFLATOR PRESSURES OF 2350 PSI
AND 2700 PSI

NOMINAL VELOCITY (MPH)	TEST NO. 2350 PSI	SEVERITY INDEX (S.I. ₁)	TEST NO. 2700 PSI	SEVERITY INDEX (S.I. ₂)	DIFFERENCE (S.I. ₁ - S.I. ₂)
15	2735	100	2832	60	40
15	2737	110	2840	60	50
15	2820	30	2833	40	-10
15	2821	80	2841	40	40
22	2829	210	2845	230	-20
25	2812	350	2831	250	100
25	2813	230	2834	210	20
25	2815	300	2842	290	10
25	2822	320	2843	220	100
25	2824	260	2830	310	-50
25	2825	350	2835	300	50

Increasing the stored gas pressure did not have a statistically significant influence upon any measure of air cushion performance other than instrument panel contact although the S.I. differences were very close to significant at the 95 percent level of confidence. Since the distance between the dummy's head and the instrument panel was not determined during most of the dummy tests conducted at the GM Proving Grounds, it is impossible to statistically evaluate the effect of these changes on this parameter. However, it is obvious from the results of the 20 successive dummy tests that there was an improvement in the remaining head-to-panel distance.

The data of Tables XXXVII and XXXVIII are also representative of a factorial experiment with 4 observations at each combination of two nominal velocities and two propellant weights. The results of performing an analysis of variance of these data are presented in Tables XXXVIIa and XXXVIIIa. For both variables the effect of velocity is significant as one would expect but the propellant effect is mixed. For the head impact Severity Indices the effect of the propellant is significant and the velocity - propellant joint effect is not significant. This result agrees with the t-test on the mean differences. For the peak chest accelerations, however, although the propellant effect is not significant, the joint effect with velocity is significant. This joint effect can be seen in Table XXXVIIb. At 15 MPH the average chest acceleration was less at 20 grams than at 25 grams of propellant while the reverse order holds at 25 MPH. Notice that the total averages over the two velocity levels are equal. This relationship may be due to the changes in pyrotechnic gas generator firing times that occur as a function of impact velocity. It does raise questions regarding the propriety of a test of mean differences across quantities of propellant.

TABLE XXXVIIa. ANALYSIS OF VARIANCE TABLE FOR CHEST
ACCELERATIONS AT TWO LEVELS OF
VELOCITY AND PROPELLANT

SOURCES OF VARIATION	DEGREES OF FREEDOM	MEAN SQUARE	F RATIO	95% SIGNIFICANCE LEVEL
Velocity (V)	1	1105.6	87.8	4.75
Propellant (P)	1	.1	.01	4.75
VxP	1	60.1	4.77	
Error	12	12.6		
Total	15			

TABLE XXXVIIb. AVERAGE CHEST ACCELERATIONS

NOMINAL VELOCITY (MPH)	AVERAGE ACCEL (G) 20 GRAMS	AVERAGE ACCEL (G) 25 GRAMS
15	13.75	17.75
25	34.25	30.5
Combined velocities	24.0	24.1

TABLE XXXVIIIa. ANALYSIS OF VARIANCE TABLE FOR SEVERITY INDICES
AT TWO LEVELS OF VELOCITY AND PROPELLANT

SOURCES OF VARIATION	DEGREES OF FREEDOM	MEAN SQUARE	F RATIO	95% SIGNIFICANCE LEVEL
Velocity (V)	1	239366	57.6	4.75
Propellant (P)	1	48731	11.73	4.75
VxP	1	13398	3.23	4.75
Error	12	4153		
Total	15			

These tables provided by Dr. Berens of University of Dayton Research Institute

A commonly accepted method of accounting for a change in the variance with an independent variable is to perform a transformation of the dependent variable. If the coefficient of variation is constant for an increasing mean, then it can be shown that a logarithmic transformation of the dependent variables will yield equal variances. A statistician, not associated with the original investigation, was consulted to accomplish an analysis using this method. The analysis of the data sets after performing a log transformation of the head impact Severity Indices and the peak chest accelerations showed the results generally agreed with those reported by the investigators.

To determine how much influence the size of the dummy had upon the test data a statistical analysis was accomplished using the data sets given in Tables XLI and XLII. The data are arranged in pairs that are matched in all experimental variables except dummy size. Tests where there was evidence that the dummy's head may have impacted the instrument panel were not used. The analysis indicates that the null hypothesis, that there is no difference, cannot be rejected using the head impact Severity Index data set. The mean difference between the Severity Indices is -30 with an estimated standard deviation of the mean difference of 21.5. The t-value in this case is -1.39. The mean difference between the peak resultant chest accelerations is -5 G with an estimated standard deviation of the mean difference of 1.25. The value of t is -4.01 which is significant at the 95 percent level of confidence. The analysis indicates that if there is a difference between these parameters for the 50th and 95th percentile dummies, and there should be, that the difference is statistically significant for the peak chest acceleration only. The difference between

TABLE XLI. COMPARISON OF HEAD IMPACT SEVERITY INDICES FROM TESTS WITH 50TH AND 95TH PERCENTILE DUMMIES

NOMINAL VELOCITY (MPH)	50TH PERCENTILE TEST NO.	SEVERITY INDEX (S.I. ₅₀)	95TH PERCENTILE TEST NO.	SEVERITY INDEX (S.I. ₉₅)	DIFFERENCE (S.I. ₅₀ -S.I. ₉₅)
27	2810	350	2811	450	-100
25	2812	270	2824	260	10
25	2815	300	2827	190	110
15	2820	30	2737	110	-80
25	2831	250	2830	310	-60
25	2834	210	2835	300	-90
15	2833	40	2832	60	-20
15	2841	40	2840	60	-20
22	2844	210	2845	230	-20

TABLE XLII. COMPARISON OF PEAK RESULTANT CHEST ACCELERATION VALUES FROM TESTS WITH 50TH AND 95TH PERCENTILE DUMMIES

NOMINAL VELOCITY (MPH)	50TH PERCENTILE TEST NO.	CHEST ACCEL. (G ₅₀)	95TH PERCENTILE TEST NO.	CHEST ACCEL. (S.I. ₉₅)	DIFFERENCE (G ₅₀ - G ₉₅)
27	2810	35	2811	37	-2
25	2812	32	2824	36	-4
25	2815	27	2827	35	-8
25	2831	32	2830	32	0
15	2820	12	2837	22	-10
25	2834	32	2835	38	-6
15	2833	14	2832	15	-1
15	2841	13	2840	17	-4
22	2844	27	2845	37	-10

the head impact S.I. values is probably hidden by the large variance in this parameter that is due to other factors such as accelerometer mounting efficacy.

The series of 20 successive impact tests that were conducted with a 50th percentile dummy to demonstrate that the instrument panel would not be contacted provides some insight into the reproducibility of test conditions and the variability of the accelerations measured with both externally and internally mounted accelerometers. A statistical analysis of these data shows that the test conditions, that is, the impact velocity and peak sled acceleration have means of 25.4 MPH and 17.08 G respectively. The estimated standard deviation of the velocity is 0.33 MPH while the estimated standard deviation of the measured peak accelerations is 0.44 G (coefficient of variation is 0.025). The relatively good reproducibility of these environmental parameters contrasts sharply with the measurements of dummy response. For example, the distances remaining between the dummy's head and the instrument panel have a mean value of 3.08 inches with an estimated standard deviation of 1.56. Head impact Severity Index values computed from accelerometers mounted on the head strap have a mean of 268 with an estimated standard deviation of 112 (coefficient of variation = 0.418). If the two highest and two lowest S.I. values are arbitrarily eliminated from this sample, the mean is changed insignificantly and, although the estimated standard deviation is reduced to 52, the coefficients of variation for the sled acceleration and the head impact Severity Index differ by nearly an order of magnitude (.025 versus .205).

The 20 successive dummy tests also provide some insight into the effects of accelerometer mounting as a source of variability in the data.

An analysis of head impact Severity Indices shows that the S.I. values computed from the internally mounted accelerometers yielded a mean of 197 with an estimated standard deviation of 22.8 (coefficient of variation = 0.116). A similar analysis of the H.I.C. data shows a mean of 212 with an estimated standard deviation of 124 (coefficient of variation = 0.585) for data computed from the externally mounted accelerometer data and a mean of 146 and an estimated standard deviation of 20 (coefficient of variation = 0.137) from the values computed from the internally measured acceleration. Statistical analysis of the resultant head accelerations shows that the mean acceleration is 43.1 with an estimated standard deviation of 8.81 (coefficient of variation = 0.204) using externally mounted transducers. The mean resultant acceleration is 33.6 with an estimated standard deviation of 2.54 (coefficient of variation = 0.075) using the data from the accelerometers mounted within the dummy head. Analysis of the accelerations measured on the chest strap and within the dummy chest reveals similar statistics. The mean resultant acceleration measured externally is 35.5 while the value of the mean is 32.7 for the internal measurements. The estimated standard deviations for the chest accelerations are 6.33 and 2.16 respectively. The respective coefficients of variation are 0.178 and 0.066.

A series of statistical comparisons were made to determine if there were significant differences between the data collected during dummy tests at the GM Proving Grounds using a horizontal acceleration facility (a 12 inch diameter Hyge machine) and the data from tests conducted with the horizontal decelerator (the Daisy facility) at Holloman AFB. The comparisons were accomplished by using a t-test to evaluate the null hypothesis

that the means of the two different samples came from the same population or from populations with the same means. A sample of 12 dummy tests conducted at a nominal velocity of 25 MPH was used to represent the data collected at the GM Proving Grounds. This sample consists of the 25 MPH tests conducted during the series from test number 2812 through 2843. Tests where the dummy's head impacted the instrument panel were eliminated. The data collected on the Daisy Decelerator at Holloman AFB were represented by the 20 successive dummy tests conducted at a nominal impact velocity of 25 MPH. Both head impact Severity Index and peak resultant chest acceleration data were used in the evaluation. The Severity Indices for both samples were computed by General Motors using the accelerations measured by the accelerometers mounted within the dummies' heads.

A t-value was calculated from head impact Severity Indices of the two samples using a pooled estimate of the estimated standard deviation. An F-test was performed to determine that it was valid to assume that the estimates of the standard deviations of the samples could be pooled to give a better estimate. Using the mean of the S.I. values from the GM sample, 264, the mean of the S.I. values from the AMRL sample, 197, and a pooled estimated standard deviation of 31.2, a t-value of 5.88 was calculated. Since the value of t for a 0.001 probability of rejecting the null hypothesis when it is true is 3.646 for 30 degrees of freedom, the hypothesis can be rejected with a minimal risk.

A t-test was not performed using the peak resultant chest accelerations because the two samples are obviously identical. The mean of the GM sample is 32.8 G while the AMRL sample is 32.7 G. The estimated standard deviations are 2.73 G and 2.16 respectively. However, Figure 72

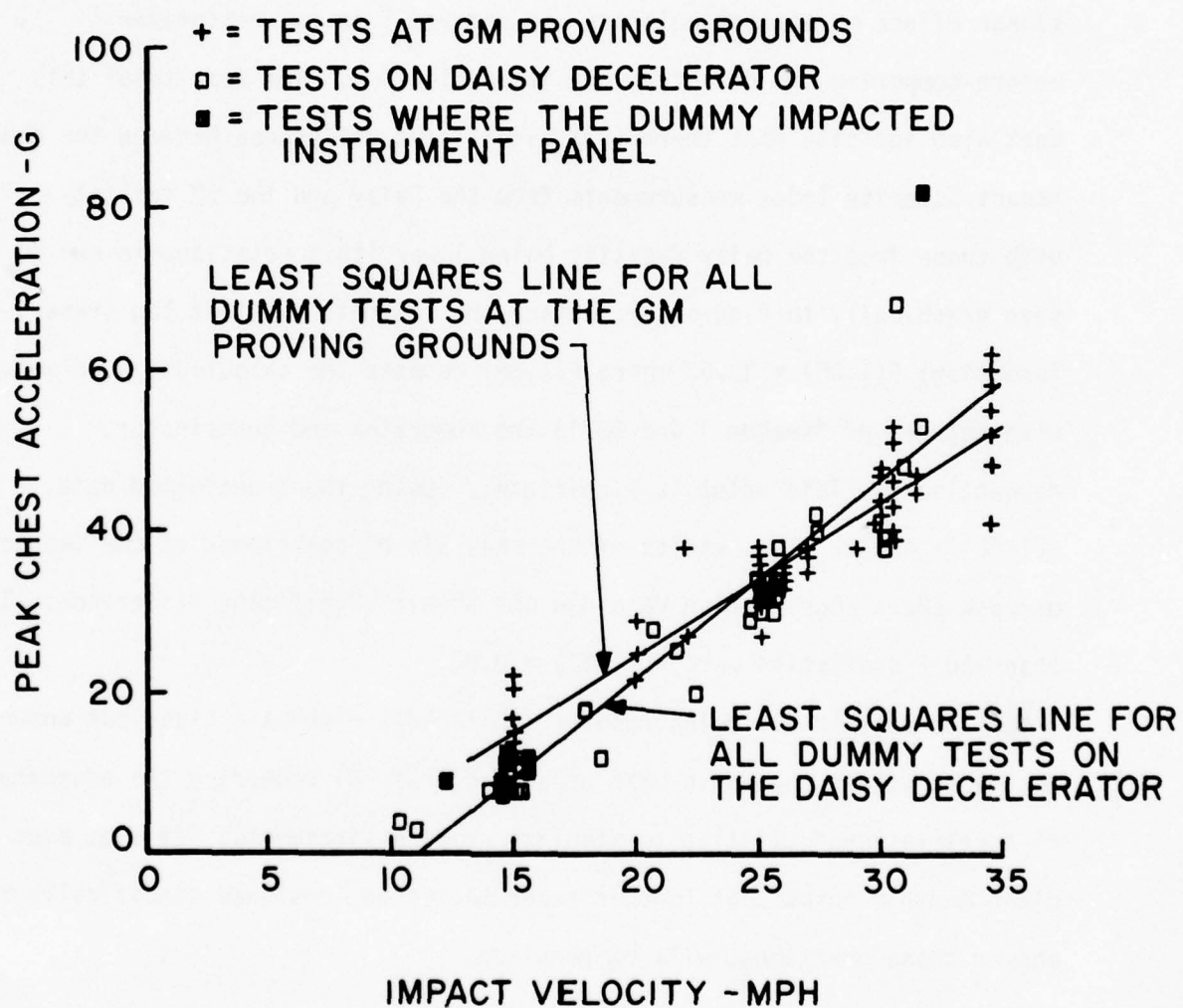


Figure 72. Comparison of Peak Chest Acceleration Data From Tests at the GM Proving Grounds and the Daisy Decelerator

shows that at the 26 MPH impact condition the differences between the two data sets is minimal.

Therefore, to provide a more complete comparison the head impact Severity Index and peak chest acceleration data for both accelerator and decelerator facilities over the total range of velocities, an analysis of covariance (ref 19) was performed. In this analysis the linear effect of nominal velocity was removed from the measurements before comparing the data from the two facilities. The results of this test also indicate that there is a significant difference between the head impact Severity Index measurements from the Daisy and the GM facility with those from the Daisy facility being lower (this relationship can be seen graphically in Figure 73). Using the raw data (without log transformation) $F(1,88) = 33.63$ where $F(1,88)$ denotes the calculated F values with degrees of freedom 1 and 88 in the numerator and denominator, respectively. This value is significant. Using the transformed data, $F(1,88) = 48.42$. The results of the analysis of covariance of the two sets of peak chest acceleration data did not show a significant difference. The observed F statistics were $F(1,112) = 0.80$.

From these conflicting results one is left without a clear cut answer to the questions that have been presented (ref 20) regarding the adequacy of acceleration facilities to simulate crash environments. It does seem clear at this point that further experimentation, designed specifically to answer these questions, will be required.

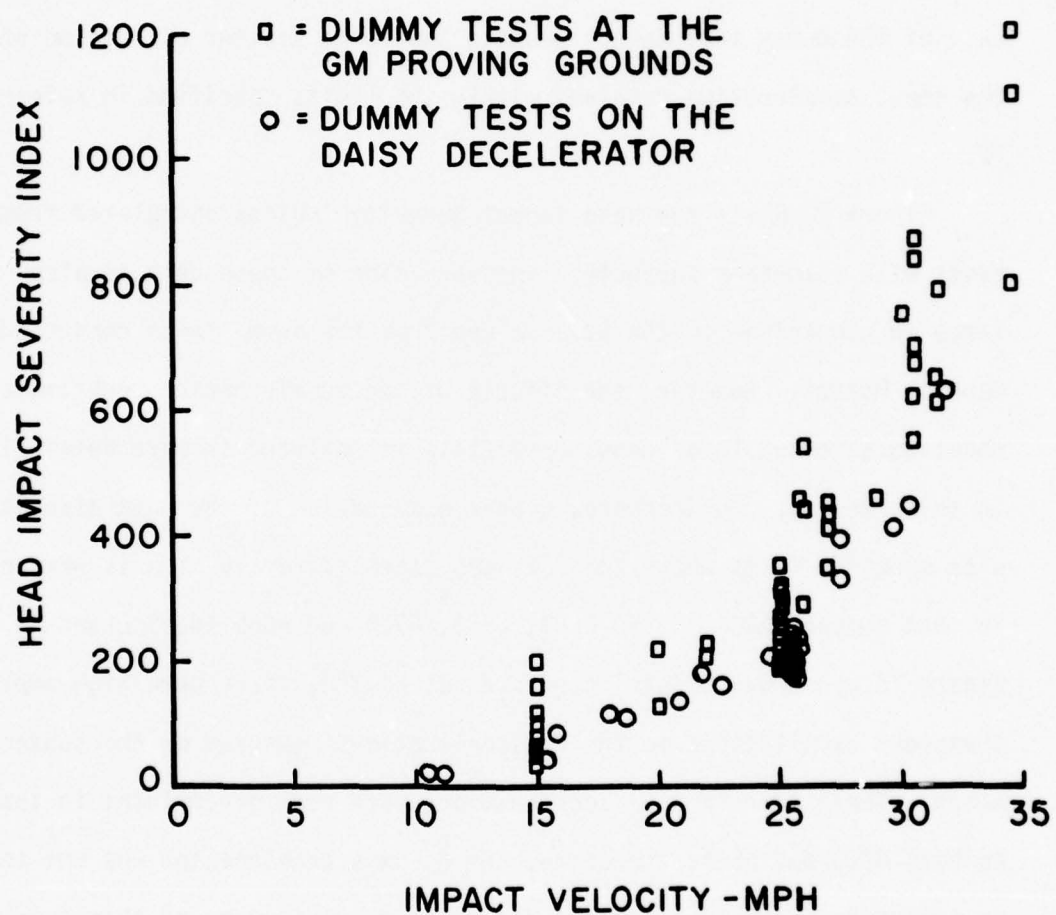


Figure 73. Comparison of Head Impact Severity Index Values From Tests at the GM Proving Grounds and the Daisy Decelerator

B. Tests With Volunteers

The acceleration data collected from the accelerometers mounted on the chests of the volunteer subjects is summarized in Figure 74 in terms of the peak resultant acceleration for each test. The most noteworthy aspect of the data is the relatively large variance; however, the variance does not appear to increase with the impact velocity as in the case of the dummy test data. Despite the large scatter of data points the chest acceleration remained within the limits specified in reference 12.

Figure 75 plots the head impact Severity Indices calculated from the tests with volunteer subjects. The variation of these data is also quite large in comparison to the S.I. values from the dummy tests conducted by General Motors. However, the effects of the accelerometer mounting and mounting site should be considered (this is analyzed in more detail later in this report). Furthermore, closer examination of the data associated with specific tests where the S.I. was extraordinarily high is warranted. In test numbers 6534, 6535, 6561, 6563, 6564 and 6566 (designated in Figure 75 by shaded points) conducted at 24 MPH, there were high amplitude transient oscillations in the G_z accelerations measured on the subjects' heads. These transient G_z accelerations were very predominant in test numbers 6563 and 6564; therefore, the G_z axis acceleration was set to zero in computing the S.I. values to determine the influence of this acceleration component. This procedure yielded S.I. values of 166 for test number 6563 and 168 for 6564. The data that was not processed in this manner yielded S.I. values of 520 and 700 respectively.

TESTS 6507 - 6575

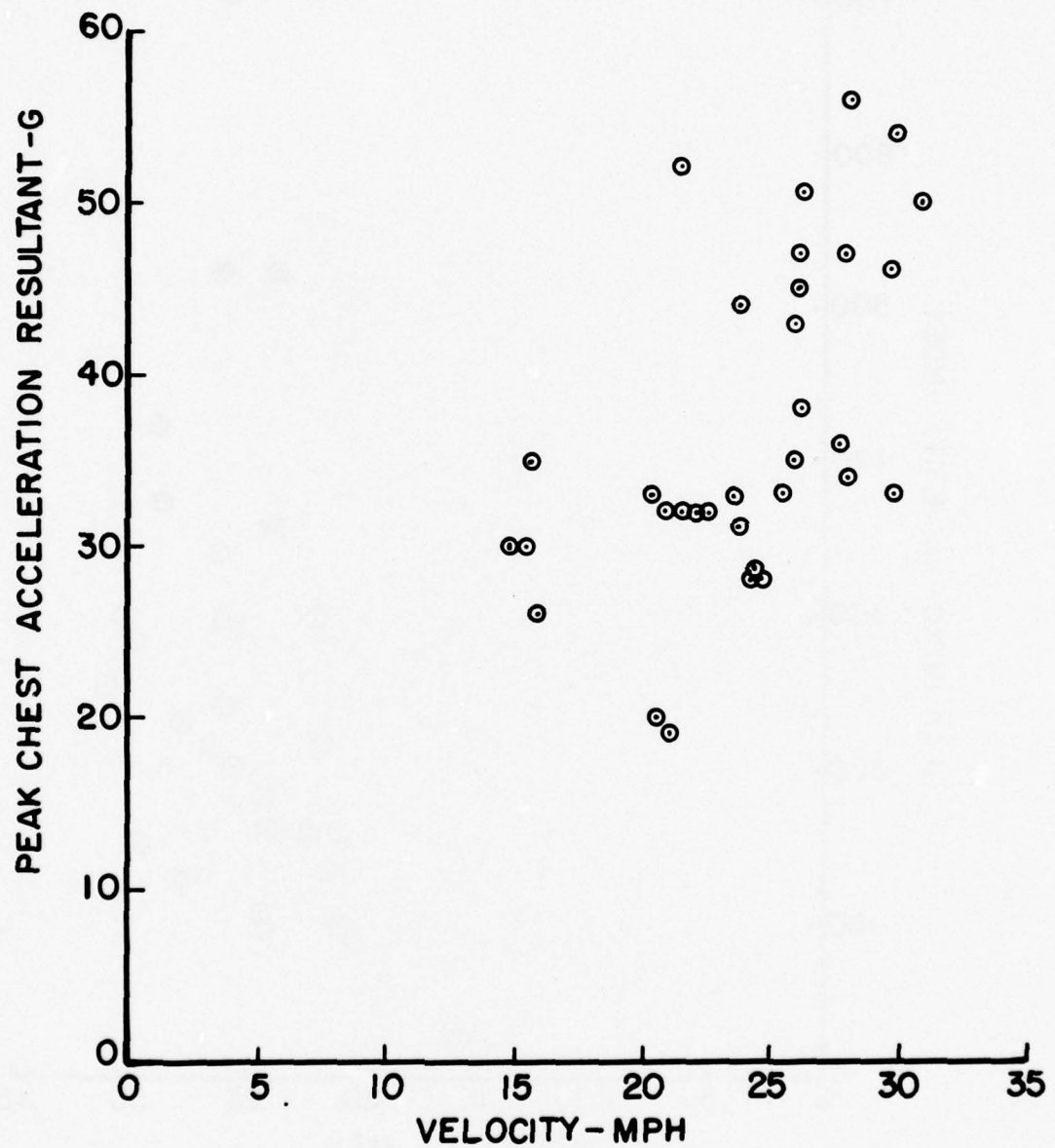


Figure 74. Peak Chest Resultant Acceleration Values From Air Cushion Tests Using Volunteer Subjects

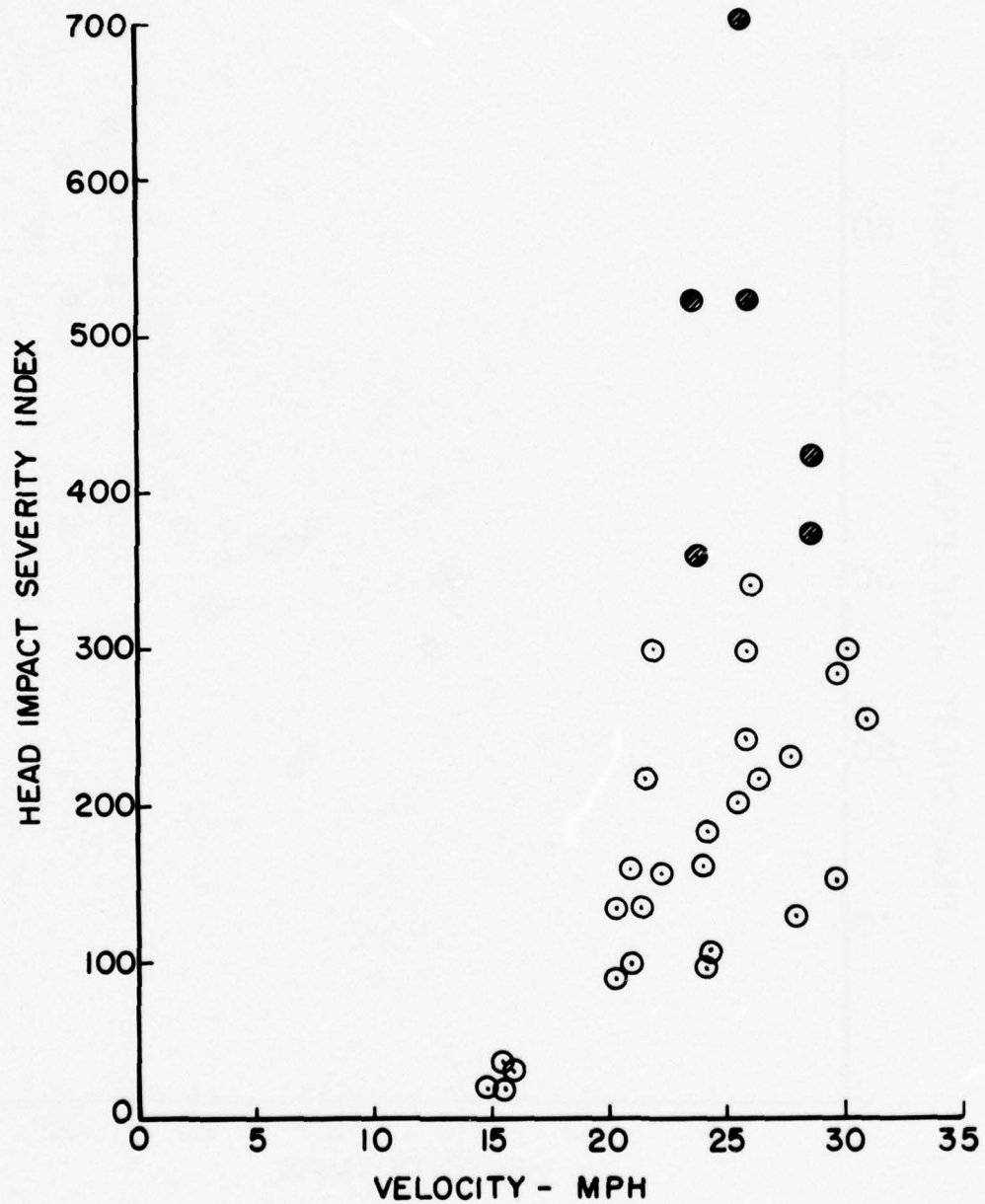


Figure 75. Head Impact Severity Indices from Air Cushion Tests 6507-6575

Closer examination of the data from the individual head accelerometers shows that the G_z accelerations had the largest variation and were the major cause of the large variation of the head impact Severity Indices. For example, the coefficients of variation of the G_x accelerations measured on the subjects' heads range from 0.03 to 0.17 for the seven impact velocity levels studied. The average of the coefficients of variation of the G_x head accelerations is 0.07. In contrast the coefficients of variation of the G_z accelerations measured on the subjects' heads range from 0.13 to 0.51 with an average of 0.32. The relatively clear trend established by the peak G_x accelerations measured on the subjects' heads is shown in Figure 76.

The relatively large variations seen in the G_z axis accelerations and to a lesser degree in the G_y axis accelerations (coefficients of variation averaged 0.30 for the G_y data) are understandable since the body tissues under the accelerometer mounts on both the head (mounted on the back of the head) and chest (mounted over the sternum) offer very little resistance to shearing motion. Thus, the accelerometer mount may react to the acceleration of the chest or head and, in the case of the chest accelerometer package, to the motion of the air bag by small shear movements that cause high amplitude, short duration accelerations that are superimposed on the true motion of the body segment.

The mouth accelerometer mount, if held firmly by the subject in a fitted mouthpiece, should provide acceleration data that are more representative of the motion of the head. Statistical analysis of the measurements from the individual accelerometers of the mouth accelerometer package shows that the coefficients of variation for the G_z measurements are improved

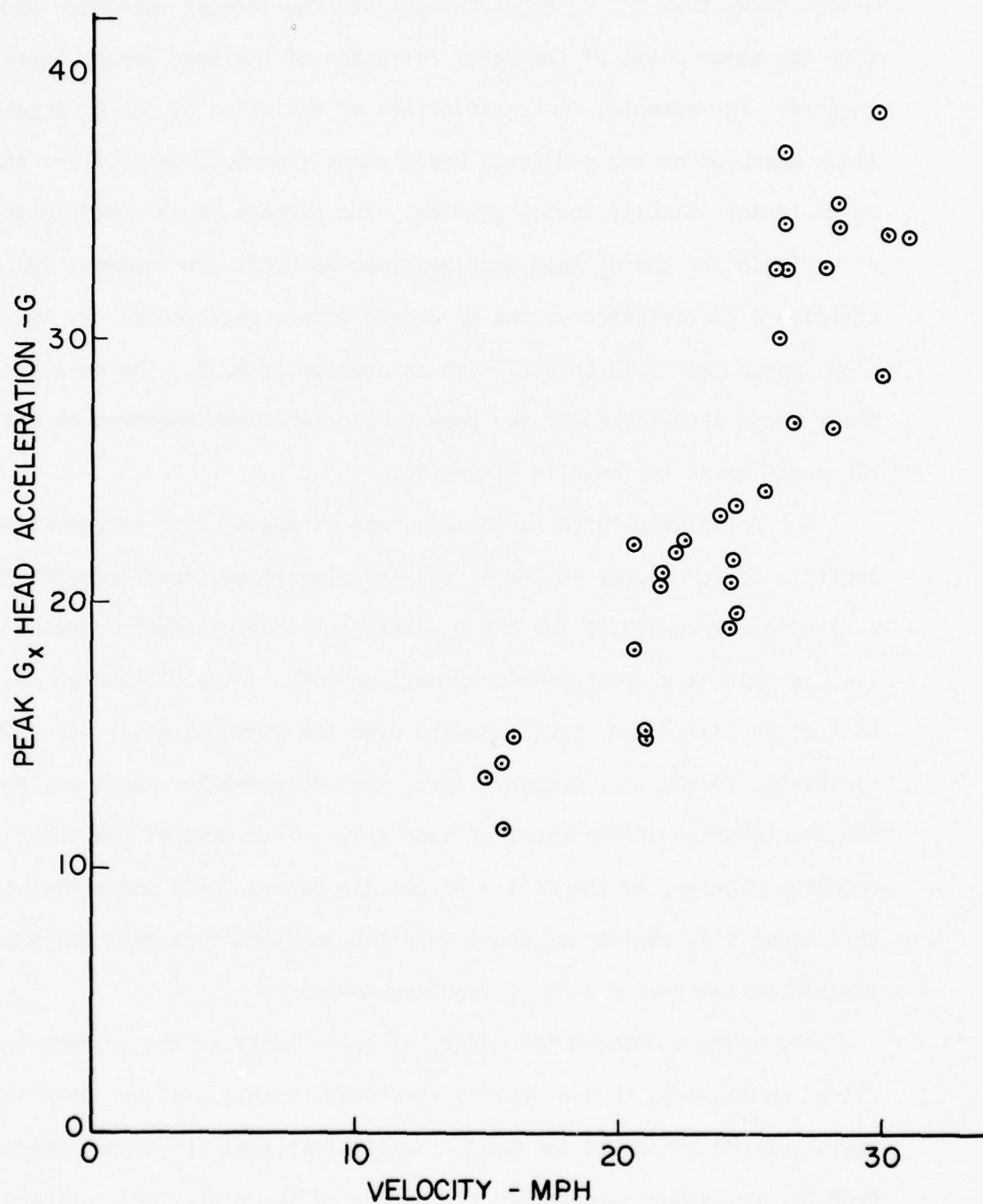


Figure 76. Peak G_x Acceleration Values Measured on the Head of Volunteers Using Externally Mounted Accelerometers

coefficient of variation from the means and standard deviations of the G_y accelerations showed only slight improvement from 0.30 to 0.27. However, the relationship of the average coefficients of variation for the G_x acceleration are reversed; the average coefficient of variation is 0.07 for the head acceleration and 0.12 for the acceleration measured in the mouth. (A statistical comparison of S.I. values computed from accelerations measured on the head and within the mouth is provided and discussed later in this section of the report.)

Figure 77 provides a plot of Head Injury Criteria (H.I.C.) values as a function of impact velocity. The H.I.C. values were plotted from the data listed in Table XXVI. The same general trend seen in the plot of S.I. versus impact velocity exists; however, there is a reduction of the scattering of data points.

The H.I.C. values provided by General Motors are compared to the H.I.C. values computed by the Aerospace Medical Research Laboratory in Table XLIII. The values calculated by GM appear to be consistently higher than those calculated by AMRL. Note that the acceleration data used by AMRL were digitized at a rate that would provide filtering of frequencies above 50 Hertz. These two groups of data were studied using a t-test to determine whether there is a statistically significant difference between the two data processing methods. The null hypothesis tested was that the mean difference is zero. The data were arranged in matched pairs and evaluated. The average difference between the means is -17.3. The value of t that was calculated is 4.325 and thus, the null hypothesis can be rejected (the value of t at the 0.5 level for 9 degrees of freedom is 2.262). H.I.C. values from tests numbers 6534,

TESTS 6507 - 6575

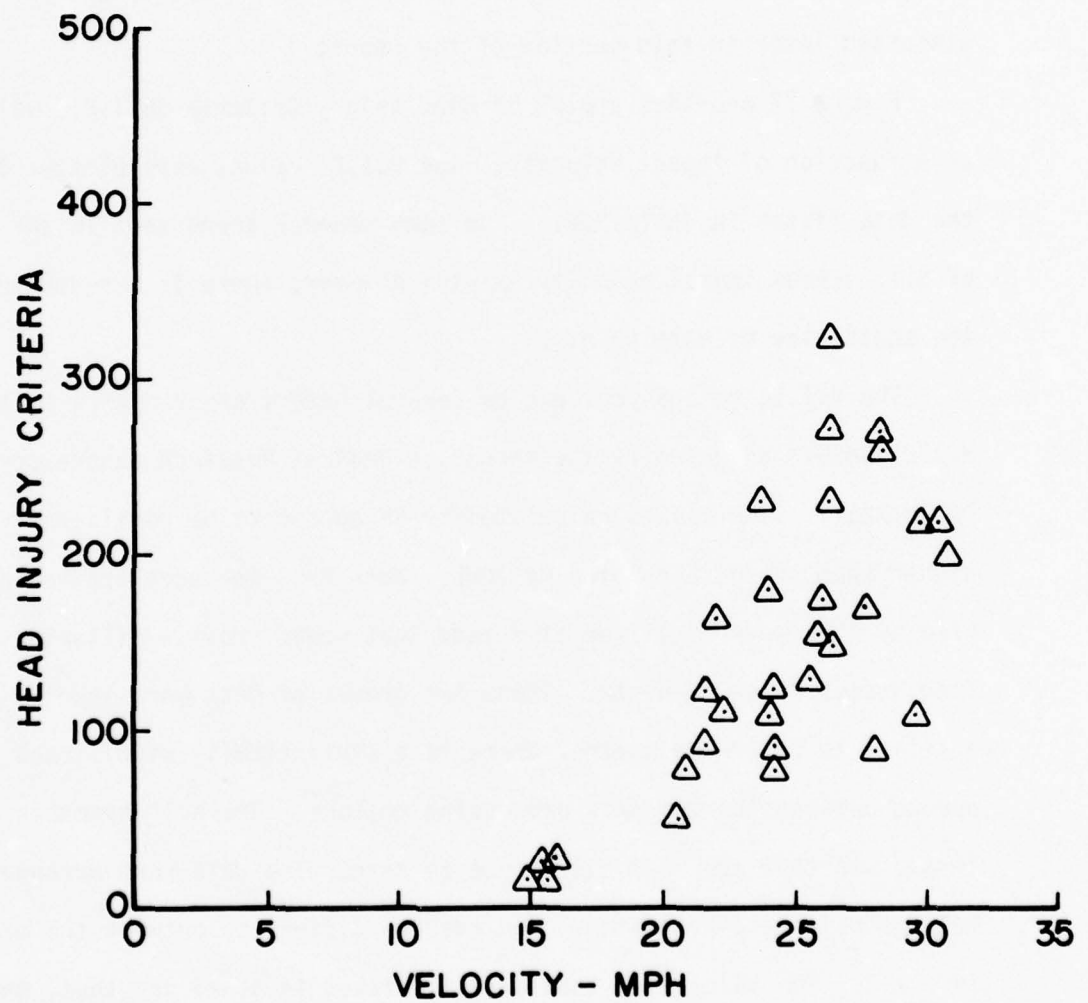


Figure 77. Head Injury Criteria Values for Tests 6507 to 6575

TABLE XLIII. COMPARISON OF H.I.C. VALUES CALCULATED
BY GENERAL MOTORS AND THE AEROSPACE
MEDICAL RESEARCH LABORATORY

TEST NO.	SLED VELOCITY (MPH)	H.I.C. (GM)	H.I.C. (AMRL)
6556	24.2	70	82
6557	24.3	90	93
6559	25.5	130	156
6561	28.1	270	274
6567	27.7	170	203
6569	28.0	90	100
6571	29.7	220	255
6572	29.8	110	113
6574	30.8	200	218
6575	30.1	220	249

6535, 6563, 6564 and 6566 were not used in this comparison because of the spurious G_z axis accelerations discussed previously.

One of the factors that could create a difference between the two methodologies is the digitization rate that was used or the introduction of other data filtering techniques. A series of t-tests of the difference between the mean and zero were accomplished to evaluate the differences between the data obtained from acceleration recordings digitized at a rate to filter frequencies above 500 Hertz and acceleration recordings digitized to filter frequencies above 50 Hertz. The data used in this analysis are summarized in Tables XLIV and XLV. The data are arranged in pairs matched in all aspects other than digitization rate.

The comparisons of peak values of sled acceleration, resultant acceleration measured on the subjects' head and resultant acceleration in the subject's mouth each showed statistically significant differences between the two digitization rates. The mean difference between the two sled acceleration data sets is -2.01 with an estimated standard deviation of the mean difference of 0.176. The t-value is 0.196 indicating that the probability the mean difference is zero is less than 0.001. The mean difference between the two head acceleration sets is -10.8 G with an estimated standard deviation of the mean difference of 3.99 ($t = 2.711$, probability $M = 0$ less than 0.02). The mean difference between the two mouth acceleration sets is -12.03 G with an estimated standard deviation of the mean difference of 3.31 ($t = 3.635$, probability of $M = 0$ less than 0.01).

TABLE XLIV. DATA FROM TESTS WHERE ACCELERATION RECORDINGS
WERE DIGITIZED TO FILTER ABOVE 500 HERTZ

TEST NO.	VEL. (MPH)	SLED ACCEL. (G _x)	HEAD ACCEL. (G _r)	HEAD IMPACT S.I.	MOUTH ACCEL. (G _r)	MOUTH IMPACT S.I.
6556	24	20.7	23.7	94	34.5	128
6557	24	20.3	24.2	108	29.4	148
6559	26	18.0	34.1	200	38.7	203
6563	26	19.9	38.3*	166*	51.5	255
6564	26	19.3	46.2*	168*	41.1	201
6561	28	21.1	58.0	373	58.4	313
6566	28	20.7	91.2	420	66.3	368
6567	28	20.0	40.9	229	68.9	382
6569	28	20.6	34.1	127	40.1	266
6571	30	21.2	45.6	282	36.9	255
6572	30	21.5	42.2	150	26.9	158
6574	30	22.7	36.8	256	34.6	225
6575	30	22.6	50.4	297	47.6	251

*G_z acceleration recording set to zero

TABLE XLV. DATA FROM TESTS WHERE ACCELERATION RECORDINGS
WERE DIGITIZED TO FILTER ABOVE 50 HERTZ

TEST NO.	VEL. (MPH)	SLED ACCEL. (G _x)	HEAD ACCEL. (G _r)	HEAD IMPACT S.I.	MOUTH ACCEL. (G _r)	MOUTH IMPACT S.I.
6556	24	19.0	22.5	104	25.0	128
6557	24	18.7	19.7	110	23.2	131
6559	26	17.3	31.3	204	37.4	215
6563	26	17.2	34.6*	169*	39.6	287
6564	26	17.6	34.9*	168*	28.8	151
6561	28	19.2	42.0	333	29.4	174
6566	28	19.1	36.0	346	34.3	199
6567	28	18.3	37.5	252	36.1	204
6569	28	18.7	29.7	134	36.1	195
6571	30	18.7	42.3	330	32.2	244
6572	30	18.8	28.0	141	27.1	156
6574	30	20.4	32.8	260	35.5	228
6575	30	19.5	33.6	291	33.7	208

*G_z acceleration recording set to zero

The t-test of the head impact Severity Index values obtained from measurements on the head showed no difference between the sets digitized at the different rates. The mean difference between the Severity Indices sets computed from acceleration measured on the head was -1.46 with a standard deviation of the mean difference of 8.14 ($t = 0.179$, probability of $M = 0$ greater than 0.8 but less than 0.9). However, the mean difference between the Severity Indices sets computed from accelerations measured within the mouth is -48.7 with a standard deviation of the mean difference of 19.5 which yield a t-value of 2.489. Thus, the Severity Indices computed from the accelerometers recorded within the subject's mouth are significantly different (less than 0.05 probability of $M = 0$) when different digitization rates are used. This may be due to two facts. First, the mouth mounted acceleration traces appear to contain more high frequency components. The head accelerometer mount and the head tissue would tend to filter out these higher frequency components since they are relatively softer than the dental appliance used to couple the mouth accelerometers to the head structure. Second, the mouth accelerometer recordings contained the high frequency anomaly that was consistently seen on the initial portion of the acceleration-time histories of both the chest and the mouth accelerometers.

The 50 Hertz digitization process had other pronounced effects. In specific tests, such as test numbers 6561 and 6566, where there were high amplitude spikes on the G_z acceleration traces, both the peak accelerations and Severity Indices were altered while in tests that were representative of the majority of the data that was collected there was generally little consistent significant effect.

The limited study of the effects of data processing techniques that has been accomplished within the scope of this program shows that the experimental results can be influenced by data processing methods such as the digitization rate. Unfortunately, only the frequency response requirements for instrumentation are currently defined in reference 14. This subject needs to be clarified in future standards.

The cord length data collected to determine the position of the head with respect to the windshield and the instrument panel reflect an interesting relationship to the impact environment. The trend that can be seen in Figure 40 in the Results section of this report is more clearly illustrated when the remaining-head-to-panel distances are averaged and plotted as a function of impact velocity as in Figure 78. This histogram shows that the average remaining distances decrease rapidly to the 22 MPH level but then appear to remain between 6 and 7.8 inches. The polynomial curve fit of the entire data set shown in Figure 79 provided the best correlation with these data.

Figure 80 attempts to show air cushion penetration trends within the individual subjects. Clear trends of remaining-head-to-panel distance decreasing with impact velocity are, in fact, seen in the cases of most of the subjects. However, subjects F, H and J seem to show a reverse trend although not to a significant degree. Several subjects such as H, J and M show remarkable similar penetrations for a fairly large range of impact velocities. Subjects J and M consistently penetrated deeply into the air bag. Subject B and E exhibited a tendency to rotate into the upper portion of the air bag during impact and, in fact, each contacted the windshield on two occasions. Subjects B and E were not selected for the 28 and 30 MPH tests because of this tendency.

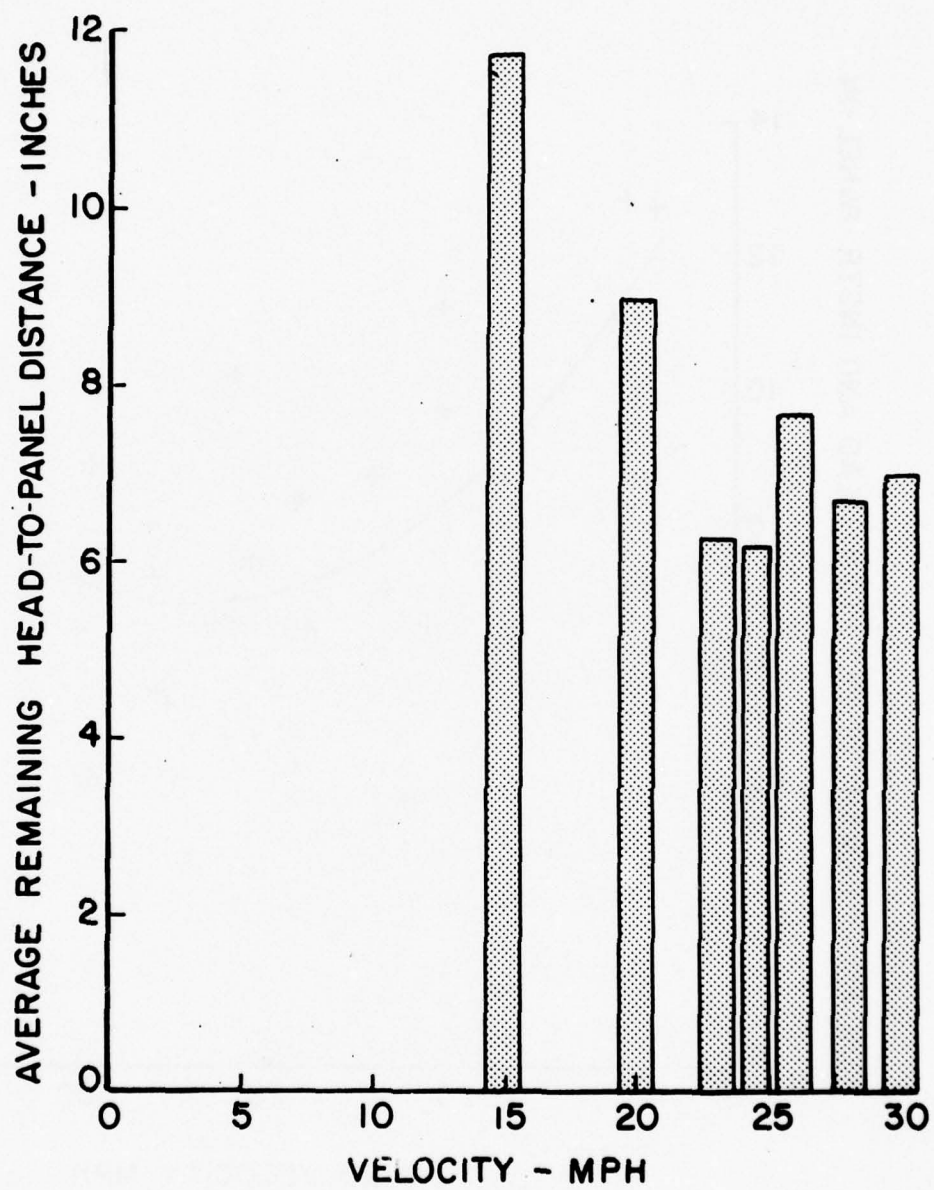


Figure 78. Average Remaining Head-to-Panel Distances for Impact Velocity Groups

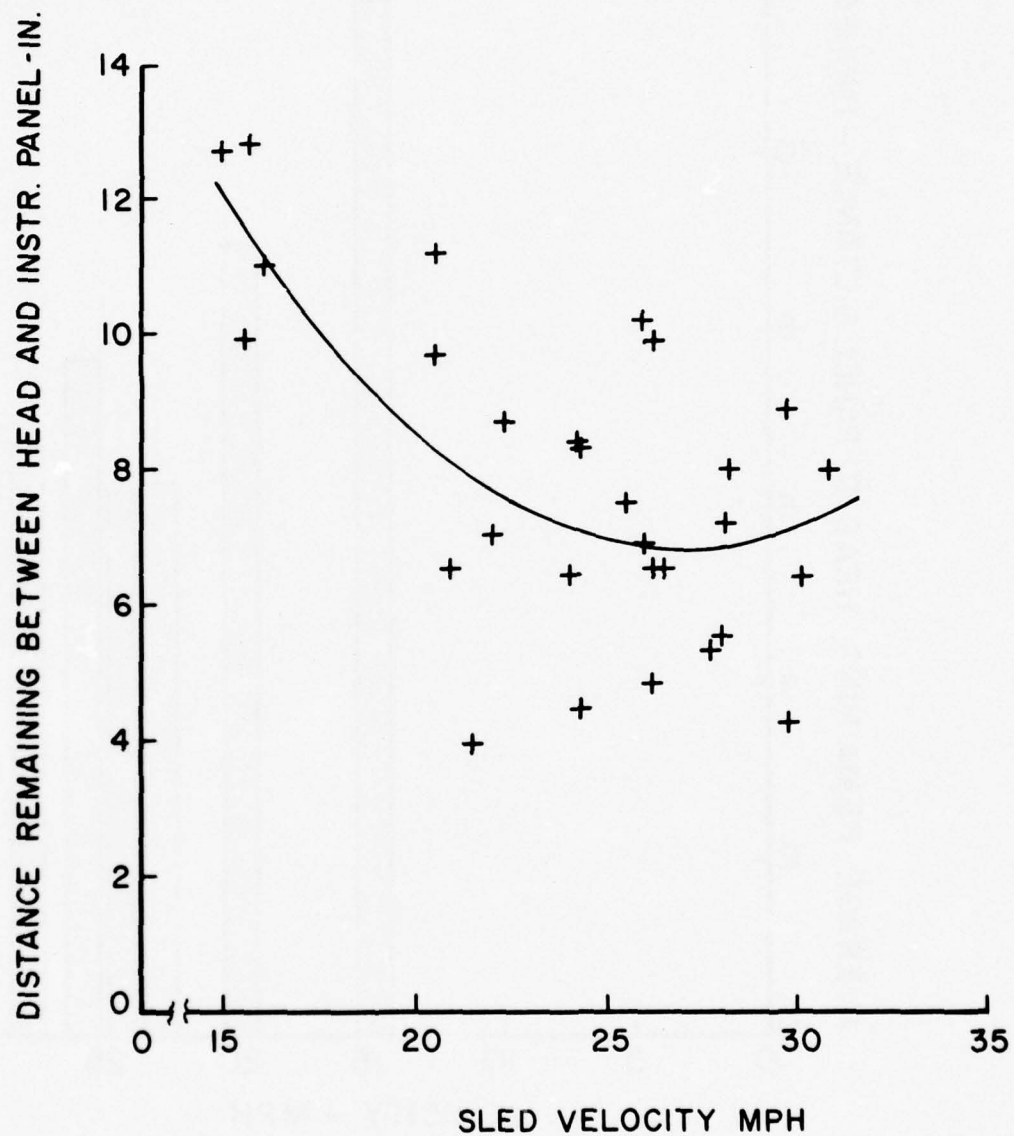


Figure 79. Distance Remaining Between Head and Instrument Panel for Each Test with Human Subjects

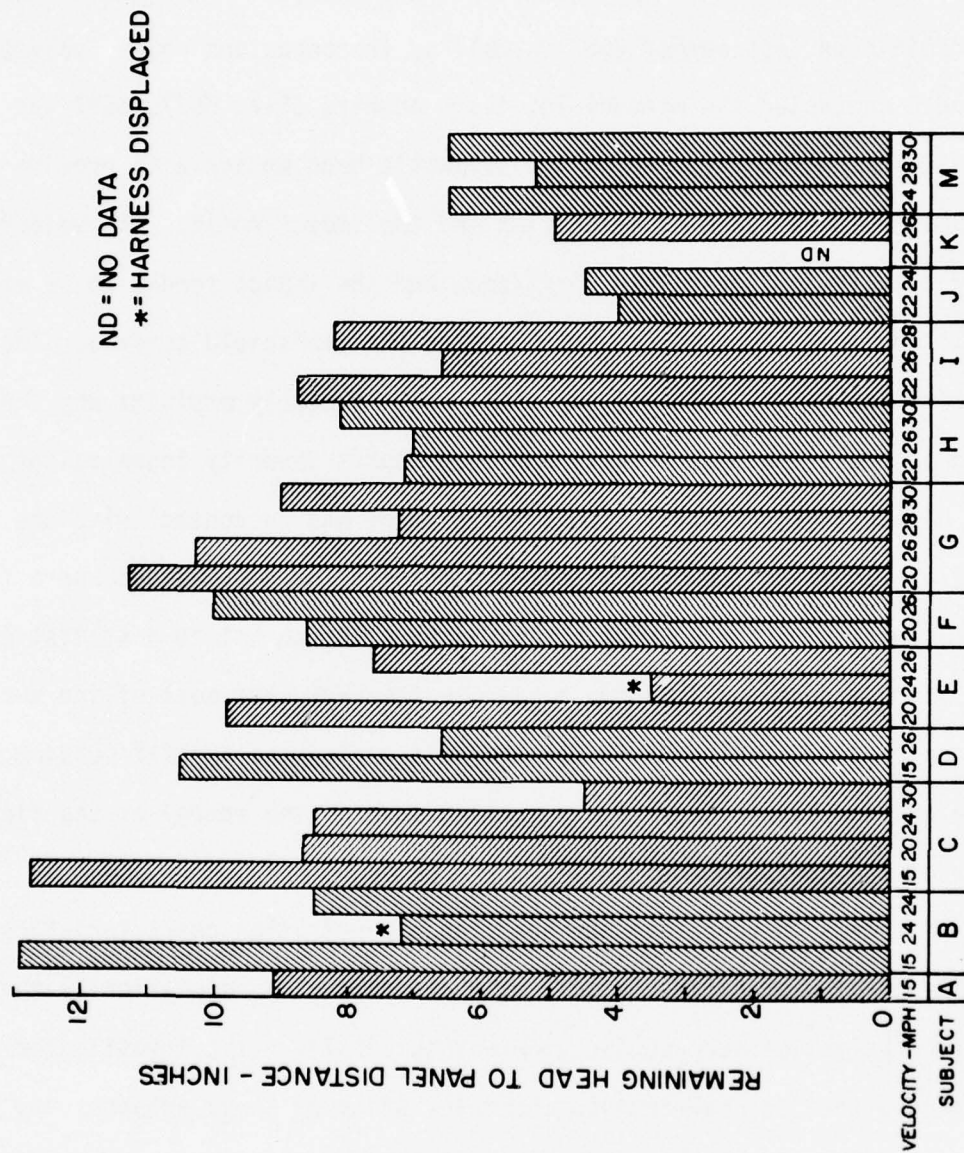


Figure 80. Remaining Head-to-Panel Distance Data Grouped for Each Subject

Although the analysis of the photometric measurements of head motion was limited to the four 30 MPH tests, and those tests where head contact with the windshield was indicated from other data, i.e., cord measurements or dye marks, it confirmed that subject A contacted the windshield on test number 6507 as well as the occasions where Subject B and E contacted the windshield, tests numbers 6514, 6537, 6557 and 6569. The motion pictures of the subject's head motion also provide an estimate of the range of velocities and the impact angle. The velocities were usually low, less than 10 ft/sec, and the impact tended to be at a small angle with respect to the plane of the windshield surface. The combination of low velocity and small angle probably explains why the head acceleration measurements and head impact Severity Index values are not higher than comparable tests where there was no contact with the windshield. In fact, the mean difference between the S.I. values where there were contacts versus no contacts is lower although not to a statistically significant degree. This may be due to the fact that most of the subjects who contacted the windshield contacted it during the initial portion of the deceleration event, thereby dissipating some of the energy of the final portion of the deceleration.

Attempts to correlate the head/torso penetration characteristics and incidents of windshield contacts with anthropometry, specifically the sitting height of each subject, were unsuccessful. The investigators suspected that the penetration characteristics of these subjects may be related to the stiffness with which the individuals maintained their leg muscles during impact. This theory was not verified by the foot load measurements but subjectively appeared to be the case from observation of the kinematics of the subjects documented by high speed photography.

Analysis of the foot load data shows a slight correlation between the sled acceleration and the resultant foot load measurements. The correlation coefficient is 0.55. The data are plotted in Figure 81. The least squares line plotted in this figure has an intercept at zero peak sled G of 1090 pounds and a slope of 32 pounds per G. Attempts to use up to third order polynomial fits did not significantly increase the goodness-of-fit. Although the linear correlation is slight, it is statistically significant. The probability of obtaining a larger correlation coefficient by chance is 0.001 if the true value of r is zero.

Attempts to obtain higher correlation of foot load data with other test parameters such as impact velocity were not fruitful. The data were also studied on a subject by subject basis; this was also fruitless.

From a medical standpoint the tests were relatively uneventful. Most subjects exhibited no significant apprehension during the tests. What little anxiety that existed initially was, in most cases, dispelled once the subjects had experienced their first test with the air cushion restraint system. Some degree of anxiety was unavoidably associated with the elaborate safety precautions that are quite apparent to the subjects in this type of experimentation. Subject K resigned from the panel after his second exposure in response to the concern that he felt regarding the possibility of impacting the instrument panel. This may have been due to the somewhat cumbersome head displacement measuring system or the unguarded comments of test personnel regarding his penetration into the air bag. Subject A resigned after his first test with the air cushion and shortly thereafter was transferred from the base. He was apparently anxious about his

Tests 6507-6575

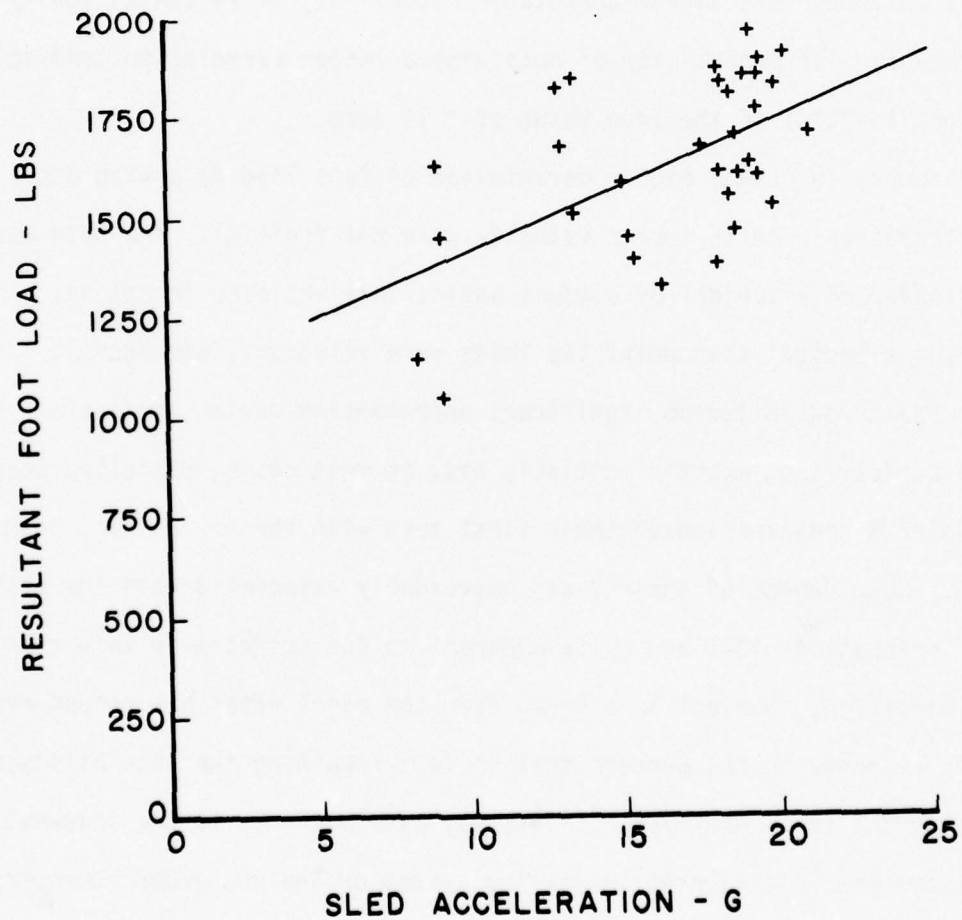


Figure 81. Resultant Foot Load Data Plotted as a Function of Impact Sled Acceleration

inability to brace his feet on the floor before impact (foot blocks were added to the following tests).

Objective medical findings and subjective complaints were minimal throughout the series of tests. The most severe adverse finding was a muscle spasm in one subject (test no. 6559) that persisted approximately seven days after the impact test. This occurrence was probably secondary to poor body and head position upon contact with the air bag.

Most of the subjects expressed the opinion that the tests were less stressful as the impact velocities increased. This subjective response may have reflected the reduced anxiety resulting from increased familiarity with the test environment rather than an actual decrease in the actual mechanical stress. Nevertheless, the objective medical findings associated with the higher velocity tests were very minimal.

The results of the earlier tests of a prototype air bag restraint (Ref 9) and the results of the air cushion tests have been graphically compared in Figures 82 and 83. Figure 82 plots the head impact Severity Indices from the respective volunteer test programs as a function of peak sled acceleration (as reported in Ref 9). This graph clearly shows a major reduction of the head impact Severity Index by the near-production air cushion restraint configuration. The average head impact Severity Index at 30 MPH from the earlier study was 851 and 258 in the tests reported herein. The scatter of the data points from the earlier tests is noticeably smaller, however.

The peak resultant chest accelerations measured in both test series, plotted in Figure 83, show that there was a decrease in the magnitude of these values in the tests with the near-production air cushion. The

scatter of the chest acceleration data about the least square lines appears to be smaller in the near-production air cushion tests than in the earlier tests.

The most dramatic difference between the data recorded from the earlier test series (Ref 9) and the data reported within this report is the difference between the head rebound accelerations. In the earlier tests the head rebound accelerations ranged from 40 to 137 G in contrast to the 1 to 12 G levels recorded on the head in the tests of the near-production air cushion restraint system.

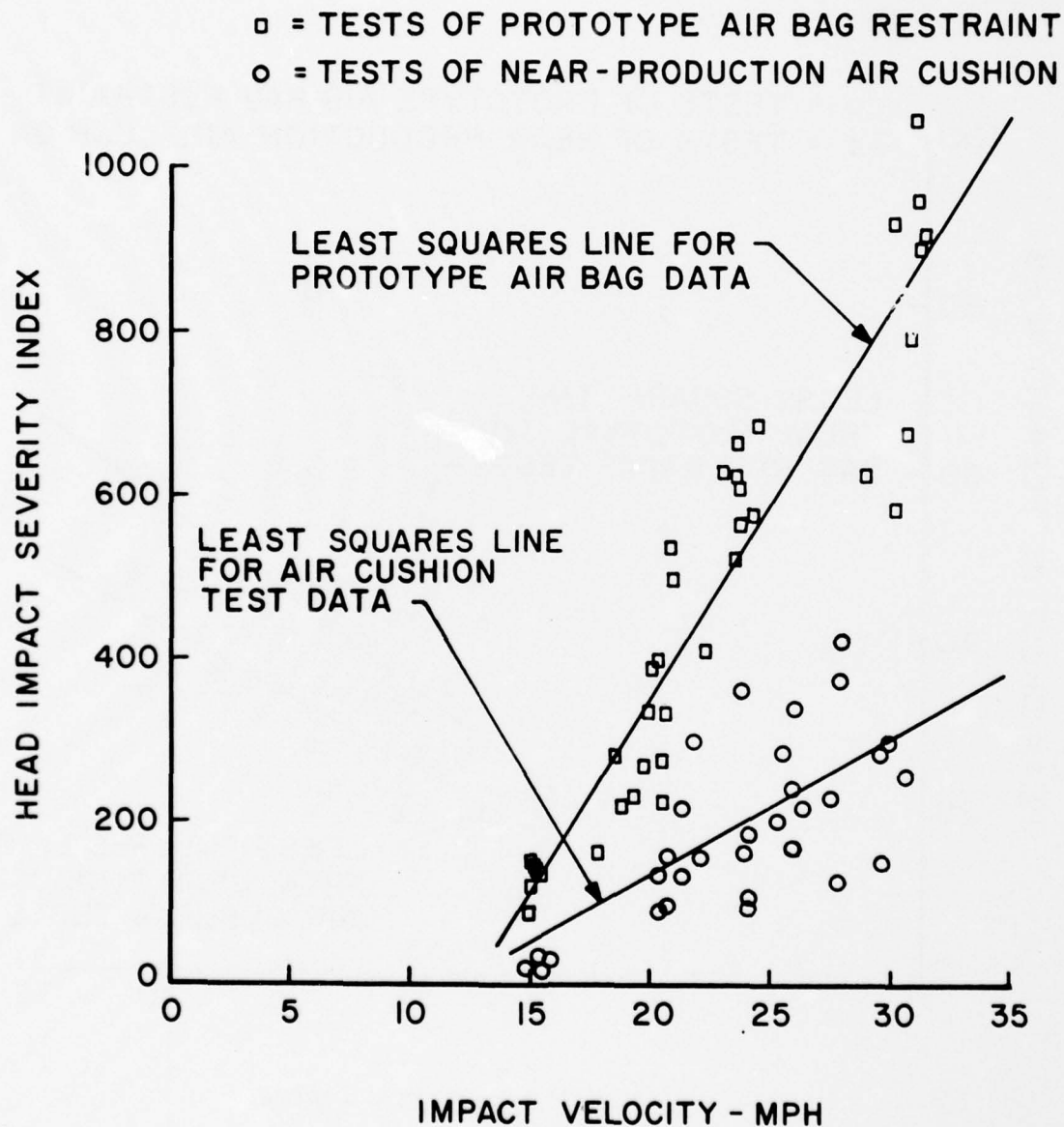


Figure 82. Head Impact Severity Index Values for Prototype Air Bag and Near-Production Air Cushion Tests with Human Subjects

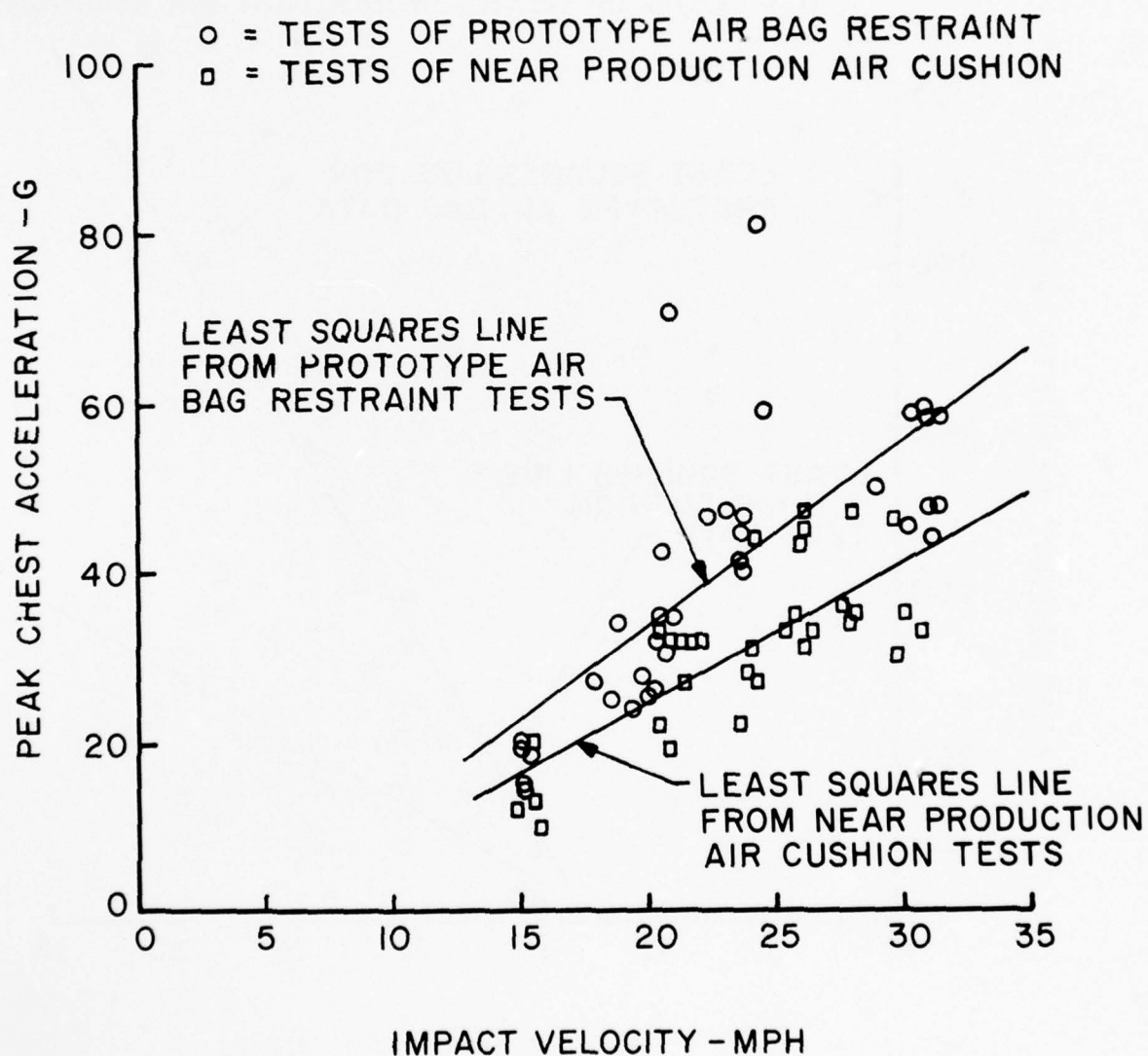


Figure 83. Peak Chest Acceleration Data for Prototype Air Bag and Near-Production Air Cushion Tests with Human Subjects

C. Comparison of Dummy and Human Tests

The peak resultant accelerations computed from the triaxial accelerations measured on the chests of the volunteer subjects are generally higher and have a larger variance than the peak resultant accelerations computed from the accelerations measured within the chest of the dummy subjects. For example, the mean of the peak resultant chest accelerations measured on the seven volunteers tested at the 26 MPH condition is 38.1 G with an estimated standard deviation of 6.62 (coefficient of variation = 0.174) while the peak values measured within the dummy chest have a mean of 32.7 G and an estimated standard deviation of 2.15 (coefficient of variation = 0.066). Analysis of these data sets using the F-test for variances resulted in an F value of 9.48 which indicates that the variances are statistically different.

A statistical comparison of the peak resultant chest accelerations from the same seven tests with volunteers and the data computed from the accelerations measured by the accelerometer package mounted on the chest of the dummy shows that the values are statistically equivalent in terms of both their means and estimated variances. The mean of the peak chest accelerations measured on the dummy chest is 35.5 G with an estimated standard deviation of 6.33 (coefficient of variation = 0.178). The means were evaluated using the t-test for differences between two means and the variances were evaluated using the F-test (ref 18). The computed value of t is 1.048 and the value of F is 1.09.

A comparison of the head impact Severity Indices from the same dummy and human tests used in the above analyses shows similar relationships. The mean S.I. from the data measured within the dummies head is 196.5 with an estimated variance standard deviation of 22.8 (coefficient

of variation = 0.116) while the S.I. values determined from measurements taken from the externally mounted accelerometers have a mean of 267.5 with an estimated standard deviation of 112.2 (coefficient of variation = 0.419). The S.I. values obtained during the seven tests with volunteers have a mean of 232.3 with an estimated standard deviation of 65.1 (coefficient of variation = 0.280). S.I. values calculated from external measurements on the dummy and the volunteers indicate that the variance estimates are probably not different and a t-test of the differences between the means, using a pooled estimate of the standard deviation also indicates no difference ($t = 0.779$). It is interesting to note that if the two lowest and the two highest S.I. values in the sample of dummy tests are eliminated, the differences between the dummy sample and the human sample are statistically negligible since the mean of the dummy sample is then 248.8 with an estimated standard deviation of 52.3.

Due to the previously expressed concern about the influence of impact velocity upon the variance of the dummy data and the human head impact S.I. values, the analysis of the results from the dummy and volunteer tests was extended to include an analysis of covariance. The peak resultant accelerations and the head impact Severity Indices from the measurements on the dummies and the volunteer subjects were compared after adjusting for impact velocity. Using untransformed data, the hypothesis of no difference could not be rejected in either comparison. The value of the F statistic is $F(1,68) = 0.163$ for the chest acceleration data sets. The F statistic for the S.I. data sets, shown in Figure 84, is $F(1,68) = 0.163$. The hypothesis could also not be rejected using the transformed data, here $F(1,68) = 1.398$.

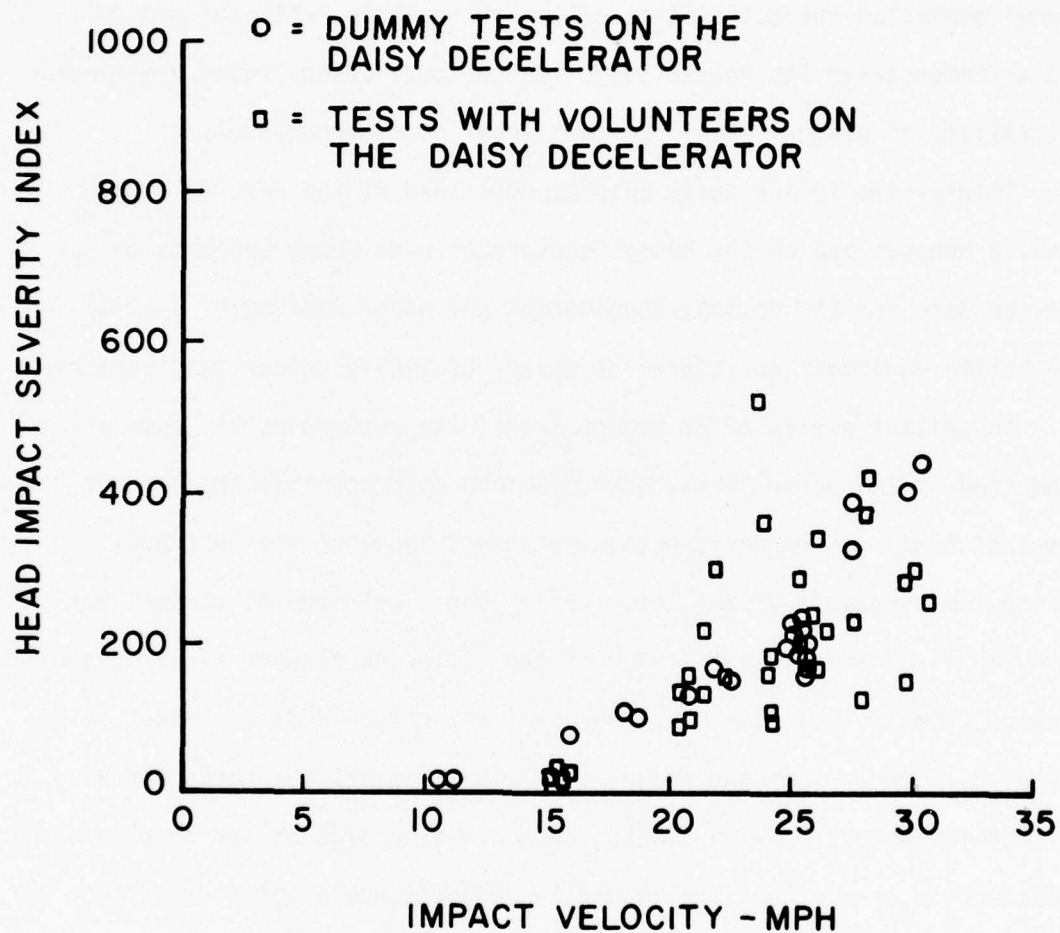


Figure 84. Head Impact Severity Index Values for Tests with Dummy and Volunteer Subjects on the Daisy Decelerator

VI. SUMMARY

A series of 50 tests with anthropometric dummies were accomplished at the General Motors Proving Grounds at impact velocities ranging from 15 to 40 MPH. The objectives of these tests were to determine the normal operating characteristics of the air cushion restraint system and to demonstrate its reliability. These tests demonstrated a minimum reliability of 0.95 at the 90 percent lower confidence level.

Thirty-nine impact tests were accomplished at the General Motors Proving Grounds and on the Daisy Decelerator with dummy subjects to provide data for the design, development and proof testing of special protective equipment to insure the safety of the volunteer test subjects.

An initial series of 28 impact tests with anthropometric dummies conducted on the Daisy Decelerator provided evidence that the head of the test dummy was contacting the instrument panel of the test buck during the subject's impact into the air bag. Evidence of contact was found in 11 of the 28 tests. Ten of the 11 incidents were at velocities ranging from 12.4 to 15.8 MPH. One incident occurred at an impact velocity of 31.8 MPH. A second series of 34 impact tests was conducted at the General Motors Proving Grounds to study this problem and develop a procedure to assure that the volunteer subjects would not contact the instrument panel during normal operation of the air cushion restraint system.

The air cushion inflator system was revised as a result of impact tests at the General Motors Proving Grounds. The pyrotechnic charges within the gas generators were increased from 20 grams to 25 grams and the pressure of the stored gas was increased from 2350 psi to 2700 psi.

Increasing the size of the pyrotechnic charges had a statistically significant influence on the head impact Severity Index but not on the peak resultant chest acceleration. It also did not prevent head contact with the instrument panel. Increasing the stored gas pressure with the inflator reduced the possibility that the subject's head would contact the instrument panel; however, increasing the pressure did not make a statistically significant difference in either the head impact Severity Index or the peak resultant chest acceleration.

A final series of 25 impact tests of the air cushion restraint system was accomplished on the Daisy Decelerator prior to initiation of tests with volunteers. The revised inflator system was used. Twenty of these tests were exact, successive replicates conducted at the 26 MPH test condition.

A total of 103 impact tests of the air cushion restraint system were conducted with 50th and 95th percentile anthropometric dummies prior to commencement of tests with human subjects. These tests successfully demonstrated that the minimum reliability of air bag deployment was 0.98 at the 90 percent lower confidence limit.

Comparisons of differences between measurements of peak chest accelerations for 50th and 95th percentile dummies showed statistically significant differences. The same comparison of head impact Severity Index values for the two dummy sizes did not show a statistically significant difference. However, the differences between head impact Severity Indices due to dummy size were probably obscured by the large variance in this parameter.

Forty-three impact tests of the air cushion restraint were accomplished with 12 volunteer subjects. Impact velocities were incrementally

increased from 14.9 to 30.8 MPH with sled accelerations ranging from 8.3 to 21.1 G. Peak resultant acceleration measured on the subject's chests ranged from 11 to 47 G. Head impact Severity Indices calculated from accelerations measured on the subject's heads ranged up to 420 (700 if the influence of G_z acceleration transients was included) while the corresponding maximum H.I.C. value was 281.

The inertial loads that were reacted through the feet of the volunteer subjects during impact were measured by two triaxial load cells mounted under the floor board of the test buck. The measured loads varied between 1100 to 1900 pounds. The loads were slightly but significantly correlated with the sled acceleration. The slope of the least squares line of the data was 32 pounds per G with an intercept of 1090 pounds. The foot load-time histories were nearly trapezoidal in waveform.

The distances remaining between the subject's head and the instrument panel were not linearly correlated with impact velocity. The data points were best fit by second and third order polynomial curves. The distances varied from 12.9 to 4.0 inches over the range of impact velocities that were studied.

Dye marks on the windshield of the test buck indicated that the volunteers contacted the windshield during four tests. Data obtained from cords attached to the subjects' heads indicated that a subject contacted the windshield during three additional tests; however, photometric data provided clear confirmation for only one of these three possible contacts. The windshield contacts were not noticed by any of the subjects during the tests and could not be detected by analysis of the head impact Severity Indices.

Objective medical findings and subjective complaints were minimal throughout the test series. The most severe adverse finding was a muscle spasm in one subject which persisted for approximately seven days. The subjects indicated that the tests were less stressful as the impact velocities increased.

Peak resultant acceleration values and head impact Severity Indices determined from measurements taken from within the chests of dummy subjects were statistically different than the values determined from measurements taken from the externally mounted accelerometers on both dummy and human subjects. When the values were obtained from accelerometers that were mounted similarly at the same anatomical sites, there was no statistically significant difference between the dummy and human test results.

Statistical comparisons of head impact Severity Index data obtained from dummy tests conducted by the General Motors Corporation using an acceleration facility and by AMRL using a deceleration facility showed that the data were significantly different. The same comparisons between the peak resultant chest accelerations measured on dummies at the two facilities failed to show a statistically significant difference.

An analysis was conducted to evaluate the influence of data sampling rates upon the test results. Sampling rate was found to have a statistically significant effect upon both peak resultant acceleration values and head impact Severity Indices.

The results of the tests of the near-production air cushion indicated that the tests were less severe than equivalent tests conducted with volunteers using an earlier prototype air bag restraint. The tests

were less severe in terms of peak resultant acceleration measured on the chest and head during both the initial impact with the air bag and impact with the seat back following rebound from the air bag.

VII. REFERENCES

1. Clarke, T. D., Sprouffs, J. F., Trout, E. M., Klopfenstein, H.S., Muzzy, W. H., Gragg, C. D., and Bendixen, C. D., "Baboon Tolerance to Linear Deceleration (-G):Lap Belt Restraint," Fourteenth Stapp Car Crash Conference. AMRL-TR-72-44, November 1970, (AD 741 739).
2. Clarke, T. D., Sprouffs, J. F., Trout, E. M., Gragg, C. D., Muzzy, W. H. and Klopfenstein, H. S., "Baboon Tolerance to Linear Deceleration (-G):Air Bag Restraint." Fourteenth Stapp Car Crash Conference. AMRL-TR-72-43, November 1970, (AD 741 724).
3. Clarke, T. D., Smedley, D. C., Muzzy, W. H., Gragg, C. D., Schmidt, R. E., and Trout, E. M., "Impact Protection Afforded by the Air Force Shoulder Harness - Lap Belt." Fifteenth Stapp Car Crash Conference. AMRL-TR-72-74, November 1972.
4. Sprouffs, J. F., Muzzy, W. H., Gragg, C. D. and Clarke, T. D., "Data Reproducibility During Impact of a Rebuilt Dummy." Fifteenth Stapp Car Crash Conference. Society of Automotive Engineers, Inc., New York, November 1971.
5. Sprouffs, J. F., Clarke, T. D., Gragg, C. D., Trout, E. M., and Muzzy, W. H., "Evaluation of the Lap Belt, Air Force Shoulder Harness - Lap Belt, and Air Bag Plus Lap Belt Restraints During Impact with Anthropomorphic Dummies." Aerospace Medicine, Vol. 43, No. 4, April 1972.
6. Bendixen, C. D., "Final Report, Daisy Track Human Tolerance Tests." Department of Transportation Technical Report No. DOT-HS-800-419, June 1970.
7. Gragg, C. D., Bendixen, C. D., Clarke, T. D., Klopfenstein, H. S., and Sprouffs, J. F., "Evaluation of the Lap Belt, Air Bag and Air Force Restraint Systems During Impact with Living Human Sled Subjects." Fourteenth Stapp Car Crash Conference, AMRL-TR-72-42, November 1970, (AD 741 731).
8. Greer, C. R., and Gragg, C. D., "Experimental Evaluation of the Deployment of an Air Bag Restraint Using Human Subjects (Stationary Body Buck)," Department of Transportation Report No. DOT-HS-800-668, May 1972.
9. Greer, C. R. and Russell, H. C., "Impact Tests of Human Subjects Using a Prototype Air Bag Restraint System," Department of Transportation Report No. DOT-HS-800-805, September 1972.
10. General Motors Corporation, "Holloman II, Dynamic Tests," Warren, Michigan, Unpublished, February 1972.

11. Gadd, C. W., "Use of Weighted Impulse Criterion for Estimating Injury Hazard," 10th Stapp Car Crash Conference, Society of Automotive Engineers, Inc., New York, Paper No. 660793, 1966.
12. Federal Motor Vehicle Safety Standard No. 208, U. S. Department of Transportation, National Highway Traffic Safety Administration, Washington, D. C., May 1972.
13. Chandler, R. F., "The Daisy Decelerator," 6571st Aeromedical Research Laboratory, Technical Report No. ARL-TR-67-3, May 1967.
14. Instrumentation for Barrier Collision Tests - SAE J 211, Society of Automotive Engineers, Inc., 1970.
15. Warner, A., Ofsevit, D. and Plank, G., "Occupant Motion Sensors: Rotational Accelerometer Development." Department of Transportation Report No. DOT-HS-820-211, April 1972.
16. Plank, G., Ofsevit, D., and Warner, A., "Occupant Motion Sensors: Development and Testing of a Piezoresistive Mouthpiece Rotational Accelerometer," Department of Transportation Report No. DOT-HS-820-211, July 1973.
17. Hertzberg, H. T. E., and Daniels, G. S., "Anthropometry of Flying Personnel - 1950." WADC Technical Report 52-321, September 1954.
18. Volk, W., Applied Statistics for Engineers. McGraw-Hill Book Co., New York, 1958.
19. Dixon, W. J. and Massey, K. J., Introduction to Statistical Analysis. McGraw-Hill Book Co., New York, 1957.
20. Johnson, A. K., "Analysis of Decelerator, Accelerator, and Shock-Cord Propelled Rebound Sleds for Evaluating Air Bag Restraints." National Highway Traffic Safety Administration, Department of Transportation Report No. DOT-HS-820-220, August 1972.

APPENDIX A

SUMMARY OF INSTALLATION, MATERIALS AND CONFIGURATION
ASPECTS DEVIATING FROM THE PRODUCTION AIR CUSHION
SYSTEM

COMPILED FROM DATA SUBMITTED BY THE
FISHER BODY DIVISION,
GENERAL MOTORS CORPORATION

The front passenger air cushion restraint system used in the human tests deviates from the proposed 1973 "C" and "E" body system in the following respects:

I. Test Buck versus Production Body

The test buck is more rigid than a car body in respect to the firewall and "A" pillar air restraint mounting; the floor pan is rigid plywood without a tunnel and the seat attachment is a rigid bracket rather than the seat adjuster assemblies.

II. Upper Instrument Panel and Windshield

The windshield has been replaced with energy absorbing styrofoam with an interior surface to duplicate the internal contours of a production windshield. The upper instrument panel, made from high energy absorbing material, follows the contour of the 1972 Oldsmobile "B" upper instrument panel to the crest but from there it goes to the windshield surface on a 45 degree angle above the normal instrument panel surface.

III. Headrest

18" x 68" x 10" Polyurethane foam

IV. Sensor and Bumper Switch

The sensor and bumper switch were removed from the air cushion restraint system and the activating signal was supplied by cam switches located on the Daisy track sled. Both gas generators will be initiated regardless of the test speed.

V. Restraint Assembly - Air Cushion Front Passenger

Production 960613

Test Article 71XP-06093

A. Manifold

Material was a nodular iron casting.

B. Diffuser and Cushion Assembly

1. Inner cushion retainer had ring ends to slip over the diffuser instead of snap-in-clamps.
2. In addition to the normal diffuser-to-manifold junction, these parts are bolted together with three 1/4-20NC bolts.
3. An inner and an outer pitot tube are added for bag pressure measurements.

C. Plate Assembly - Reaction

The reaction plate had three 1/2-inch diameter holes which were filled with rubber plugs on the interrupt wire switches.

D. Interrupt Switch

Three interrupt switches were added to trigger the explosive nut which anchors the safety harness.

E. Inflator Assembly

71XP-06104 inflator assembly differs from proposed production as follows:

1. Inflator was shipped with 15 psi argon gas and pressurized to 2700 psi after installation in buck.
2. The fill valve was replaced with a port connection to the fill hose. This hose was 1/4" ID and approximately 6 feet

long. This added 2.7 cubic inches to the 100 cubic inch volume of the vessel.

3. The electrical connection was made through a pigtail and standard Packard Electric snap-on connector instead of the production plug-in connector.
4. The low pressure monitoring switch was removed.
5. The shipping cap was smaller than the production cap because the vessel was not charged.
6. The high level pyrotechnic gas generator chamber was ported for a pressure transducer.

NOTE: A pressure transducer in the fill hose measured vessel pressure.

7. A wire interrupt switch was added across the low level gas generator output nozzle to signal the release of the secondary restraint system.
8. Redundant squibs with separate switches, batteries and circuits were provided in the high and low gas generators.
9. The amount of propellant within first mode gas generator was increased from 20 grams to 25 grams.

APPENDIX B

TSC 4 CHANNEL LINEAR/ROTATIONAL MOUTHPIECE ACCELEROMETER SPECIFICATIONS

PHYSICAL PROPERTIES

Configuration: Consists of four miniature piezoresistive accelerometers (Endevco Model 2264-150), three of which are mounted on mutually perpendicular axes ($x = A - P$, $y = Lateral$, $z = longitudinal$). The fourth is also mounted on the z axis and the spacing of the two z accelerometers is 0.58". The device measures three linear accelerations and rotational acceleration in the sagittal plane.

Size: Approximately $1\frac{1}{2}" \times \frac{3}{4}" \times \frac{1}{4}"$ (including mounting flanges). $\frac{3}{4}" \times \frac{3}{4}" \times \frac{1}{4}"$ (excluding mounting flanges).

Weight: Less than 10 grams

DYNAMIC CHARACTERISTICS

Range: -150 g to +150 g (linear)
-200,000 r/sec² to +200,000 r/sec² (rotational)

Sensitivity: 2.0 mv/g (linear)
.003 mv/r sec² rotational

Frequency response: (linear and rotational)
1 db 0-500 Hz
3 db 0-1000 Hz

Linear error: (maximum)
13 r/sec²/g (uncorrected)
3.3 r/sec²/g (corrected)

Linearity: Less than $\pm 3\%$

ELECTRICAL CHARACTERISTICS

Excitation: 10v DC regulated battery supply

Resistance: $1700 \pm 20\%$ per arm

APPENDIX C

TWO BIT DISPLACEMENT MEASURING SYSTEM

CHARLES S. CLARK
SENIOR ELECTRONIC ENGINEER
DYNALECTRON CORPORATION
LAND-AIR DIVISION

CONTRACT DAAD07-69-C-0032

An urgent requirement was presented for a method to measure the travel of the subject's head during deceleration into an air bag. Photographic measurements could not be used since the air bag obscured the field of view. A string harness and friction brake were used, but this method gave only a single data point, i.e., the maximum displacement of the head. It was decided to design and fabricate an electronic system based on the principle of a photo cell tape reader. The system was specified to provide two channels of displacement time information.

The system consists of: (1) two read heads on the sled, (2) blockhouse instrument chassis containing a two-channel counter with a shared numerical read-out, (3) two tape recorder output circuits, (4) two galvanometer output circuits, and (5) power supply. The read heads, which were mounted on the sled, use a pair of photo interrupter modules to detect a horizontal stripe pattern on an exposed strip of 16 mm film (see figure C1). Each module has an infrared light emitting diode and phototransistor. When an exposed strip of tape passes through the read head, a pulse is generated. This pulse is transmitted through the whip cable to the counter and record output circuits in the blockhouse. Since the electronics cannot distinguish the direction of motion, a pressure pad on the read heads prevents reverse motion of the film after maximum pull-out.

The system was designed to resolve a displacement of .2 inch for a total travel of 39.8 inches (199 counts), with a one count ambiguity. Maximum anticipated pulse rate is 3 kHz which corresponds to a film velocity of 600 inches per second which is approximately 34 mph. During bench tests, pulse rates of 5 kHz were easily recovered.

The read modules are bilaterally symmetrical such that each cell reads a half track on the film, thus generating two bits of data (hence the name of the device). The film is designed such that four consecutive stripes .2 inches apart cover half the width of the film. The fifth strip is full width and is thus read by both cells. This is shown in Figure C1.



Figure C1. Film Stripe Pattern

The bits are electrically summed to yield a recording output which duplicates the appearance of the film. The width of the recorded pulses are proportional to film speed through the head as shown in Figure C2.

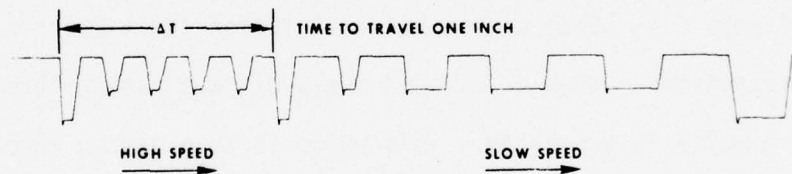


Figure C2. Recorded Output Pulses

Bit #1 is fed into the electronic counter. The totalized count, up to a maximum of 199, is displayed on a light emitting diode readout. The readout is shared between two counters. The contents of either counter can be displayed by a selector switch. A fixed decimal point is placed between the first and second digit. This means that displacement in inches can be determined by multiplying the counter reading by two. Example: 10.2 equals 20.4 inches of displacement.

The film as it passes under the read head generates a pulse train which, when totalized, gives the incremental displacement of the film. This, of course, is not the displacement of the subject's head since there is slack in the pulling string prior to impact. In order to determine the maximum displacement, it is necessary to know the exact amount of slack before the film is placed in tension. This is illustrated in Figure C3.

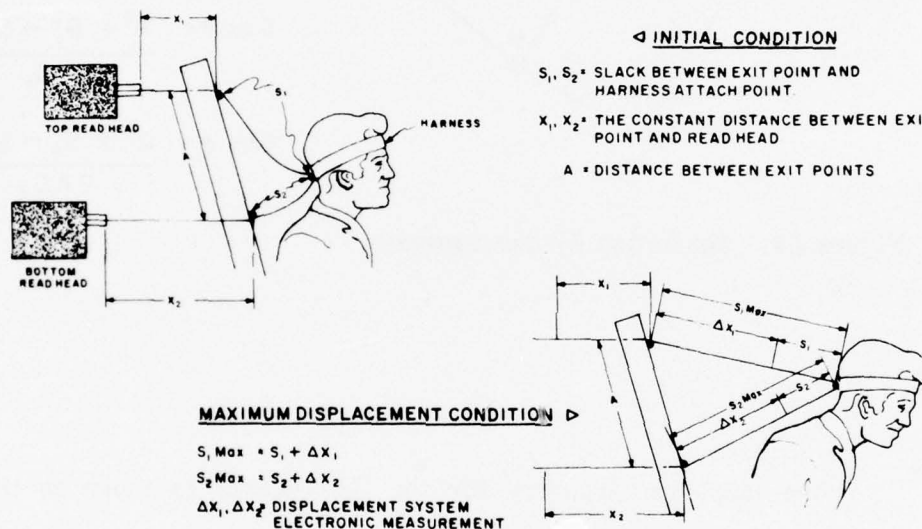


Figure C3. Measurement System Initial and Maximum Displacement Conditions

It should be noted that if there is no slack between the exit point and the read heads the absolute value of X_1 and X_2 do not enter the calculation.

Provided A is known, and careful pre-run measurement is made of S_1 and S_2 , then maximum displacement can be solved for graphically or analytically as shown in figure C4.

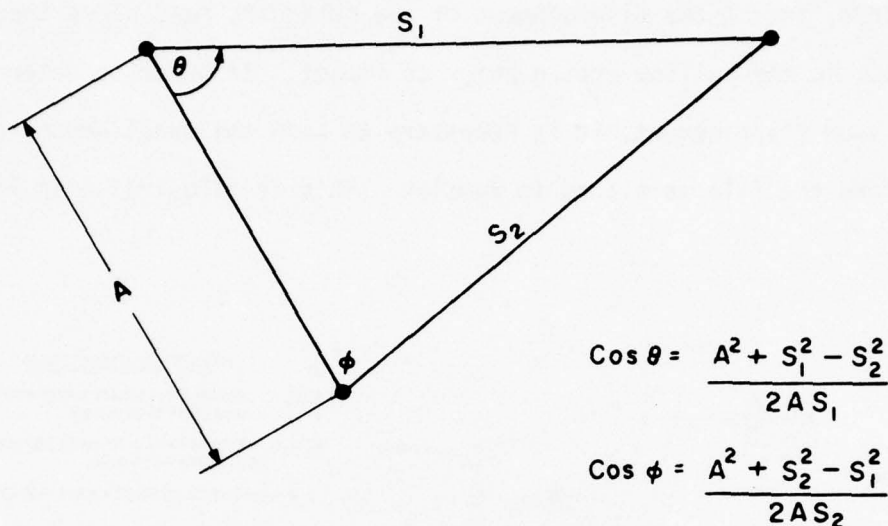


Figure C4. Measuring System Geometry

The complete circuitry for the instruments is shown on the electronic schematic. Digital logic was implemented using Teledyne HiNIL circuits. This is a family of 12 volt DTL logic offering excellent noise immunity, and modest speed. The family uses an open collector output transistor to drive loads of variable impedance. The galvanometer drive circuit is formed by current summing the drive capability of two open collector NAND gates. The tape recorder drive circuit is somewhat unusual in that optoisolators are used to form a ground referenced voltage summing circuit which is shown in simplified form in figure C5.

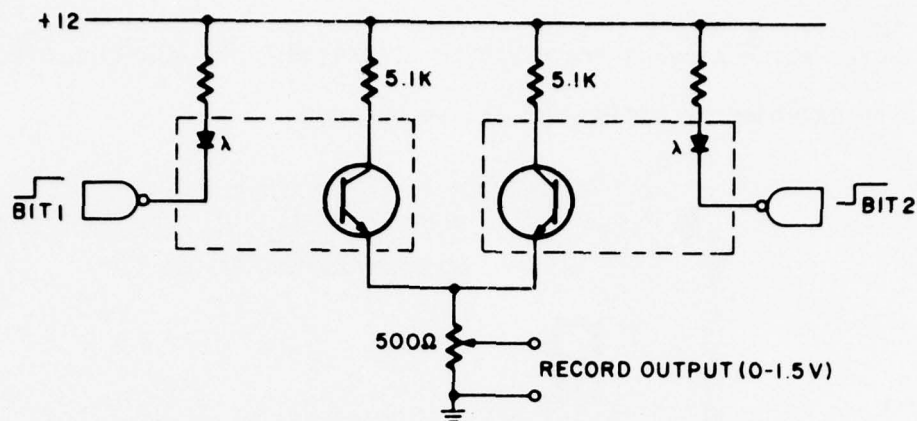


Figure C5. Ground Referenced Voltage Summing Circuit

FUTURE CONSIDERATIONS

There are circuit additions which can be made to the system to yield improved performance and more information. These include: (1) coincidence circuit for controlled pulse outputs to recorders, (2) electronic quadrature detection and mechanical take-up mechanism for bidirectional readings, (3) thumbwheel presets for entering value of slack in pulling string, and (4) digital to analog converter for continuous analog output of displacement.

The mechanical design aspect of a bidirectional reader would probably be difficult. Previous experimentation with spring-loaded, angular pickoff resistive potentiometers showed that overshoot control at reasonable force levels under impact conditions was difficult to achieve.

It is felt that a related design can be used for other applications. For example, by attaching a pulling cord to the moving part, it would be possible to measure the displacement and peak velocity of the HYGEE thrust column and sled. There is no limit except length of film on the distance

over which a pulse train can be generated. The counting circuits can be extended by adding successive decades.

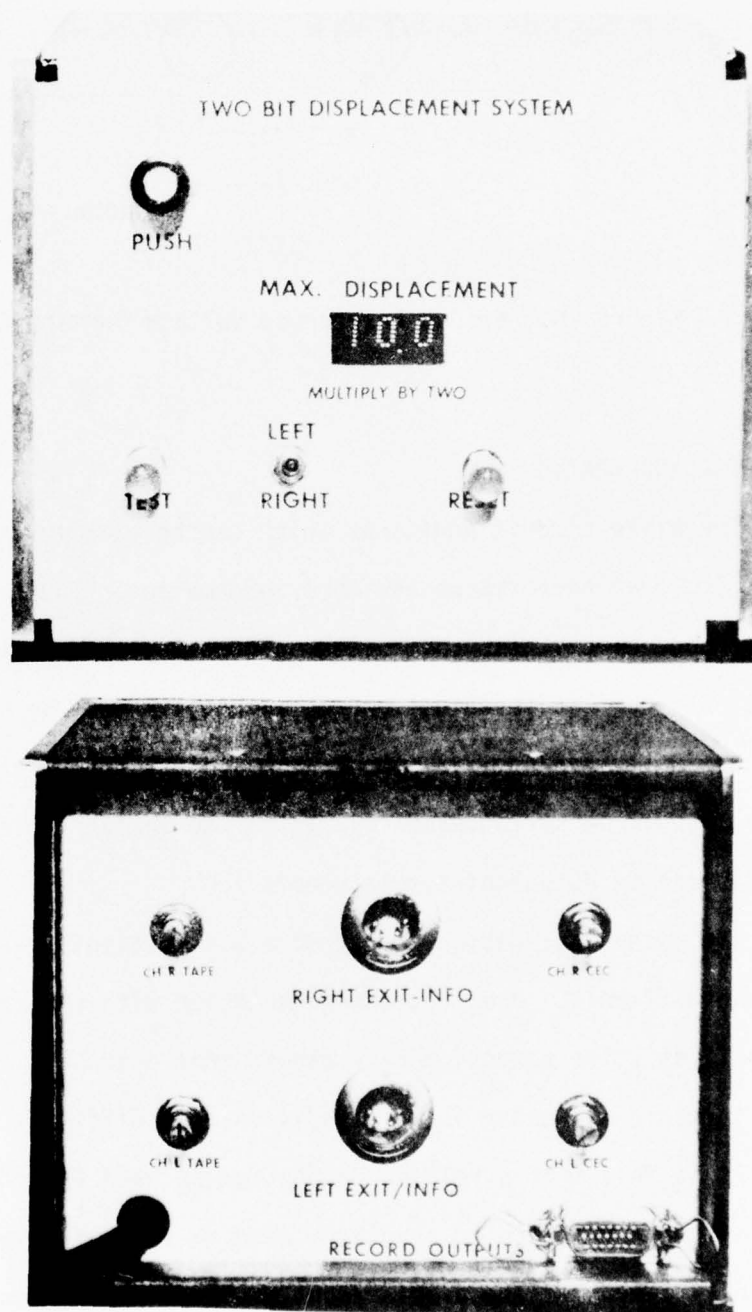
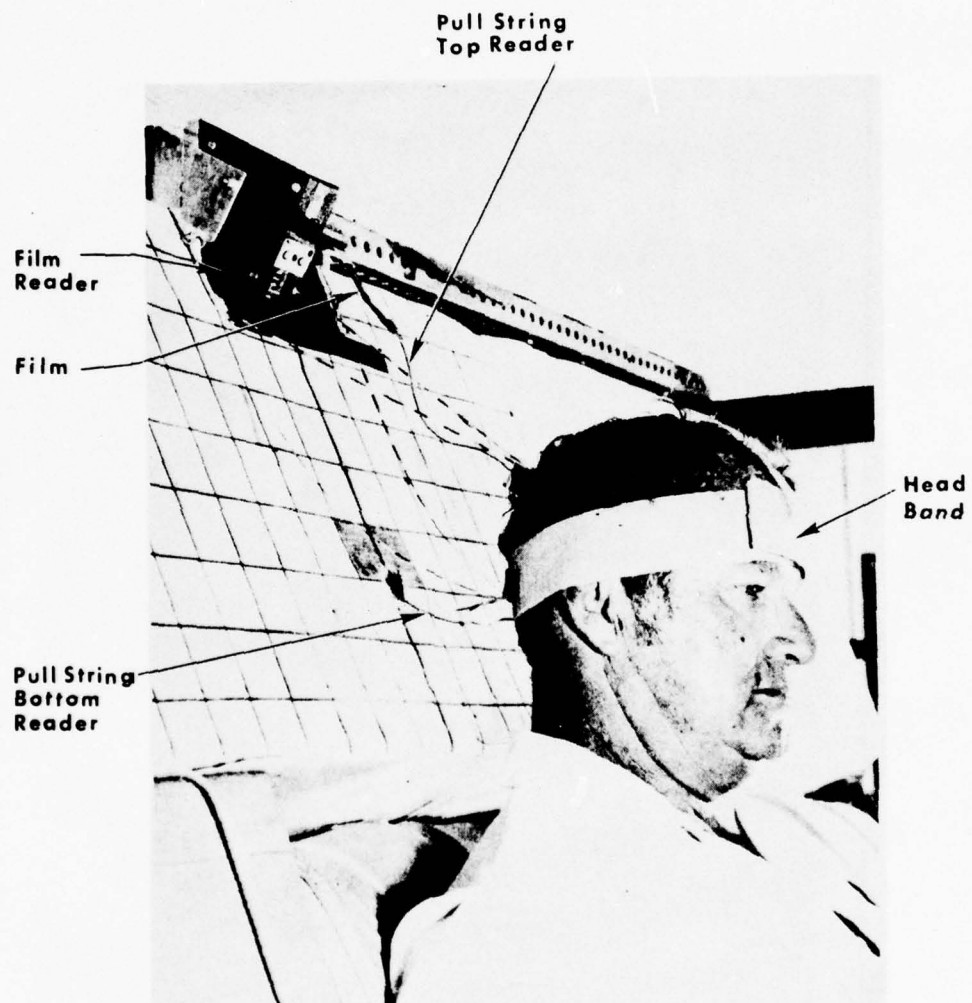


Figure C6. Front and Rear View of Two Bit Displacement System Control/Display Module



PRERUN INSTALLATION

Figure C7. Prerun Configuration with Subject

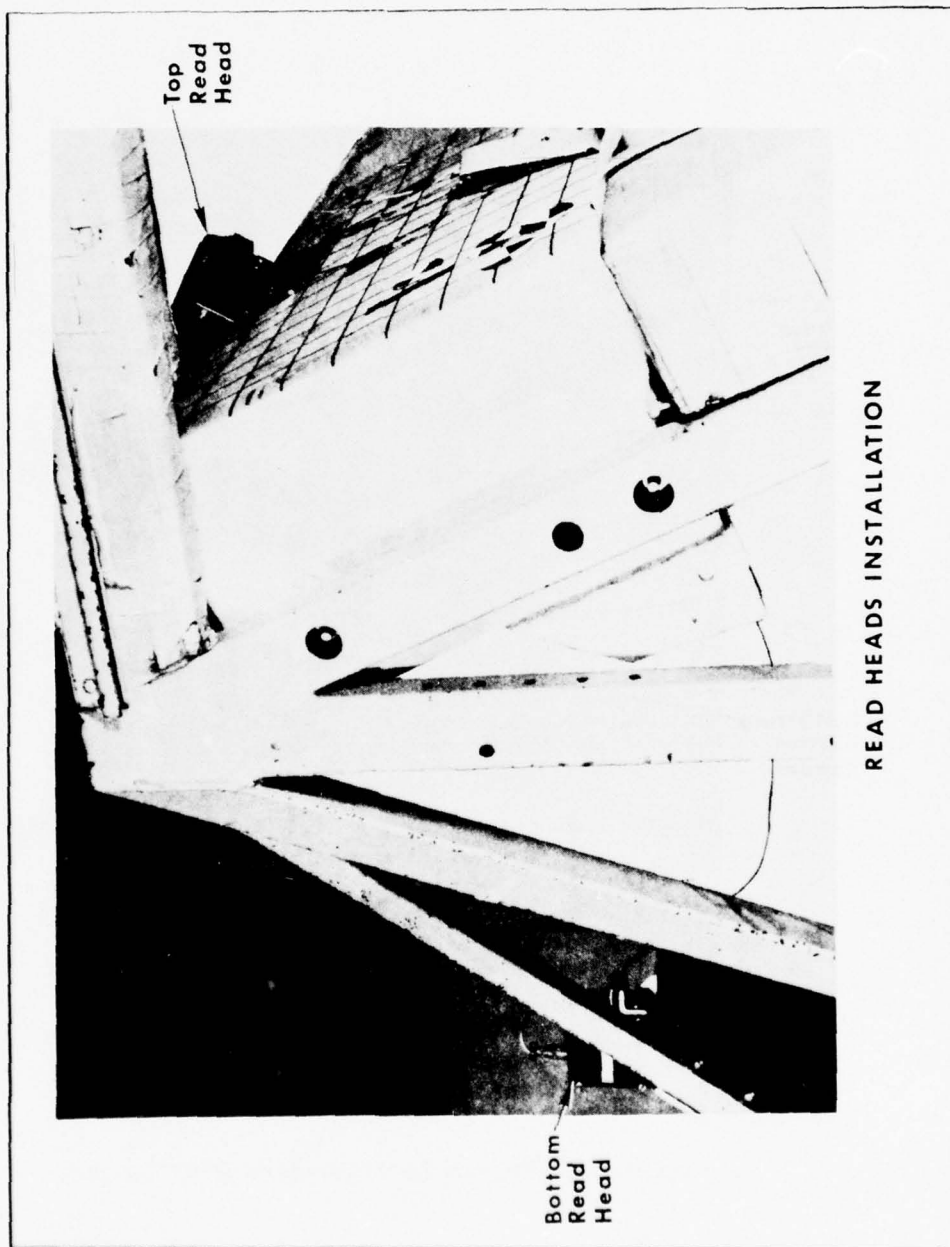


Figure C8. Bottom and Top Read Heads Positions

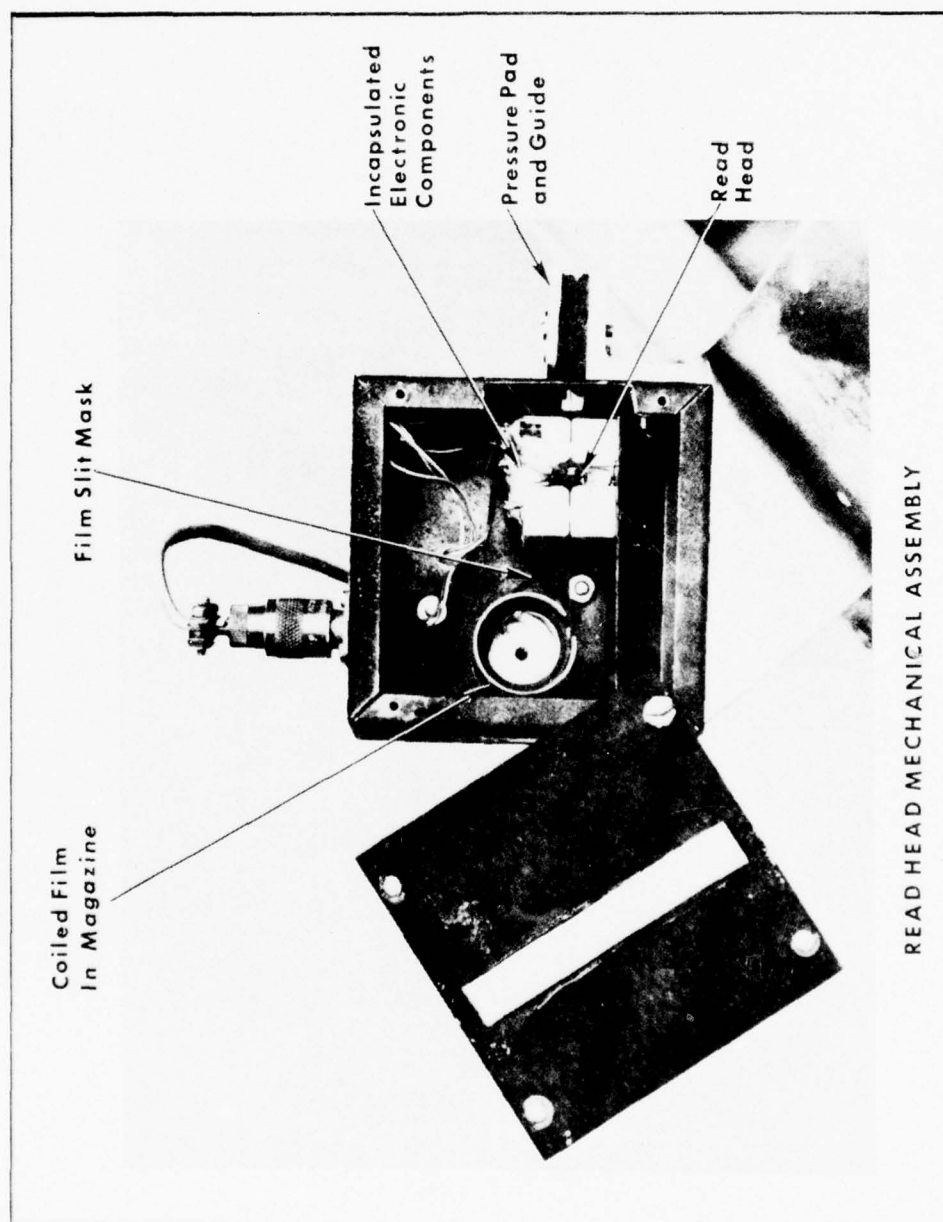


Figure C9. Interior View of the Read Head

APPENDIX D

PHOTOMETRIC DATA PROCESSING METHODS

CAPT. JOHN P. KILIAN, USAF

PREPARED FROM INFORMATION SUBMITTED BY

COMPUTING AND SOFTWARE, INC.

CONTRACT NO. DAAD07-69-C-0006

These methods failed to provide any useful photo-data for two primary reasons. The first was the unique physical aspects of the experiments. For example, subject interaction with the air cushion during the impact event made it nearly impossible for any two cameras to track the same reference point on the subject. In addition, other instrumentation equipment such as strings, cables, tapes, etc. masked both reference and subject fiducials for short periods of time making it difficult for even one camera to follow the subject through the impact event. The second was probably the complexity of the data reduction methods combined with poor data reduction quality control. The method discussed here required more and better input photo-data than were available from the high speed films of the impact events.

This procedure is presented as a valid semi-automatic data processing method which would be useful for processing body segment position data providing the data requirements of this method are considered as a primary aspect of the overall experimental design.

The objective of this Photometric Data Analysis Program was to develop body segment position data describing human kinematics during impact with a near-production prototype air cushion restraint system. The photometric test data are derived from six high speed, 16 mm cameras positioned to provide maximum coverage of the impact event. Three of the cameras were mounted on the moving impact sled. The other three cameras were mounted adjacent to and approximately 30 feet from the test track. All of the cameras were fixed to their mounts and did not track moving body segments. Figure D1 illustrates the camera positions with respect to the test track.

Reference fiducials were positioned on the test vehicle frame, floor, and Lexan side panel as illustrated in Figure D2. These reference fiducials were standard SAE type with target diameters of one and two inches. They were positioned at six inch intervals in both the X and Z directions to allow continuous observation of at least two reference fiducials by any camera during the impact event.

A Sled Coordinate System (SCS) was defined. The SCS was a left-handed rectangular coordinate system. The origin of the SCS was located at the center, rear bottom edge of the sled floor. The x-axis was positive in the direction from the rear to the front of the sled. The X-Y plane was parallel to the plane defined by the sled floor. The Y-axis was positive in the direction 90 degrees clockwise from the X-axis when viewed from above. The Z-axis was positive upwards. See Figure D3.

A reference grid of squares, two inches on a side, (14 rows and 14 columns) was surveyed into the Sled Coordinate System (SCS) at two locations identified as Grid A and Grid B. The three corners of each reference grid surveyed into the SCS are given in Figure D3. Grid A was used as the reference grid for onboard cameras one and two with Grid B used for onboard camera three. The three surveyed corners of Grid A are plotted in Figure D3. The numbering used for grid rows and columns is given in Figure D4b. The grid was installed in the sled, its corners were surveyed, and it was photographed using the cameras which would use the grid for orientation. For example, onboard cameras one and two were used to photograph grid A. Next, the grid was removed and the sled was prepared for the impact test to be monitored.

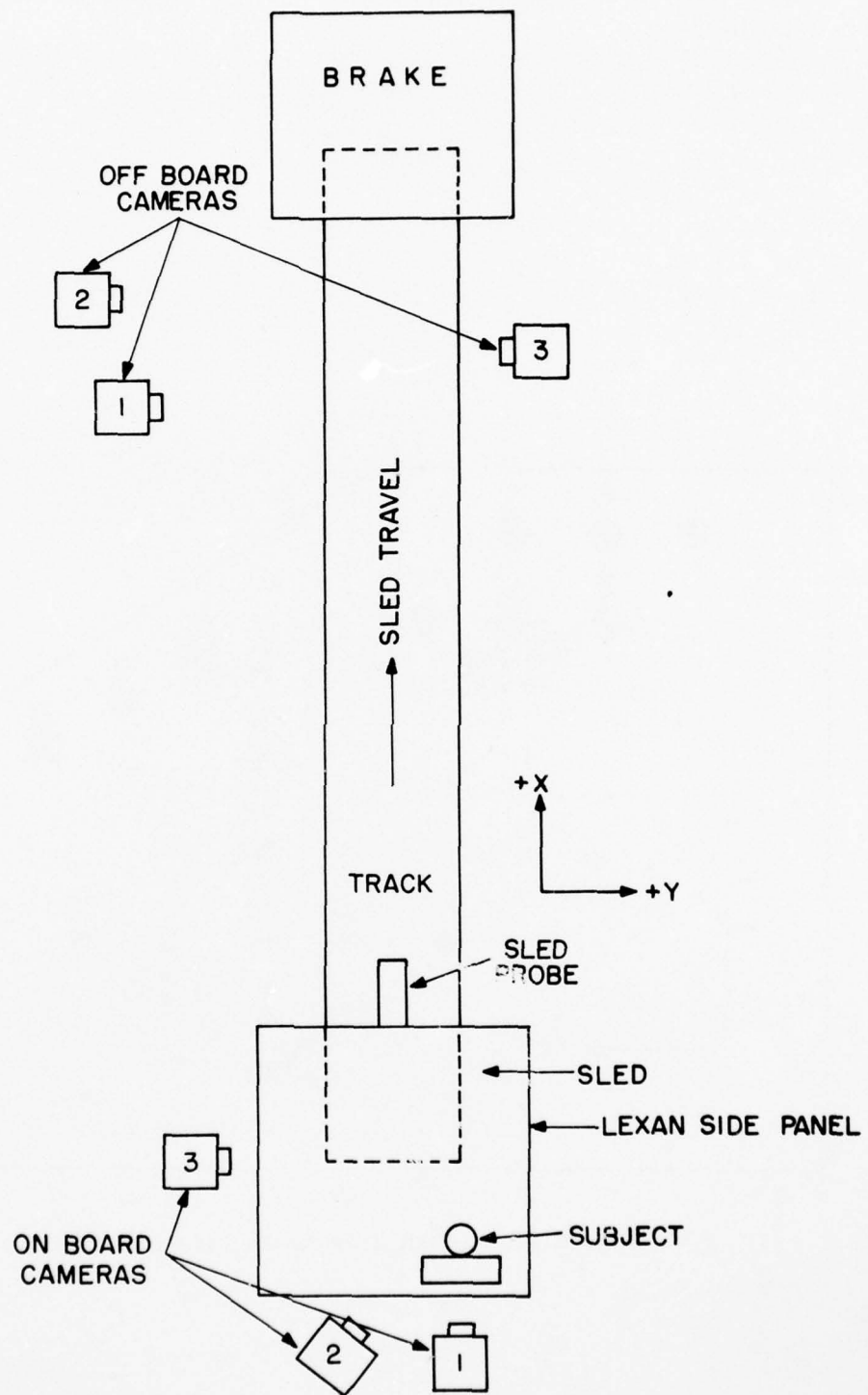


Figure D1. Camera Locations

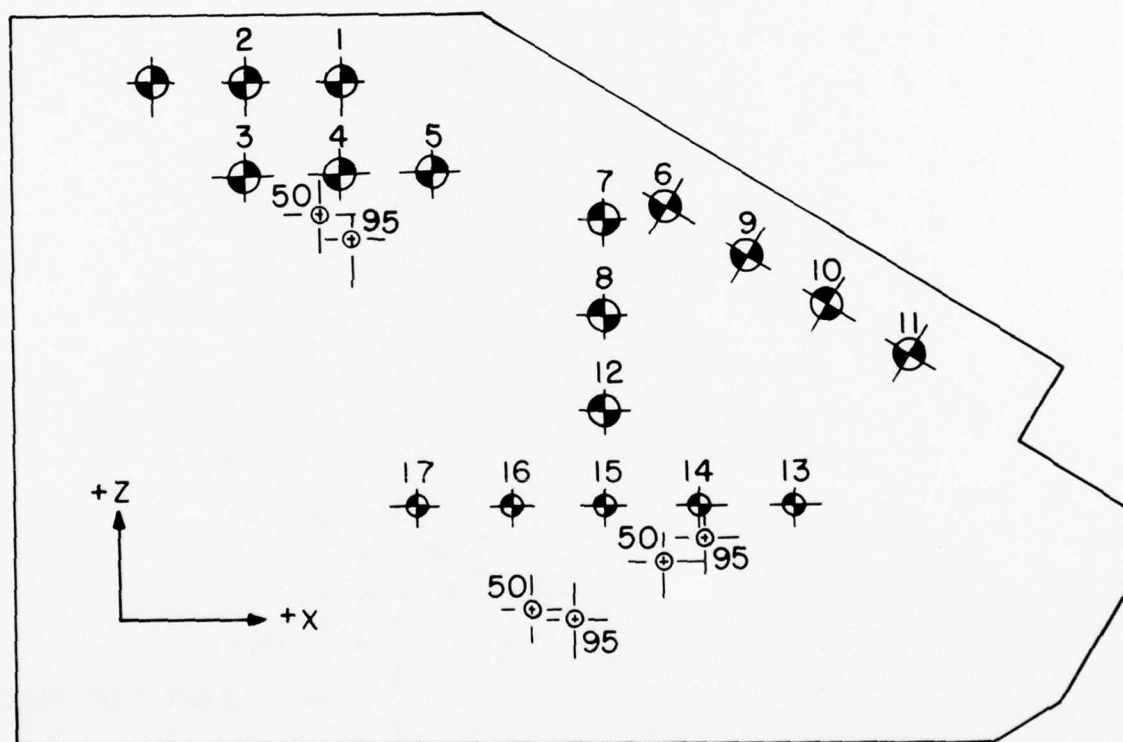


Figure D2. Lexan Side Panel (Scale 1 to 10)

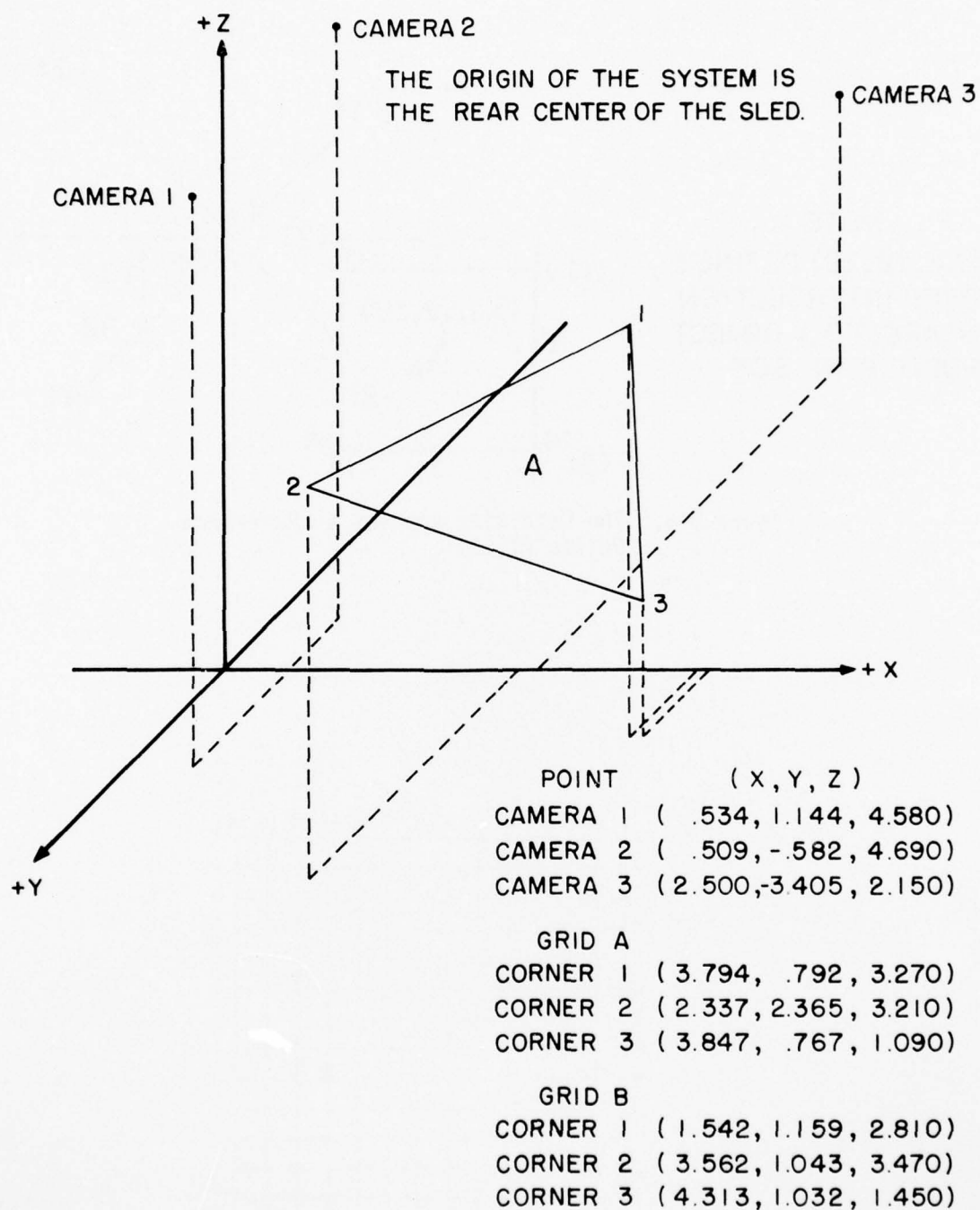


Figure D3. Grid and Camera Location in the Sled Coordinate System

NOTE :
 (X2,Y2,Z2) DEFINES
 GRID INTERSECTION
 NEAREST TO OBJECT
 POINT P IN SCS

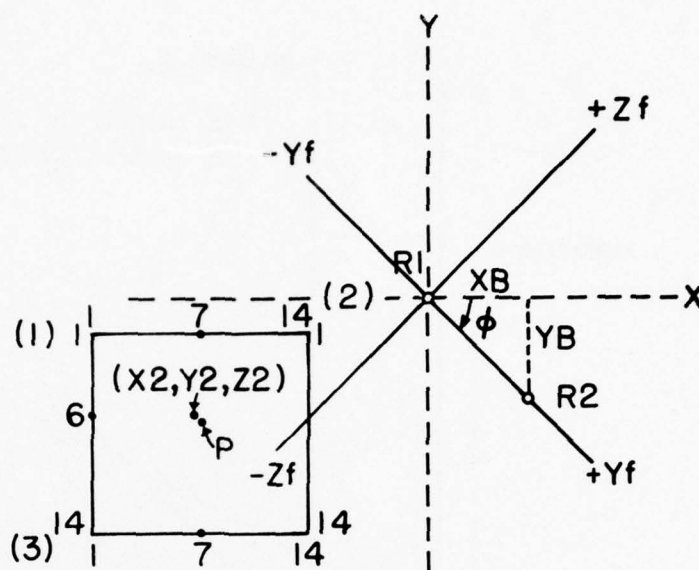


Figure D4a. The Grid With Respect to Reference Points R1, R2

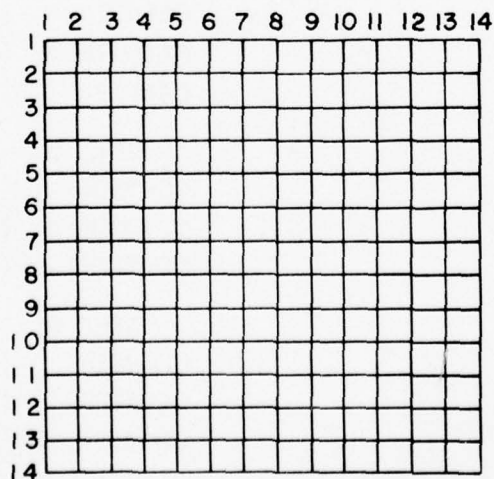


Figure D4b. The Onboard Camera Grid

A description of how the grid was used to determine object position will be provided later in this report.

Two separate computer programs were written in Fortran V language to operate on the UNIVAC 1108 EXEC 8 computer under the Data Reduction Operating System (DROPSYS) by Computing and Software, Inc. to develop position data. The first program (PBP066), reference D1, was designed to compute position data from boresight camera data derived from one or more of the onboard cameras. The second program (PPM067), reference D2, was designed for position data computations from only one of the off-board cameras. Due to factors such as lens aberration, parallax, image quality, lighting variation, and nonlinear frame rates, accurate position data were difficult to obtain from film reading. An effort was made to minimize some of the inherent inaccuracies by using a constant film reading method and by incorporating corrective mathematical operations within the two computer programs.

Program PBP066 was the more complex of the two programs. Data from any combination of cameras 1, 2, and 3 (the on-board cameras) was used to compute body segment position using as reference points, the fiducials painted on the sled side panel and the grid surveyed into the Sled Coordinate System (SCS). This program can calculate body segment position using data from one or more of the on-board cameras. The following discussion applies primarily to the single station (or camera) solution to body segment location. The direction cosines calculated by this procedure are also used in the multiple station solution and the point where the procedure diverges for multiple station solutions will be identified.

To describe the single station solution, assume the camera is located at X_1, Y_1, Z_1 (SCS) and uses reference fiducials R1 and R2. The 14 row and 14 column grid (shown in Figure D4b) was photographed installed in the sled by the same camera used for data collection prior to collecting data. Orientation data is obtained by reading the grid photographs in the following manner. The Telecordex (digitizer) was zeroed on reference fiducial R1. The position of R2 with respect to R1 was then read as an X and a Y value in digitizer counts. Next, without rezeroing the digitizer, each grid intersection was read. The end result was the recording of an X and Y value, in digitizer counts, between R1 and each grid intersection and between R1 and R2. Now the data collected by the camera was read using the same digitizer. The digitizer was again zeroed on reference fiducial R1 and X and Y readings were obtained between R1 and R2 and between R1 and the point of interest on the object. The film readings were all made using a 20 power lens on the reader to minimize differences in image size and the same operator made both orientation and data readings.

In order to minimize errors caused by misalignment of the film in the reader all digitizer X and Y readings (reading coordinate system) were translated and rotated into a Film Plane Coordinate System (FCS). The FCS was defined as being in the film plane with the Y axis passing through reference fiducials R1 and R2 and positive in the direction from R1 to R2. The origin at R1 and the Z axis was perpendicular to the Y axis, located in the film plane, and negative in the direction 90° clockwise from the positive Y axis (see Figure D4a). Where the digitizer Y counts between R1 and R2 are Y_B and the X counts between R1 and R2 are

X_B then the angle between the FCS Y axis and the X axis of the digitizer can be defined as follows:

$$\phi = \tan^{-1} \frac{Y_B}{X_B}$$

Locations read in X and Y values on the digitizer can now be related to the FCS by:

$$YF = X \cos \phi + Y \sin \phi$$

$$ZF = Y \cos \phi - X \sin \phi$$

where YF and ZF represent Y and Z values of a location in the FCS and X and Y are digitizer counts to the same point in the Reading Coordinate System (RCS). This rotation from the RCS to the FCS will compensate for errors in film angular alignment during the film reading process. The rotated coordinates of the grid intersections and of the object position (point P) were the input data from which the body segment positions were calculated.

The next step in the procedure was the calculation by the computer of the direction cosines between the camera located at $X1, Y1, Z1$ (SCS) and the object represented by point P. The computer had established a 14 x 14 matrix of the FCS Y and Z values of each grid intersection. The grid intersection nearest to where the line of sight from the camera to point P pierces the grid is selected by the program by comparing grid Y, Z coordinates with object Y, Z coordinates. Because the grid corners were surveyed into the Sled Coordinate System an SCS X, Y, Z value can be calculated by the computer for every grid intersection. The azimuth (a) and elevation (e) angles between the camera at $X1, Y1, Z1$ and the grid intersection at $X2, Y2, Z2$ can be determined as follows:

$$\Delta X1 = X2 - X1$$

$$\Delta Y1 = Y2 - Y1$$

$$\Delta Z1 = Z2 - Z1$$

$$Q = (\Delta X1^2 + \Delta Y1^2)^{1/2}$$

$$\tan e = \frac{\Delta Z}{Q}$$

$$e = \tan^{-1} \frac{\Delta Z1}{(\Delta X1^2 + \Delta Y1^2)^{1/2}} \quad (1)$$

$$\tan a = \frac{\Delta Y1}{\Delta X1}$$

$$a = \tan^{-1} \frac{\Delta Y1}{\Delta X1} \quad (2)$$

$$R = (\Delta X1^2 + \Delta Y1^2 + \Delta Z1^2)^{1/2} \quad (3)$$

We now know the azimuth angle (a), the elevation angle (e), and the slant range (R) to the grid intersection nearest to the line of sight from the camera to point P (see Figure D5).

Each grid square was two inches on a side, a factor which can be used to make the final correction to the direction cosine from the camera to point P.

GY and GX represent the digitizer count difference between X2, Y2, Z2 and the point P (Figure D6). The "size" of each grid square in counts is known from the input data and were called CX and CY. The X distance from X2, Y2, Z2 to P is:

$$X = \frac{\Delta GX}{CX} \times 2 \text{ inches}$$



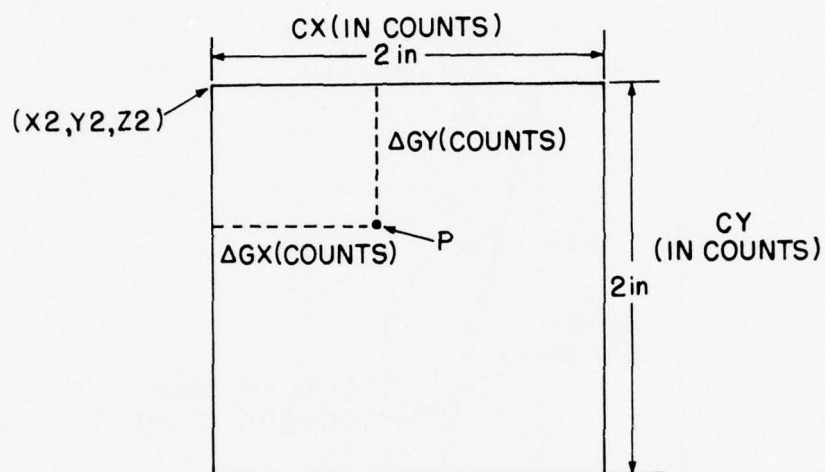


Figure D6. Relative Location of Point "P"

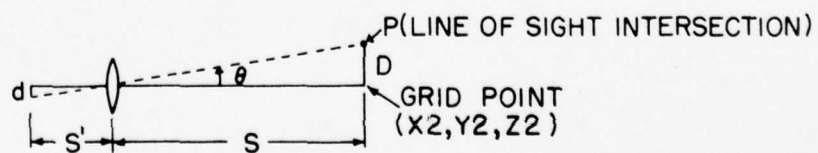


Figure D7. Correction to Grid Direction Cosines

and for Y

$$\Delta Y = \frac{\Delta GY}{CY} \times 2 \text{ inches}$$

The distance identified as s in Figure D7 was sufficiently close to R (eg. 3) to allow the direction cosines between the line of sight to the grid point (X2, Y2, Z2) and the line of sight to P (angle θ) to be calculated as follows:

$$R^1 = (R^2 + (\Delta X)^2 + (\Delta Y)^2)^{1/2}$$

$$\lambda^1 = \frac{R}{R^1} \quad (4)$$

$$\mu^1 = \frac{Y}{R^1} \quad (5)$$

$$\gamma^1 = \frac{Z}{R^1} \quad (6)$$

Geometrically these direction cosines represent a camera coordinate system (CCS) with the positive X^1 axis being along the line of sight from the camera to X2, Y2, Z2. The origin of the CCS is at X2, Y2, Z2 with the Y^1 axis perpendicular to the X axis, in the film plane, and positive to the right. The Z^1 axis lies in the film plane perpendicular to the $X^1 Y^1$ plane and positive up.

The direction cosines obtained in equations 4, 5, and 6 are first rotated through the angle of elevation between the camera and X2, Y2, Z2 and then through the azimuth angle. The resulting rotations give the direction cosines between the camera and the object.

$$\begin{aligned}\lambda &= \cos(a) \cos(e) \lambda^1 - \sin(a) \mu^1 - \cos(a) \sin(e) \gamma^1 \\ \mu &= \sin(a) \cos(e) \lambda^1 + \cos(a) \mu^1 - \sin(a) \sin(e) \gamma^1 \\ \gamma &= \sin(e) \lambda^1 + \cos(e)\end{aligned}$$

These direction cosines can be used to calculate object position in the SCS using either a single or a multiple station solution.

The single station solution starts with the assumption that the object's lateral movement (along the Y axis in SCS) was negligible. With this assumption, it was possible to determine the distance r between the object point P and the camera. The calculations made were as follows:

$$Y = Y_c + \mu r$$

where Y = Y coordinate in SCS

Y_c = known camera Y coordinate in SCS

μ = Y axis direction cosine

r = distance from camera to P (Slant Range)

Now where $Y = K$ (a constant) then:

$$Y_c + r = K$$

$$r = \frac{K - Y_c}{\mu}$$

The The position in the SCS of the object can now be determined by using the above value of r. For example:

$$X = X_c + \lambda r$$

where X_c = camera X coordinate in SCS

λ = direction cosine in SCS with respect to X axis

X = SCS X coordinate of object

Next, consider the multiple station solution for the SCS position of P.

AD-A038 525

AEROSPACE MEDICAL RESEARCH LAB WRIGHT-PATTERSON AFB OHIO F/G 13/12

IMPACT TESTS OF A NEAR-PRODUCTION AIR CUSHION RESTRAINT.(U)

FEB 77 J W BRINKLEY, G C MOHR, H C RUSSELL

DOT-HS-017-1-017-1A

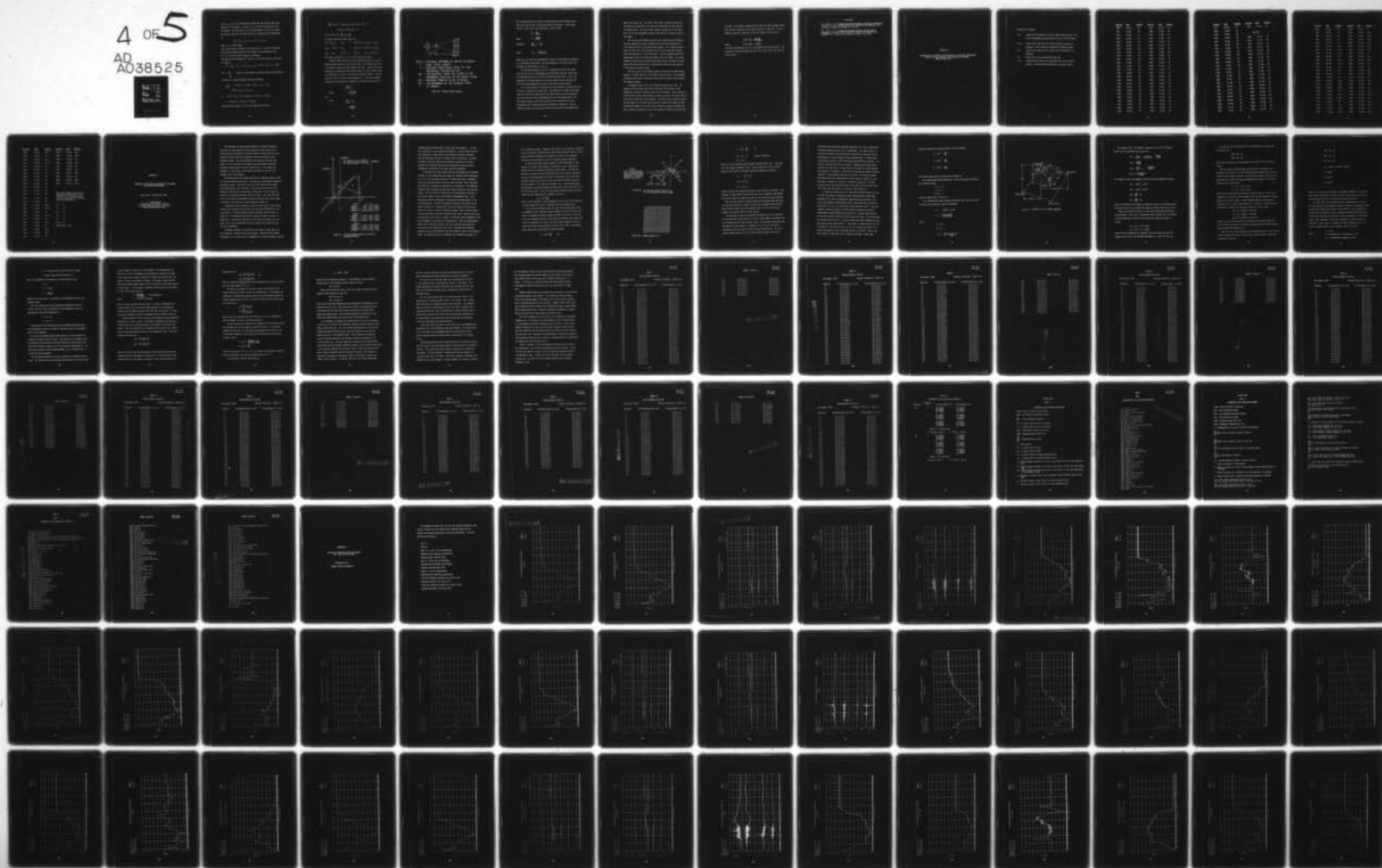
UNCLASSIFIED

AMRL-TR-75-47

DOT-HS-802-248

NL

4 OF 5
AD
A038525



Let $(\lambda_i, \mu_i, \gamma_i)$ be the direction cosines for the line of sight from camera i to the object. Let (X_i, Y_i, Z_i) be the coordinates of the i th camera. The position (X, Y, Z) of the object is now to be found. Any point on the line of sight from the i th camera may be represented by

$$(X_i + r_i \lambda_i, Y_i + r_i \mu_i, Z_i + r_i \gamma_i),$$

where r is a slant range.

For a multi-station solution, the position (X, Y, Z) will be defined as that point where the sum of the squares of the distances from (X, Y, Z) to the lines of sight is a minimum.

The square of the distance D_i^2 from (X, Y, Z) to any point on the line of sight is

$$D_i^2 = (X_i + r_i \lambda_i - X)^2 + (Y_i + r_i \mu_i - Y)^2 + (Z_i + r_i \gamma_i - Z)^2$$

Let $S = \sum_{i=1}^n D_i^2$ where n is the number of stations used in the solution

A value for r_i may be obtained from the following

$$\frac{D_i^2}{r_i} = 2(X_i + r_i \lambda_i - X)\lambda_i + 2(Y_i + r_i \mu_i - Y)\mu_i + 2(Z_i + r_i \gamma_i - Z)\gamma_i = 0$$

$$\text{or } r_i (\lambda_i^2 + \mu_i^2 + \gamma_i^2) = (X - X_i)\lambda_i + (Y - Y_i)\mu_i + (Z - Z_i)\gamma_i$$

$$r_i = (X - X_i)\lambda_i + (Y - Y_i)\mu_i + (Z - Z_i)\gamma_i$$

Substituting the value r_i into S and taking the partials

$$\frac{\partial S}{\partial X} = X(\lambda_i^2 - 1) + Y \sum \lambda_i \mu_i + Z \sum \lambda_i \gamma_i - [\sum X_i (\lambda_i^2 - 1) + \sum Y_i \lambda_i \mu_i + \sum Z_i \lambda_i \gamma_i] = 0$$

and similarly for $\frac{\partial S}{\partial Y}$ and $\frac{\partial S}{\partial Z}$

The three equations formed reduce to

$$\begin{aligned} \sum (\lambda_i^2 - 1) \sum \lambda_i \mu_i & \quad \sum \lambda_i \gamma_i & \quad X & \quad \sum X_i (\lambda_i^2 - 1) + Y_i \lambda_i \mu_i + Z_i \lambda_i \gamma_i \\ \sum \lambda_i \mu_i & \quad (\mu_i^2 - 1) & \quad \sum \mu_i \gamma_i & \quad Y & \quad \sum X_i \lambda_i \mu_i + Y_i (\mu_i^2 - 1) + Z_i \mu_i \gamma_i \\ \sum \lambda_i \gamma_i & \quad \sum \mu_i \gamma_i & \quad \sum (\gamma_i^2 - 1) & \quad Z & \quad \sum X_i \lambda_i \gamma_i + Y_i \mu_i \gamma_i + Z_i (\gamma_i^2 - 1) \end{aligned}$$

The object position (X, Y, Z) in SCS can now be solved.

Program PPM067 developed for the offboard cameras was used to analyze motion within the film plane only. This program uses only a one camera solution to body segment position. Lateral motion was assumed to be negligible leaving only motion in the XZ plane (SCS). The reference grid was not used for the offboard cameras. For any point (Xi, Zi) for which a displacement (X, Z) from the reference fiducial R1 was desired was computed as follows (see Figure D8):

$$\frac{DX}{X_2 - X_1} = \frac{X}{X_1}$$

where

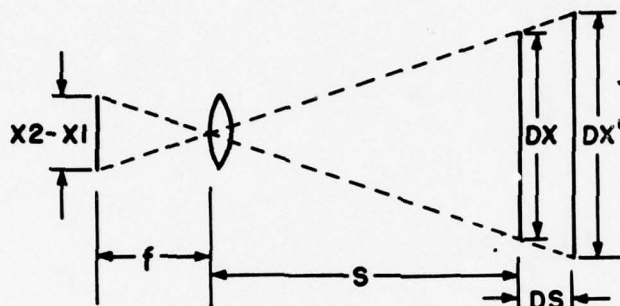
$$X = \frac{DX (X_i)}{X_2 - X_1}$$

and

where

$$\frac{DX}{X_2 - X_1} = \frac{Z}{Z_1}$$

$$Z = \frac{DX (Z_i)}{X_2 - X_1}$$



- $X2-X1$ = DISTANCE BETWEEN R1 AND R2 IN COUNTS
- f = LENS FOCAL LENGTH
- S = DISTANCE FROM NODAL POINT TO THE
REFERENCE FIDUCIALS(R1, R2)
- DS = THE DISTANCE FROM THE PLANE OF THE
REFERENCE FIDUCIALS TO THE OBJECT PLANE
- DX = DISTANCE FROM R1 TO R2 IN INCHES
- DX' = THE MOVEMENT OF THE SUBJECT POINT
IN INCHES

Figure D8. Offboard Camera Geometry

The calculation must be further corrected because the reference fiducials (R1, R2) are not in the same plane as the object. Given values for DX, f, and X2-X1 (see Figure D8), s can be found

$$\frac{S}{f} = \frac{DX}{X2-X1}$$

where: $S = \frac{f(DX)}{X2-X1}$

Therefore $\frac{DX}{S+\Delta S} = \frac{Xi}{f}$

where: $DX^1 = \frac{Xi(S + \Delta S)}{f}$

Where (Xi, Zi) was the displacement in counts of the subject as measured on a Telereadex (digitizer). The same approach is used for the Z displacement by substituting Zi for Xi.

The distance between R1 and R2 is measured for every film frame used and the X and Z displacements are translated from the origin used for computations (R1) to the Sled Coordinate System (SCS). The y displacement is assumed constant for any one camera for any one test and was the distance between the center of the sled and the subject.

All of the previously discussed film data readings of object position included a reference to a base time. The beginning of impact data (base time) was marked by electronically initiated flash units positioned on the test sled to be seen simultaneously by all the cameras used. For the onboard cameras, the flash was seen at the intersection of the instrument panel simulation and the simulated A Frame post. For the offboard cameras, the flash units were positioned along the bottom floor

edge of the test sled. The time of the frame in which the flash was activated was considered to be time zero indicating the initiation of the impact event. The flash event normally occurred 20 to 30 frames prior to air bag deployment depending upon the film transport speed of the camera.

The initial body segment positions were established by beginning the data readings at least 20 frames prior to flash activation on a film frame which has a preprinted frame number. This frame was designated as frame 100. The top edge of the film has preprinted numbers which were indexed by 1 every 20 frames. The hand numbered individual frames should fall on a preprinted number every 20 frames. This check procedure insured that the preprinted numbers were a constant 20 frames apart which helped prevent the introduction of errors by the operator or the machine skipping frames.

The film used by the offboard cameras was marked with IRIG timing. However, for data reduction, only delta times were used. The averaging procedure established to determine delta time was used for both onboard and offboard cameras.

To determine delta time, the following procedure was used. The exposed film had timing pips (marks) located at the bottom of each frame with a timing pip having a value of .001 second. It was necessary to get a delta time at the beginning, middle, and end of the data due to the erratic frame rate of the cameras. The delta time is found by counting the number of pips that occur within an interval of frames and then dividing the number of pips that occur within an interval of frames and then dividing the number of pips by the number of frames and multiplying

by 0.001. For example, beginning with frame 100 locate another frame that had the timing pip in the same location as frame 100. In this example assume the frame was 140 and the number of pips was 39.

$$\text{delta time} = \frac{39 \text{ pips}}{40 \text{ frames}}$$

where:

$$\text{delta time} = 0.000975$$

The same technique was used for the middle and end of the data. The average of the three deltas was used as the delta time per frame for that station.

REFERENCES

D1. Goode, J. E., Program Description Document, Biodynamic Photometric (PBP066), Task No. S1-1039, Version 00, Computing and Software, Inc., Contract No. DAAD07-69-C-0006, 26 Sep 1972.

D2. Moore, R. L., Program Description Document, Single Station Photometric (PPM067), Task No. S2-1057, Version 00, Computing and Software, Inc., Contract No. DAAD07-69-C-0006, 2 Oct 1972.

APPENDIX E

CHRONOLOGICAL LISTING OF TESTS CONDUCTED ON THE DAISY DECELERATOR
DURING THE NEAR PRODUCTION AIR CUSHION TEST PROGRAM
MARCH TO SEPT 1972

Definition of Symbols

- BP = Impact tests conducted to develop water brake patterns or to verify deceleration profile prior to tests with volunteers.
- AC-X = Impact tests where the air cushion restraint system was deployed. Third character designates volunteer subject.
- ND = Impact tests where the air cushion was intentionally not deployed.
- PT = Proof test of the experimental apparatus
- IT-X = Indoctrination impact test conducted with torso restraint harness. Third character designates volunteer subject.

<u>Test No.</u>	<u>Date</u>	<u>Purpose</u>	<u>Test No.</u>	<u>Date</u>	<u>Purpose</u>
6310	22 Mar	BP	6335	06 Apr	BP
6311	22 Mar	BP	6336	11 Apr	BP
6312	22 Mar	AC	6337	11 Apr	ND
6313	23 Mar	AC	6338	11 Apr	AC
6314	23 Mar	BP	6339	11 Apr	ND
6315	23 Mar	BP	6340	11 Apr	AC
6316	23 Mar	BP	6341	12 Apr	PT
6317	24 Mar	BP	6342	12 Apr	BP
6318	24 Mar	ND	6343	14 Apr	AC
6319	24 Mar	ND	6344	14 Apr	AC
6320	27 Mar	AC	6345	14 Apr	BP
6321	27 Mar	AC	6346	17 Apr	AC
6322	28 Mar	ND	6347	17 Apr	AC
6323	28 Mar	ND	6348	17 Apr	AC
6324	28 Mar	BP	6349	18 Apr	AC
6325	28 Mar	ND	6350	18 Apr	BP
6326	28 Mar	ND	6351	18 Apr	AC
6327	29 Mar	ND	6352	18 Apr	AC
6328	29 Mar	ND	6353	19 Apr	BP
6329	29 Mar	ND	6354	19 Apr	AC
6330	29 Mar	ND	6355	19 Apr	AC
6331	30 Mar	ND	6356	19 Apr	AC
6332	30 Mar	ND	6357	19 Apr	AC
6333	06 Apr	BP	6365	23 May	BP
6334	06 Apr	BP	6366	23 May	BP

<u>Test No.</u>	<u>Date</u>	<u>Purpose</u>	<u>Test No.</u>	<u>Date</u>	<u>Purpose</u>
6367	23 May	BP	6392	14 Jun	AC
6368	23 May	BP			
6369	23 May	BP		SEE NOTE	
6370	24 May	BP	6469	26 Jul	BP
6371	24 May	BP	6470	27 Jul	AC
6372	24 May	BP	6471	28 Jul	AC
6373	24 May	BP	6472	28 Jul	AC
6374	24 May	BP	6473	28 Jul	AC
6375	25 May	BP	6474	31 Jul	AC
6376	25 May	BP	6475	31 Jul	AC
6377	25 May	BP	6476	31 Jul	AC
6378	31 May	BP	6477	01 Aug	AC
6379	31 May	BP	6478	01 Aug	AC
6380	31 May	AC	6479	01 Aug	AC
6381	31 May	AC	6480	01 Aug	AC
6382	01 Jun	BP	6481	01 Aug	AC
6383	01 Jun	AC	6482	01 Aug	AC
6384	01 Jun	AC	6483	02 Aug	AC
6385	05 Jun	BP	6484	02 Aug	AC
6386	08 Jun	AC	6485	02 Aug	AC
6387	08 Jun	AC	6486	02 Aug	AC
6388	09 Jun	AC	6487	02 Aug	AC
6389	09 Jun	AC	6488	03 Aug	AC
6390	12 Jun	BP	6489	03 Aug	AC
6391	12 Jun	AC	6490	03 Aug	AC

<u>Test No.</u>	<u>Date</u>	<u>Purpose</u>	<u>Test No.</u>	<u>Date</u>	<u>Purpose</u>
6491	03 Aug	AC	6516	15 Aug	BP
6492	03 Aug	AC	6517	15 Aug	IT-J
6493	04 Aug	AC	6518	15 Aug	IT-I
6494	04 Aug	AC	6519	15 Aug	IT-H
6495	07 Aug	BP	6520	15 Aug	IT-K
6496	07 Aug	IT-E	6521	15 Aug	IT-L
6497	07 Aug	IT-F	6522	15 Aug	IT-M
6498	07 Aug	IT-G	6523	16 Aug	BP
6499	08 Aug	BP	6524	16 Aug	AC-C
6500	08 Aug	IT-D	6525	16 Aug	AC-G
6501	08 Aug	IT-A	6526	16 Aug	BP
6502	08 Aug	IT-C	6527	17 Aug	BP
6503	08 Aug	BP	6528	17 Aug	AC-H
6504	08 Aug	BP	6529	17 Aug	AC-I
6505	08 Aug	BP	6530	18 Aug	BP
6506	09 Aug	AC-A	6531	18 Aug	AC-K
6507	09 Aug	AC-A	6532	18 Aug	AC-J
6508	09 Aug	AC-B	6533	21 Aug	BP
6509	10 Aug	BP	6534	21 Aug	AC-M
6510	10 Aug	AC-C	6535	21 Aug	AC-B
6511	10 Aug	AC-D	6536	22 Aug	BP
6512	11 Aug	BP	6537	22 Aug	AC-E
6513	11 Aug	BP	6538	22 Aug	AC-J
6514	11 Aug	AC-E	6539	23 Aug	BP
6515	11 Aug	AC-F	6540	23 Aug	AC-G

<u>Test No.</u>	<u>Date</u>	<u>Purpose</u>	<u>Test No.</u>	<u>Date</u>	<u>Purpose</u>
6541	23 Aug	AC-H	6566	15 Sep	AC-I
6542	24 Aug	BP	6567	15 Sep	AC-M
6543	24 Aug	AC-I	6568	18 Sep	BP
6544	24 Aug	AC-K	6569	18 Sep	AC-B
6545	24 Aug	BP	6570	19 Sep	BP
6546	25 Aug	BP	6571	19 Sep	AC-G
6547	07 Sep	BP	6572	19 Sep	AC-C
6548	07 Sep	BP	6573	20 Sep	BP
6549	07 Sep	BP	6574	20 Sep	AC-H
6550	07 Sep	BP	6575	20 Sep	AC-M
6551	08 Sep	BP			
6552	11 Sep	BP			
6553	11 Sep	BP			
6554	11 Sep	BP			
6555	12 Sep	BP			
6556	12 Sep	AC-B			
6557	12 Sep	AC-C			
6558	13 Sep	BP			
6559	13 Sep	AC-E			
6560	14 Sep	BP			
6561	14 Sep	AC-G			
6562	14 Sep	BP			
6563	14 Sep	AC-D			
6564	14 Sep	AC-F			
6565	15 Sep	BP			

NOTE: Test numbers 6393 to 6468 conducted during period of 6 Jul 1972 to 20 Jul 1972 were accomplished in support of B-1 aircraft escape system program.

BP = 70

PT = 01

AC = 53

ND = 14

IT = 12

AC-X = 33

TOTAL TESTS = 133

APPENDIX F

PHOTOMETRIC DATA ANALYSIS PROCEDURE TO DETERMINE
HEAD MOTION TRAJECTORIES

Capt. John P. Kilian, BSC, USAF

Impact Branch
Biodynamics and Bionics Division
Aerospace Medical Research Laboratory
Wright-Patterson AFB, Ohio

This photometric Data Reduction Method was created to develop head position data describing head kinematics during impact with a near-production prototype air cushion restraint system after the semi-automatic method discussed in Appendix D failed to provide useful photometric data. The raw photometric test data were derived from camera 2, the high speed, 16 mm camera best positioned to provide coverage of head motion during the impact event. This camera was mounted to a fixed mount on the impact sled with an over the left shoulder view of the subject.

The head position was established within a reference system called the Sled Coordinate System (SCS). The SCS was a left-handed rectangular coordinate system. The origin of the SCS was located at the center, rear bottom edge of the sled floor. The X-axis was positive in the direction from the rear to the front of the sled. The X-Y plane was parallel to the plane defined by the sled floor. The Y-axis was positive in the direction 90 degrees clockwise from the X-axis when viewed from above. The Z-axis was positive upwards (Figure F1).

A reference grid of squares, two inch by two inch, (14 rows and 14 columns) was surveyed into the SCS at two locations identified as Grid A and Grid B. The three corners of each reference grid are given in Figure F1. The numbering used for grid rows and columns is given in Figure F2b. The grid was installed in the sled, its corners were surveyed, and it was photographed using the cameras which would use the grid for orientation.

A computer program (in two parts) was written in Super Basic for the "Tymshare"* computer time sharing system. Basically this program
*"Tymshare" is the trade name of a commercially available computer service.

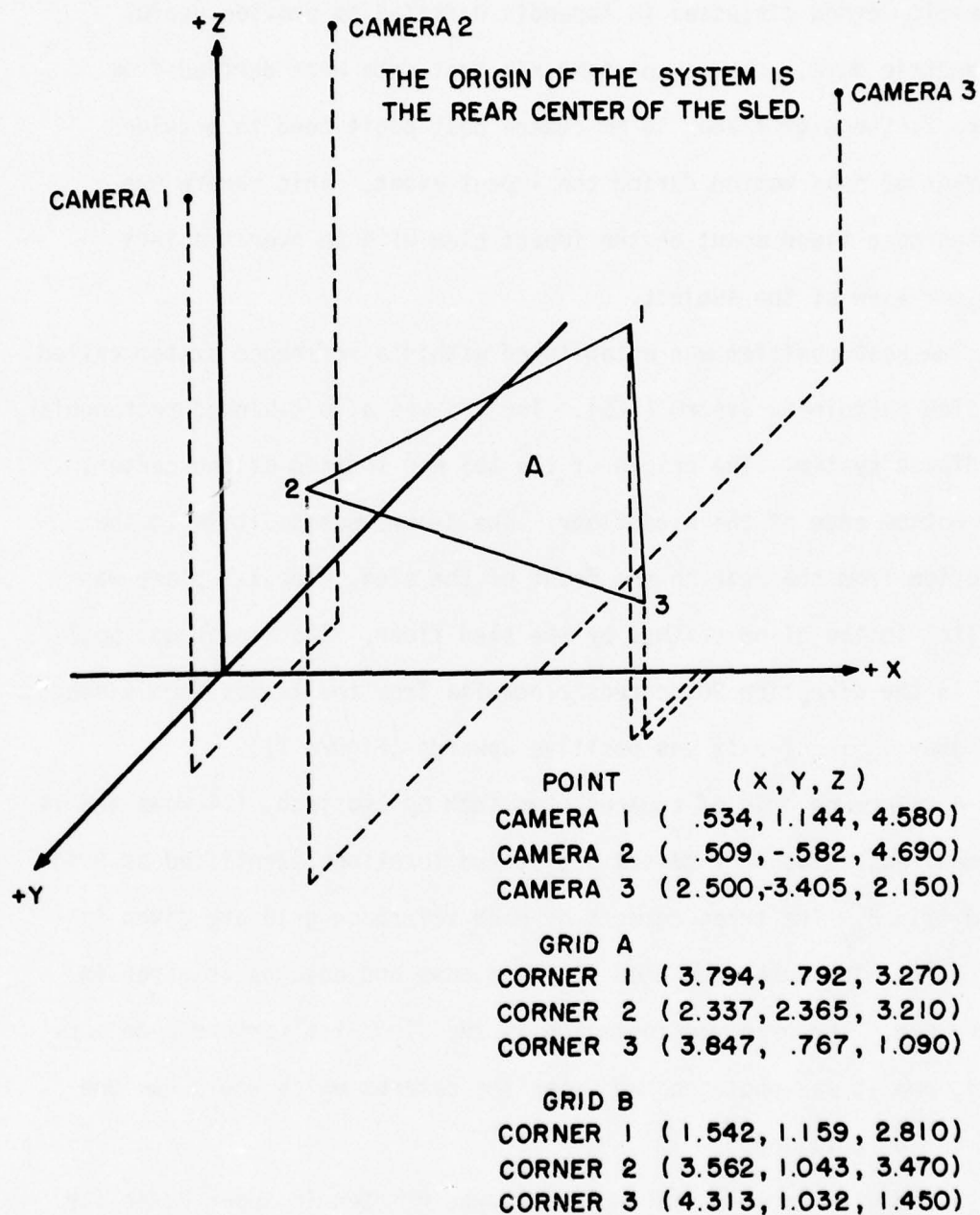


Figure F1. Grid and Camera Location in the Sled
Coordinate System

computed head positions based on photo data from camera 2. For the SCS coordinates of this camera see Figure F1. Due to factors such as lens aberration, image quality, and lighting variation, accurate position data were difficult to obtain from film reading. An effort was made to minimize some of the inherent inaccuracies by using a constant film reading method and by incorporating some corrective mathematical operations in the data reduction procedure.

To describe the single camera solution calculated by the computer program, it was assumed that the camera was located at SCS coordinates $X1$, $Y1$, $Z1$, and reference fiducials $R1$ and $R2$ were used. Reference fiducials were positioned on the test vehicle frame, floor, and Lexan side panel as illustrated in Appendix D, in Figure D2. The reference fiducials were standard SAE type with target diameters of one and two inches. The 14 row and 14 column grid was photographed installed in the sled by camera 2 prior to collecting experimental data. Grid orientation data was obtained by reading the grid photographs in the following manner. The PSC Film Reader (digitizer) was zeroed on reference fiducial $R1$. The position of $R2$ with respect to $R1$ was then read as an X and a Y value in digitizer counts. Next, without rezeroing the digitizer, each grid intersection was read. The end result was the recording of an X and a Y value, in digitizer counts, between $R1$ and $R2$ and between $R1$ and every grid intersection. Next, the experimental photo data collected by camera 2 was read using the same digitizer. The digitizer was zeroed on $R1$ and X and Y readings were obtained between $R1$ and $R2$ and between $R1$ and the reference point on the subject's head. The complete grid, once obtained, was permanently stored as a

file in computer memory. Numerous spot checks of the reference fiducial to grid intersection relationships established that there were no significant differences between grid readings as stored in the computer initially, and those made as the film reading program progressed.

In order to minimize errors caused by film misalignment in the reader, all subject head readings in digitizer X and Y counts were rotated into a Grid Reading Coordinate System (GRCS). The GRCS was defined as being in the film plane with the X-axis passing through R1. This axis was represented by the zero Y coordinate of the digitizer. The GRCS X-axis was positive to the right while the GRCS Y-axis was positive upward. The origin was located at R1. The reference angle was defined as the angle between the GRCS X-axis and a line from R1 to R2 (see Figure F2a). Let ϕ_s be the standard reference angle as determined from the reference grid readings as follows:

$$\phi_s = \tan^{-1} \frac{Y_r}{X_r}$$

where Y_r was digitizer Y counts between R1 and R2 and X_r was digitizer X counts between R1 and R2 as recorded from the reference grid.

Let ϕ_f be the reference angle for every data frame read; X_f and Y_f represent X and Y digitizer counts between R1 and R2¹ on each data frame; θ represent the angle between the GRCS X-axis and a line from R1 to the reference fiducial on the subject's head for each frame; and X_o and Y_o represent the X and Y digitizer counts between R1 and the reference located on the subject's head for each frame. Considering these conditions, the following steps were taken:

$$\phi_f = \tan^{-1} \frac{Y_f}{X_f} \quad \text{and}$$

NOTE :
 (X_2, Y_2, Z_2) DEFINES
 GRID INTERSECTION
 NEAREST TO OBJECT
 POINT P IN SCS

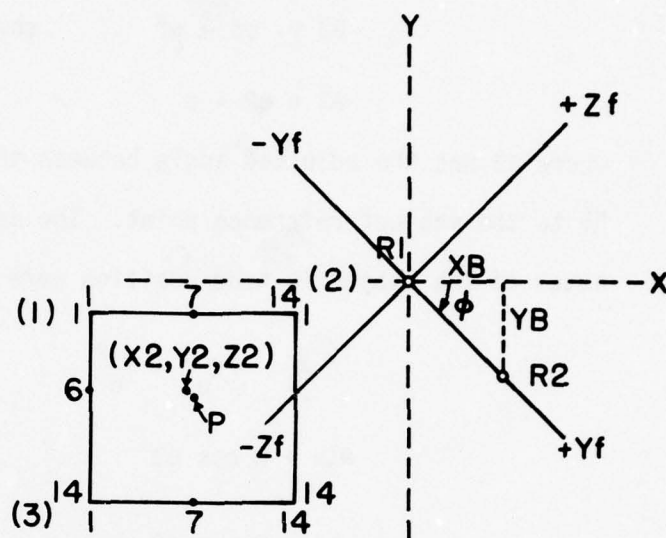


Figure F2a. The Grid and Typical Point "P" in the Grid Reading Coordinate System

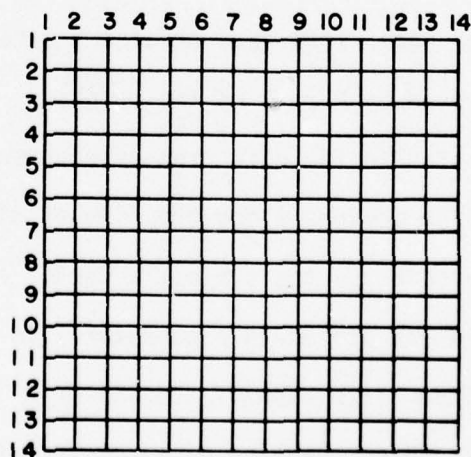


Figure F2b. Onboard Camera Grid

$$\theta = \tan^{-1} \frac{Y_o}{X_o} \quad \text{if}$$

$$\theta_2 = \phi_s - \phi_f \quad \text{then by definition}$$

$$\theta_3 = \theta_2 + \theta$$

where θ_3 was the adjusted angle between the CRCS X-axis and a line from R1 to the subject reference point. The new digitizer X and Y coordinates of the subject's head position were determined as follows:

$$R = \sqrt{X_o^2 + Y_o^2}$$

$$X_a = R \cos \theta_3$$

$$Y_a = R \sin \theta_3$$

where X_a and Y_a are adjusted digitizer X and Y values in the GRCS. This rotation of data values insured that errors due to angular misalignment of the film frame in either the camera or the digitizer were minimized.

Part 1 of the computer program accepted the punched paper tape output from the digitizer, rotated the data into alignment with the standard reference angle (ϕ_s), and created a data file with the correct format to be used by Part 2 of the program.

The next step in the data processing procedure was the calculation of the direction cosines along the line of sight between the camera and the reference point on the subject's head. As mentioned previously, the reference grid was stored in a computer file as X and Y digitizer coordinates from R1 to each of the 196 grid intersections. The grid square through which the line of sight from the camera to the head

reference point passed was found by comparing grid X and Y coordinates with head reference point X and Y coordinates. The three corners of each grid surveyed into the SCS made it possible to calculate the SCS coordinates of a point located on the reference grid. To make these calculations possible, a Grid Coordinate System (GCS) was defined. The origin of the GCS was the row 1 column 1 reference grid intersection. The GCS X-axis was row 1 of the grid and was positive in the direction from column 1 to column 14. The Y-axis of the GCS was column 1 and was negative in the direction from row 1 to row 14. The three surveyed grid points were the intersections of row 1-column 1 (corner 1), row 14-column 1 (corner 3), and row 1 - column 14 (corner 2). The GCS positive X-axis was then from corner 1 to corner 2 while the GCS negative Y-axis was from corner 1 to corner 3 (see Figure F1).

To locate the pierce point "P", which was the point where the line of sight from camera 2 through the head reference point pierced the reference grid, several mathematical operations were required. Part two of the computer program begins with a search routine to locate the individual 2 in. by 2 in. grid square which contains point P. The grid "square" as seen by camera 2 was not usually a square but normally approximated a parallelogram (see Figure F3). The next operation was to find the location of point P within the grid square. All calculations for the position of P within the grid square were made referenced to the grid square corner above point P. This corner is identified as (IR, IC) in Figure F3. Each one of the 2 in. by 2 in. squares had each of its corners recorded as X and Y digitizer counts in the GRCS. Point P was also located in digitizer X and Y counts in the GRCS. These known

positions allowed the following angles to be calculated:

$$\alpha = \tan^{-1} \frac{XP}{YP}$$

$$\beta = \tan^{-1} \frac{X2}{Y2}$$

$$\beta1 = \tan^{-1} \frac{X3}{Y3}$$

where these angles were as identified on Figure F3.

Once these angles were determined, it was then possible to define the following angles:

$$Q = \beta + \beta1$$

$$\gamma = \beta - \alpha$$

$$\beta2 = Q - \gamma$$

which are identified on Figure F3.

The altitude (h) of the triangle defined by point (IR, IC), point P and the side labeled XSI can be determined.

$$R = (\Delta XP)^2 + (\Delta YP)^2$$

$$h = R \frac{\sin \gamma \sin \beta2}{\sin (\gamma + \beta2)}$$

Since

$$Q = \beta2 + \gamma$$

$$\beta2 = Q - \gamma$$

$$h = R \frac{\sin \gamma \sin (Q - \gamma)}{\sin Q}$$

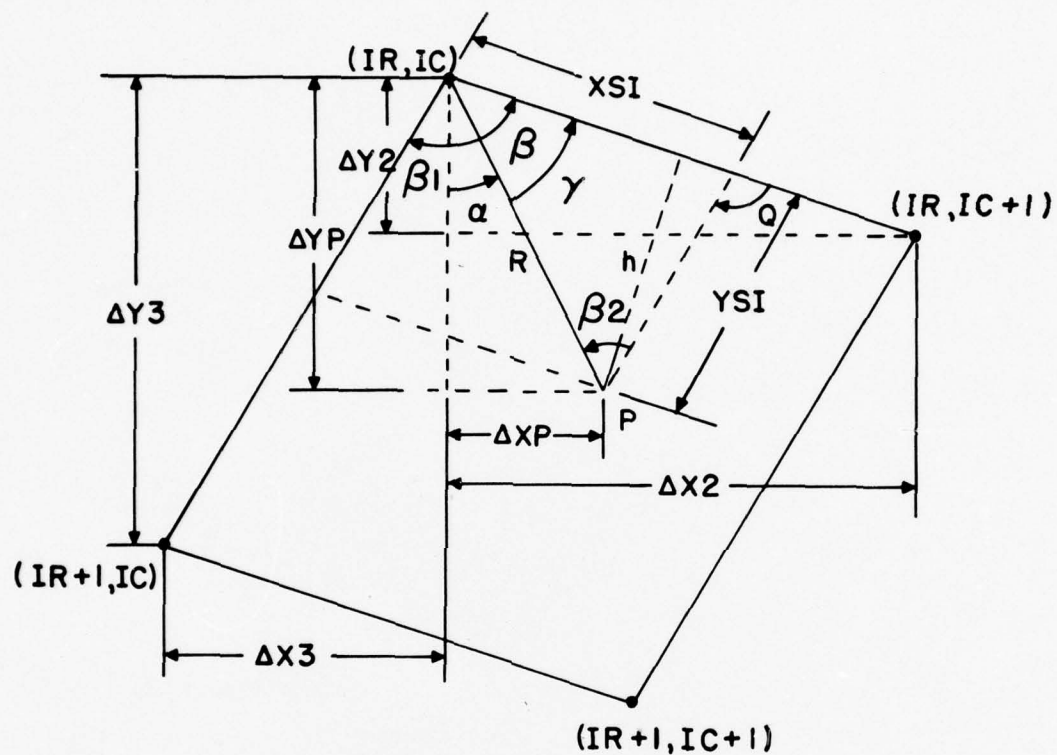


Figure F3. TYPICAL 2" x 2" GRID SQUARE

The length of the line segments labeled XSI and YSI in digitizer counts can be determined (see Figure F3).

$$YSI = \frac{h}{\sin \beta_2} = \frac{h}{\sin(Q-\gamma)} = \frac{R \sin \gamma}{\sin Q}$$

$$YSI = \frac{R \sin \gamma}{\sin Q}$$

$$XSI = \frac{h}{\sin \gamma} = R \frac{\sin(Q-\gamma)}{\sin Q}$$

$$XSI = R \frac{\sin(Q-\gamma)}{\sin Q}$$

The lengths of the line segments SX and SY were calculated as follows:

$$R1 = (\Delta X2)^2 + (\Delta Y2)^2$$

$$R2 = (\Delta X3)^2 + (\Delta Y3)^2$$

$$SX = \frac{XSI}{R1} \quad (2)$$

$$SY = \frac{YSI}{R2} \quad (2)$$

where R1 and R2 were the length in digitizer counts of the sides of the grid square and SX and SY were the lengths in inches from (IR, IC) to P.

Next, the location of point P in the Grid Coordinate System (GCS) was determined. The X and Y coordinates (GCS) of point (IR, IC) located at the intersection of the Ith row and the Ith column was found as follows:

$$Xg = (IC - 1) \cdot 2 \text{ inches}$$

$$Yg = (IR - 1) \cdot 2 \text{ inches}$$

where IC and IR respectively represent the grid column and grid row numbers and Xg and Yg are the GCS coordinates in inches of (IR, IC).

The last step in locating point "P" in the GCS was to add SX and SY to Xg and Yg.

$$X_{gp} = SX + X_g$$

$$Y_{gp} = SY + Y_g$$

where Xgp and Ygp were the coordinates of the point "P" in the GCS in inches.

The next step in the analytical procedure was to determine the location of the point "P" in the Sled Coordinate System (SCS) by transforming from the GCS to the SCS. The direction of each of the GCS axes was defined as an SCS unit vector originating at corner 1 of the grid. These two unit vectors were:

$$X = A_1 i + A_2 j + A_3 k$$

$$Y = B_1 i + B_2 j + B_3 k$$

where A1, A2 and A3 were the direction cosines of the X, Y and Z SCS components of the GCS X axis and where B1, B2 and B3 represent the same factors for the GCS Y-axis. These direction cosines can be used to determine the X, Y and Z coordinates of P in the SCS. Letting the SCS coordinates of Corner 1 of the grid be X2, Y2, and Z2, then:

$$X_p = X_2 + X_{gp}(A_1) + Y_{gp} (B_1)$$

$$Y_p = Y_2 + X_{gp}(A_2) + Y_{gp} (B_2)$$

$$Z_p = Z_2 + X_{gp}(A_3) + Y_{gp} (B_3)$$

where Xp, Yp and Zp were the SCS coordinates of the point where the line of sight from camera 2 through the reference point on the subject's head pierced the reference grid.

The next step in the procedure was the determination of the direction cosines between the line of sight and the three SCS Axes. These were determined as follows:

$$DXp = Xp - X1$$

$$DYp = Yp - Y1$$

$$DZp = Zp - Z1$$

$$R = (DXp)^2 + (DYp)^2 + (DZp)^2$$

$$A = DXp/R$$

$$B = DYp/R$$

$$C = DZp/R$$

Where $X1$, $Y1$, and $Z1$ were the SCS coordinates of camera 2, R was the slant range from camera 2 to point P and A, B and C were the direction cosines between the line of sight and respective SCS axis.

The final step in the procedure was to determine the X, Y and Z SCS coordinates of the reference fiducial located on the subject's head. To make this determination from a single camera, it was necessary to assume that the subject's lateral movement (movement along the Y-axis in SCS) was negligible (the validity of this assumption is considered later in this appendix). With this assumption, it was possible to determine a slant range (r) between the camera located at $X1$, $Y1$, $Z1$ and the reference point on the subject's head as follows:

$$Y = Y1 + Br$$

where

Y = reference point Y coordinate in SCS

$Y1$ = Y coordinate of camera 2 in SCS

$B = Y$ axis direction cosine of line of sight

$r =$ slant range from the camera to P

When Y was assumed to be constant (no lateral motion) then:

$$Y = Y_c$$

$$Y_c = Y_1 + Br$$

$$r = \frac{Y_c - Y_1}{B}$$

where Y_c was the initial Y coordinate of the reference point on the subject's head.

With this expression and the previously determined direction cosines, the SCS X and Z coordinates of the reference fiducial on the subject's head were determined by:

$$X = X_1 + Ar$$

$$Z = Z_1 + Cr$$

These general calculations made by the computer program yielded the tabulated raw data on a frame by frame basis that are included as part of this appendix.

In order to estimate subject head velocity, it was necessary to estimate an elapsed time per frame. The beginning of the impact event was marked by electronically initiated flash units positioned on the test sled to permit viewing by all of the cameras simultaneously. The flash event normally occurred approximately 10 to 30 frames prior to visible air bag deployment.

The following procedure was used to establish an average time per frame. All head position data readings were started at the flash event

on each frame at intervals of 0.001 seconds. The average time per frame for a given film segment was determined by counting the number of pips that occur within an interval of frames and then dividing the number of pips by the number of frames. For example, beginning with frame zero locate another frame with the timing pip in the same location as frame zero. In this example, assume the frame was 40 and the number of pips was 39 which leads to:

$$t = \frac{39 \text{ pips}}{40 \text{ frames}} \times .001 \text{ seconds or}$$

where

$$t = .0009975 \text{ sec/frame}$$

where t was the average time per frame. In order to compensate for variable frame rates by the high speed cameras, this procedure was repeated for the middle and the end of the data run and then all three values were averaged to obtain an average time per frame for each run.

Selected portions of the raw data were smoothed and then graphically presented in the basic report. The method of smoothing the data was a sliding three point average centered on the middle of the three data points. Let $X1$ through $X4$ and $Z1$ through $Z4$ be the SCS X and Z coordinates of the head reference point at four sequential times. The first average point would be:

$$X2a = \frac{X1 + X2 + X3}{3}$$

$$Z2a = \frac{Z1 + Z2 + Z3}{3}$$

where $X2a$ and $Z2a$ were the coordinates of the average point and were labeled with the frame number of point $X2$, $Z2$. The next point in the smoothed path was calculated by dropping $X1$ from the calculation and

adding X4 giving

$$X_{3a} = \frac{X_2 + X_3 + X_4}{3} \quad \text{and}$$

$$Z_{3a} = \frac{Z_2 + Z_3 + Z_4}{3}$$

where X_{3a} and Z_{3a} represented the second averaged point and were labeled with the frame number of X_3 , Z_3 .

The data, as presented in the basic report, was plotted with a "range" envelope on either side of the average path. This envelope was determined by summing the absolute value of the differences between the sliding averaged value and the 3 points which made up the average value and dividing by 3.

$$DX = \sum_{i=n}^{n+2} \frac{X_a - X_i}{3}$$

$$DZ = \sum_{i=n}^{n+2} \frac{Z_a - Z_i}{3}$$

where X_a was the average X over the interval n to $n + 2$ and where Z_a was the average Z value for the same interval.

The next step was to determine the component of the variation which was perpendicular to the average direction of travel. If the angle between the direction of travel and the horizontal were called θ , and if the angle formed by vector addition of the elements DX and DZ was called ϕ , then:

$$\theta = \tan^{-1} \frac{Z(n+1)_a - Z_{na}}{X(n+1)_a - X_{na}}$$

$$\phi = \tan^{-1} \frac{DZ}{DX}$$

where X_{na} , Z_{na} and $X(n+1)_a$, $Z(n+1)_a$ were the average X , Z coordinates at the point n and the next average point $(n+1)$.

The resultant variation was found by:

$$U = (DZ)^2 + (DX)^2$$

where U was the resultant variation. The component of the variation perpendicular to the average path was found as follows:

$$U_p = U \sin \phi .$$

Next, U_p was broken up into X, and Z SCS values for plotting with respect to the location of X_{na} , Z_{na} .

$$U_{px} = U_p \sin \theta$$

$$U_{pz} = U_p \cos \theta$$

These values were then plotted positive and negative originating at the average point X_{na} , Z_{na} . This was done for each of the averaged values calculated, with the end result being an envelope of varying width around the average path. This envelope provided an indication of the variation between points used to calculate the average point.

In an attempt to evaluate the reproducibility of the film readings, a test was run in which three different operators read the same two film frames three times each. The first frame selected was one in which the standard reference fiducials were clear and distinct as was the reference fiducial on the subject's head. Three readings were taken by each of the three operators and processed through the computer as if it were a data run. The same format was followed for the second frame read except that the standard reference fiducials were partially obstructed by the strings attached to the subject's head. There was some blurring due to impact vibrations and the reference fiducial on the subject's head was at an angle to the camera, making it difficult to locate the center of the fiducial. In general, the first film frame represented

the best reading conditions which were encountered while the second frame represented the other extreme and was nearly unreadable.

For the first or the good frame, the X coordinate was $23.208 \pm .154$ inches and the Z coordinate was $33.093 \pm .088$ inches. The \pm values represent one standard deviation from the mean and were less than 1% of the mean for both X and Y coordinates indicating good reproducibility.

For the second frame read, the X coordinate was $43.395 \pm .242$ inches and the Z coordinate was $31.372 \pm .328$ inches. The \pm values again represent one standard deviation from the mean. The standard deviation for the X coordinate was still less than 1% however, the standard deviation for the Z coordinate was slightly greater than 1%. These values indicate the results from the poor data frame were not as good; however, the deviations from the mean were not excessive, indicating reasonably good reproducibility.

There were several potential errors which were not mathematically accounted for in the photometric processing methods. The three potential error modes to be considered here were magnification errors, errors caused by subject lateral motion, and operator film reading errors.

Magnification errors could result from the film deflecting within the film plane of the high speed cameras during periods of high deceleration. This could cause some change in image size as recorded by the camera. This was probably a random error and was probably not constant across the film frame. To provide a number to represent this potential error, the distance in counts between the reference fiducials

for 36 sequential values of the raw data from run 6528 was analyzed. The distance between R1 and R2 ranged from 413 counts to 424 counts with a mean value of 418 counts and a standard deviation of + 3 counts. This was not a large variation and could possibly result from operator reading variations as well as from changes in image size.

Subject lateral motion was assumed to be negligible in the position calculations made by the computer. To minimize the lateral motion error, the overhead camera film (camera 1) for each run was reviewed prior to making photometric data readings. Subject lateral motion was easily observed by this camera and an estimate was made of when lateral motion became significant. Generally speaking, the amount of lateral motion was small until after rebound from the air bag.

The final potential source of error to be considered was operator reading error. An attempt to provide numbers for this item was made in the paragraph discussing reproducibility of results. Only a small number of operators (3) were used and these operators worked closely with the individual who processed the data to obtain the final results. The end result was a reasonably standard method of reading the same two sled reference fiducials and a reasonably standard method of establishing and reading the head reference point.

Tables 1 through 11 are the unsmoothed position data for each of the experimental runs for which photometric data was analyzed. Table 12 gives the numerical values used to estimate the reproducibility of the photometric data. Finally, the last few pages of this appendix include Part 1 and Part 2 of the computer program used to process photometric data.

BEST COPY
AVAILABLE

TABLE 1

HEAD REFERENCE POSITION

Run Number: 6507

Average Time/Frame: .001074 sec

Frame No.	X Displacement (in.,scs)	Z Displacement (in.,scs)
10	19.121139	32.550243
20	19.160566	32.643275
30	19.40653	32.542673
40	19.233351	32.532033
50	21.032443	32.673154
60	22.025435	33.217673
70	23.203475	33.662174
80	25.322627	34.090301
90	23.500679	34.233513
100	31.232626	34.366723
105	32.667033	34.370025
110	34.013024	34.512419
115	35.215351	34.562332
120	36.553474	34.524347
125	37.230636	34.502231
130	33.952364	34.225326
132	32.541722	3.622134
134	32.743231	34.307253
136	40.311606	34.740725
138	40.56471	34.631544
140	40.932064	34.341243
142	41.030123	34.525647
144	41.412177	34.632323
146	41.317311	34.621741
148	41.236732	34.54224
150	42.157253	34.442122
152	42.153752	34.526374
154	42.30122	34.512543
156	42.473442	34.410216
158	42.613703	34.502151
160	42.752513	34.456324
162	42.363476	34.437524
164	42.220033	34.5126
166	42.223432	34.306746
168	42.263312	35.033352
170	42.205244	34.244166
172	42.12535	35.154704
174	41.266205	35.072044
176	41.723273	35.367553
178	41.253123	35.400237
180	41.237334	35.625432
182	41.243173	35.604343
184	40.262544	35.342677

BEST COPY
AVAILABLE

TABLE 1 (Contd.)

136	40.343736	35.830542
133	40.403743	36.121613
120	40.03322	36.034453
125	37.474044	36.545035
200	33.230037	36.527433
205	33.17302	37.101366
207	33.230433	37.064327
210	37.602763	37.073722
215	37.135722	37.130761
220	36.376343	37.201611

BEST AVAILABLE COPY

BEST COPY
AVAILABLE

TABLE 2

HEAD REFERENCE POSITION

Run Number: 6514

Average Time/Frame: .00105 sec

Frame No.	X Displacement (in.,scs)	Z Displacement (in.,scs)
40	17.205044	36.132252
41	20.303721	36.350556
37	30.213223	37.343633
20	32.135273	37.344215
25	33.770534	37.315731
100	35.663621	37.620412
105	37.343413	37.670224
103	33.267466	37.563221
110	33.726132	37.437326
112	32.323222	37.501155
114	32.232215	37.624022
116	40.43634	37.531723
113	40.722371	37.50742
120	41.210242	37.332437
122	41.332127	37.424265
124	42.36725	37.22221
126	42.623123	37.0663
123	42.23205	37.225714
130	43.26413	37.101437
132	43.522312	37.023164
134	43.320263	36.703443
136	43.335322	36.52641
133	44.123335	36.630423
140	44.11013	36.553527
142	44.36552	36.414602
144	44.424362	36.272005
146	44.435677	36.04302
143	44.53074	35.257534
150	44.602441	35.361133
152	44.722036	36.026512
154	44.351253	35.352325
156	44.775232	35.635177
160	44.665373	35.227225
162	44.304463	36.027503
165	45.022343	35.661222
170	45.373406	35.325061
175	45.547261	36.011302
130	45.615456	36.132022
135	45.720477	36.554236
120	45.372644	36.736744
115	44.873226	37.037224
200	44.273433	37.264372
205	43.567721	37.26052
210	42.32633	37.446577
220	41.443602	37.72475

BEST AVAILABLE COPY

BEST COPY
AVAILABLE

TABLE 3

Run Number: 6528

Average Time/Frame: .001037 sec

Frame No.	X Displacement (in.,scs)	Z Displacement (in.,scs)
0	20.121541	33.335674
10	20.074436	33.213435
20	20.406377	33.717025
30	21.022717	33.432057
40	22.343335	33.474474
43	23.746343	33.440311
53	26.5763	33.752714
65	23.32316	33.737743
70	30.237452	33.636727
75	31.727655	33.665762
80	33.765137	33.570627
85	35.663764	33.352677
90	37.545701	33.027503
95	39.330373	32.949031
100	40.623323	32.401336
102	41.20223	32.301154
104	41.734705	31.345534
106	42.762606	31.653407
108	43.05337	31.542462
110	43.555023	31.076303
112	43.372602	31.036524
114	44.335402	30.623727
116	44.30776	30.352231
118	44.332377	30.111319
120	45.147254	29.35075
122	45.432213	29.436204
124	45.321166	29.136273
126	45.232775	23.303453
128	46.442435	23.524545
130	46.333362	23.547561
132	46.333752	23.455276
134	46.512537	27.246227
136	46.73744	27.752361
138	46.723547	27.700024
140	46.775144	27.750137
142	47.062165	27.353126
144	47.166172	27.313037
146	47.300372	27.026362
148	47.232341	26.235223
150	47.34332	27.149333
152	47.555752	26.379736
154	47.547333	26.326237
156	47.527220	26.222522
158	47.323225	26.334562

BEST COPY
AVAILABLE

TABLE 3 (Cont'd)

160	47.617237	27.027601
162	47.471232	27.213646
164	47.20122	27.332231
166	46.733122	27.531421
168	47.162312	27.374934
170	46.763516	27.533552
172	47.064522	27.543333
174	46.467752	27.324033
176	46.441064	27.36541
178	46.002353	23.04747
180	45.333242	23.421651
182	45.042352	23.362726
184	44.336236	23.623521
186	44.235356	23.933567
190	43.246225	22.552231
195	42.033523	30.040523
200	41.32263	30.441704
205	40.377653	30.315414
210	33.205123	31.306322

BEST AVAILABLE COPY

BEST COPY
AVAILABLE

TABLE 4

HEAD REFERENCE POSITION

Run Number: 6534

Average Time/Frame: .001038 sec

Frame No.	X Displacement (in.,scs)	Z Displacement (in.,scs)
0/	19.262246	33.534540
10	20.037273	33.475119
20	20.406240	33.3591
30	21.36366	33.071397
40	23.072304	33.173267
50	25.7313	33.541393
53	23.27905	33.951247
70	33.353676	34.123962
75	35.325563	34.163456
30	37.546431	34.162539
35	37.352427	34.360636
90	42.24706	34.330717
95	43.661773	34.04103
100	45.621341	34.097352
102	46.306226	33.466
104	46.774025	33.611369
106	47.772693	33.193333
103	43.106607	33.170479
110	43.901342	32.273203
112	47.393416	32.161336
114	47.722907	31.534331
116	50.173025	31.679453
113	51.04535	30.964995
120	51.305946	30.543525
122	51.766513	30.646561
124	52.072901	30.252661
126	52.594533	29.701656
123	53.123526	29.507593
130	53.363346	29.296373
132	53.963359	29.174377
134	54.439379	23.519751
136	54.233209	23.269615
133	54.653769	27.979517
140	54.370939	27.56995
142	54.91603	27.909311
144	54.324407	27.913103
146	55.672152	27.663657
143	55.455632	27.245353
150	55.531223	27.664446
152	55.562653	26.604105
154	55.161429	26.375941
156	55.413341	27.436763
153	55.352939	27.073331

BEST AVAILABLE COPY

BEST COPY
AVAILABLE

TABLE 4 (Cont'd)

160	55.55751	27.12233
162	54.316647	27.000244
164	54.132415	27.667643
166	55.103722	23.166007
163	54.740132	23.165222
170	54.453377	27.735577
175	54.040234	23.341373
130	53.422505	22.022301
135	52.700367	22.262441
137	52.627027	22.730236
120	52.222326	22.225373
125	51.445401	31.055374
200	50.235437	31.333332
205	43.265142	32.146014

BEST AVAILABLE COPY

BEST COPY
AVAILABLE

TABLE 5
HEAD REFERENCE POSITION

Run Number: 6537

Average Time/Frame: .001052 sec

Frame No.	X Displacement (in.,scs)	Z Displacement (in.,scs)
0	10.30473	34.334461
10	10.340175	34.373711
20	20.200405	34.304455
30	21.043001	34.233550
40	22.600276	34.262453
50	30.502321	35.52002
60	32.53303	35.624462
70	34.603333	35.505342
80	36.233002	35.417000
90	37.43265	35.530102
100	41.217335	35.323312
110	42.014302	35.713365
120	42.642435	35.547725
130	43.350540	35.513939
140	44.024100	35.530303
150	44.452024	35.474633
160	45.132332	35.431162
170	45.697447	35.033477
180	46.113391	34.24337
190	46.435656	34.700131
200	46.237703	34.470334
210	47.130672	34.273116
220	47.335652	33.702313
230	47.45531	33.434101
240	47.726001	33.13351
250	43.006132	32.346054
260	43.24342	32.572213
270	43.670337	32.013075
280	43.54135	31.60530
290	40.153054	31.105014
300	40.143671	30.333341
310	40.210777	30.574442
320	40.50170	30.254373
330	40.750641	29.919337
340	40.577004	29.654307
350	40.337152	29.424619
360	40.300365	29.32333
370	50.235031	23.303103
380	50.301043	23.636407
390	50.604253	23.356274
400	51.065770	23.151000
410	51.41507	23.177000
420	51.354503	27.340014

BEST COPY
AVAILABLE

TABLE 5 (Cont'd)

156	51.431632	27.741135
158	51.411245	27.623002
160	51.324753	27.513233
162	51.25555	27.423013
164	52.1223	27.47074
166	52.026714	27.276707
168	52.127733	27.15140
170	52.243253	26.737717
172	52.433002	27.047137
174	52.374325	26.735643
176	52.53222	26.302355
178	52.275332	26.350774
180	52.633633	26.627031
182	52.131157	26.343622
184	52.413235	26.323724
186	52.014405	26.52502
188	52.127553	26.306023
190	51.357176	26.643227
192	51.34036	26.723123
195	50.711243	26.712024
200	50.421503	27.035374
205	40.739346	27.427314
210	42.743343	27.634246
215	40.20225	23.213655
220	43.573511	23.532076

BEST AVAILABLE COPY

BEST COPY
AVAILABLE

TABLE 6

HEAD REFERENCE POSITION

Run Number: 6556

Average Time/Frame: .001049 sec

Frame No.	X Displacement (in.,scs)	Z Displacement (in.,scs)
40	12.270352	37.005424
44	20.237316	37.05012
20	36.722341	33.743662
25	35.244677	33.203064
100	40.344021	33.525422
102	40.635533	33.412347
104	41.032513	33.212163
106	41.525325	33.213623
103	42.04246	33.007402
110	42.356252	37.322706
112	42.534227	37.733027
114	42.760512	37.553426
116	42.734237	37.44213
113	42.763216	36.222433
120	43.010022	37.003563
122	43.021311	36.373773
124	43.13011	36.310716
126	43.207615	36.622526
123	43.331302	36.613324
130	43.222315	36.22335
132	43.357372	36.146314
134	43.372346	36.157337
136	43.326553	36.012302
133	43.562124	36.152315
140	43.332725	36.163023
142	43.673022	36.342242
144	43.504416	35.252205
146	43.513262	36.045303
143	43.333431	35.332105
150	43.235422	36.110072
152	43.272223	36.112034
154	43.217333	36.212115
156	43.071204	36.166302
153	43.02136	36.132304
160	43.073772	36.456071
162	42.72457	36.441301
164	42.705327	36.611402
166	42.273726	36.453213
170	42.260557	36.720322
175	41.566017	36.771315
130	40.231343	36.21013
135	40.520737	37.274302
120	37.366453	37.012322
125	37.224623	37.137627
200	33.702355	37.216125

BEST AVAILABLE COPY

BEST COPY
AVAILABLE

TABLE 7
HEAD REFERENCE POSITION

Run Number: 6569

Average Time/Frame: .001058 sec

Frame No.	X Displacement (in.,scs)	Z Displacement (in.,scs)
30	19.56572	34.504305
35	20.333337	34.360032
40	21.030453	34.305019
44	21.433637	35.263231
66	23.764234	35.717667
70	30.436366	35.640537
75	32.735966	35.333935
80	35.234536	35.913656
85	37.212612	35.322641
90	39.237323	35.639077
95	42.711636	35.9243
100	44.626266	35.346114
105	46.631223	35.141147
107	47.403223	34.354003
110	47.377523	34.400277
112	43.274011	34.333361
114	43.402043	34.432223
116	43.664633	34.042734
118	43.601002	33.534634
120	43.617333	33.903522
122	43.123477	33.664363
124	43.26639	33.537723
126	43.164343	33.633307
128	43.007271	33.995036
130	47.237262	34.121753
132	47.577202	33.021422
134	47.522076	33.743513
136	47.162443	33.334275
138	47.050233	33.415939
140	46.302242	32.605732
142	46.32633	33.224414
144	46.210742	33.275622
146	46.572122	33.25766
148	47.137213	33.712732
150	46.61555	33.225127
152	46.222122	33.37725
154	46.35043	32.921531
156	47.027122	33.146507
158	47.173341	32.430256
160	46.333334	32.622271
165	47.313732	32.221013
170	43.023313	32.373235
175	43.406637	31.357302

BEST COPY
AVAILABLE

TABLE 7 (Cont'd)

130	43.762226	31.656711
135	42.103022	31.251462
140	43.341647	30.662063
145	43.422762	30.170234
200	43.20633	30.137204
205	43.03352	30.056213
210	47.021533	30.133216
215	46.253077	30.115319
220	46.003142	30.202322
225	45.443375	30.073332
230	44.637322	30.253421
235	44.376623	30.542403
240	43.523372	30.722605
245	43.237434	30.377332
250	42.305432	30.967332

BEST AVAILABLE COPY

BEST COPY
AVAILABLE

TABLE 8

HEAD REFERENCE POSITION

Run Number: 6571

Average Time/Frame: .001 sec

Frame No.	X Displacement (in.,scs)	Z Displacement (in.,scs)
0	20.733172	35.021227
10	20.343256	34.703673
20	21.403751	34.630433
30	22.431446	34.51301
35	22.652237	34.910435
60	33.343265	39.245207
70	33.255574	34.897133
100	44.73645	35.315309
103	45.536145	35.10447
107	46.333017	34.022156
111	47.121303	33.669464
115	47.104176	33.023175
117	47.075054	32.226795
120	47.05325	32.237073
122	47.144251	32.333767
124	47.030176	31.706162
126	46.92261	31.303301
128	46.857027	31.770363
130	46.446435	31.117353
132	46.671076	31.513403
134	46.699622	30.961166
136	46.162267	31.253011
138	45.955337	31.104533
140	45.332333	30.995517
142	45.744534	31.256337
144	45.75572	31.145655
146	45.575996	31.276521
148	45.39419	31.01079
150	45.036152	30.642641
155	45.19354	30.343721
160	44.317525	30.261752
165	45.073775	30.034303
170	45.325343	29.913433

BEST AVAILABLE COPY

BEST COPY
AVAILABLE

TABLE 9

HEAD REFERENCE POSITION

Run Number: 6572

Average Time/Frame: .001052 sec

Frame No.	X Displacement (in.,scs)	Z Displacement (in.,scs)
0	12.003705	36.235536
10	12.110303	36.16973
20	12.731744	35.327743
30	20.716451	35.61733
33	22.021077	35.623649
60	26.625242	36.231402
65	23.024765	36.237235
73	31.472756	35.77371
32	37.30535	36.153351
100	41.467663	36.14342
132	47.710633	32.573621
140	47.795325	32.732327
145	47.406722	32.623022
150	47.125253	32.325172
152	47.201511	33.120736
154	47.217422	33.027343
156	46.210014	32.742013
153	46.344637	33.017365
160	46.64422	32.320376
162	46.377742	32.352172
164	46.213341	33.022302
166	45.315652	32.606527
163	46.210233	33.542224
170	45.200163	33.253667
172	45.247623	32.32211
175	46.624336	31.763234
180	44.355133	33.23222
185	44.215555	33.162652
190	43.702234	33.053247
195	42.262313	33.021247
200	42.407355	33.365732
210	40.757736	33.354261

BEST AVAILABLE COPY

BEST COPY
AVAILABLE

TABLE 10

HEAD REFERENCE POSITION

Run Number: 6574

Average Time/Frame: .001052 sec

Frame No.	X Displacement (in.,scs)	Z Displacement (in.,scs)
0	10.513416	33.623336
10	10.53144	33.523227
20	20.03615	33.347636
30	21.0212	33.143303
40	22.006724	32.970133
50	30.704774	32.757312
60	32.343647	32.721347
70	34.463177	32.744667
80	36.756765	32.420333
90	33.37134	32.462573
100	41.036034	32.403421
110	41.331135	32.054707
120	42.326317	31.460014
130	42.757734	31.704232
140	43.126313	31.424412
150	43.72535	31.407412
160	44.266373	31.363327
170	44.533027	31.226145
180	45.327733	30.712127
190	45.636423	30.363232
200	45.273463	30.415077
210	45.332007	30.246205
220	46.21627	30.003232
230	46.02243	29.723122
240	46.11673	29.60462
250	46.45507	28.920337
260	46.560142	29.062273
270	46.325416	28.340427
280	47.034121	28.173134
290	47.003654	28.327063
300	47.431113	27.565413
310	47.442074	27.600614
320	47.63026	27.323531
330	47.604075	27.414263
340	47.637337	27.032255
350	47.733652	26.376631

BEST AVAILABLE COPY

BEST COPY
AVAILABLE

TABLE 10 (Cont'd)

143	47.32461	26.7301
150	47.220633	26.630356
152	46.770316	26.233135
154	46.237403	27.071231
156	46.364053	26.332566
157	46.647040	26.220036
160	46.667230	27.031400
165	45.320516	27.12271
170	45.416055	27.153763
175	44.437131	27.201352
180	43.445327	27.423207
185	42.562370	27.633416

BEST AVAILABLE COPY

BEST COPY
AVAILABLE

TABLE 11
HEAD REFERENCE POSITION

Run Number: 6575

Average Time/Frame: .00104 sec

Frame No.	X Displacement (in.,scs)	Z Displacement (in.,scs)
0	21.040506	32.274572
10	21.202534	32.14357
20	21.446314	32.177627
30	22.073306	31.526024
40	24.664305	31.363673
70	33.602673	32.013275
80	37.723603	33.102321
90	41.532022	33.036233
100	44.067527	33.223125
105	45.015072	32.006567
110	45.672637	32.440001
112	45.515127	32.633171
114	45.672433	31.274763
116	45.676304	32.52655
118	45.554403	31.375573
120	45.436126	32.02523
122	45.413272	31.274156
124	45.067367	31.332441
126	45.116203	31.36733
128	44.727352	31.311767
130	44.322514	31.107607
132	44.635162	31.365743
134	44.300553	30.273632
136	44.116142	31.002452
138	44.053573	31.122231
140	43.966113	31.133252
142	43.565352	31.032272
144	43.202136	30.322224
146	43.323554	30.257475
148	43.023252	31.120251
150	43.02433	31.550003
152	42.733355	31.45552
154	42.756426	31.465302
156	42.902363	31.332713
158	42.560752	31.475322
172	41.675771	31.542147
175	41.525577	32.07206
180	41.543036	32.446324
190	40.761353	32.625137
200	40.00372	32.327523

TABLE 12
PHOTOMETRIC DATA PROCESSING CAPABILITY

Frame No.	Operator No.	X Displacement (in)	Y Displacement (in)
40	1	23.227796	33.138415
		22.914095	33.257364
		23.194362	33.115913
	2	23.119479	33.106136
		23.324361	33.074295
		23.253653	33.084518
	3	23.485258	32.915271
		23.287051	33.011622
		23.065698	33.137854

Mean \pm 1 std deviation

$$\bar{X} = 23.208 \pm .154 \text{ in} \quad \bar{Y} = 33.093 \pm .088 \text{ in}$$

98	1	43.279906	31.051893
		43.344916	31.338242
		43.089645	31.147184
	2	43.776671	31.915067
		43.354318	31.162637
		43.029435	31.941104
	3	43.602501	31.843233
		43.376973	31.319838
		43.69998	31.624812

Mean \pm 1 std deviation

$$\bar{X} = 43.395 \pm .242 \text{ in} \quad \bar{Y} = 31.372 \pm .328 \text{ in}$$

DEFINITIONS

PART 1

PHOTOMETRIC DATA PROCESSING PROGRAM

Terms listed in order of occurrence.

GRCS - Grid Reading Coordinate System

R1)
R2) - Sled reference fiducials

X1 - X Counts from R1 to R2 in the GRCS

Y1 - Y counts from R1 to R2 in the GRCS

PHOI - Unprocessed (input) data file

PHOD - Rotated (output) data file

PH)
PX) Intermediate data files
PY)

H - Frame number

X2 - X counts from R1 to R2¹

Y2 - Y counts from R1 to R2¹

X3 - X counts from R1 to head reference point

Y3 - Y counts from R1 to head reference point

0 - Angle between the GRCS X axis and a line from R1 to R2 for the reference grid.

01 - Angle between the GRCS X axis and a line from R1 to R2¹ for a data frame.

03 - Angle between the GRCS X axis and a line from R1 to the reference point on the subject's head.

R - Distance in counts from R1 to the subject's head reference point in the GRCS.

X - Rotated (output) counts from R1 to head reference point

Y - Rotated (output) counts from R1 to head reference point

PART 1

BEST COPY
AVAILABLE

PHO

PHOTOMETRIC DATA PROCESSING PROGRAM

```

10 PRINT "REF IN"
20 INPUT X1,Y1
30 PRINT "NO OF FRAMES"
31 INPUT N
40 OPEN "PHO1",INPUT,1
41 OPEN "PH",OUTPUT,2
42 OPEN "PX",OUTPUT,3
43 OPEN "PY",OUTPUT,4
50 FOR I=1 TO N
60 INPUT FROM 1:H,X2,Y2,X3,Y3
70 O=ATN(Y1,X1)
80 O1=ATN (Y2,X2)
90 O2=O-O1
100 O3=ATN(Y3,X3)
110 O4=O3+O2
120 R=SQR(Y32+X32)
130 X=R*(COS(O4))
140 Y=R*(SIN(O4))
150 WRITE ON 2:H
190 WRITE ON 3:X
200 WRITE ON 4:Y
210 NEXT I
220 CLOSE 2,3,4
230 OPEN "PH",INPUT,2
260 OPEN "PHOD",OUTPUT,5
270 FOR J=1 TO N
280 INPUT FROM 2:H
290 WRITE ON 5:H
300 NEXT J
301 CLOSE 2
302 OPEN "PX",INPUT,3
310 FOR K=1 TO N
320 INPUT FROM 3:X
330 WRITE ON 5:X
340 NEXT K
341 CLOSE 3
342 OPEN "PY",INPUT,4
350 FOR L=1 TO N
360 INPUT FROM 4:Y
370 WRITE ON 5:Y
380 NEXT L
390 CLOSE 4
480 CLOSE 1
481 PRINT "F"
482 CLOSE "PH","PX","PY","PHO1"
490 END

```

BEST AVAILABLE COPY

DEFINITIONS

PART 2

PHOTOMETRIC DATA PROCESSING PROGRAM

Terms listed in order of occurrence.

GCS - Grid Coordinate System

GRCS - Grid Reading Coordinate System

SCS - Sled Coordinate System

PHOD - Rotated subject data file

PHOG - Permanent reference grid file

P - Intermediate file used for velocity calculations

A1)

A2) GRCS X axis direction cosines in the scs

A3)

B1)

B2) GRCS Y axis direction cosines in the scs

B3)

X1)

Y1) SCS coordinates of grid corner 1 of the grid used

Z1

X2)

Y2) SCS coordinates of camera 2

Z2)

Y3 - SCS coordinate of subject's plane of motion

L - Matrix variable for frame number

H - Matrix variable for X and Y of the subject's head reference point in the GRCS

F - Matrix variable for X values of grid intersections in the GRCS

K - Matrix variable for Y values of grid intersections in the GRCS

G1) X and Y GRCS coordinates of the 2" by 2"

G2) grid square corner above point P (Ith row, Ith col)

G3) X and Y GRCS coordinates of the 2" by 2"

G4) grid square corner at (Ith row + 1, Ith col)

G5) X and Y GRCS coordinates of the 2" by 2" grid
G6) square corner at (Ith row, Ith col + 1)

G7) X and Y GRCS coordinates of the grid
G8) pierce point P

D1) Difference in counts between the X coordinates of G5,
D3) G3, G7 and G1 ($D1 = G5 - G1$)
P1

D2) Difference in counts between the Y coordinates
D4) of G6, G4, G8 and G2 ($D2 = G6 - G2$)
P2)

R - Distance in counts between (IR, IC) and the point p in counts

S1 - X GCS counts between (IR, IC) and P
S2 - Y GCS counts between (IR, IC) and P

S3 - X GCS distance (inches) between (IR, IC) and P
S4 - Y GCS distance (inches) between (IR, IC) and P

X5 - X GCS coordinate (inches) of P
Y5 - Y GCS coordinate (inches) of P

X6)
Y6) SCS coordinates of the grid pierce point P
Z6)

D6) X, Y and Z differences (in inches) between the location
D7) of camera 2 and the pierce point P
D8)

A) X, Y and Z axis direction cosines between the line
B) of sight from camera 2 to P and the appropriate axis
C)

D - slant range from camera 2 to reference point on subject head

X) Final scs coordinates of the reference point
Y) on the subject's head
Z)

PART 2

BEST COPY
AVAILABLE

PHO

PHOTOMETRIC DATA PROCESSING PROGRAM

10 OPEN 'PHOD', INPUT, 1
 11 OPEN "PHOC", INPUT, 2
 12 OPEN "P", OUTPUT, 3
 20 READ A1, A2, A3, B1, B2, B3, X1, Y1, Z1, X2, Y2, Z2, Y3
 21 DATA -.6793, .7334, -.0240, -.0243, .0115, .9996, 45.528
 22 DATA 9.504, 39.240, 6.103, -6.984, 56.230, 13.728
 30 PRINT "N"
 31 INPUT N
 40 DIM L(N), H(2, N), F(14, 14), K(14, 14)
 50 MAT INPUT FROM 1: L, H
 51 MAT INPUT FROM 2: F, K
 55 PRINT " FR X Y"
 60 FOR K=1 TO N
 70 G7=H(1, K)
 80 G8=H(2, K)
 81 GOSUB 460
 90 D1=G5-G1
 100 D2=G6-G2
 110 D3=G3-G1
 120 D4=G4-G2
 130 P1=G7-G1
 140 P2=G8-G2
 150 R=(P1*2+P2*2)*.5
 160 O1=ATN(ABS(D1/D2))
 162 IF P1*P2<0 THEN 164 ELSE 170
 164 O2=-ATN(ABS(P1/P2))
 165 GO TO 180
 170 O2=ATN(ABS(P1/P2))
 180 O3=ATN(ABS(D3/D4))
 190 Q=ABS(O3)+ABS(O1)
 200 O4=ABS(O1)+O2
 210 S1=R*(SIN(Q-O4)/SIN(Q))
 220 S2=-R*(SIN(O4)/SIN(Q))
 230 R1=(D1*2+D2*2)*.5
 240 R2=(D3*2+D4*2)*.5
 250 S3=2*(S1/R1)
 260 S4=2*(S2/R2)
 270 X5=X4+S3
 280 Y5=Y4+S4
 290 X6=X1+X5*A1+Y5*B1
 300 Y6=Y1+X5*A2+Y5*B2
 310 Z6=Z1+X5*A3+Y5*B3
 320 D6=X6-X2
 330 D7=Y6-Y2
 340 D8=Z6-Z2

BEST AVAILABLE COPY

PART 2 (Cont'd)

BEST COPY
AVAILABLE

350 S=(D6²+D7²+D8²)*.5
360 A=D6/S
370 P=D7/S
380 C=D8/S
390 D=(Y3-Y2)/P
400 X=X2+(D*A)
410 Y=Y2+(D*C)
420 Z=Z2+(D*C)
430 WRITE ON 3:L(X),X,Z
440 PRINT L(X),X,Y,Z
441 IF X=N THEN 2000
450 NEXT K
455 GO TO 2000
460 FOR J=1 TO 14
470 FOR I=1 TO 14
480 IF F(J,I)=0 THEN 930
490 IF F(J,I)>G7 THEN 990
491 I1=I+1
492 IF I1=15 THEN 990
500 IF F(J,I1)<G7 THEN 980
510 G1=F(J,I)
520 G2=X(J,I)
521 J1=J+1
522 IF J1=15 THEN 441
530 G2=X(J1,I1)
535 IF G2<G2 THEN 560
540 J2=J-1
541 IF J2=0 THEN 450
542 I3=I-1
543 IF I3=0 THEN 971
544 G1=F(J2,I3)
545 G2=X(J2,I3)
546 G3=F(J,I3)
547 G4=X(J,I3)
548 G5=F(J2,I)
549 G6=X(J2,I)
550 X4=2*(I3-I)
551 Y4=-2*(J2-I)
555 GO TO 90
560 IF G3<G2 THEN 990
570 G3=F(J1,I)
580 G4=X(J1,I)
590 G5=F(J,I1)
600 G6=X(J,I1)
610 P1=G7-G1
620 P2=G3-G2
630 D1=G5-G1
640 D2=G6-G2

PART 2 (Cont'd)

BEST COPY
AVAILABLE

650 IF ABS(P1/P2)<ABS(D1/D2) THEN 749
651 J2=J-1
660 G1=F(J2,I)
670 G2=K(J2,I)
680 G3=F(J,I)
690 G4=K(J,I)
700 G5=F(J2,I1)
710 G6=K(J2,I1)
720 X4=2*(I-1)
730 Y4=-2*(J2-1)
740 GO TO 90
749 IF G2>=K(J,I1) THEN 800
750 D3=F(J1,I1)-F(J,I1)
760 D4=K(J1,I1)-K(J,I1)
770 P1=G7-F(J,I1)
780 P2=G3-K(J,I1)
790 IF ABS(P1/P2)>ABS(D3/D4) THEN 890
800 G1=F(J,I1)
810 G2=K(J,I1)
820 G3=F(J1,I1)
830 G4=K(J1,I1)
831 I2=I+2
832 IF I2=15 THEN 990
840 G5=F(J,I2)
850 G6=K(J,I2)
860 X4=2*(I)
870 Y4=-2*(J-1)
880 GO TO 90
890 G1=F(J,I)
900 G2=K(J,I)
910 G3=F(J1,I)
920 G4=K(J1,I)
930 G5=F(J,I1)
940 G6=K(J,I1)
950 X4=2*(I-1)
960 Y4=-2*(J-1)
970 GO TO 90
971 D1=F(J,I)-F(J2,I)
972 D2=K(J,I)-K(J2,I)
973 P1=G7-F(J2,I)
974 P2=G3-K(J2,I)
975 IF ABS(P1/P2)<ABS(D1/D2) THEN 660
976 GO TO 441
980 NEXT I
990 IF J=14 THEN 441
1000 NEXT J
2000 END

APPENDIX G

**AD Plots of Test Data from Test Numbers
6571, 6572, 6574 and 6575**

**Provided by the
General Motors Corporation**

This Appendix provides plots of data and computed parameters from the four highest velocity impact tests conducted during the Air Cushion test program conducted on the Daisy Decelerator. The plots include the following:

Sled X-1

Sled X-2

Chest x, y, and z axis accelerations

Computed chest resultant acceleration

Computed chest Severity Index

Head x, y and z axis accelerations

Computed head resultant acceleration

Computed head Severity Index

Mouth x, y and z accelerations

Computed mouth resultant acceleration

Left foot downward, forward and lateral forces

Computed resultant left foot force

Right foot downward, forward and lateral forces

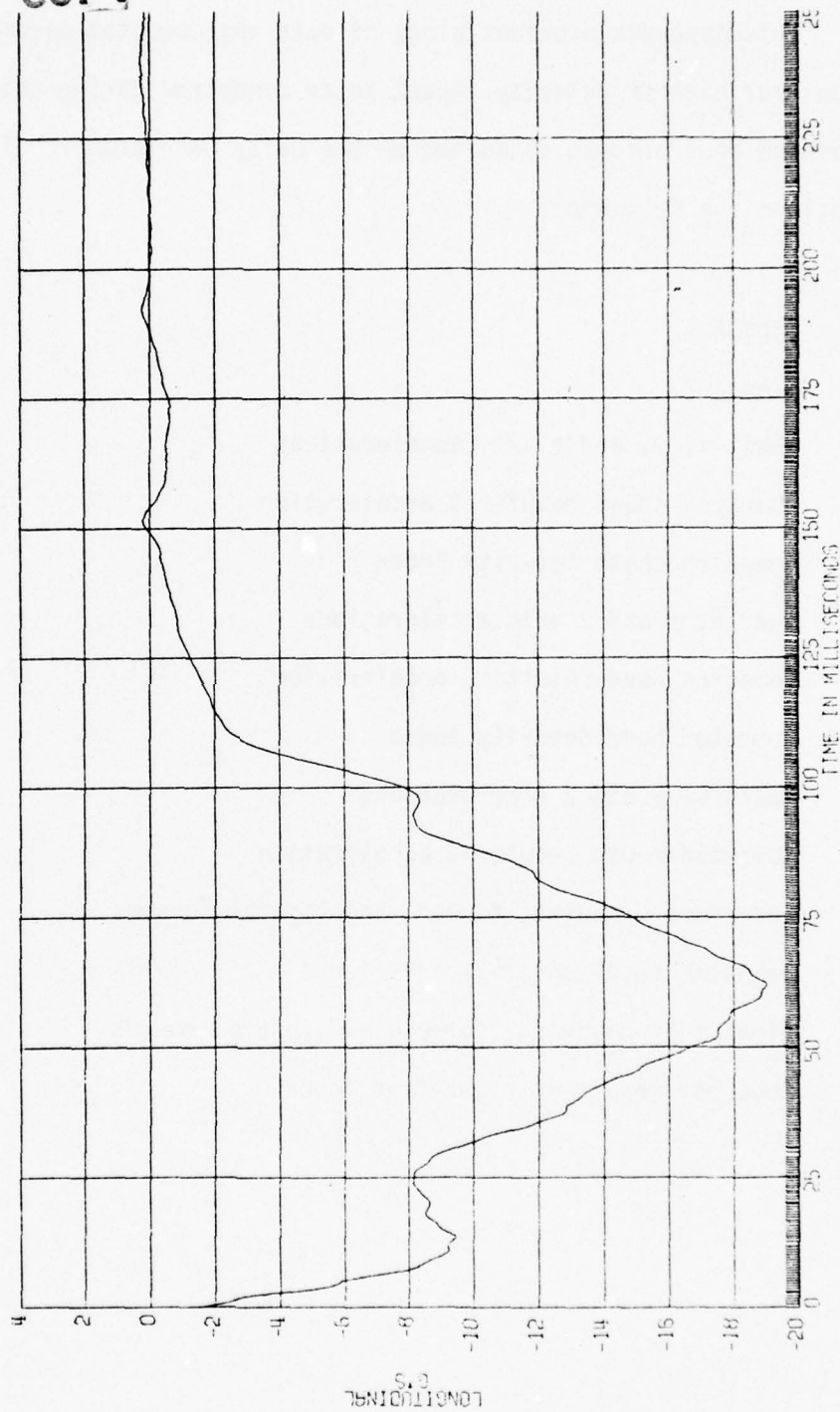
Computed resultant right foot force

BEST AVAILABLE COPY

FIGURE
REPORT PG-
09-19-72

AIR CUSHION RESTRAINT SYSTEM-HUMAN RUN
SLED X-1

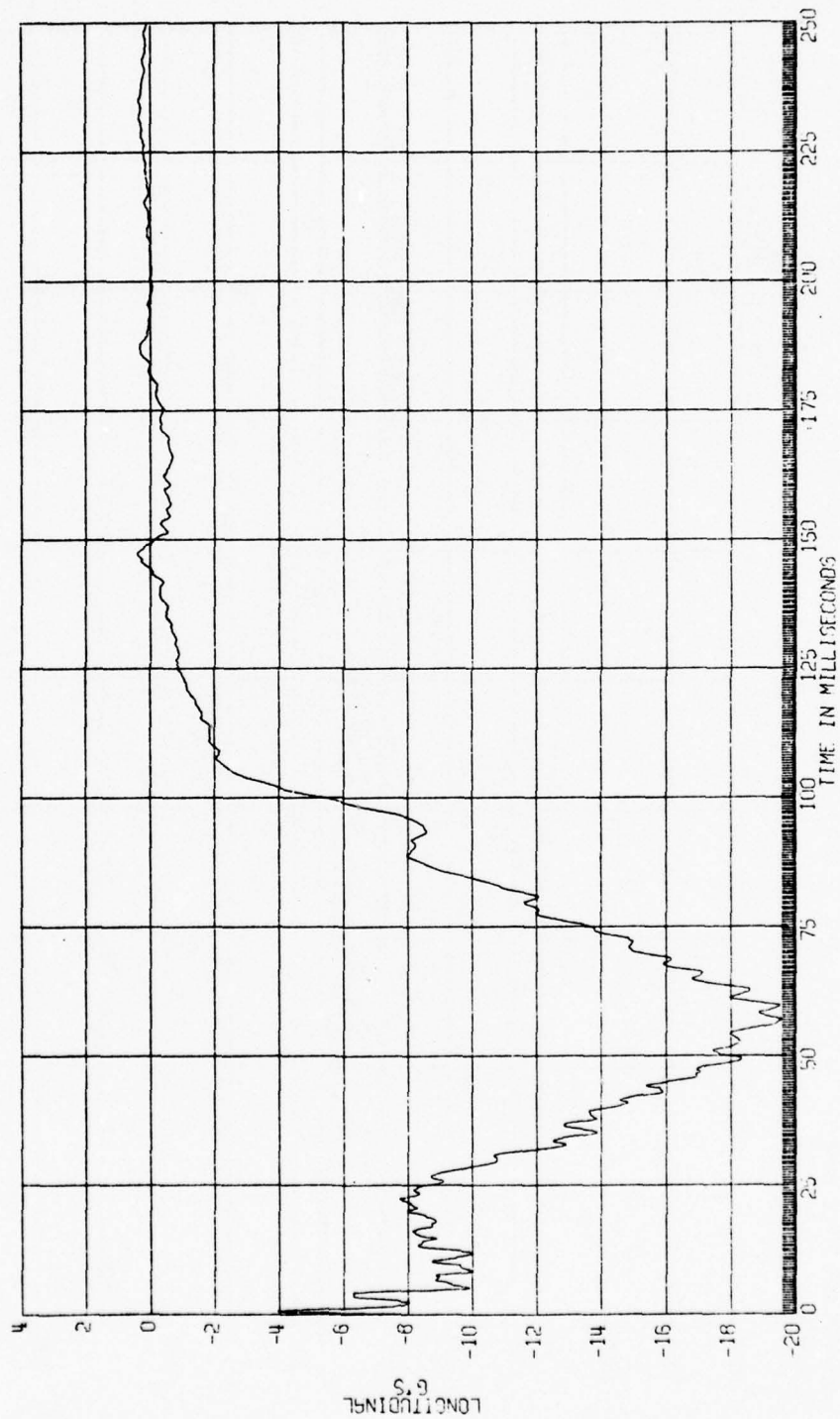
H6571A SLED IMPACT TEST
90-116-016
HOLLOWEN AIR FORCE BASE
A-D DATA SAE CLASS 60



H65718 SLED IMPACT TEST
90-116-016
HOLLOWMAN AIR FORCE BASE
R-D DATA SAE CLASS 60

AIR CUSHION RESTRAINT SYSTEM-HUMAN RUN
SLED X-2

FIGURE
REPORT PG-
09-19-72



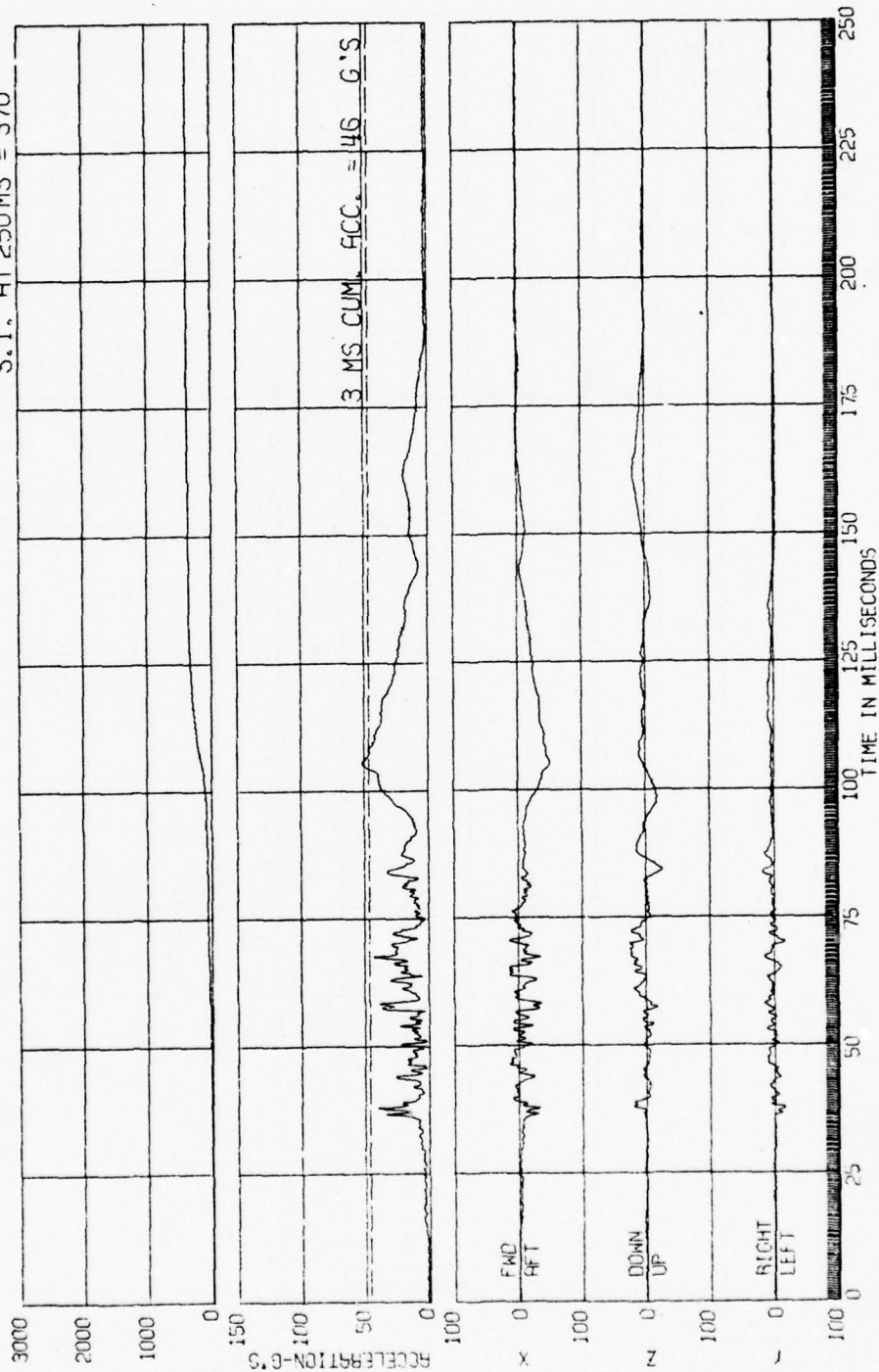
BEST AVAILABLE COPY

FIGURE
REPORT PG-
09-19-72

AIR CUSHION RESTRAINT SYSTEM-HUMAN RUN
CHEST ACCEL.

H6571B SLED IMPACT TEST
DU-116-016
HOLLOMAN AIR FORCE BASE
A-D DATA SAE CLASS 180

S.I., AT 250 MS = 370



H6571B SLED IMPACT TEST
 90-116-015
 HOLLAND AIR FORCE BASE
 A-D DATA

AIR CUSHION RESTRAINT SYSTEM-HUMAN RUN
 HEAD ACCEL.

FIGURE
 REPORT PG-
 09-19-72

S.I. AT 250 MS = 280

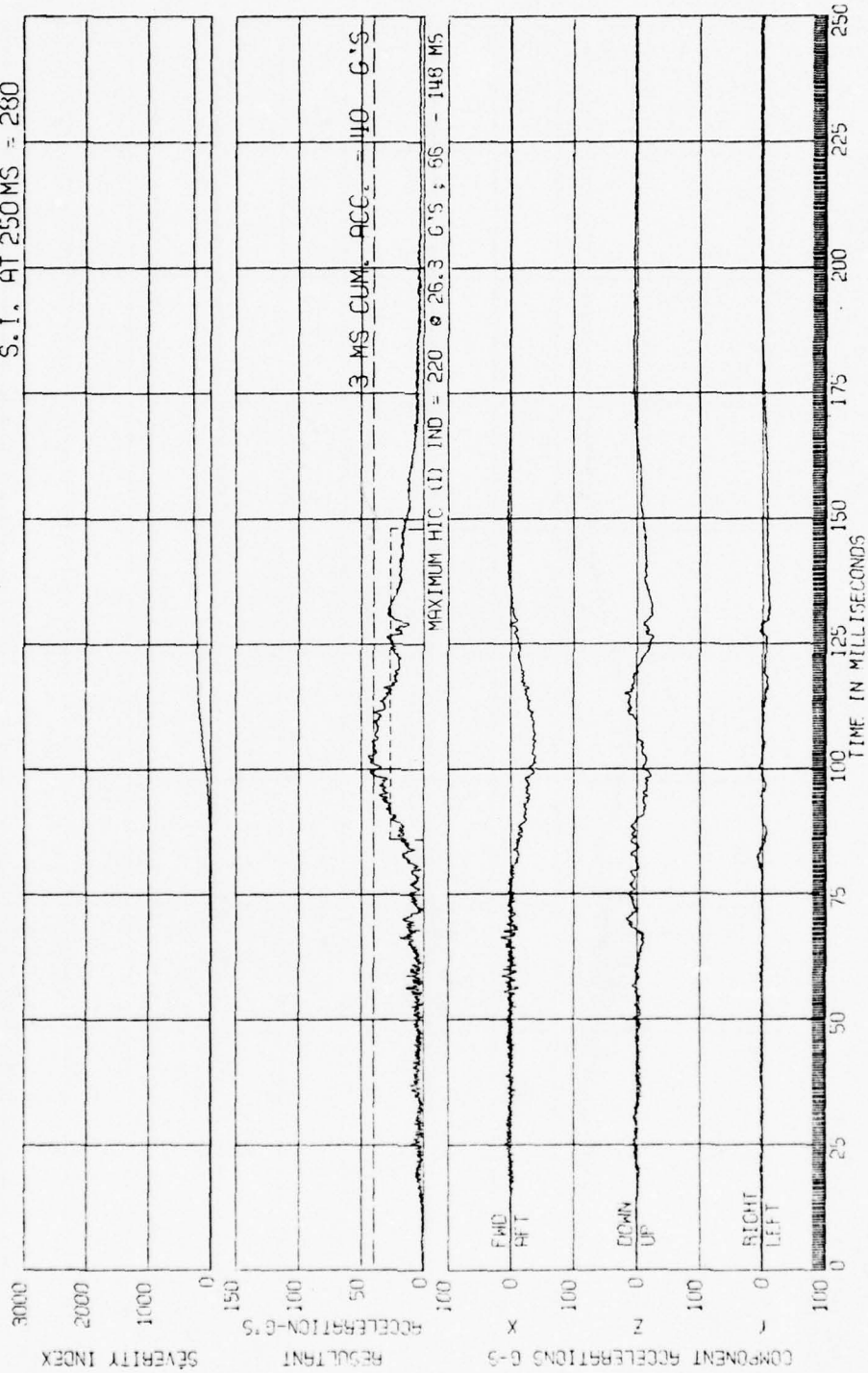


FIGURE
REPORT PC-
09-19-72

AIR CUSHION RESTRAINT SYSTEM-HUMAN RUN
MOUTH

H6571B SLED IMPACT TEST
90-116-016
HOLLoman AIR FORCE BASE
A-D DATA

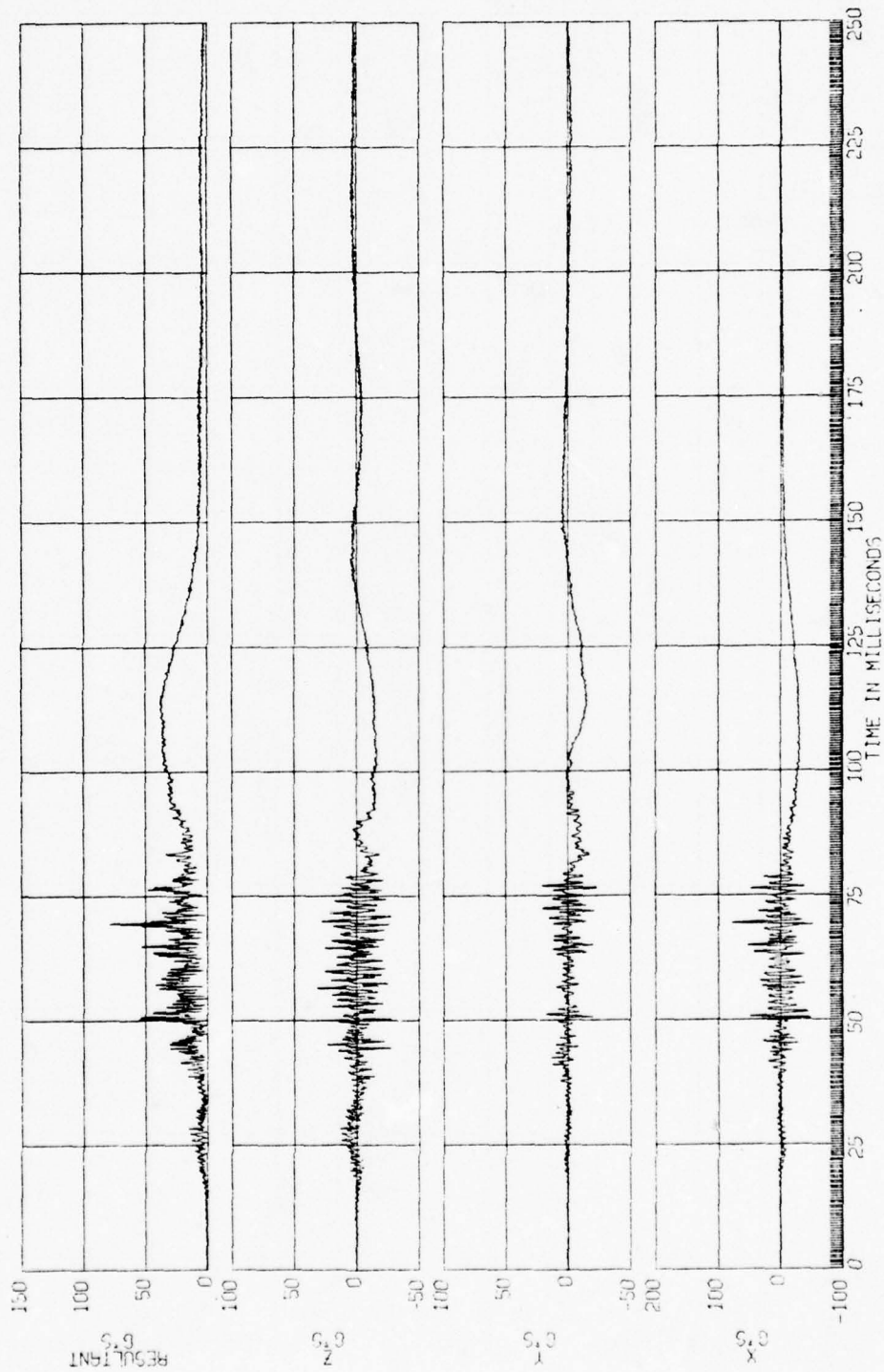


FIGURE
REPORT PG-
00-13-72

AIR CUSHION RESTRAINT SYSTEM-HUMAN RUN
LEFT FOOT

H6571A SLED IMPACT TEST
90-116-016
HOLLOWMAN AIR FORCE BASE
A-0 DATA SHE CLASS 600

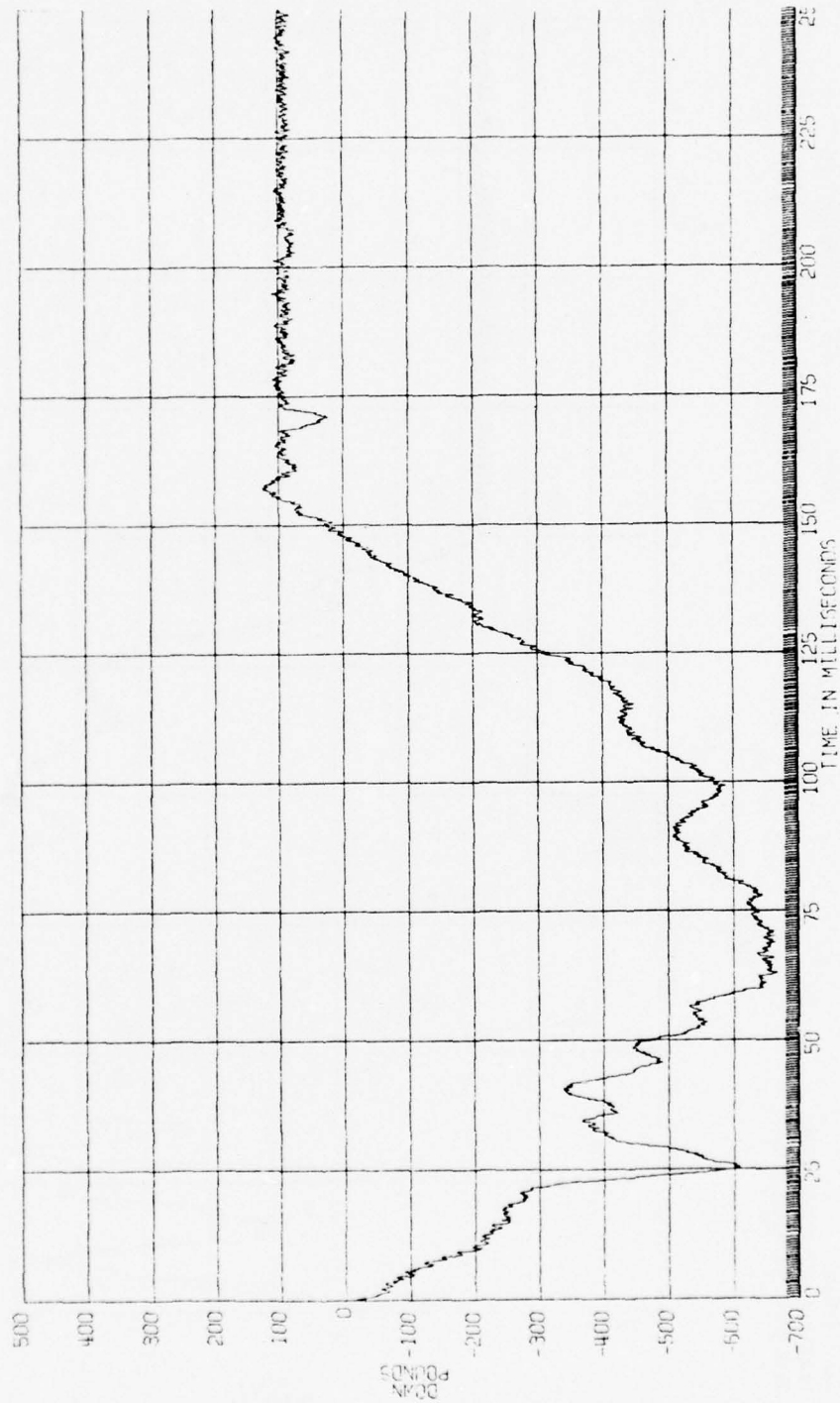
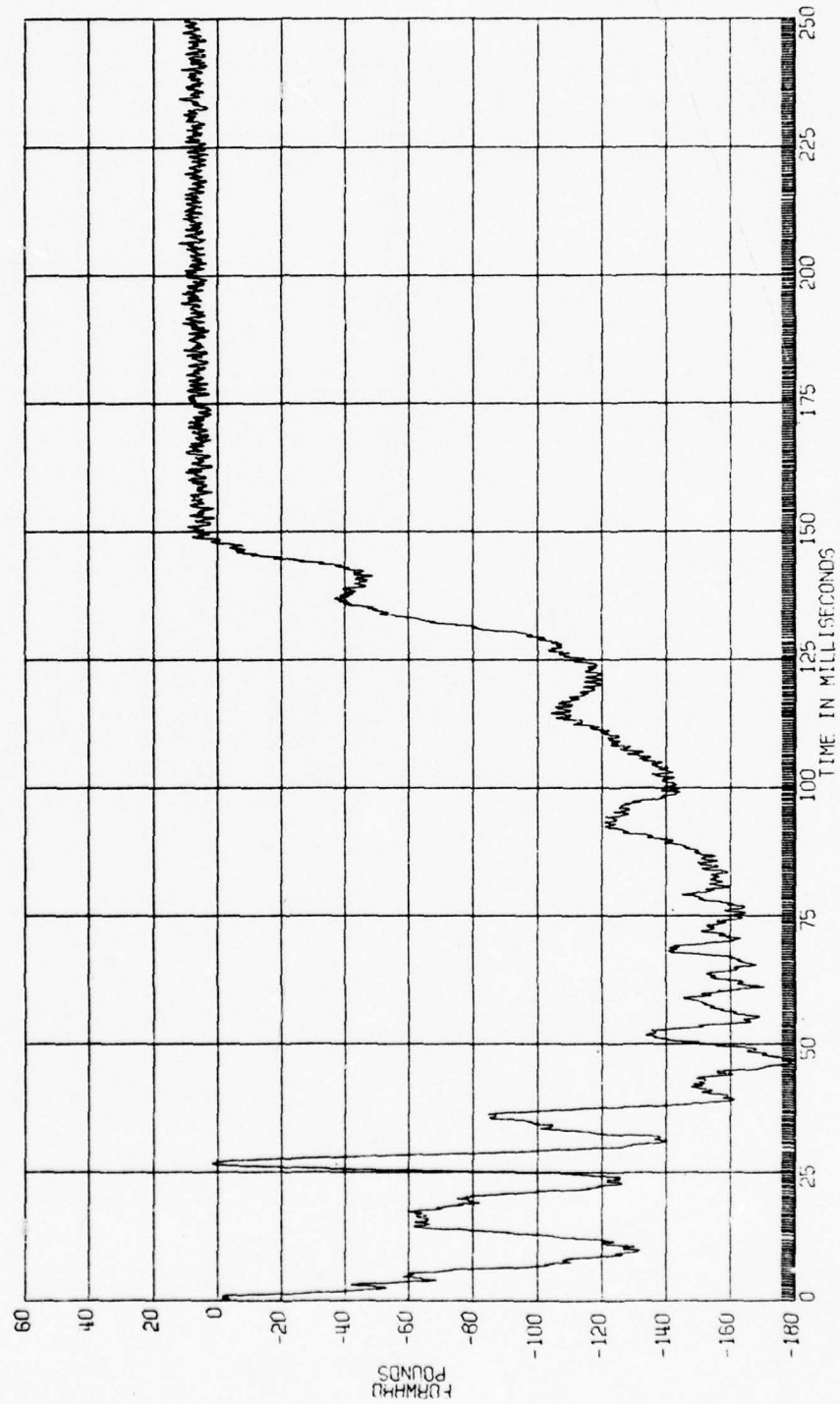


FIGURE
REPORT PC-
09-19-72

AIR CUSHION RESTRAINT SYSTEM-HUMAN RUN
LEFT FOOT

H6571A SLED IMPACT TEST
90-1116-016
HOLLOMAN AIR FORCE BASE
A-D DATA SRE CLASS 600



H6571A SLED IMPACT TEST
90-116-016
HOLLOWMAN AIR FORCE BASE
A-D DATA SHE CLASS 000

AIR CUSHION RESTRAINT SYSTEM-HUMAN RUN
LEFT FOOT

FIGURE
REPORT PG-
09-19-72

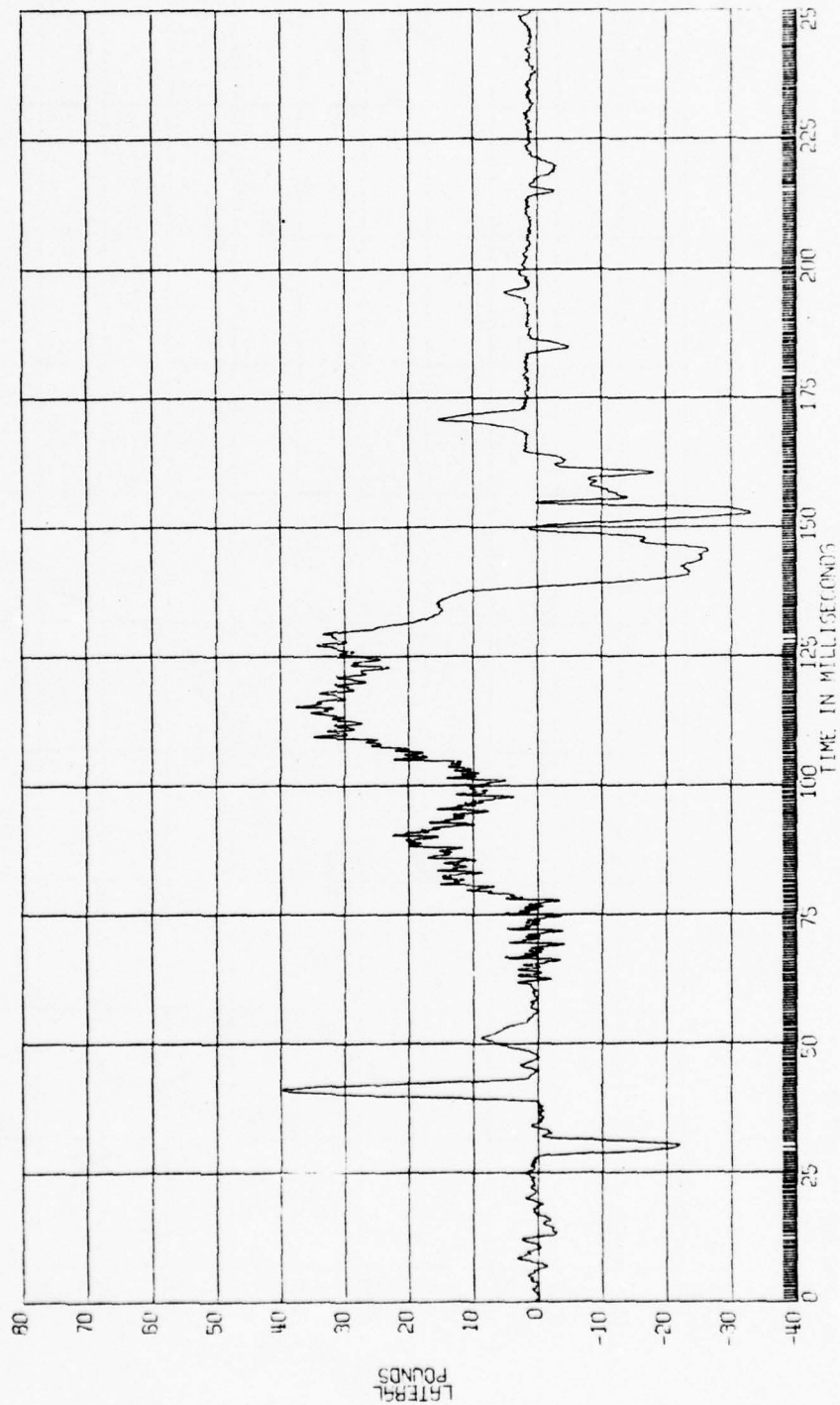
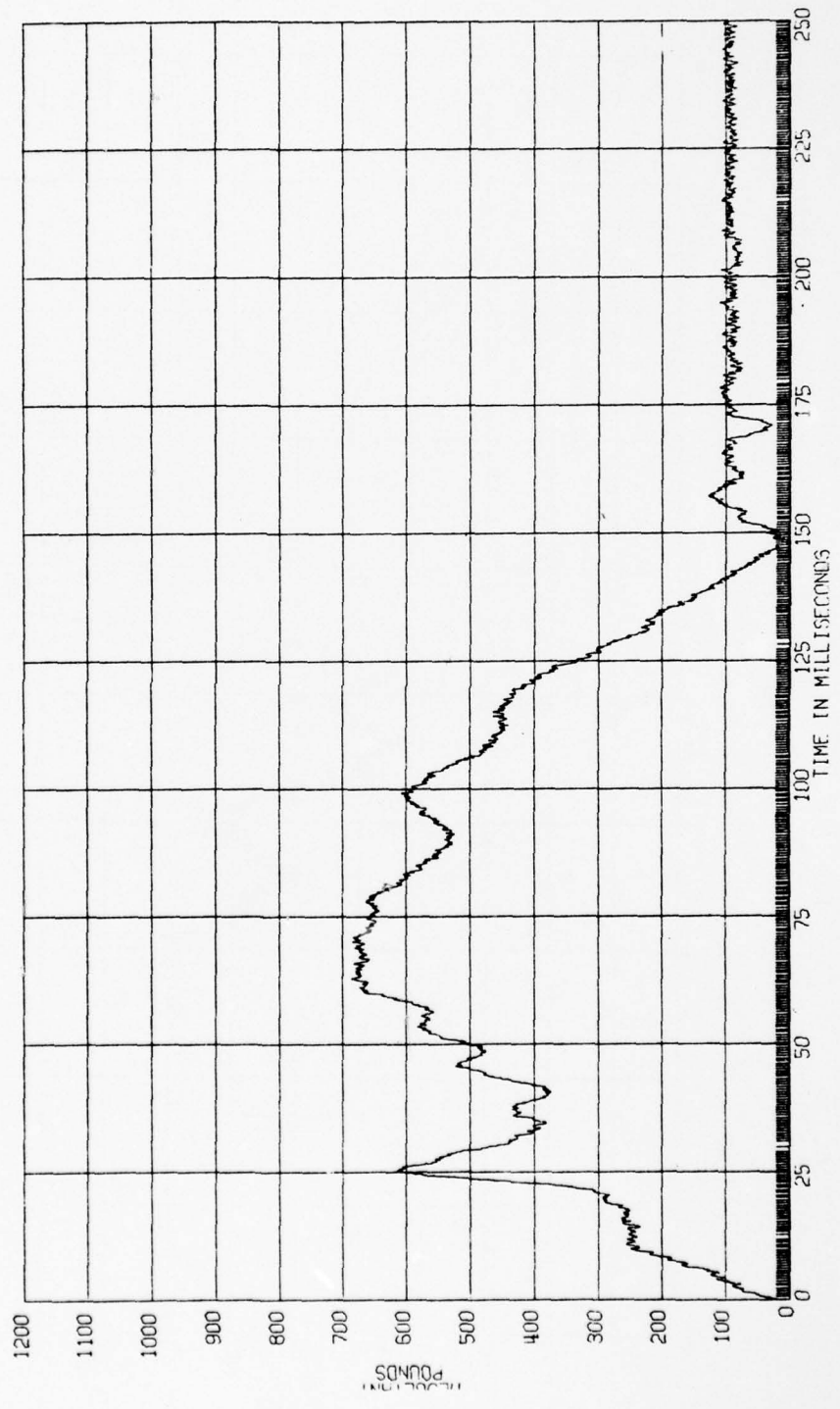


FIGURE
REPORT PG-
09-19-72

AIR CUSHION RESTRAINT SYSTEM-HUMAN RUN
LEFT FOOT
LEFT FOOT RESULTANT

H6571A SLED IMPACT TEST
90-116-016
HOLLOWMAN AIR FORCE BASE
A-D DATA SAE CLASS 600



H65714 SLED IMPACT TEST
 90-116-015
 HOLLOWMAN AIR FORCE BASE
 R-D DATA SRE CLASS 500

AIR CUSHION RESTRAINT SYSTEM-HUMAN RUN
 RIGHT FOOT

FIGURE
 REPORT FC-
 09-19-72

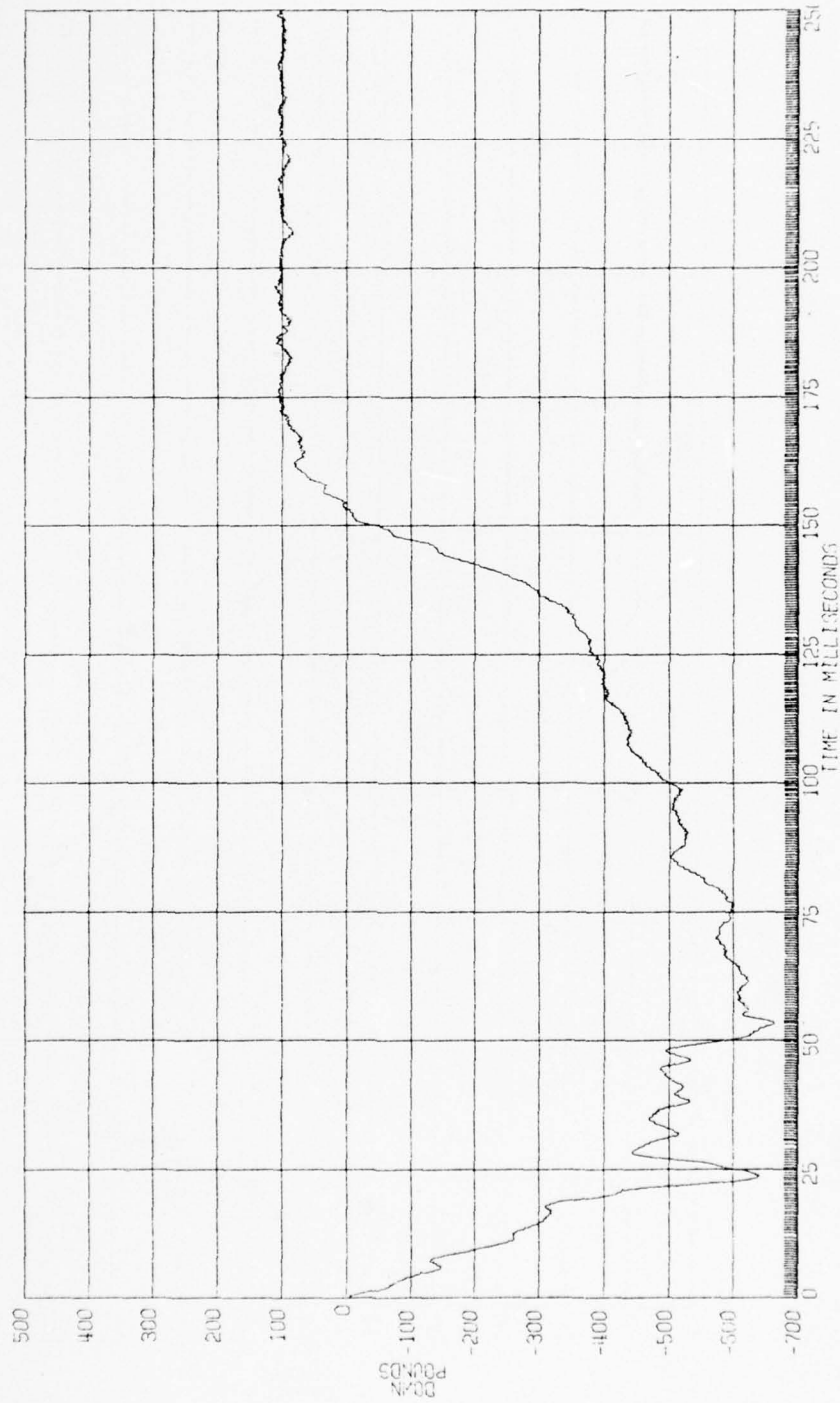
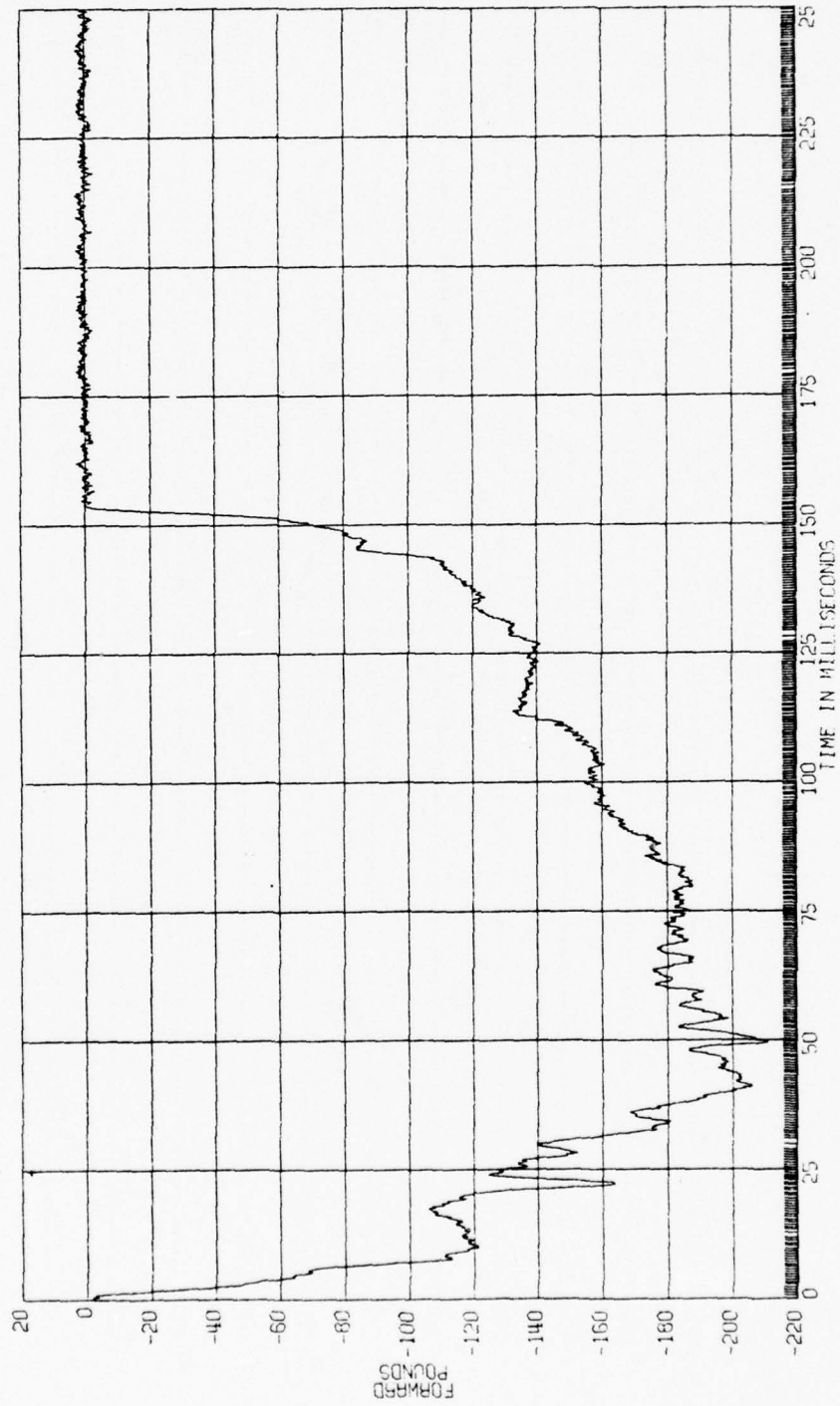


FIGURE
REPORT PG-
09-19-72

AIR CUSHION RESTRAINT SYSTEM-HUMAN RUN
RIGHT FOOT

H6571A SLED IMPACT TEST
90-116-016
HOLLOWMAN AIR FORCE BASE
A-D DATA SHE CLASS 600



H55716 SLED IMPACT TEST
90-115-015
HOLLOW-4N AIR FORCE PAGE
R-0 DATA SHEET CLASS C-00

AIR CUSHION RESTRAINT SYSTEM-HUMAN RUN
RIGHT

FIGURE
REPORT PG-
09-10-72

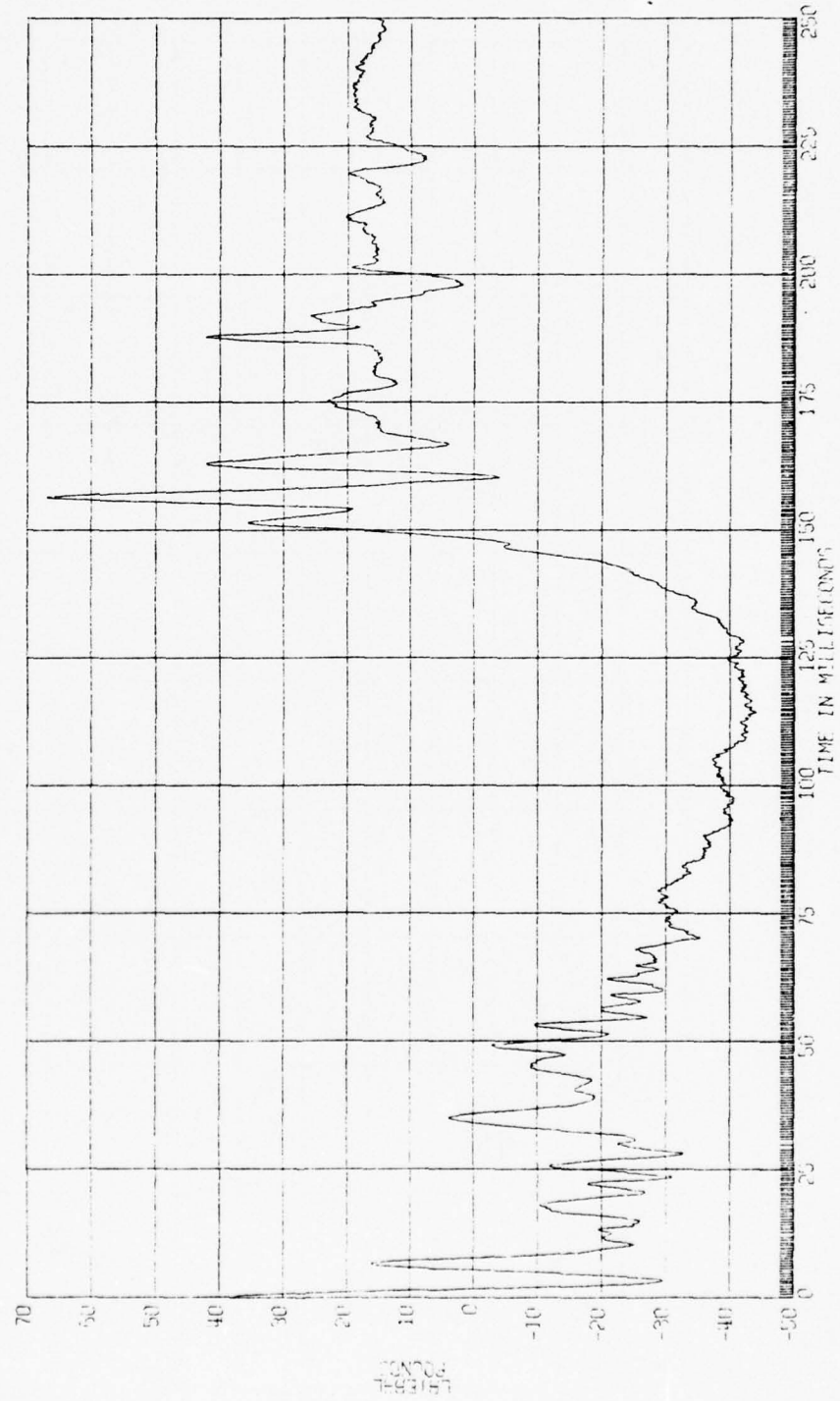


FIGURE
REPORT PG-
09-19-72

AIR CUSHION RESTRAINT SYSTEM-HUMAN RUN

RIGHT FOOT RESULTANT

H6571A SLED IMPACT TEST
90-116-016
HOLLOMAN AIR FORCE BASE
A-D DATA SHE CLASS 600

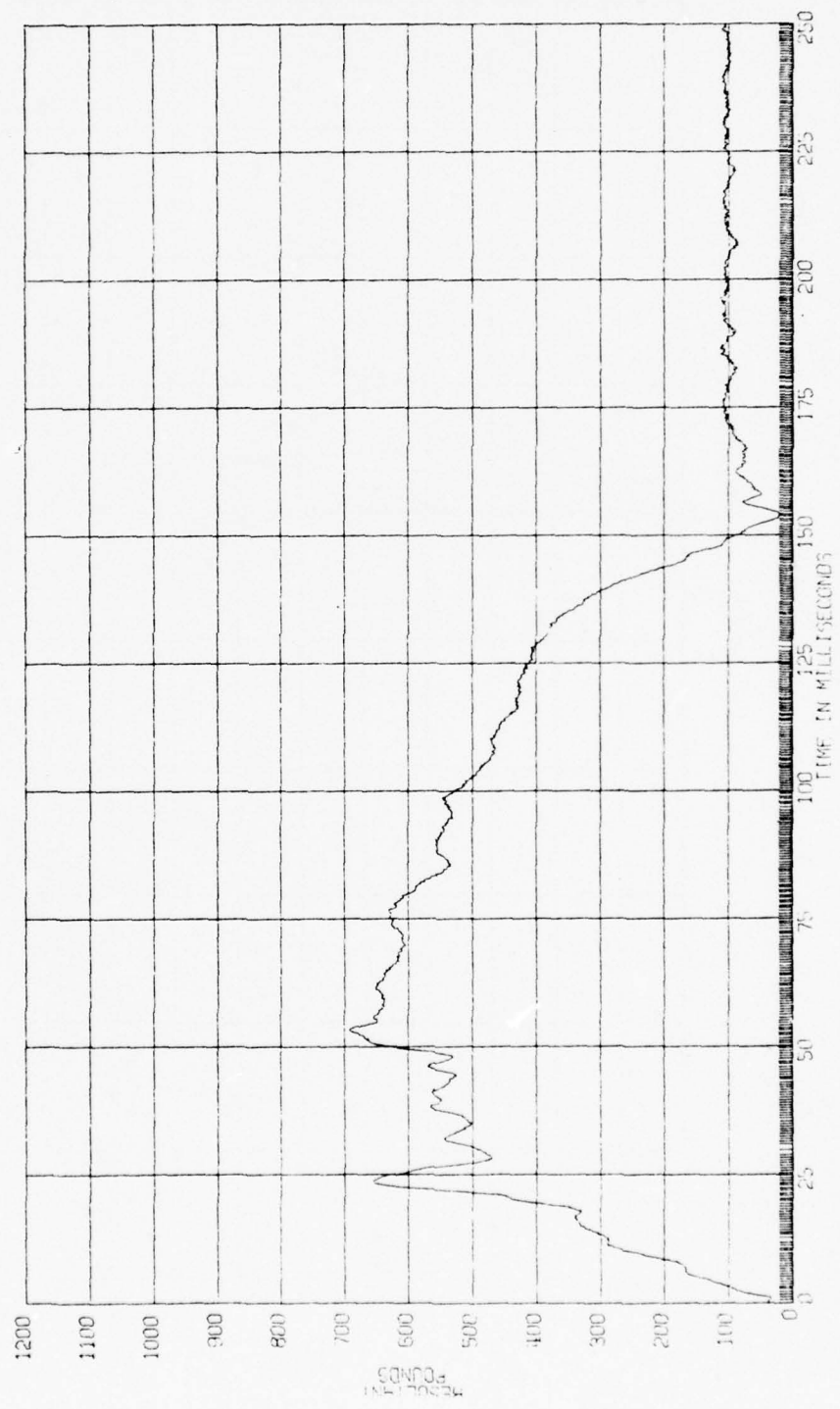


FIGURE
REPORT PC-
09-19-72

AIR CUSHION RESTRAINT SYSTEM-HUMAN RUN
SLED X-1

H6572A SLED IMPACT TEST
90-115-016
HOLLAND AIR FORCE BASE
A-D DATA SAE CLASS 60

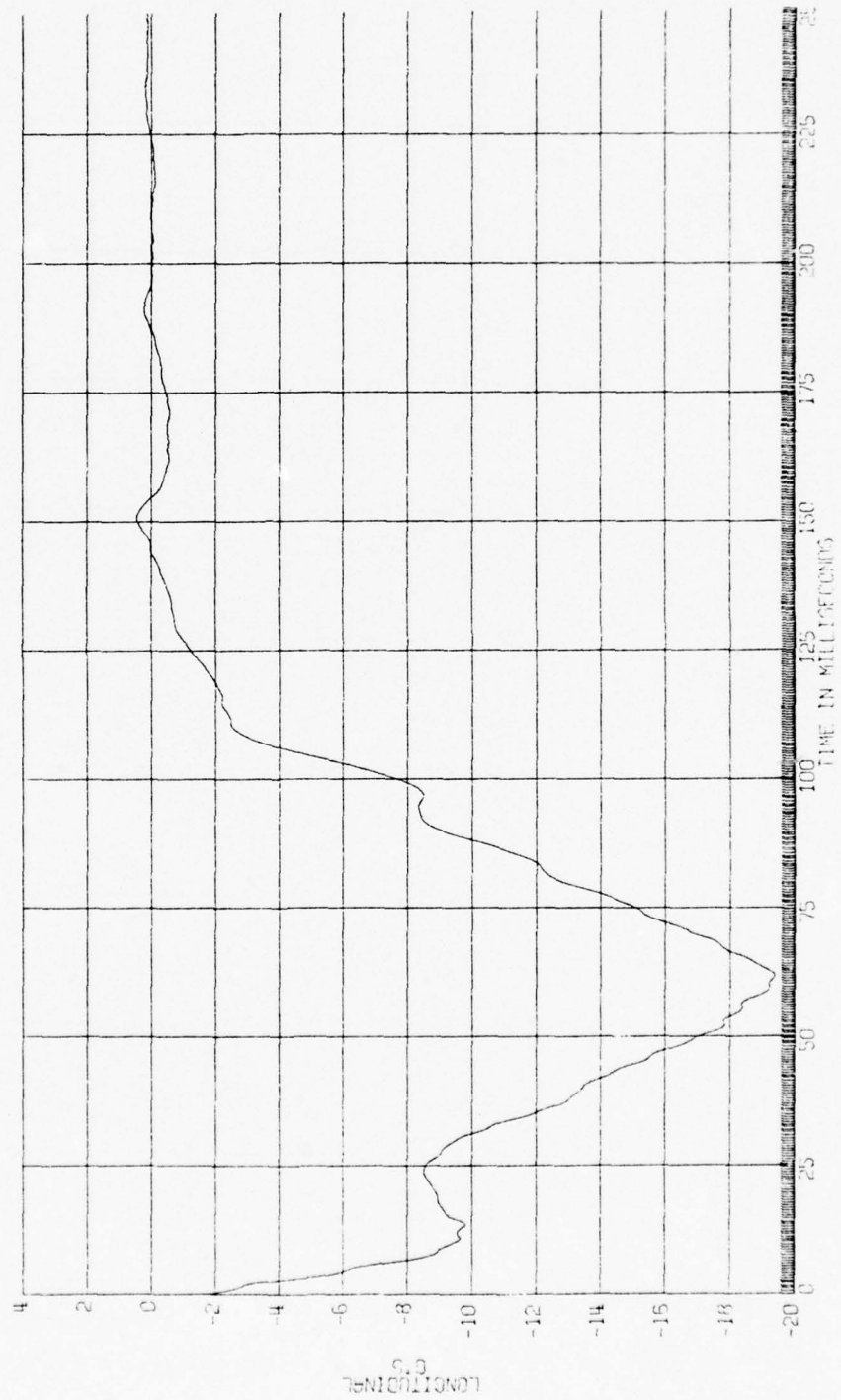
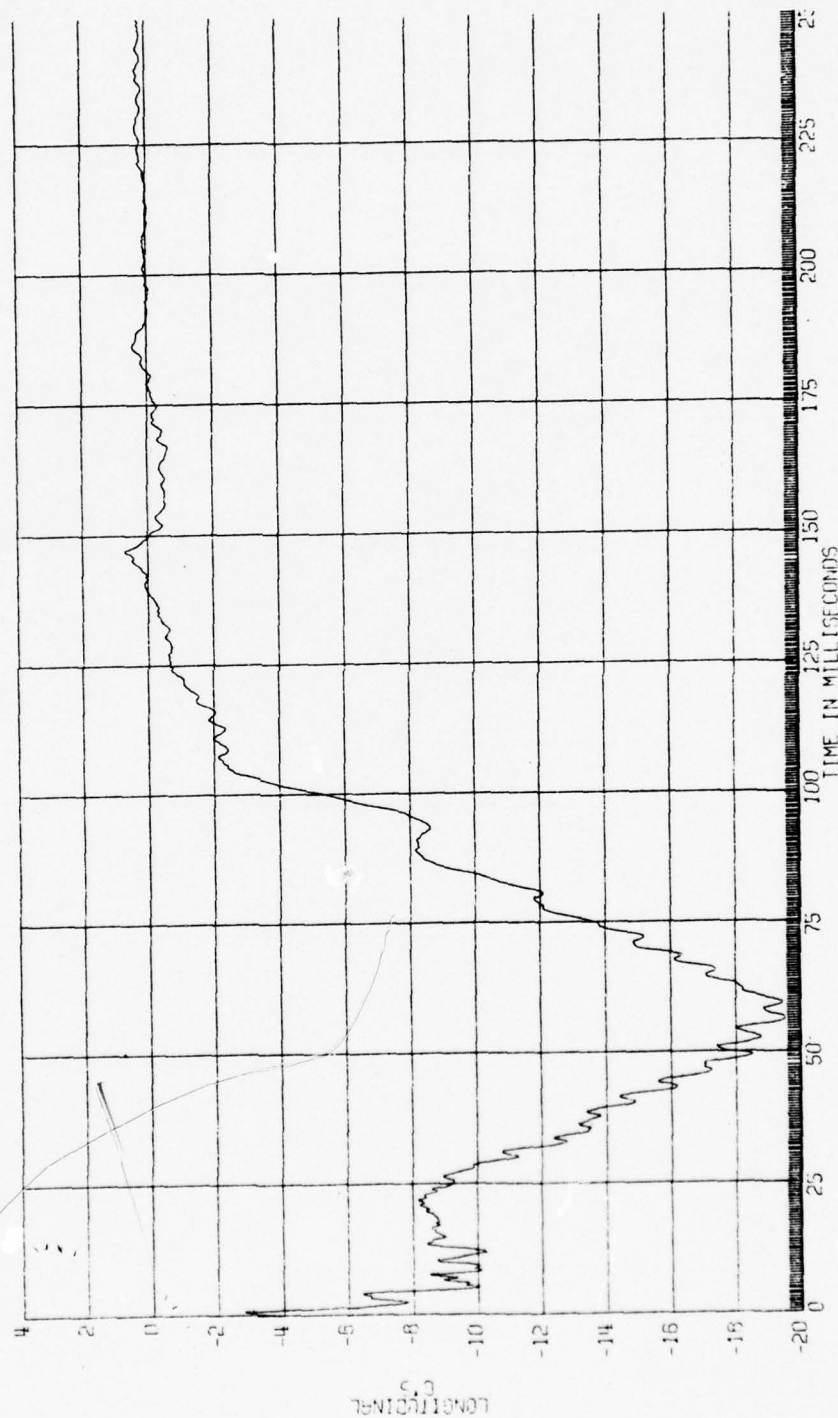


FIGURE
REPORT PG-
09-19-72

AIR CUSHION RESTRAINT SYSTEM-HUMAN RUN
SLED X-2

H6572R SLED IMPACT TEST
90-116-016
HOLLOMAN AIR FORCE BASE
A-D DATA SAE CLASS 60



H65728 SLID IMPACT TEST
 90-116-016
 HOLLOWMAN AIR FORCE BASE
 A-D DATA SAE CLASS 180

AIR CUSHION RESTRAINT SYSTEM-HUMAN RUN
 CHEST ACCEL.

FIGURE
 REPORT PG -
 09-19-72

S.I. AT 250 MS = 210

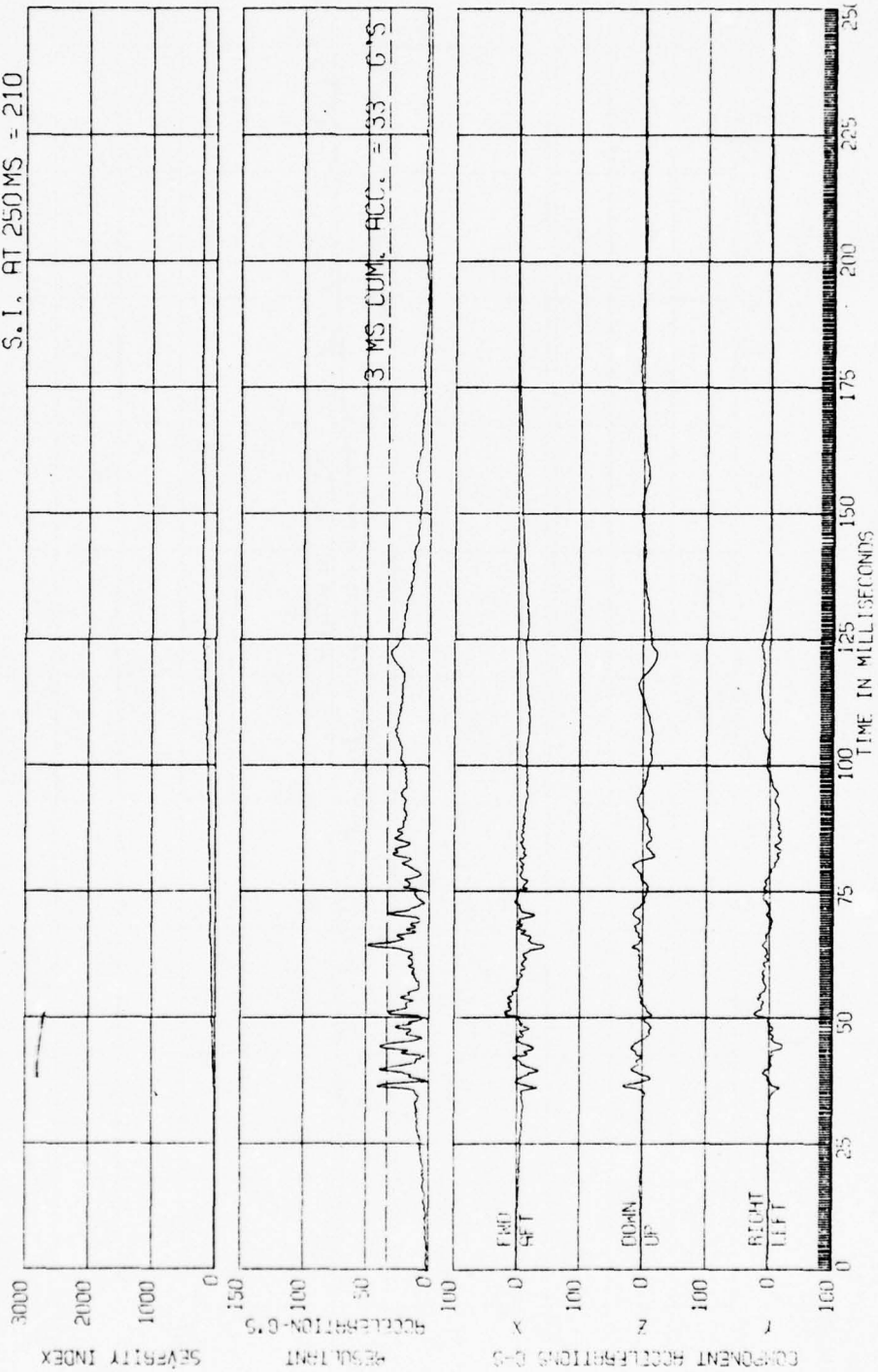
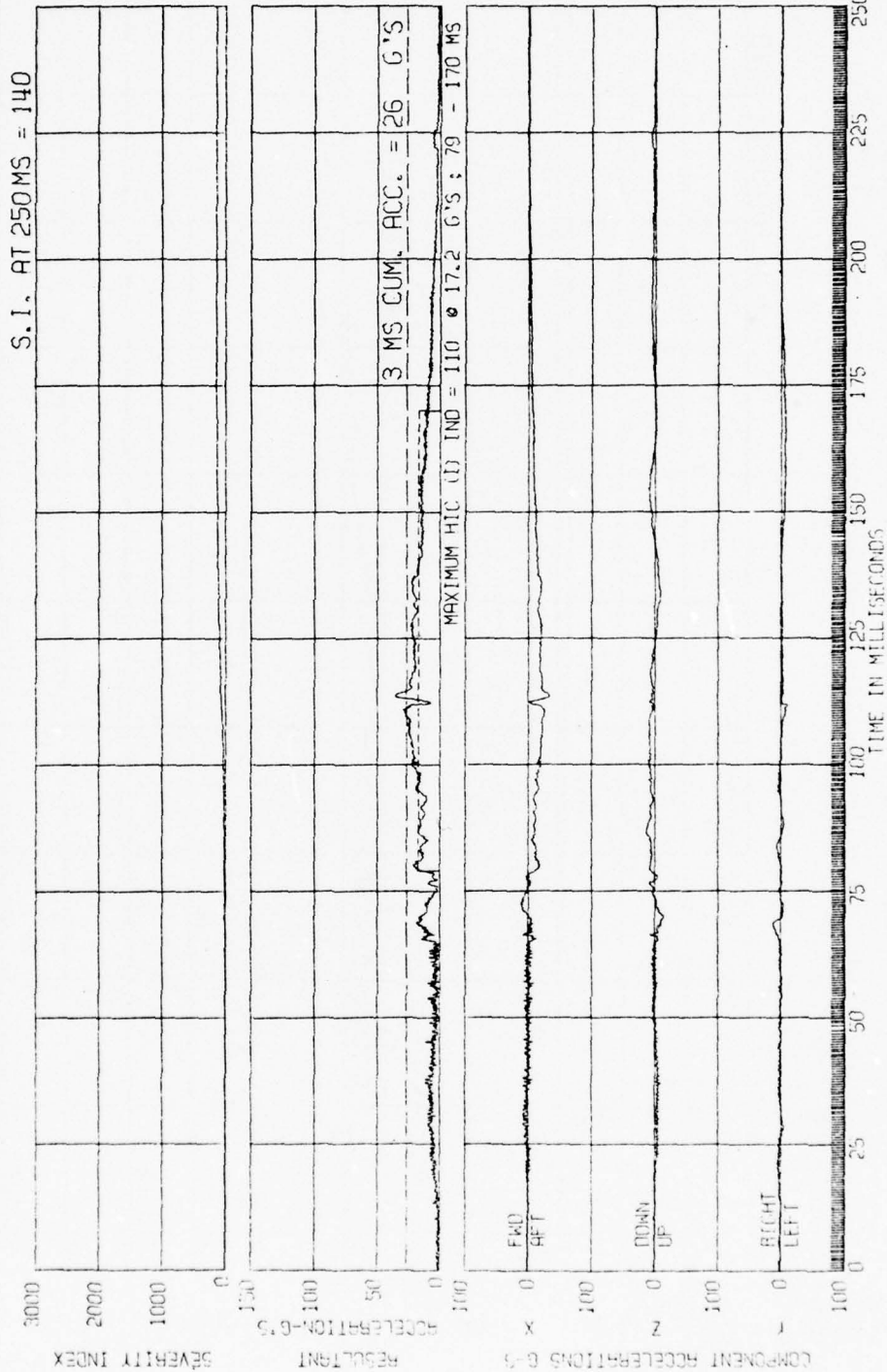


FIGURE
REPORT PG-
09-19-72

AIR CUSHION RESTRAINT SYSTEM-HUMAN RUN
HEAD ACCEL.

H6572B SLED IMPACT TEST
90-115-015
HOLLOMAN AIR FORCE BASE
A-D DATA



H6572B SLED IMPACT TEST
 90-116-016
 HOLLOWMAN AIR FORCE BASE
 A-D DATA

AIR CUSHION RESTRAINT SYSTEM-HUMAN RUN
 MOUTH

FIGURE
 REPORT PG-
 09-19-72

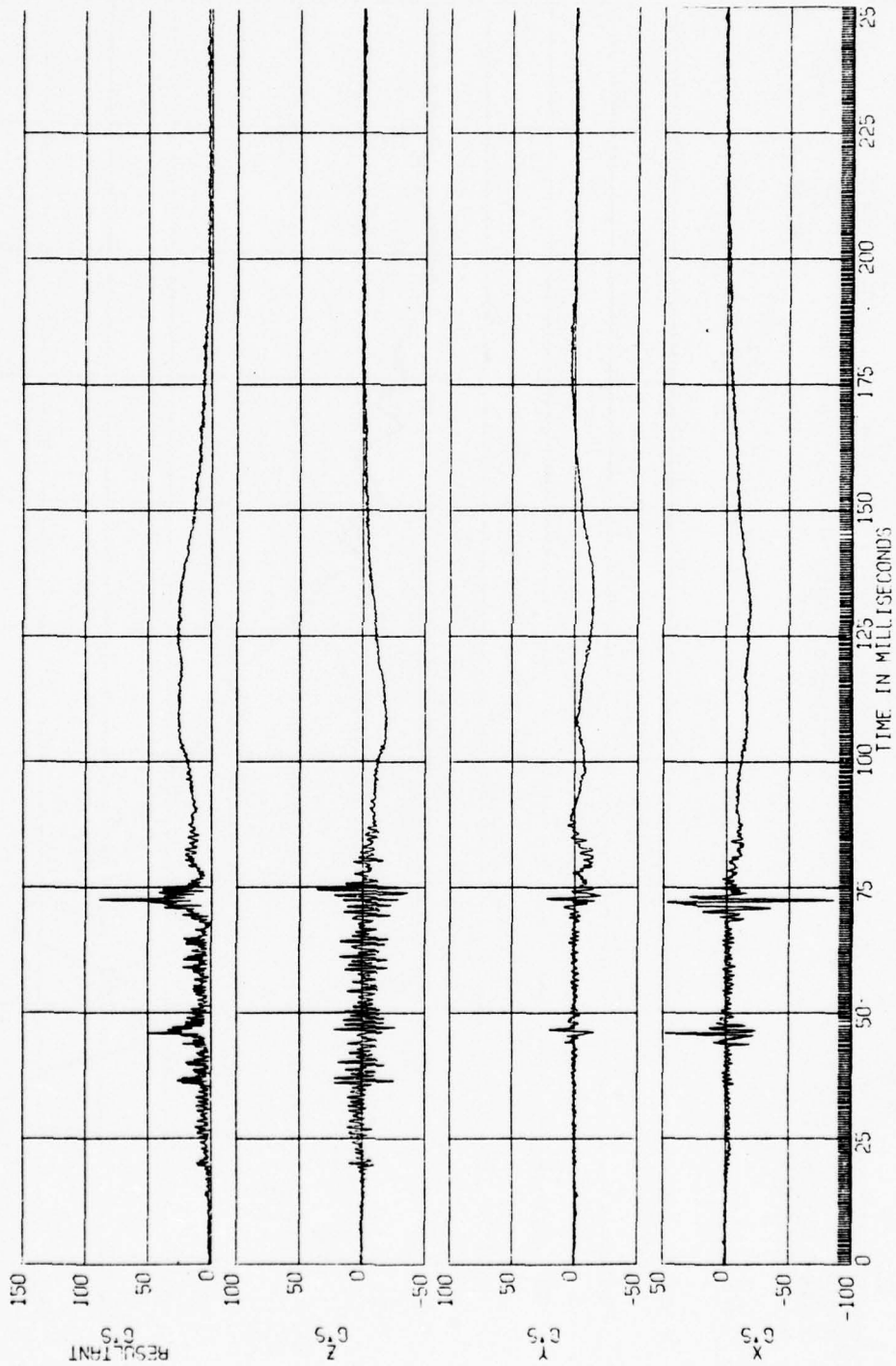
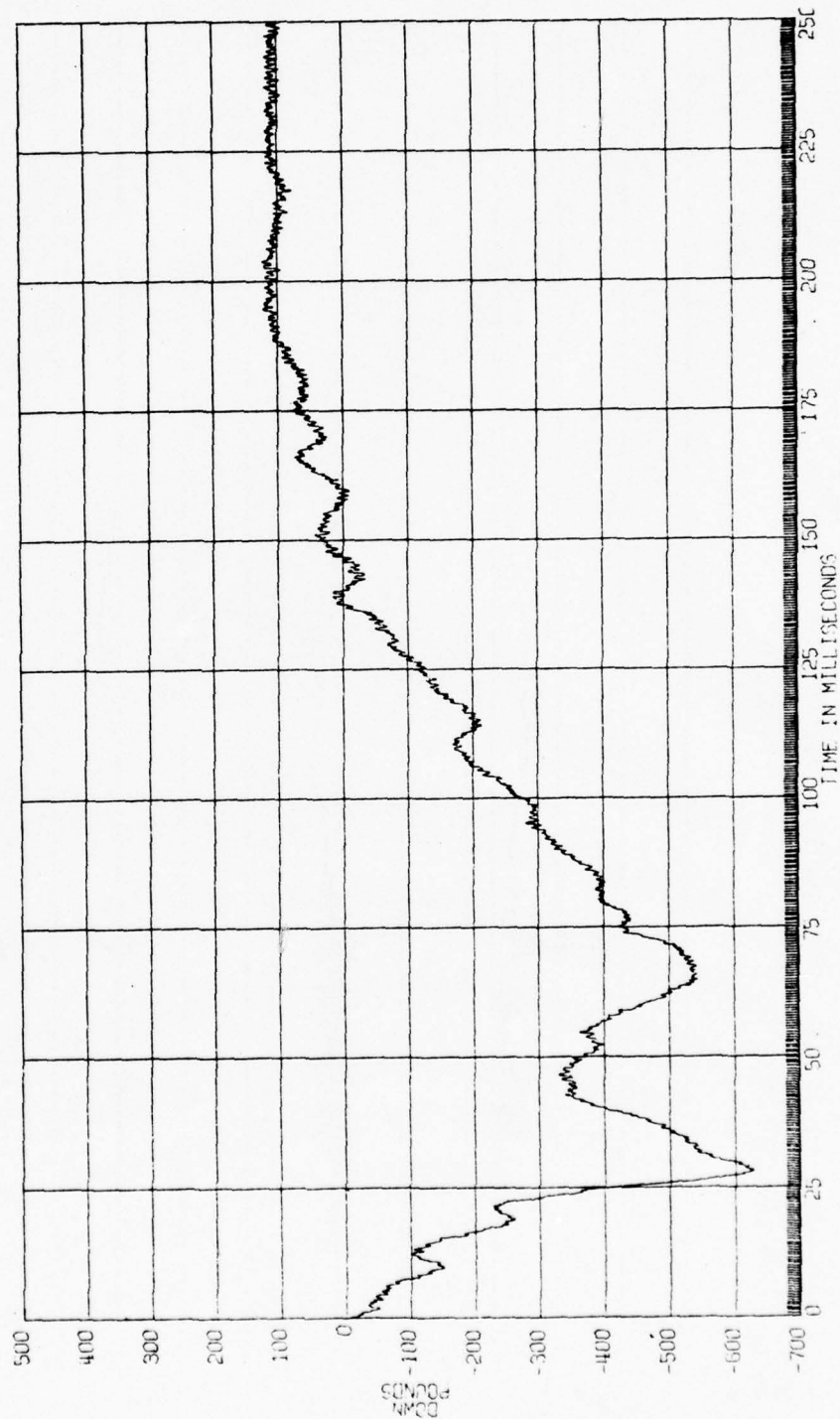


FIGURE
REPORT PG-
09-19-72

AIR CUSHION RESTRAINT SYSTEM-HUMAN RUN
LEFT FOOT

H6572A SLED IMPACT TEST
90-116-016
HOLLAND AIR FORCE BASE
A-D DATA SHE CLASS 600



H6572A SLED IMPACT TEST
90-116-016
HOLLOWMAN AIR FORCE BASE
A-0 DATA SHE CLASS 600

AIR CUSHION RESTRAINT SYSTEM-HUMAN RUN
LEFT FOOT

FIGURE
REPORT PG-
09-19-72

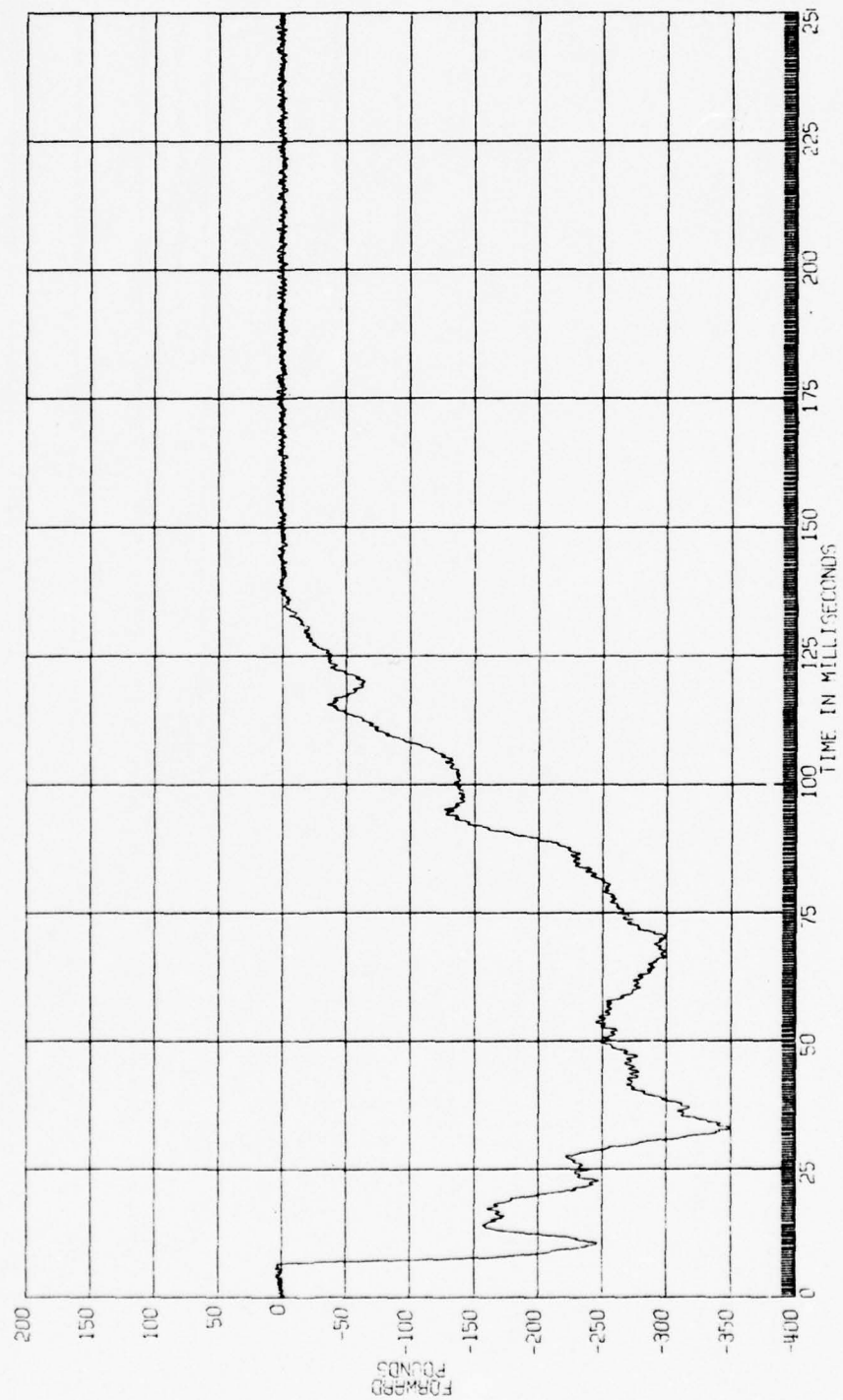
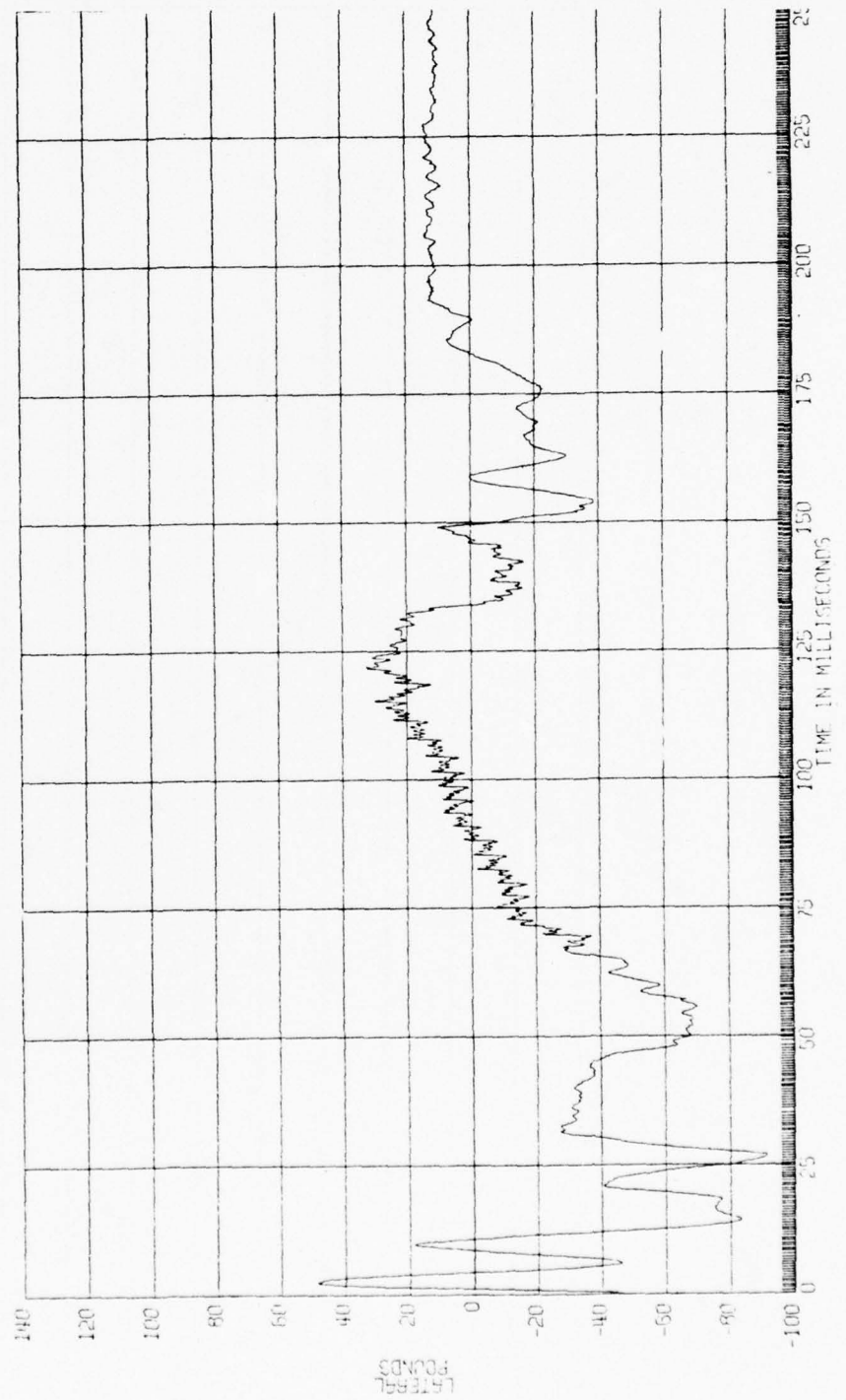


FIGURE
REPORT PG-
09-19-72

AIR CUSHION RESTRAINT SYSTEM-HUMAN RUN
LEFT FOOT

H51724 SLED IMPACT TEST
90-115-016
HOLLOWMAN AIR FORCE BASE
A-D DATA SHE CL455 600



H6572A SLED IMPACT TEST
90-116-016
HOLLOWMAN AIR FORCE BASE
A-D DATA SHE CLASS 600

AIR CUSHION RESTRAINT SYSTEM-HUMAN RUN

LEFT FOOT

LEFT FOOT RESULTANT

FIGURE
REPORT PG-

09-19-72

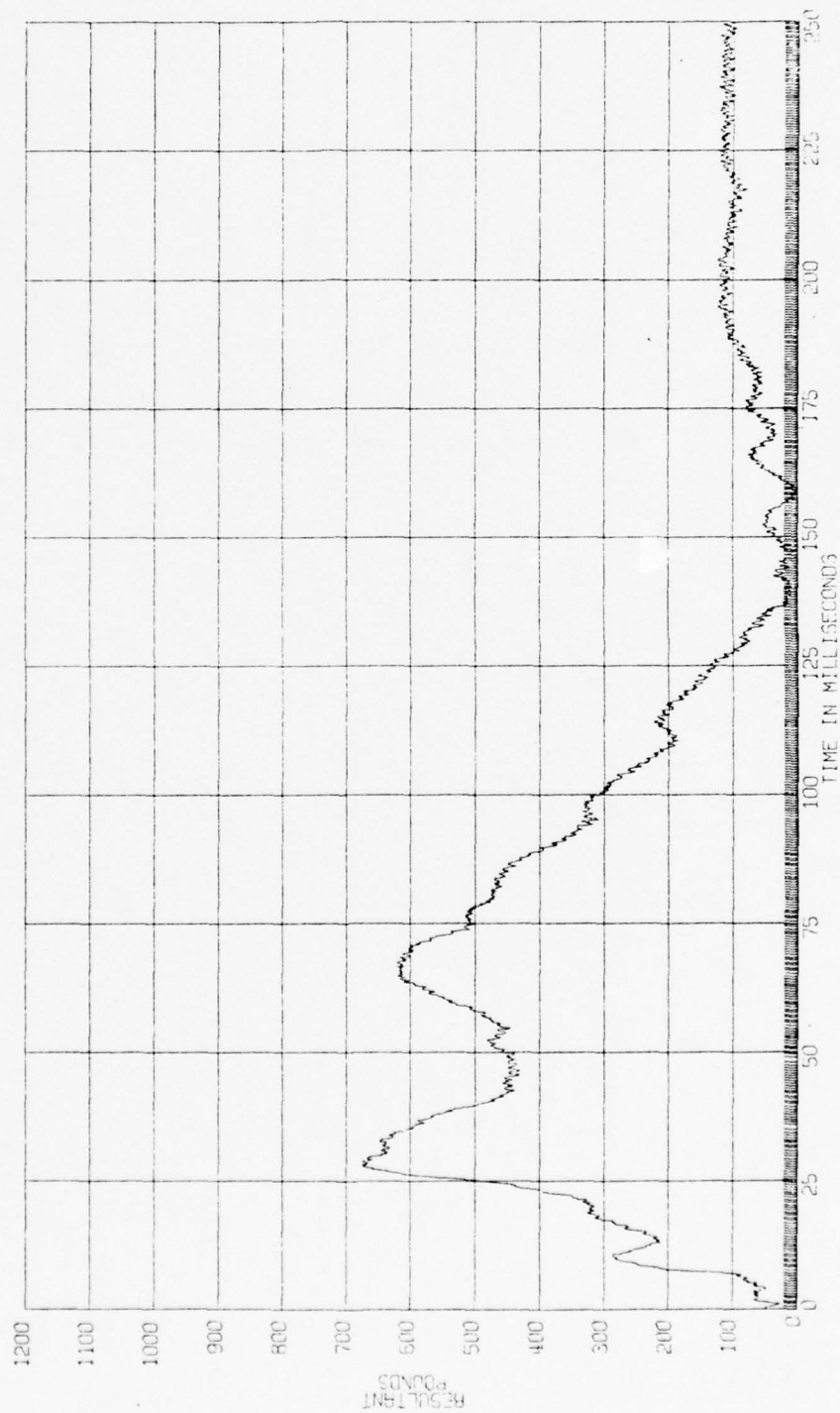


FIGURE
REPORT PG-
09-19-72

AIR CUSHION RESTRAINT SYSTEM-HUMAN RUN
RIGHT FOOT

H6572A SLED IMPACT TEST
90-116-016
HOLLOWMAN AIR FORCE BASE
A-D DATA SHE CLASS 600

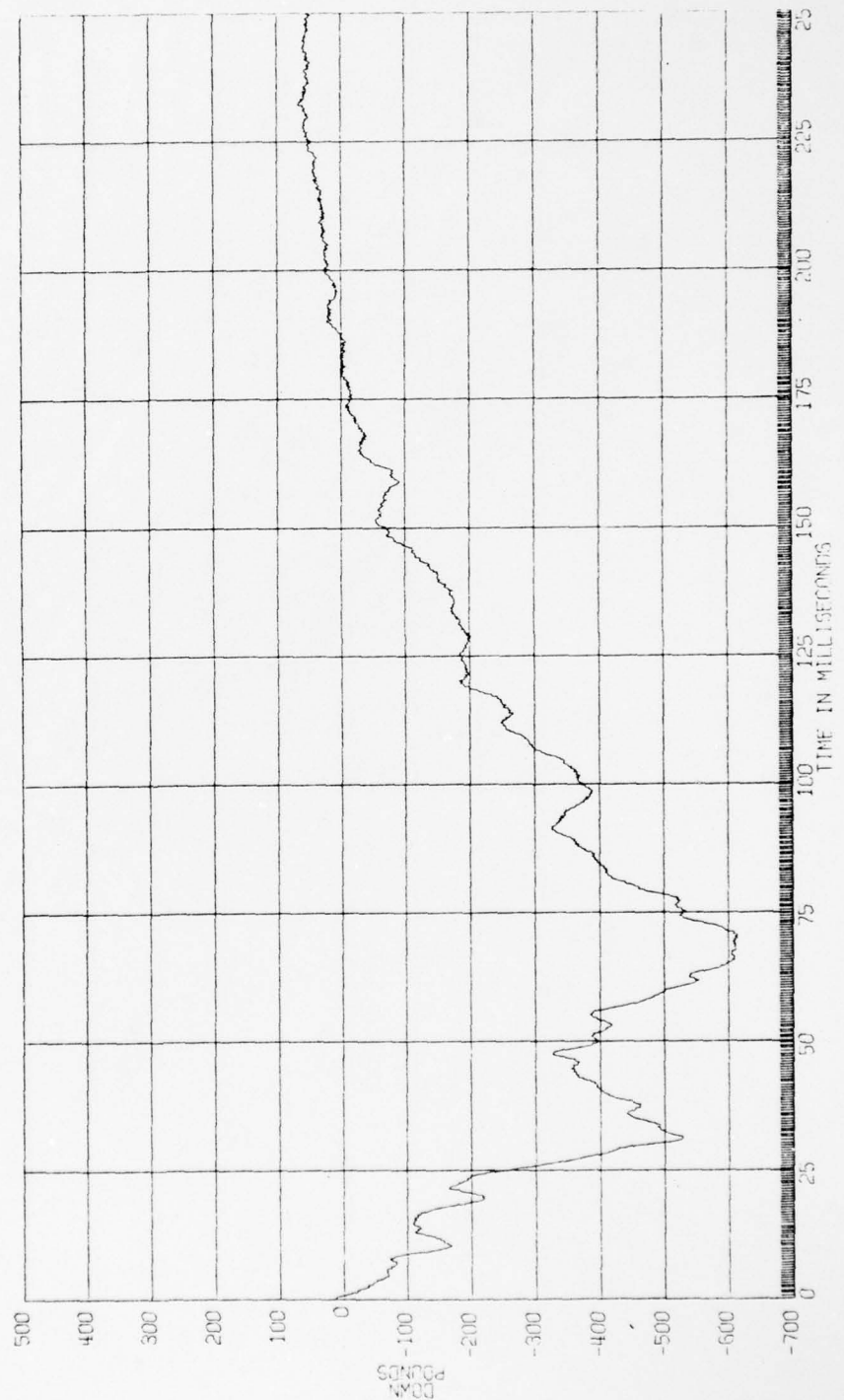


FIGURE
REPORT PG-
09-19-72

AIR CUSHION RESTRAINT SYSTEM-HUMAN RUN
RIGHT FOOT

H65724 SLED IMPACT TEST
90-116-016
HOLLOWMAN AIR FORCE BASE
A-D DATA SAE CLASS 600

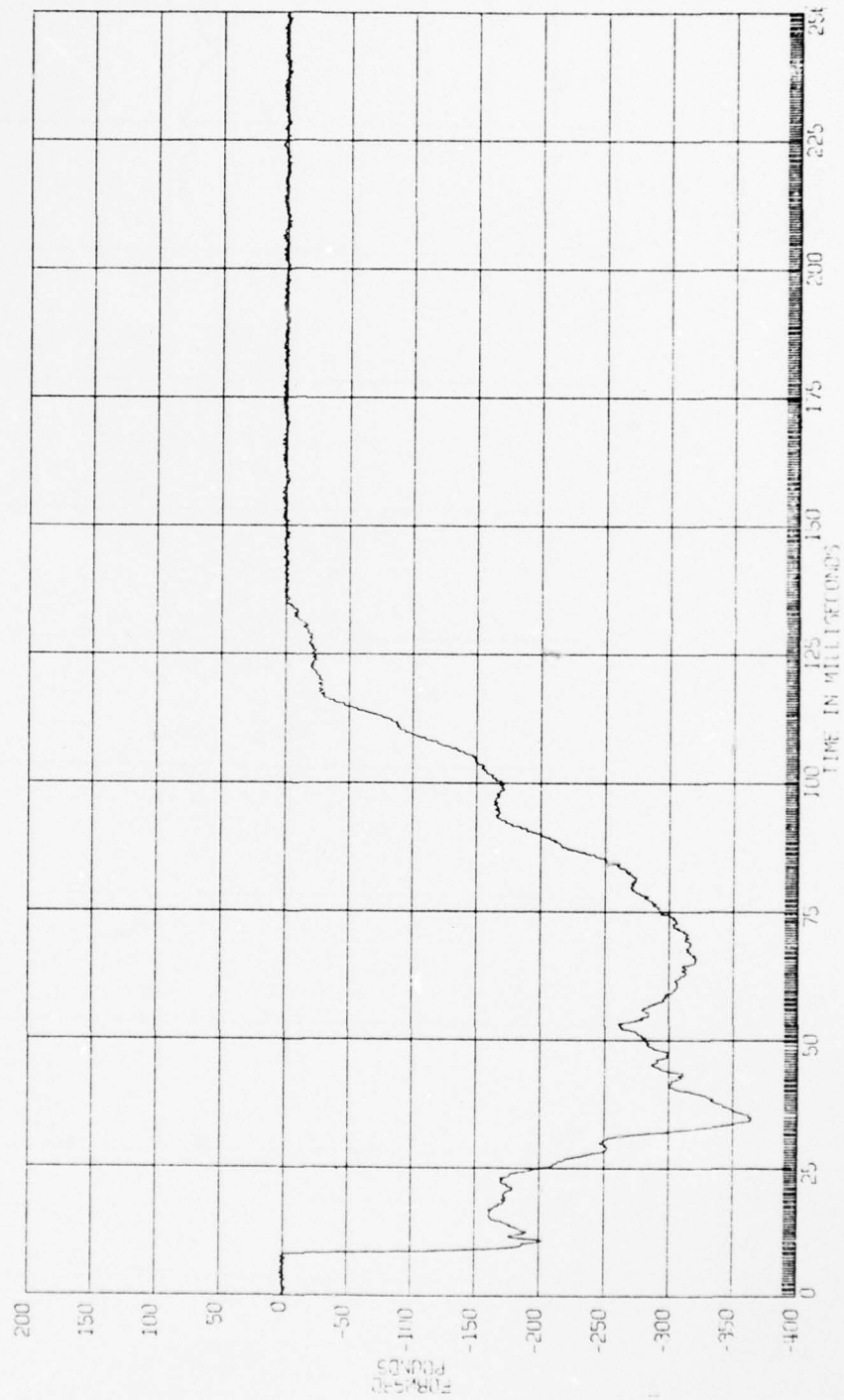


FIGURE
REPORT PG-
09-19-72

AIR CUSHION RESTRAINT SYSTEM-HUMAN RUN
RIGHT

H65724 SLED IMPACT TEST
90-116-016
HOLLOWMAN AIR FORCE BASE
A-D DATA SHE CLASS 500

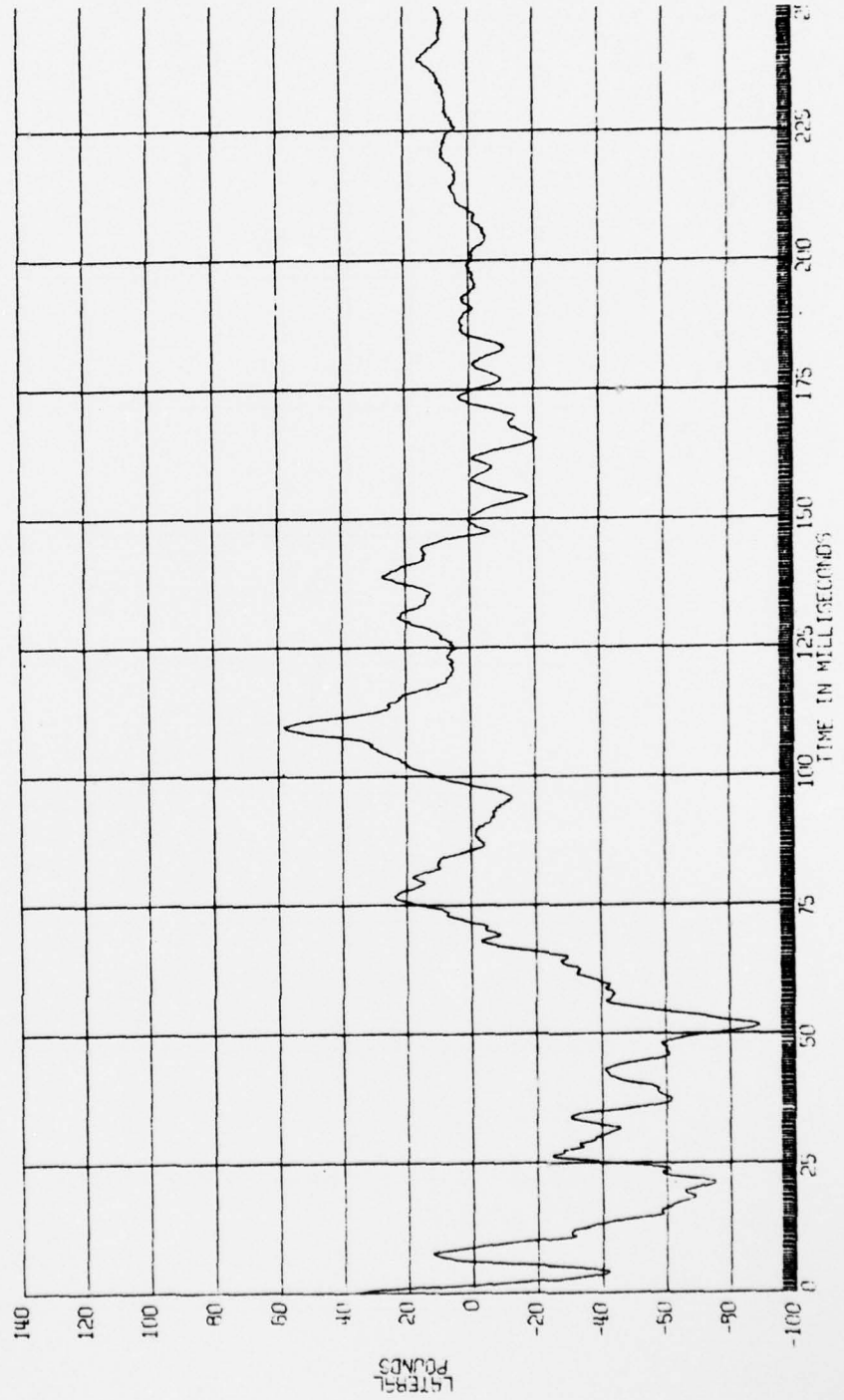


FIGURE
REPORT PG-
09-19-72

AIR CUSHION RESTRAINT SYSTEM-HUMAN RUN

RIGHT FOOT RESULTANT

H6572A SLED IMPACT TEST
90-116-016
HOLLOWMAN AIR FORCE BASE
A-D DATA SHE CLASS 600

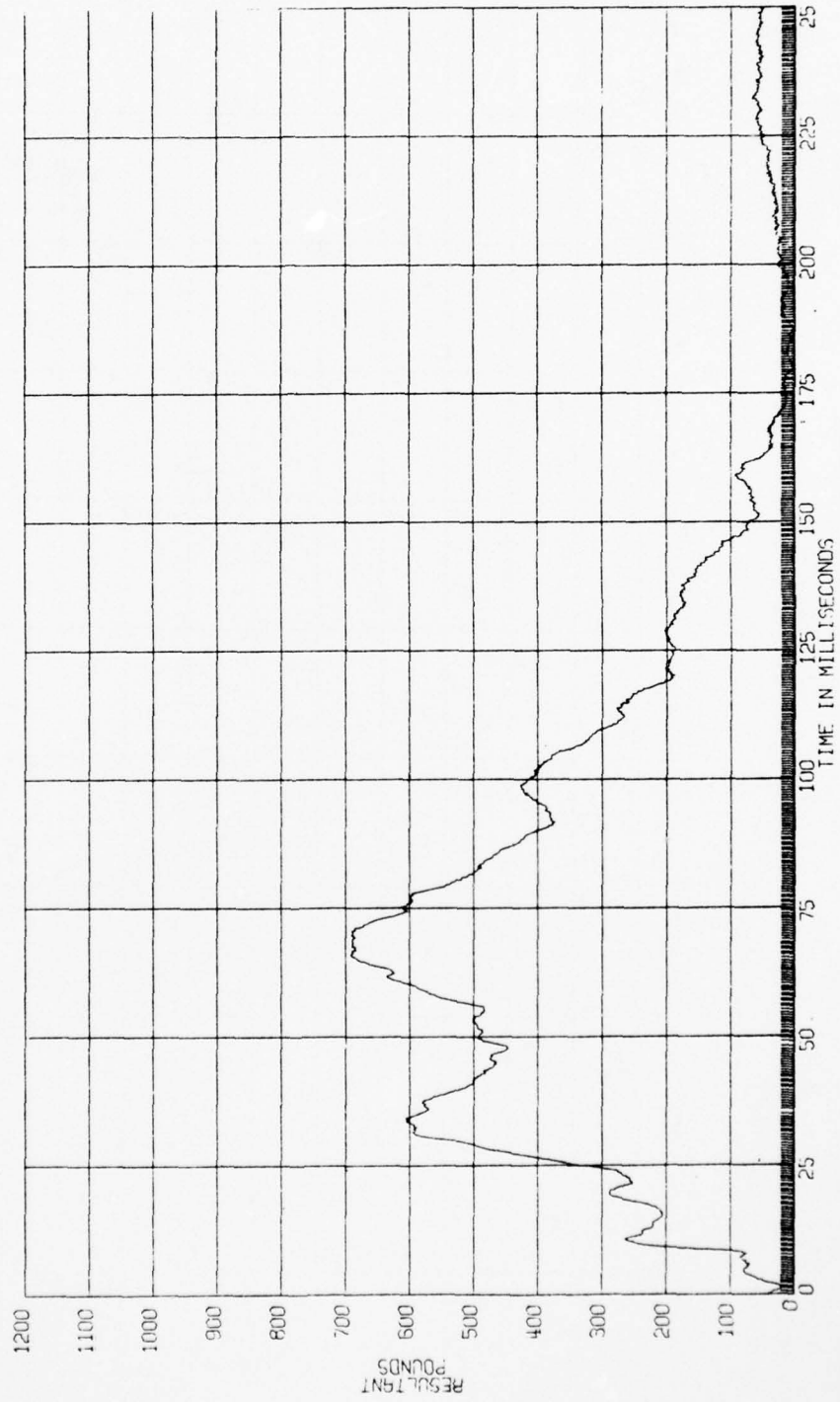
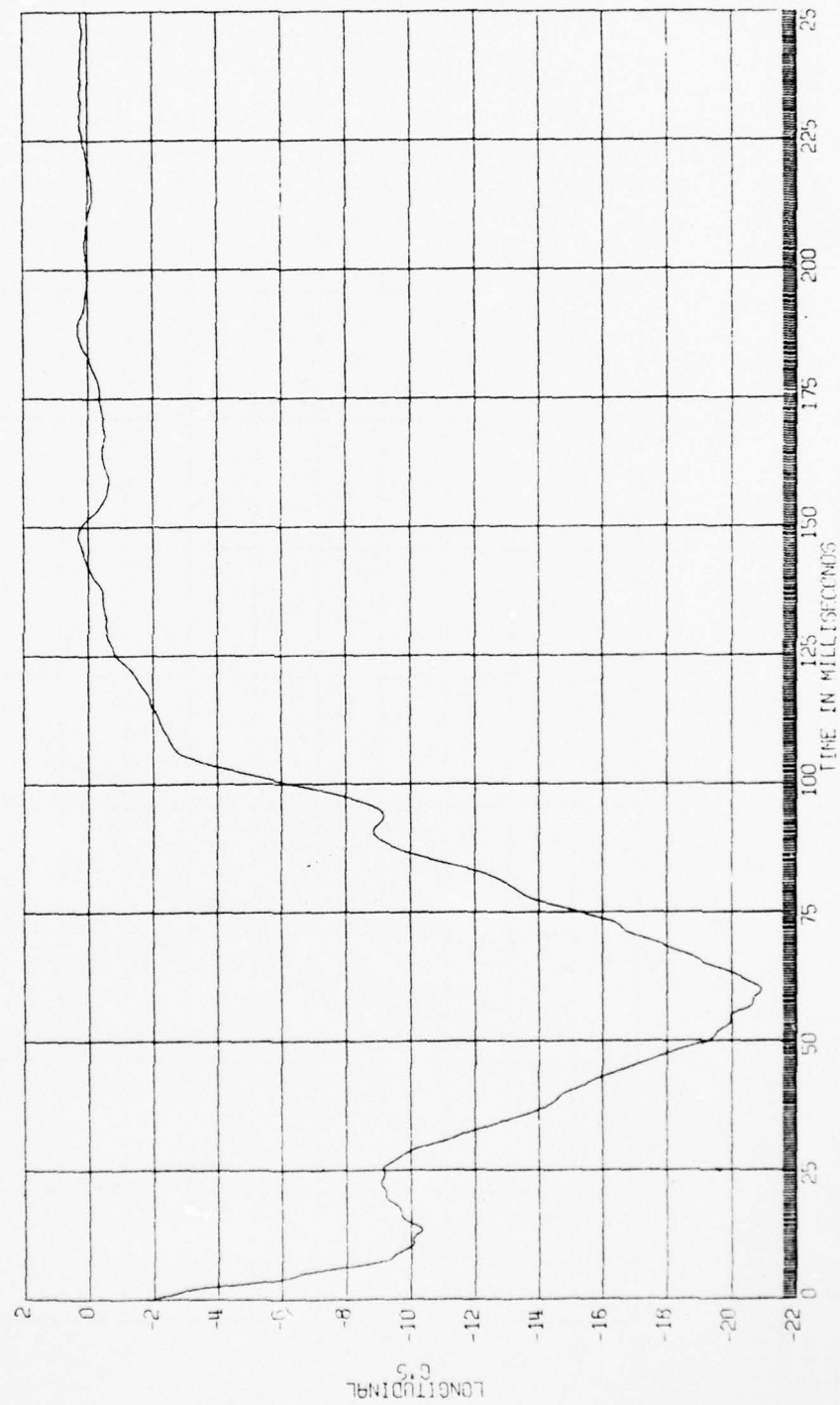


FIGURE
REPORT PC-
09-20-72

AIR CUSHION RESTRAINT SYSTEM-HUMAN RUN
SLED X-1

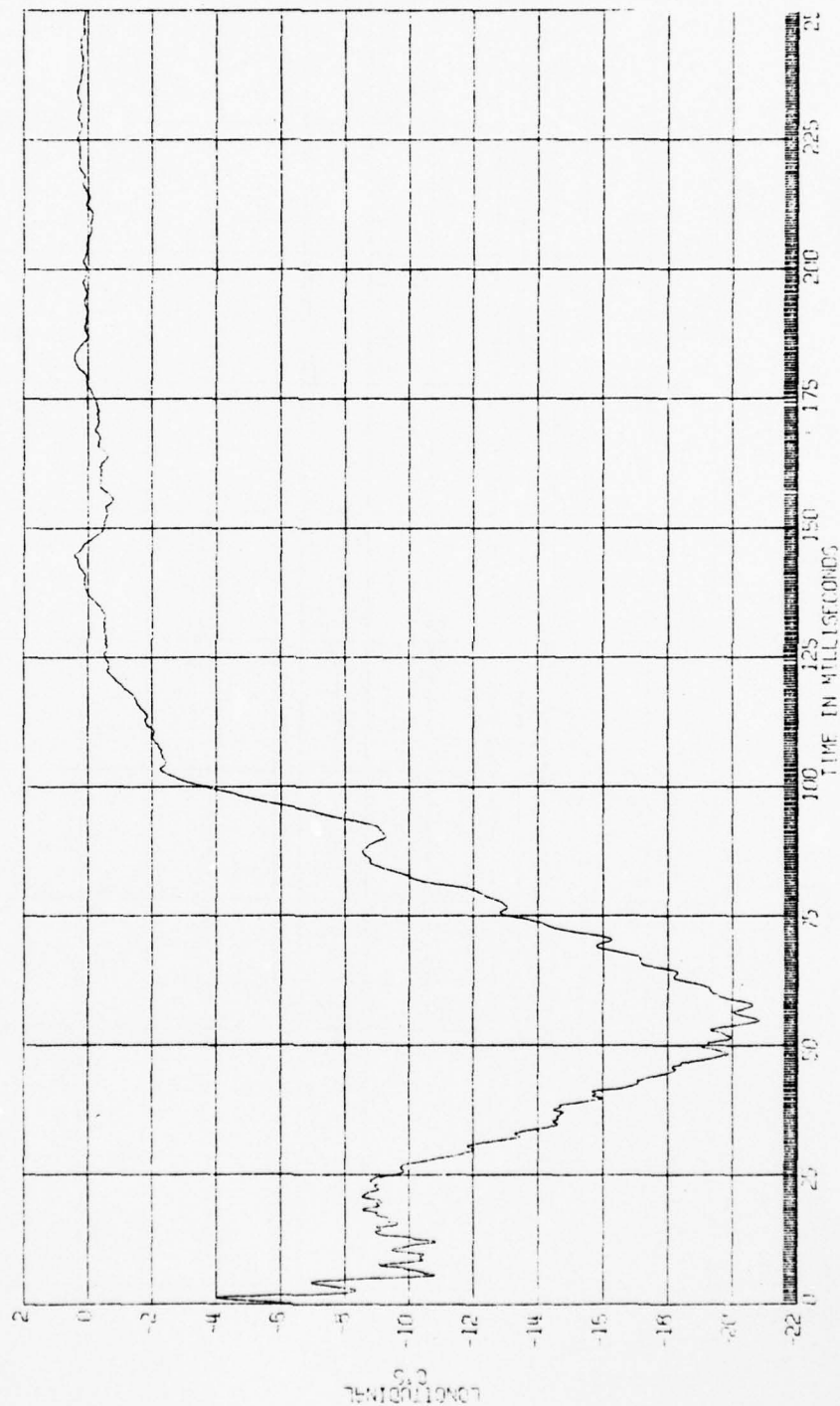
H6571A SLED IMPACT TEST
90-116-016
HOLLOWMAN AIR FORCE BASE
A-D DATA SAE CLASS 60



HRS712 SLED IMPACT TEST
 90-115-015
 HOLLOWMAN AIR FORCE BASE
 A-D DATA SHE CLASS 60

AIR CUSHION RESTRAINT SYSTEM-HUMAN RUN
 SLED X-2

FIGURE
 REPORT FC-
 09-20-72

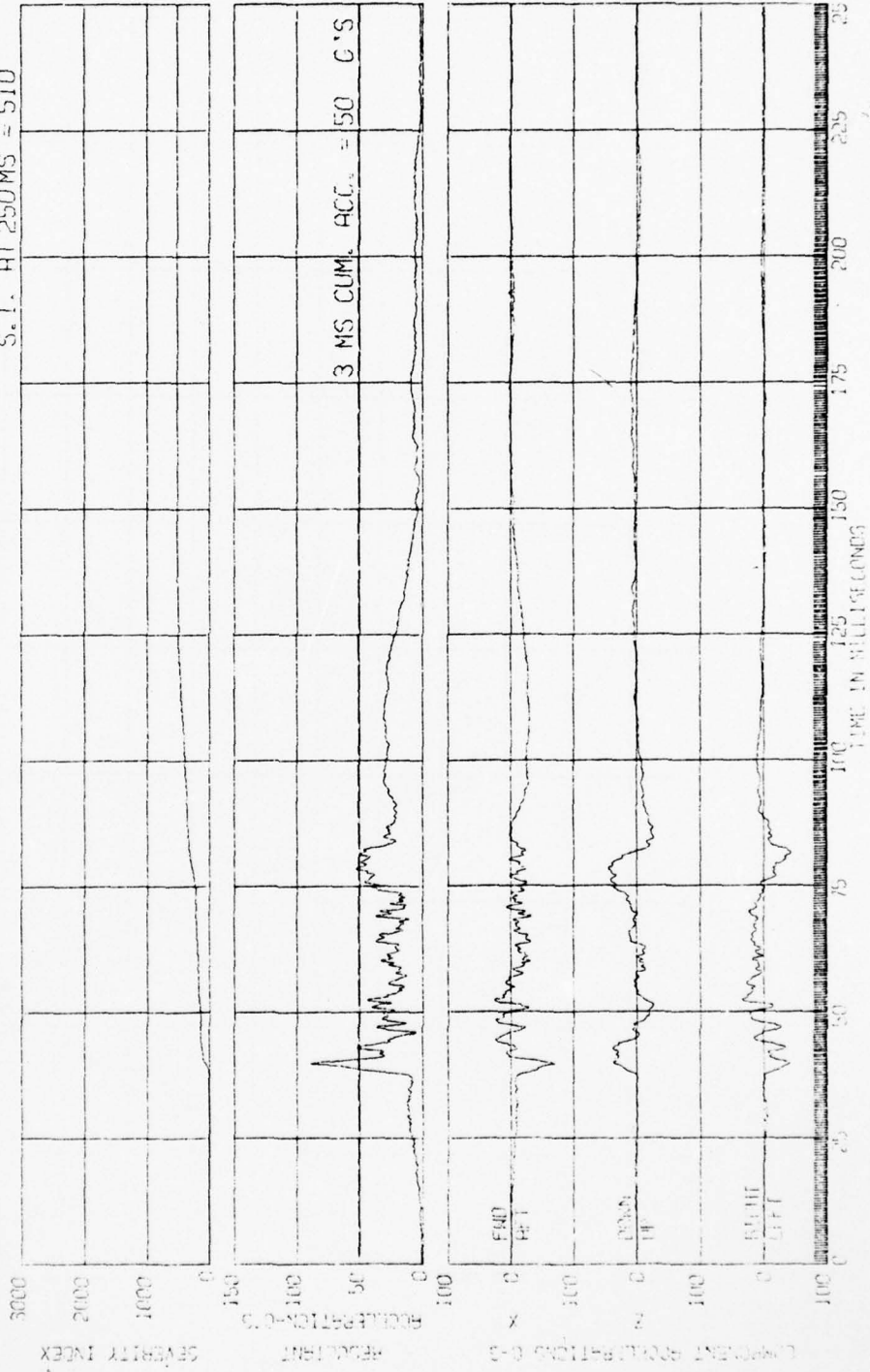


HSC24B SLED IMPACT TEST
 30-116-016
 HOLLOWMAN AIR FORCE BASE
 H-O DATA 54E CLASS 180

AIR CUSHION RESTRAINT SYSTEM-HUMAN RUN
 CHEST ACCEL.

FIGURE
 REPORT NO.
 09-20-72

S.I. AT 250 MS = 510

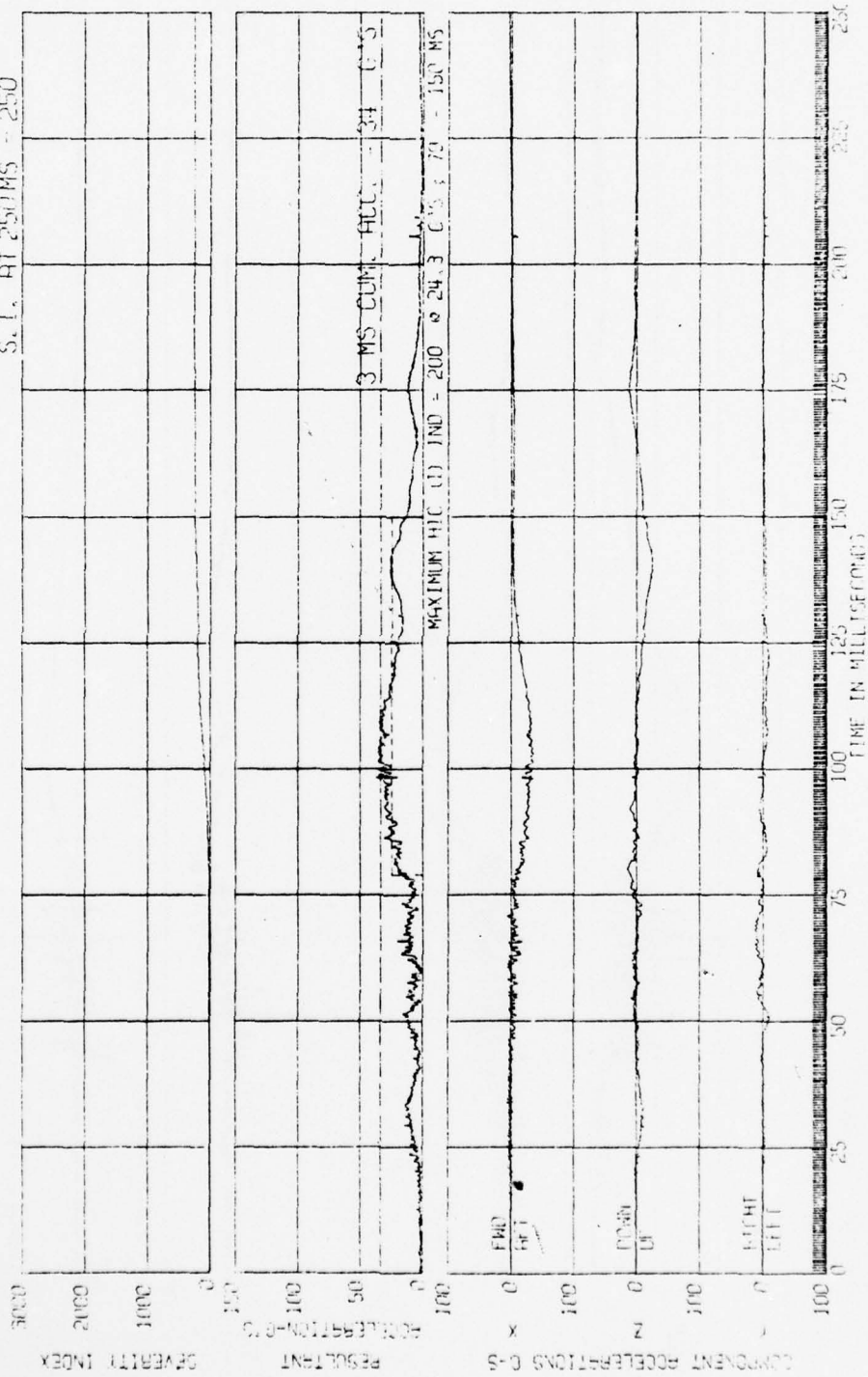


15574B SLED IMPACT TEST
90-116-015
HOLLOWMAN AIR FORCE BASE
A-D DATA

AIR CUSHION RESTRAINT SYSTEM-HUMAN RUN
HEAD ACCEL.

FIGURE
REPORT PG-
09 20-72

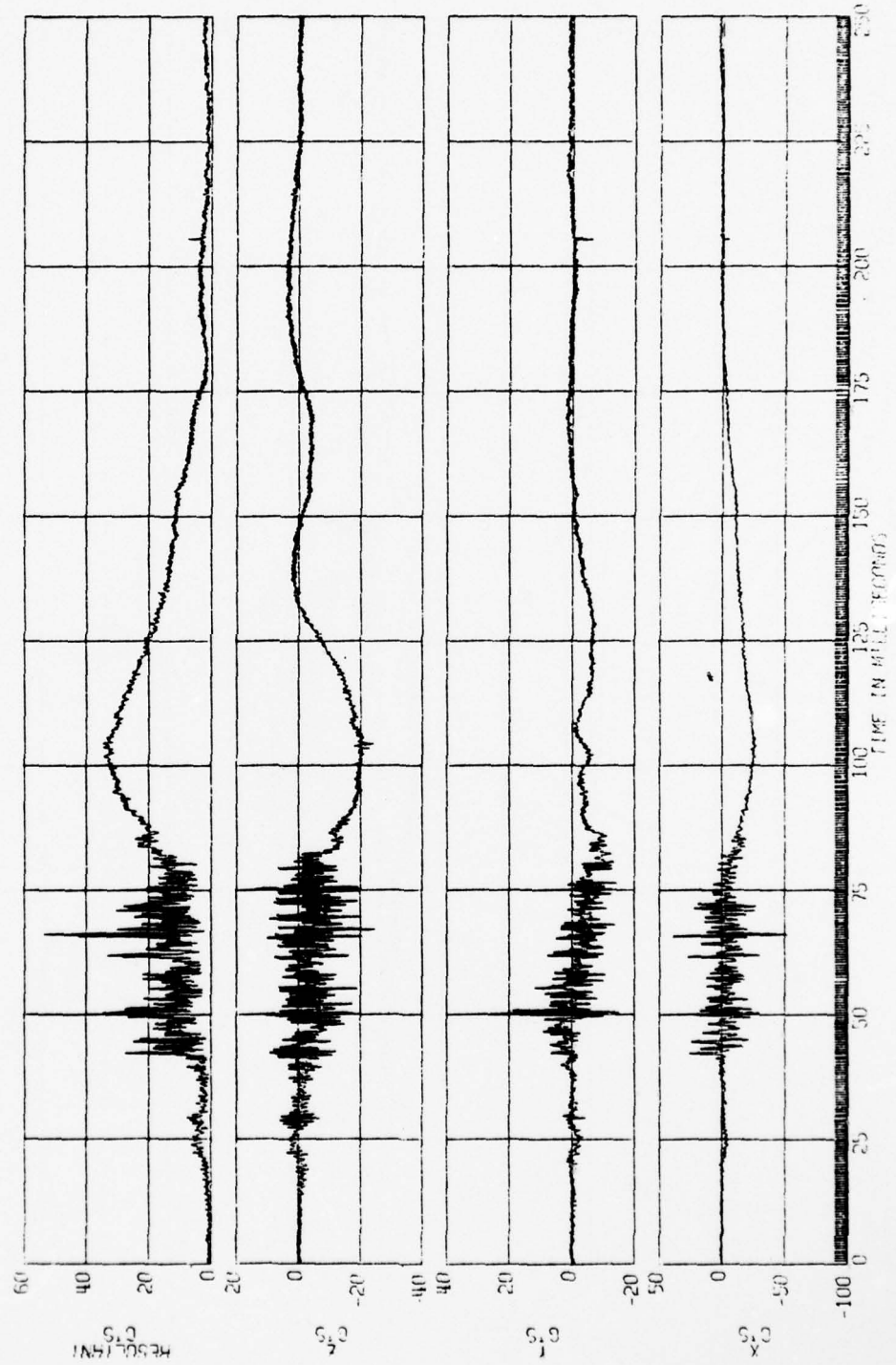
S.I. AT 250MS - 250



H6574B SLED IMPACT TEST
90-115-016
HOLLOWMAN AIR FORCE BASE
A-O DATA

AIR CUSHION RESTRAINT SYSTEM-HUMAN RUN
MOUTH

FIGURE
REPORT PG-
09-20-72



H6574A SLED IMPACT TEST
90-116-016
HOLLOWMAN AIR FORCE BASE
A-D DATA SAE CLASS 600

AIR CUSHION RESTRAINT SYSTEM-HUMAN RUN
LEFT FOOT

FIGURE
REPORT PG-
09-20-72

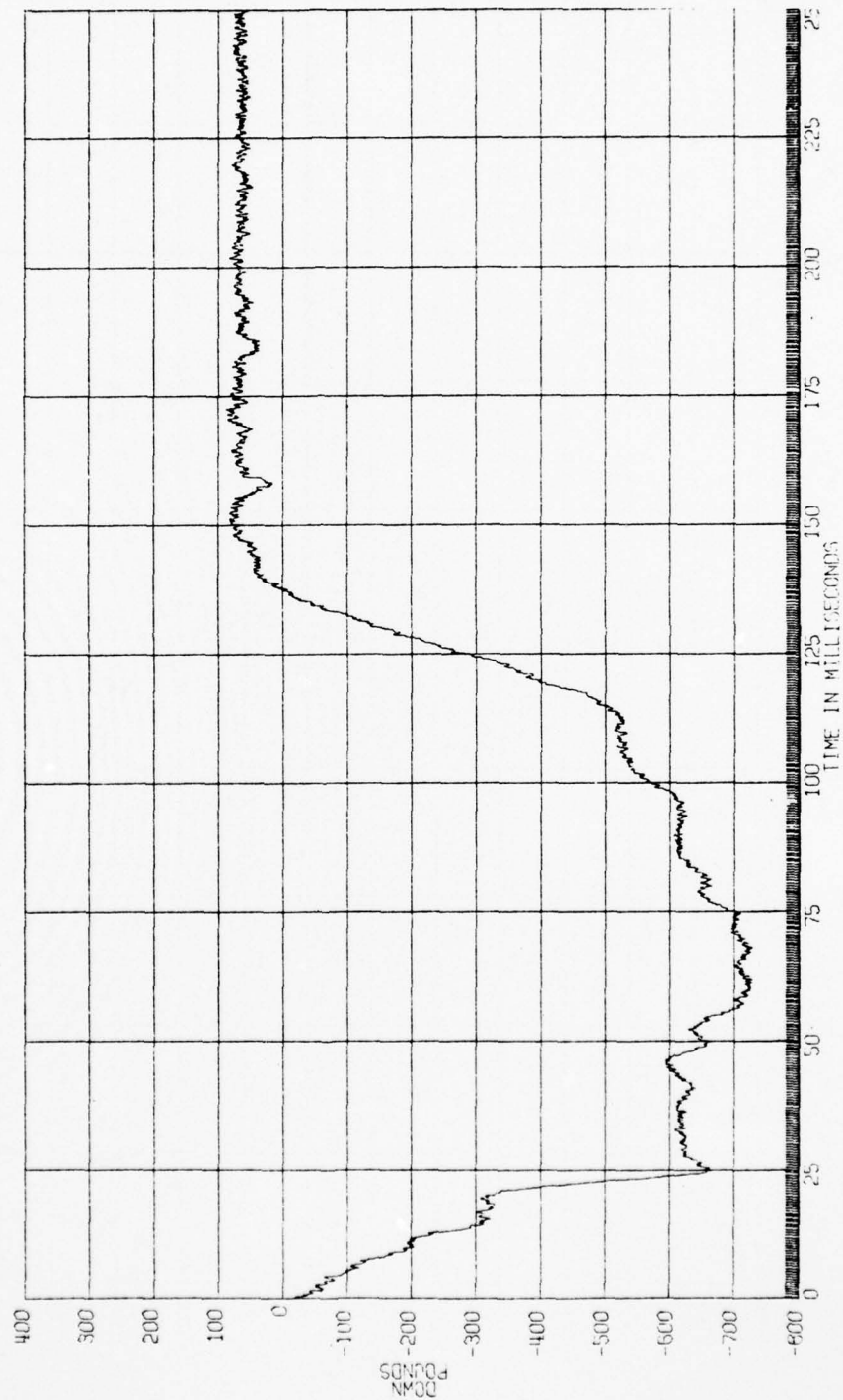
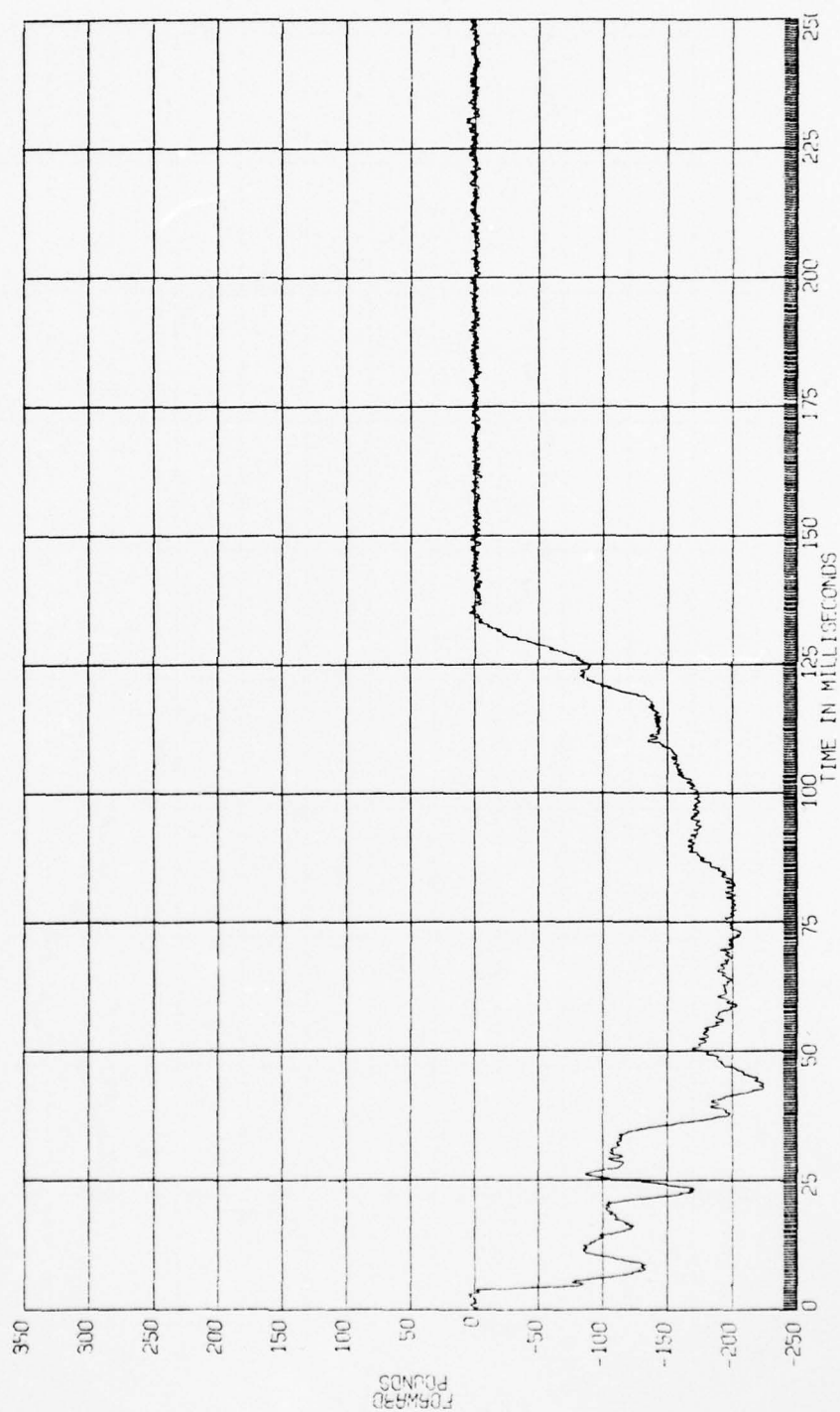


FIGURE
REPORT FC-
09-20-72

AIR CUSHION RESTRAINT SYSTEM-HUMAN RUN
LEFT FOOT

H6574A SLED IMPACT TEST
90-115-016
HOLLOWMAN AIR FORCE BASE
A-D DATA SAE CLASS 600



H65744 SLED IMPACT TEST
00-115-016
HOLLOWMAN AIR FORCE BASE
H-D DATA SHE CLASS 000

AIR CUSHION RESTRAINT SYSTEM-HUMAN RUN
LEFT FOOT

FIGURE
REPORT PG--
09-20-72

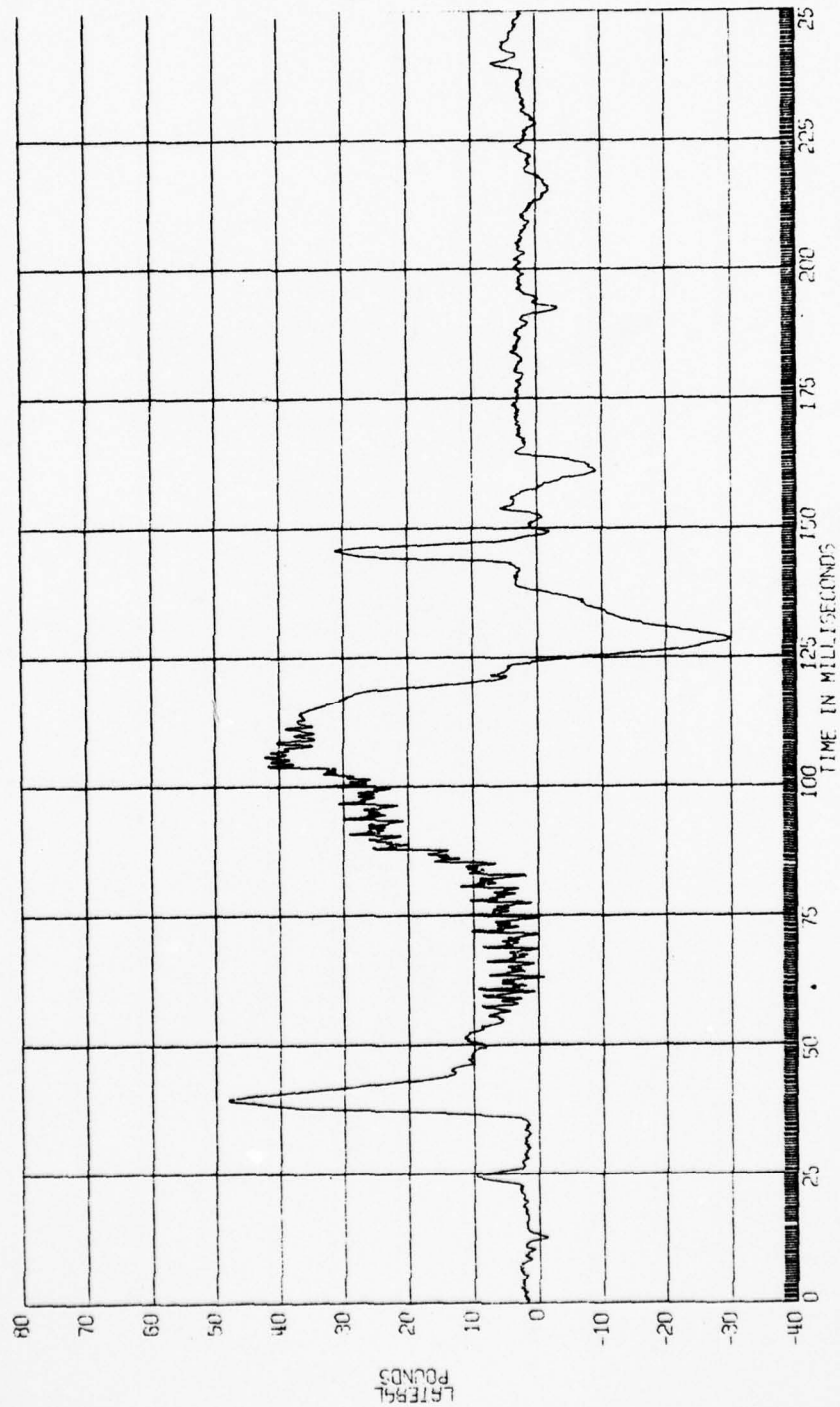
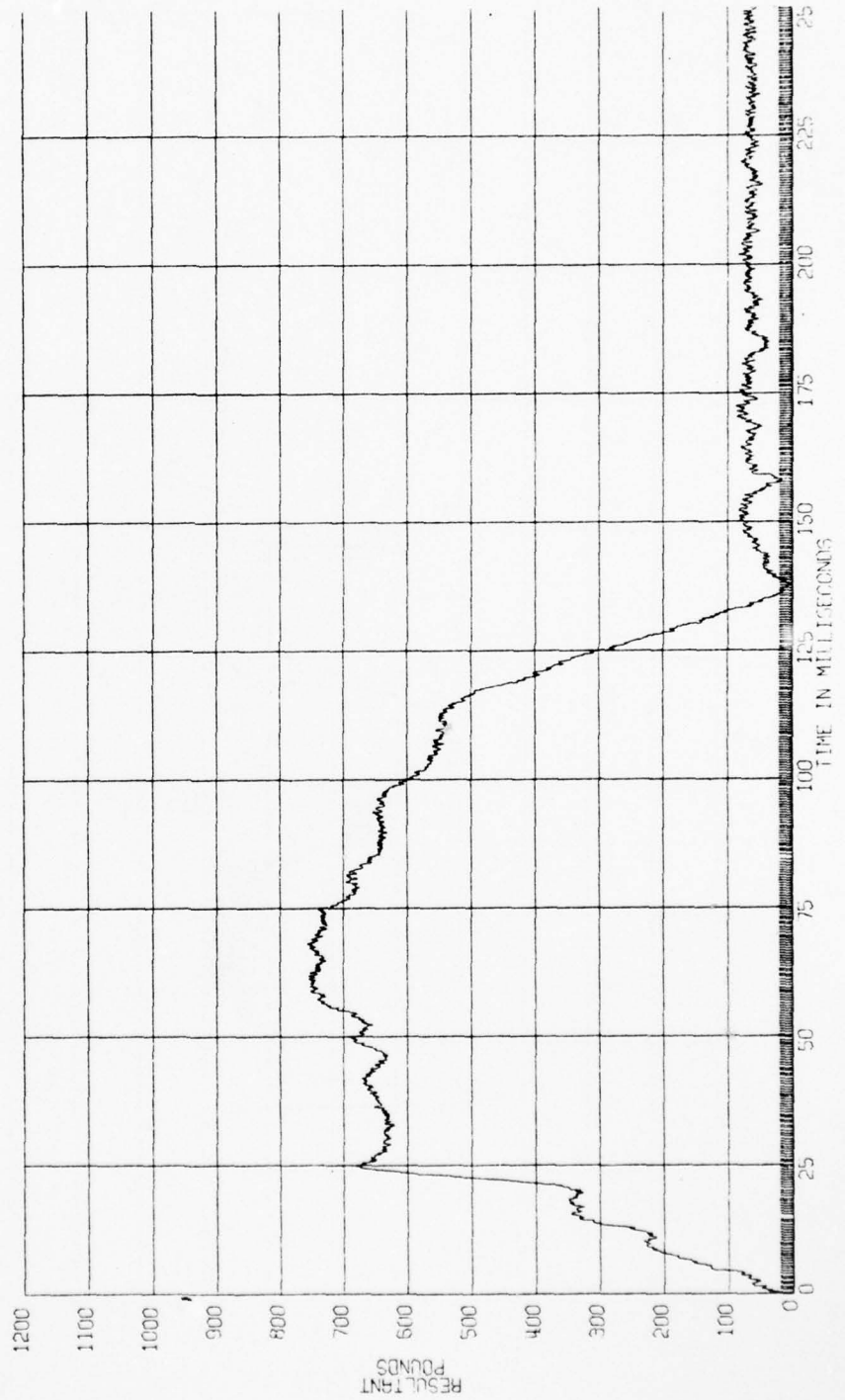


FIGURE
REPORT PG-
09-20-72

AIR CUSHION RESTRAINT SYSTEM-HUMAN RUN
LEFT FOOT
LEFT FOOT RESULTANT

H6574A SLED IMPACT TEST
90-116-016
HOLLOMAN AIR FORCE BASE
A-D DATA SAE CLASS 600



H6574A SLED IMPACT TEST
90-116-016
HOLLOMAN AIR FORCE BASE
A-D DATA SAE CLASS 600

AIR CUSHION RESTRAINT SYSTEM-HUMAN RUN
RIGHT FOOT

FIGURE
REPORT PC-
09-20-72

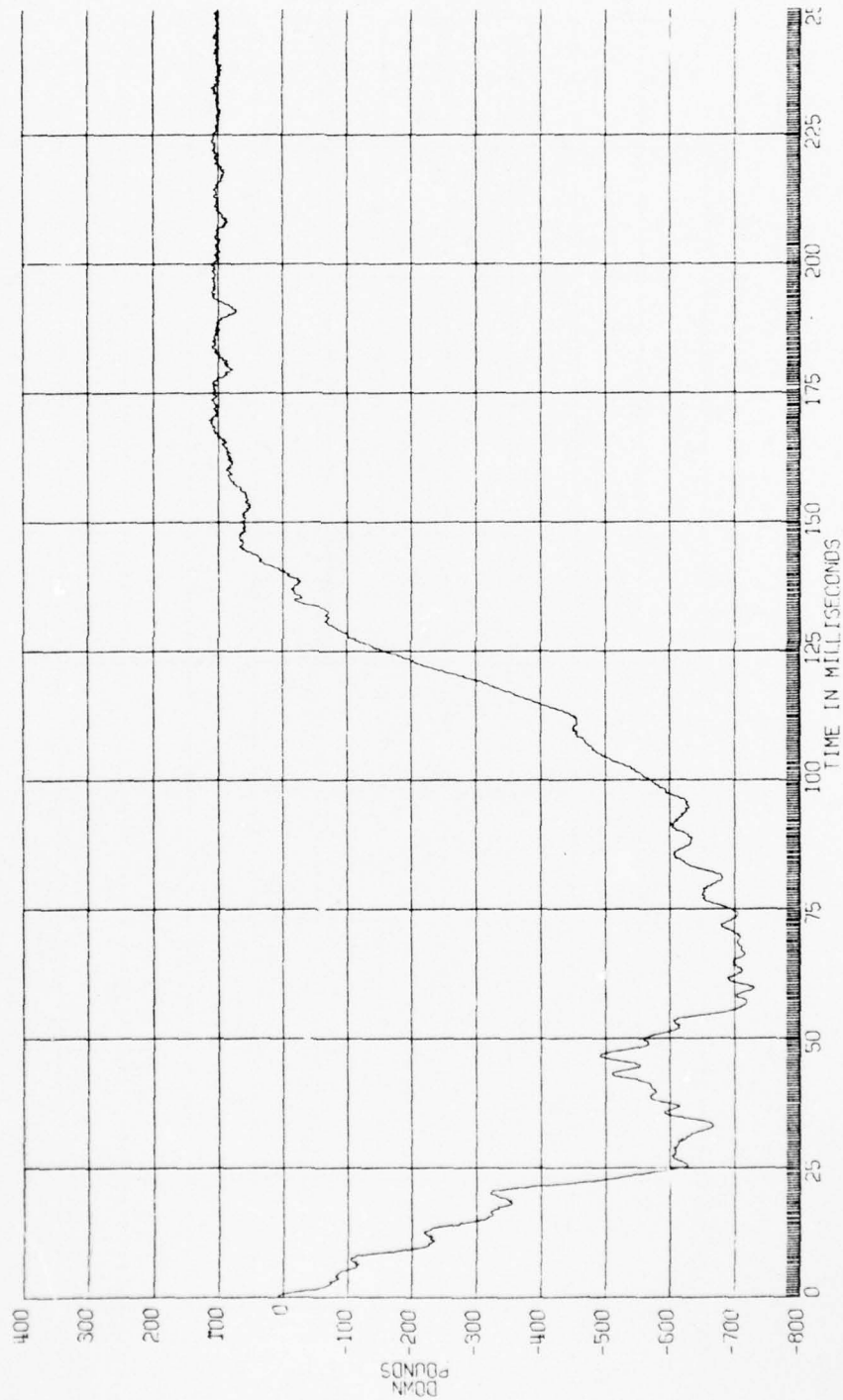
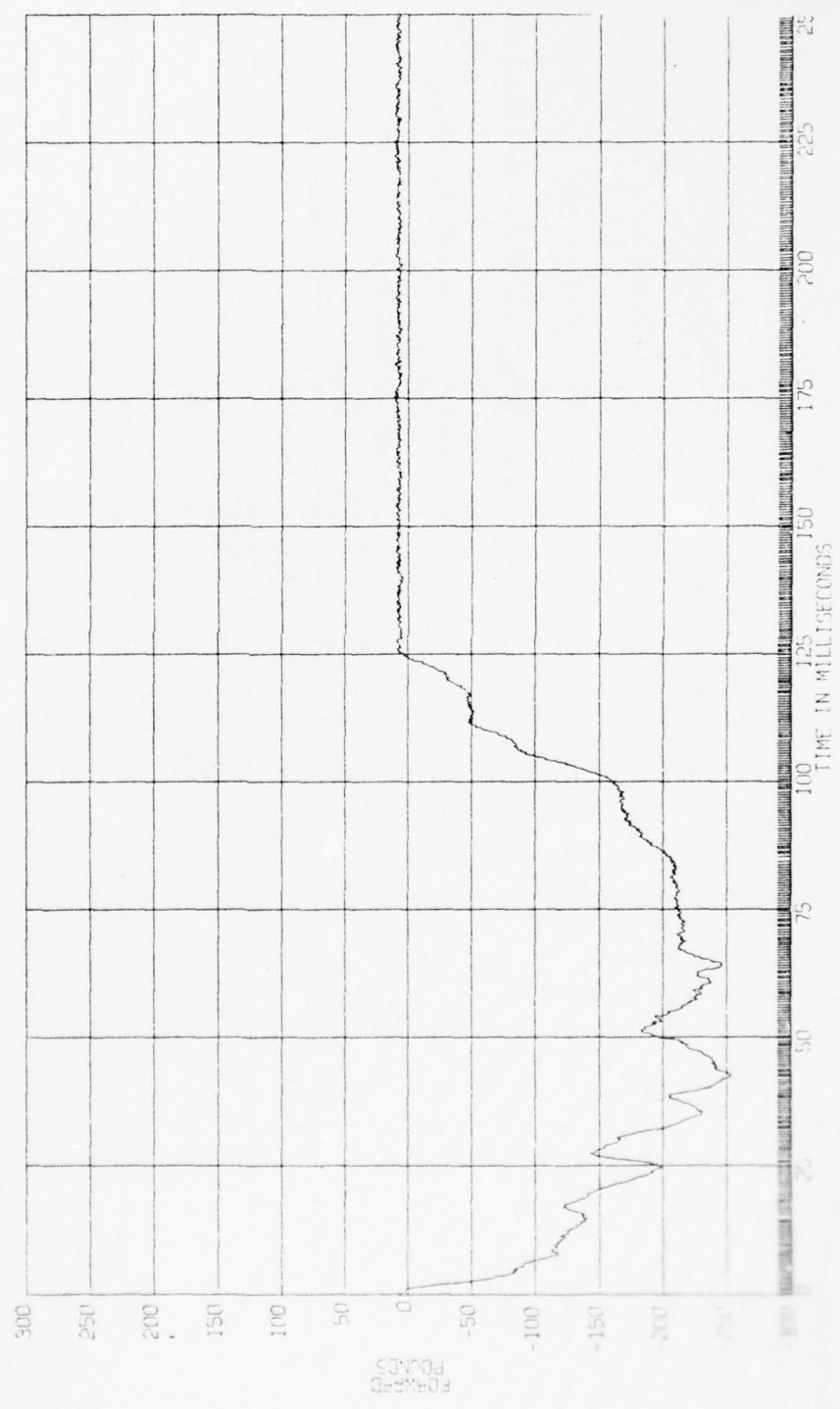


FIGURE
REPORT PG-
09-20-72

AIR CUSHION RESTRAINT SYSTEM-HUMAN RUN
RIGHT FOOT

H6574A SLED IMPACT TEST
90-116-016
HOLLOWEN AIR FORCE BASE
A-D DATA SFE CLASS 600



AD-A038 525

AEROSPACE MEDICAL RESEARCH LAB WRIGHT-PATTERSON AFB OHIO F/G 13/12
IMPACT TESTS OF A NEAR-PRODUCTION AIR CUSHION RESTRAINT.(U)

UNCLASSIFIED

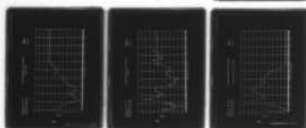
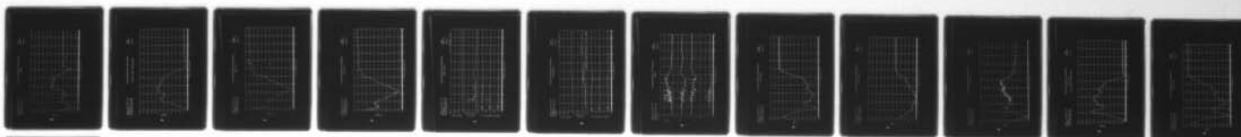
FEB 77 J W BRINKLEY, G C MOHR, H C RUSSELL DOT-HS-017-1-017-IA

AMRL-TR-75-47

DOT-HS-802-248

NL

5 OF 5
AD
A038525



END

DATE
FILMED

5-77

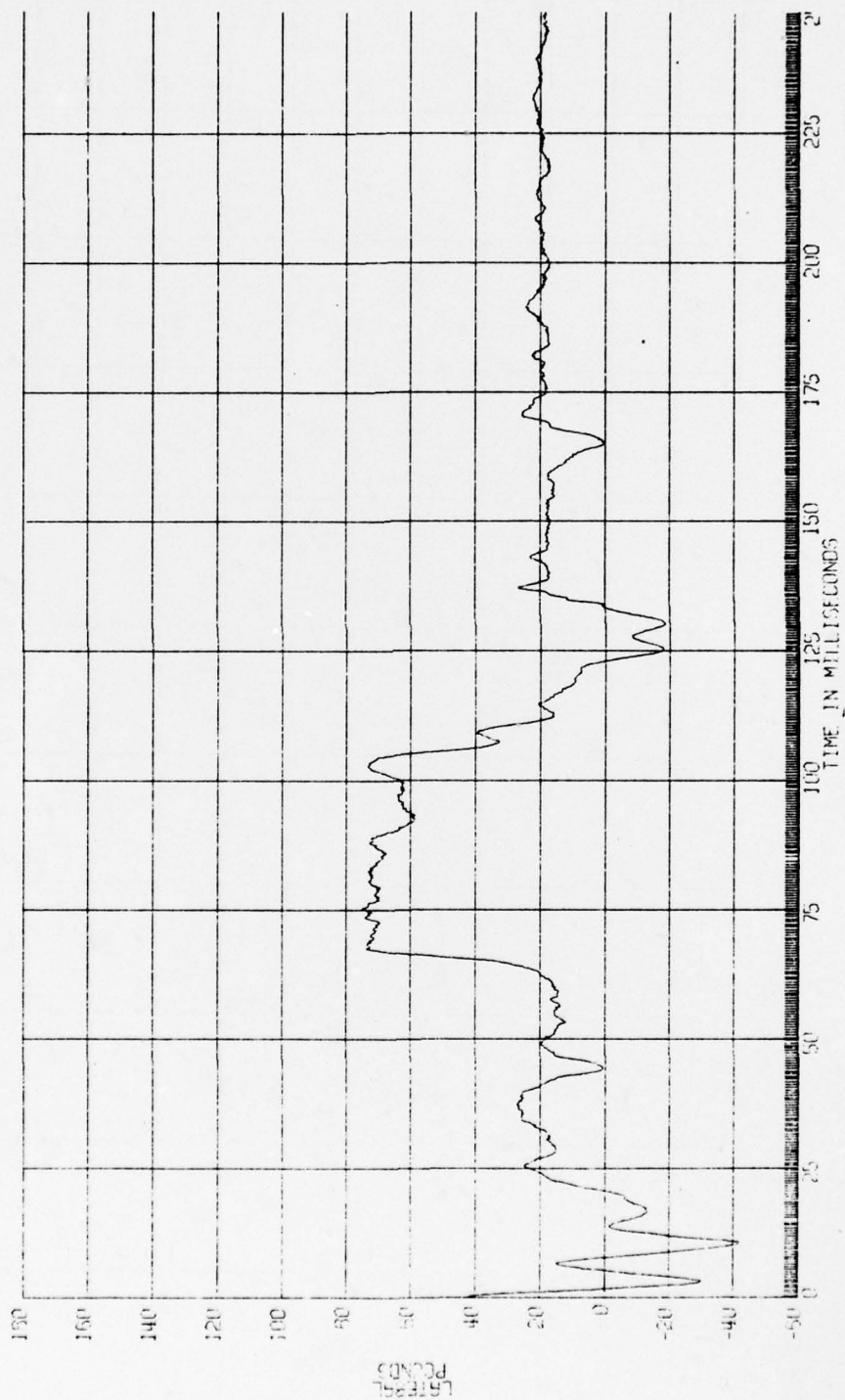
H6574A SLED IMPACT TEST
90-116-016
HOLLOWMAN AIR FORCE BASE
4-U DATA 54E CLASS 000

AIR CUSHION RESTRAINT SYSTEM-HUMAN RUN

RIGHT

FIGURE
REPORT FG-

09-20-72



H6574A SLED IMPACT TEST
90-116-016
HOLLOWAY AIR FORCE BASE
A-D DATA SAE CLASS 600

AIR CUSHION RESTRAINT SYSTEM-HUMAN RUN

FIGURE
REPORT PG-
09-20-72

RIGHT FOOT RESULTANT



FIGURE
REPORT PG-
09-20-72

AIR CUSHION RESTRAINT SYSTEM-HUMAN RUN
SLED X-1

H6575A SLED IMPACT TEST
90-116-016
HOLLOWMAN AIR FORCE BASE
A-D DATA SAE CLASS 60

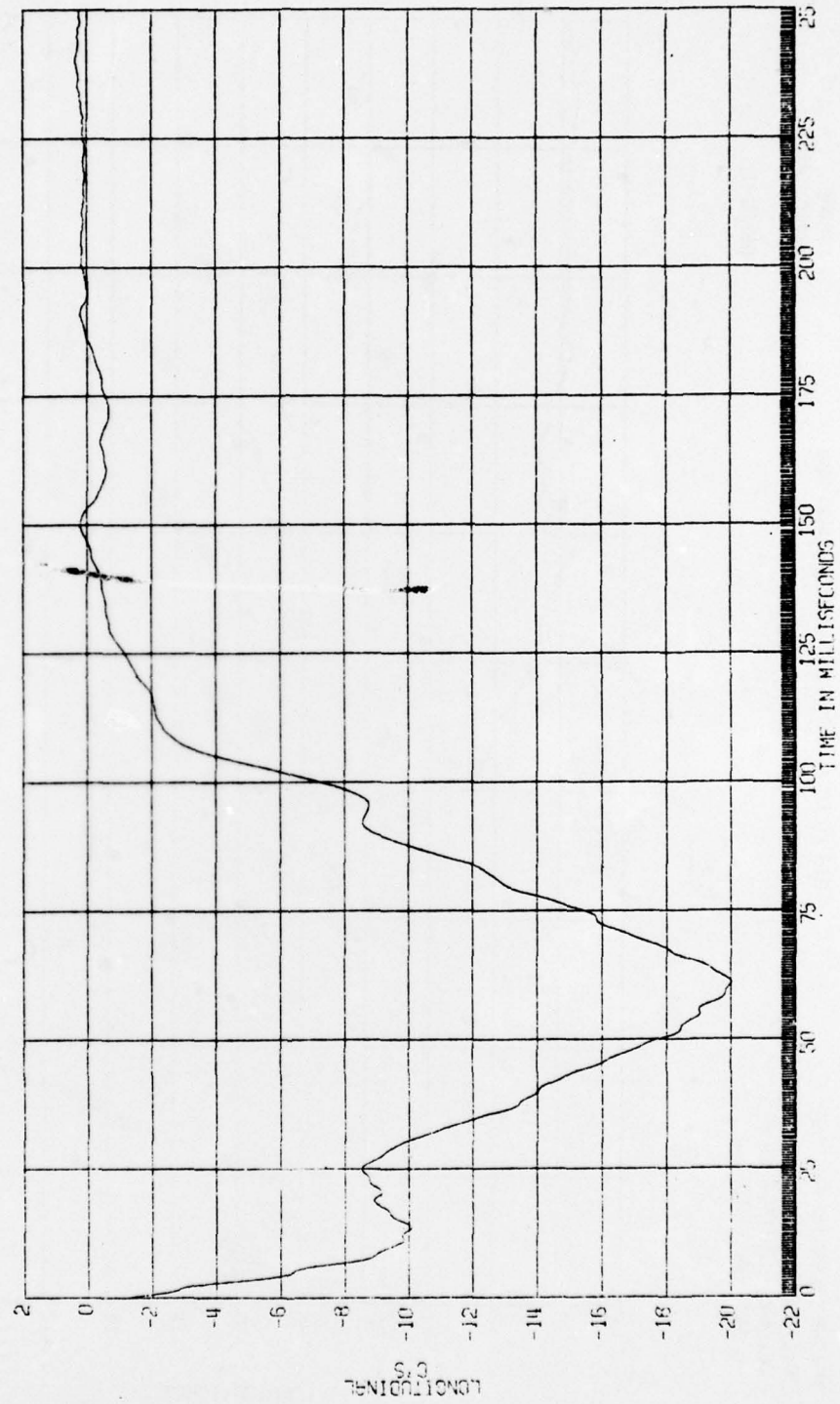
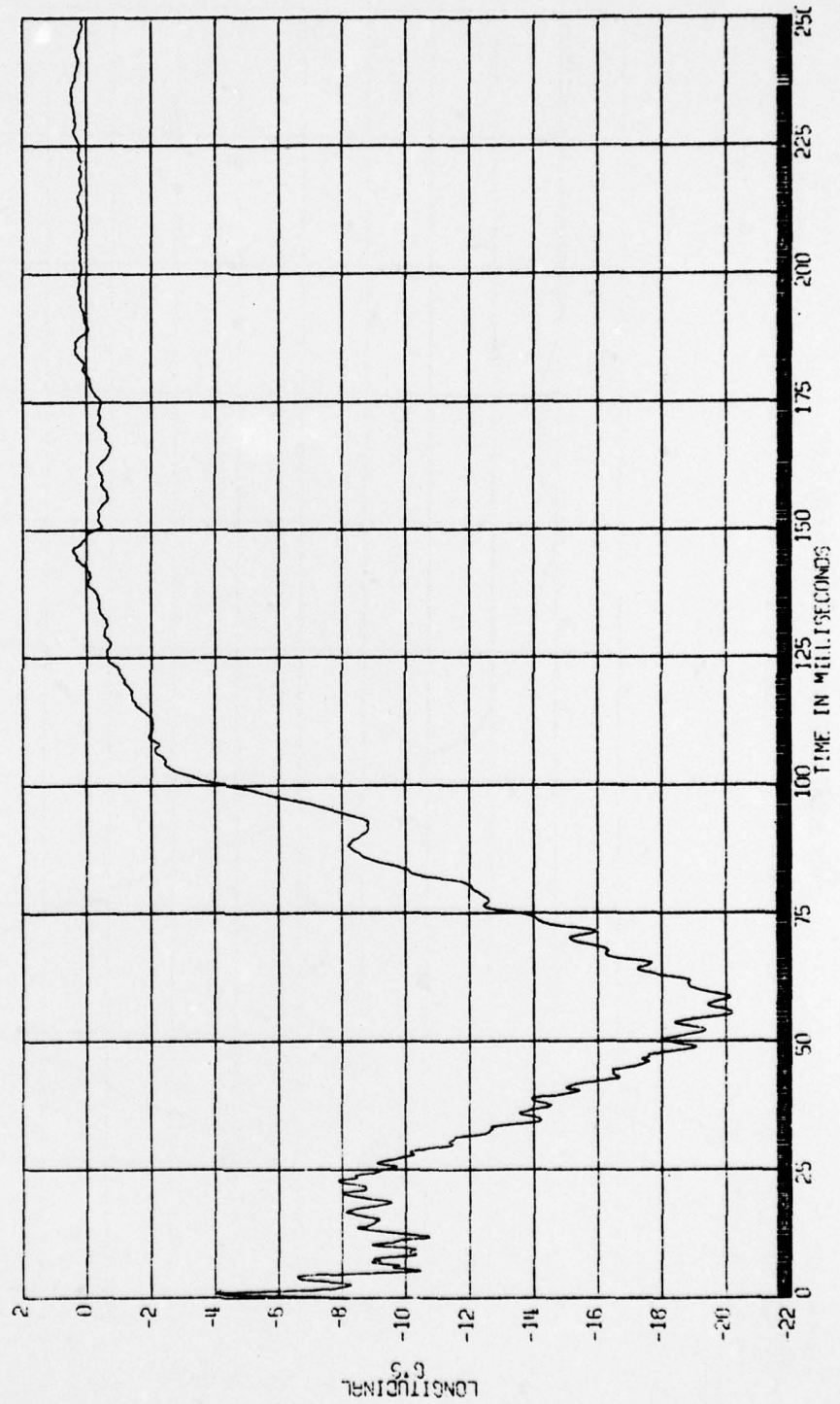


FIGURE
REPORT PG--
09-20-72

AIR CUSHION RESTRAINT SYSTEM-HUMAN RUN
SLED X-2

H6575B SLED IMPACT TEST
90-116-016
HOLLOWMAN AIR FORCE BASE
A-D DATA SAE CLASS 60

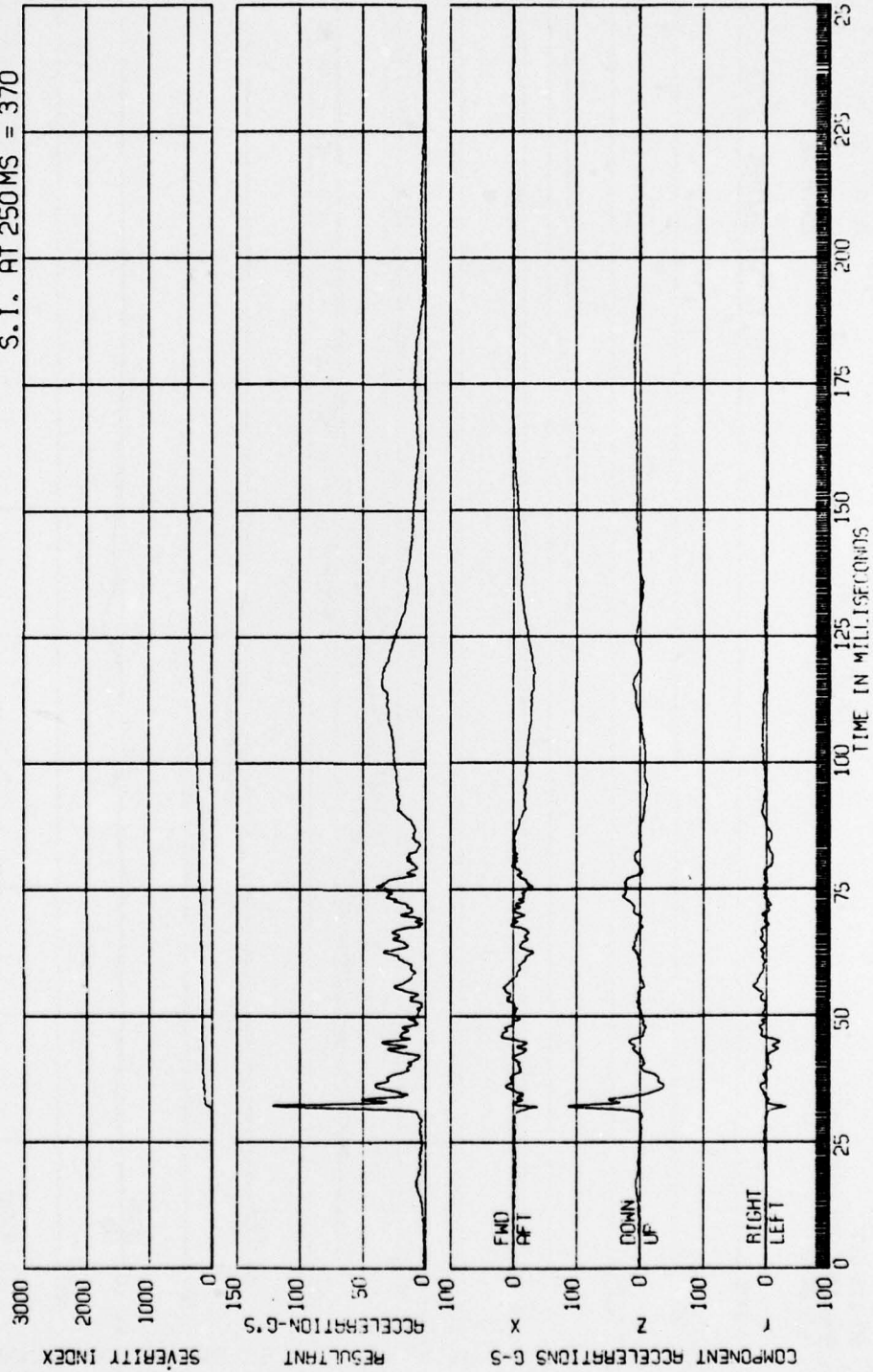


H6575R SLED IMPACT TEST
 90-116-015
 HOLLOWMAN AIR FORCE BASE
 A-D DATA SAE CLASS 160

AIR CUSHION RESTRAINT SYSTEM-HUMAN RUN
 CHEST ACCEL.

FIGURE
 REPORT PG-
 09-20-72

S.I. AT 250 MS = 370



H8575B SLED IMPACT TEST
90-116-015
HOLLOWMAN AIR FORCE BASE
A-D DATA

AIR CUSHION RESTRAINT SYSTEM-HUMAN RIN
HEAD ACCEL.

FIGURE
REPORT PG-
09-20-72

S.I. AT 250 MS = 270

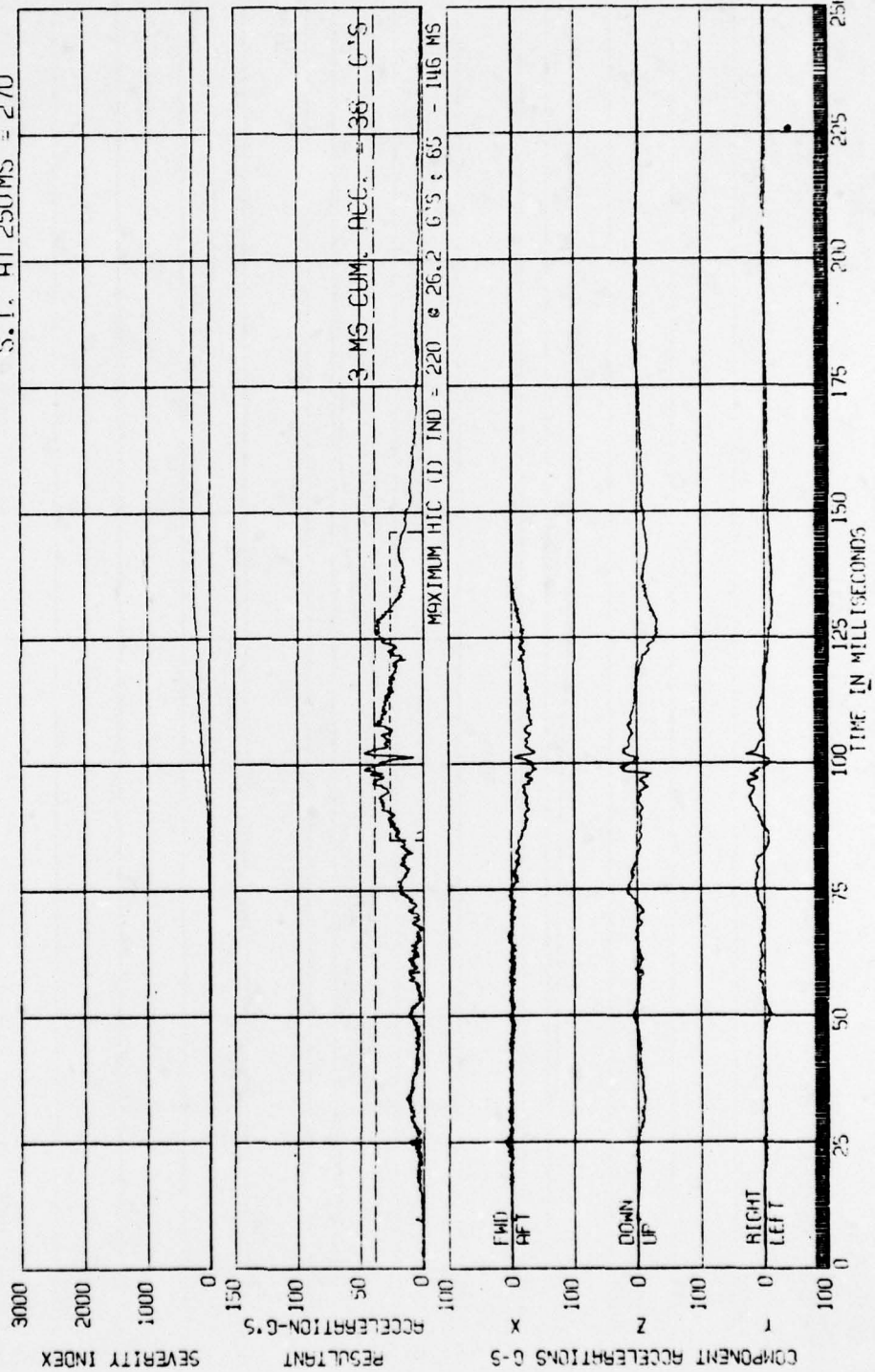
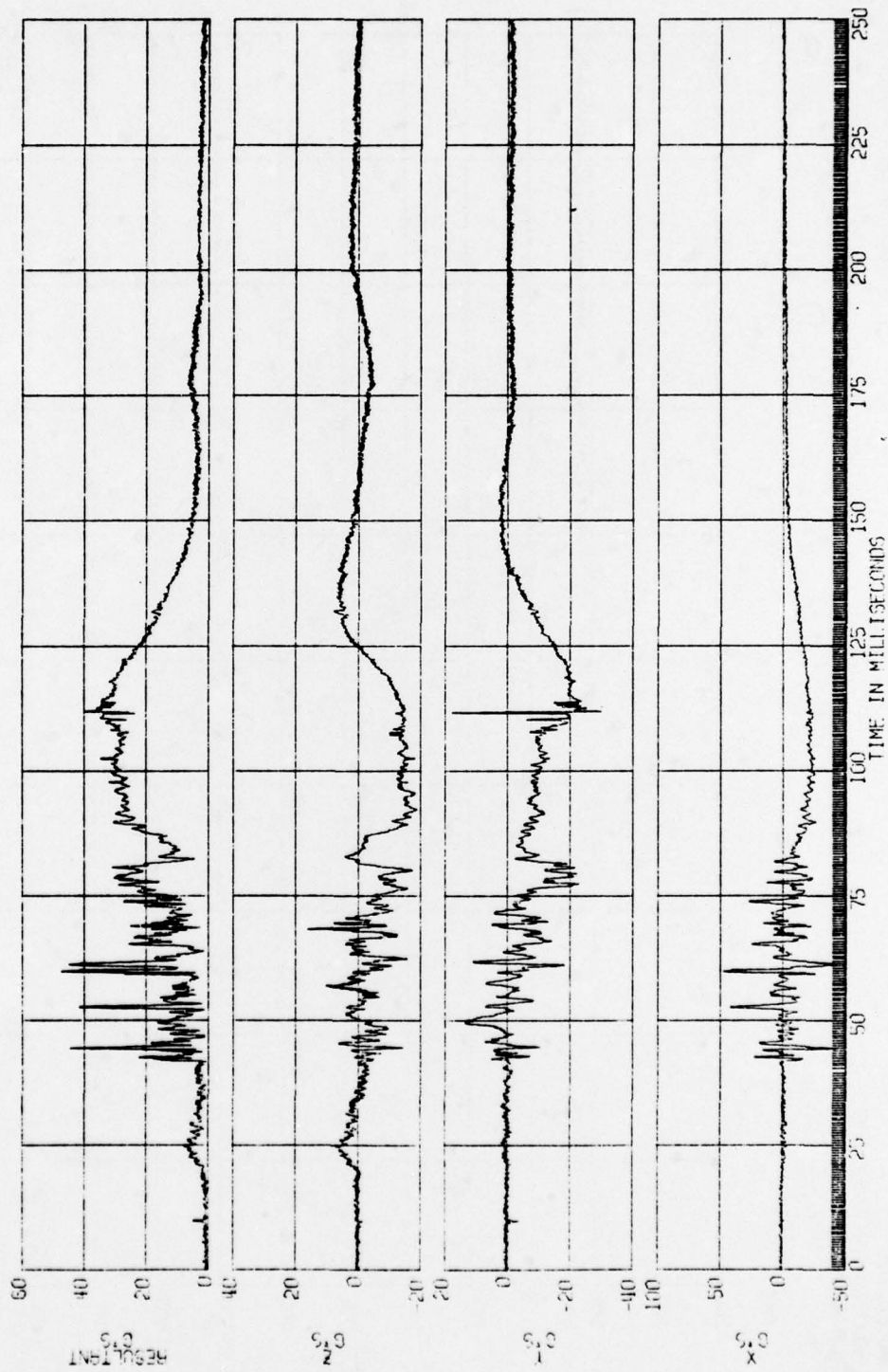


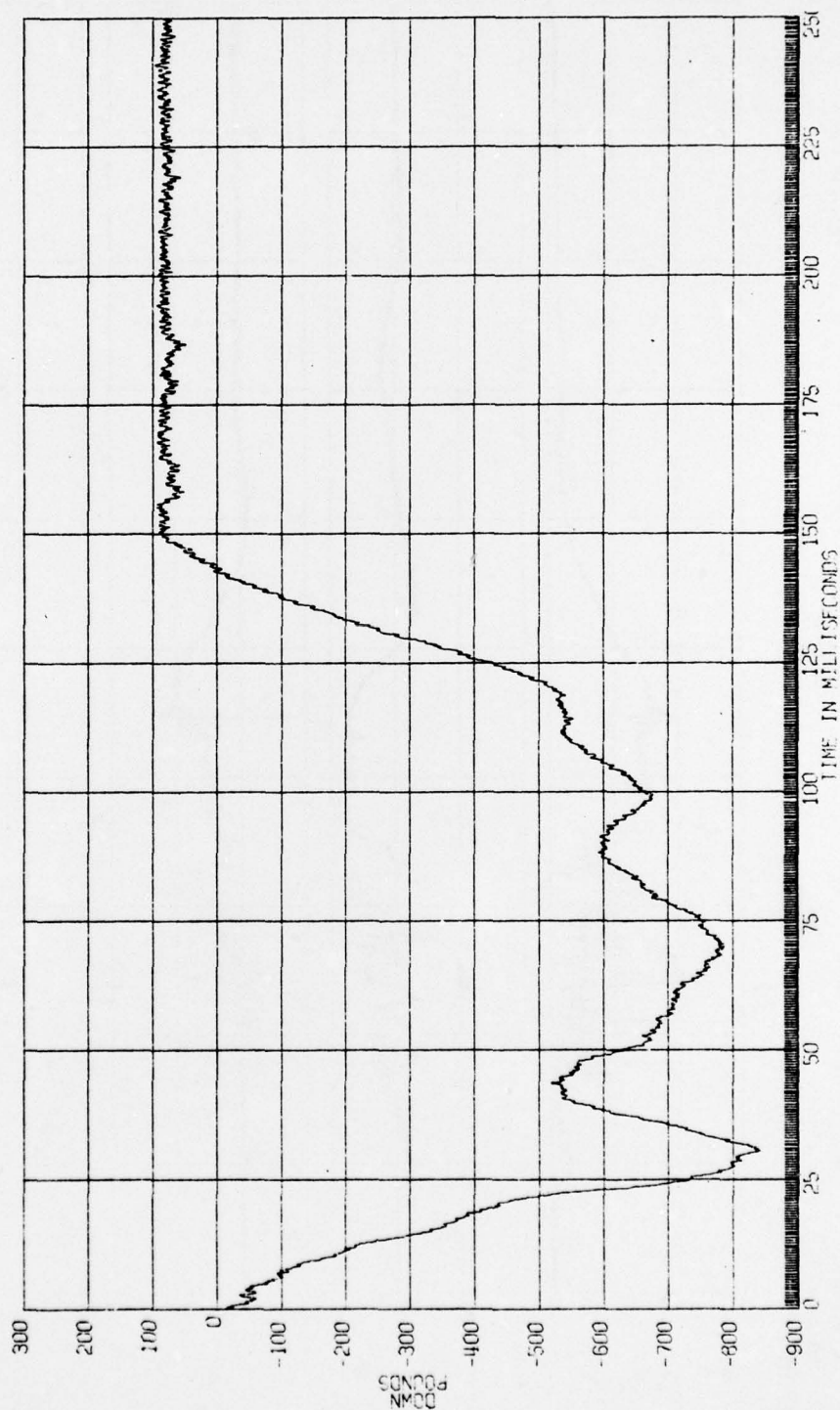
FIGURE
REPORT PG-
09-20-72



H6575A SLED IMPACT TEST
90-116-016
HOLLOWMAN AIR FORCE BASE
A-D DATA SAE CLASS 600

AIR CUSHION RESTRAINT SYSTEM-HUMAN RUN
LEFT FOOT

FIGURE
REPORT PG-
09-20-72



H6575A SLED IMPACT TEST
90-116-016
HOLLOMAN AIR FORCE BASE
A-D DATA SEE CLASS 600

AIR CUSHION RESTRAINT SYSTEM-HUMAN RUN
LEFT FOOT

FIGURE
REPORT PG-
09-20-72

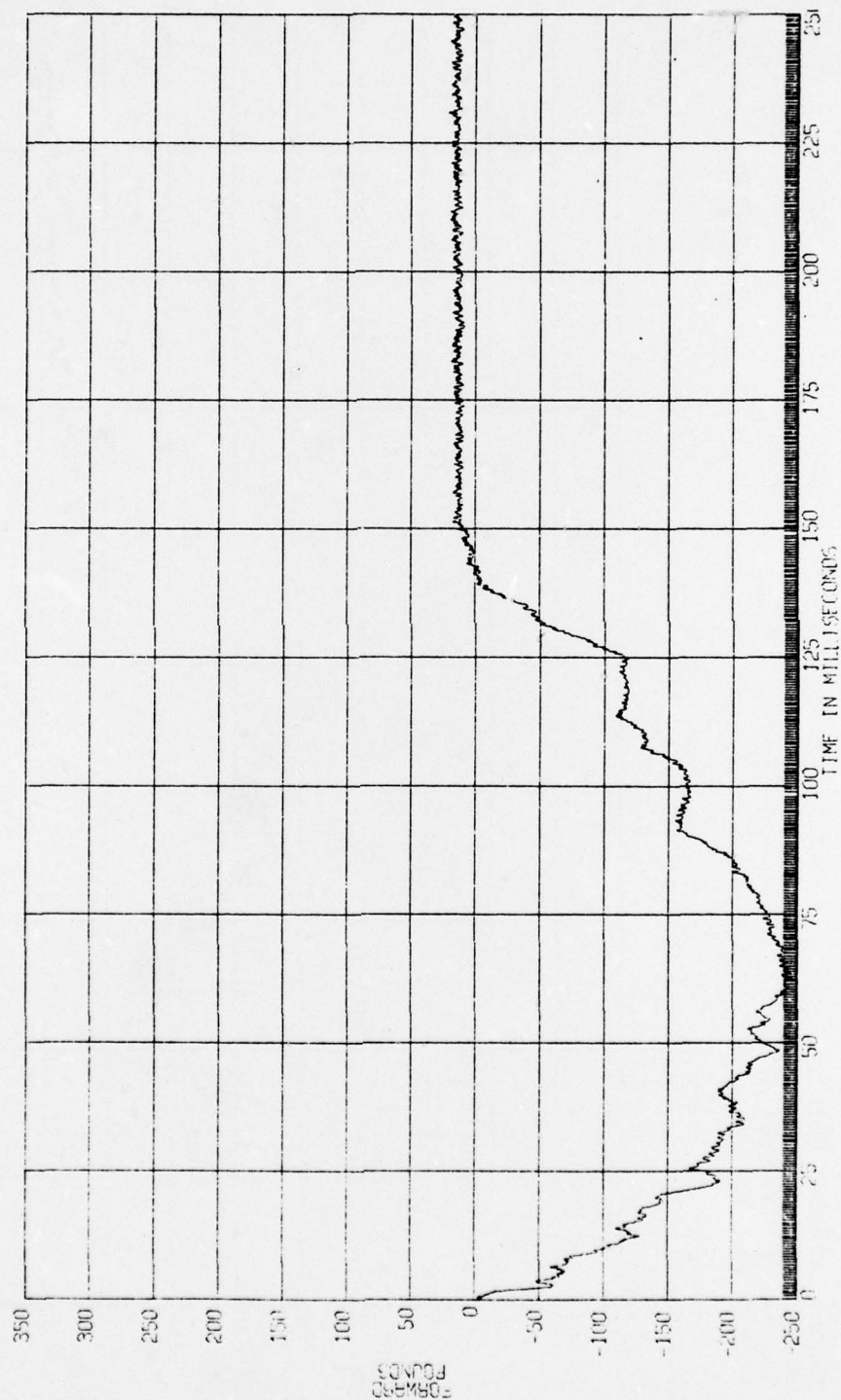
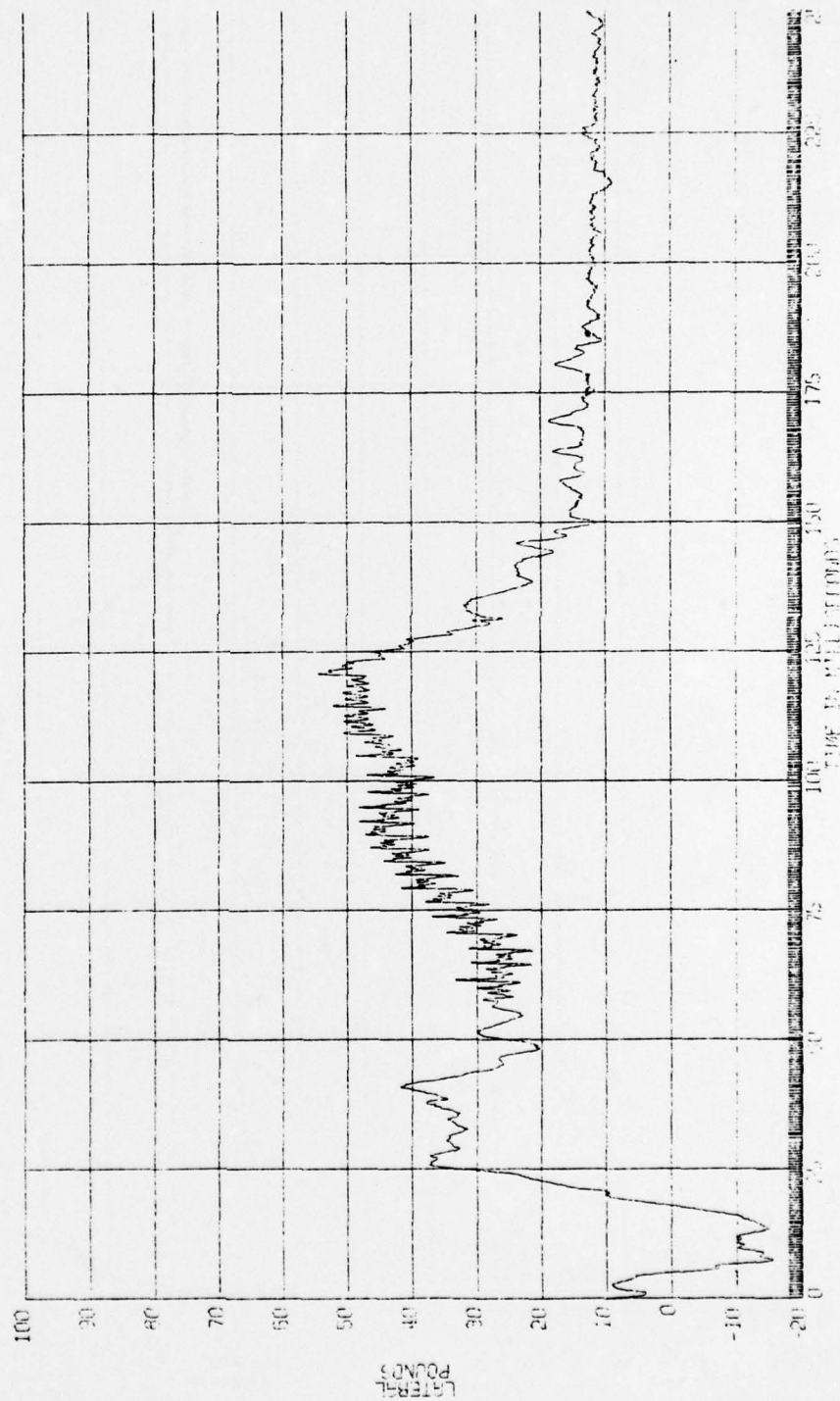


FIGURE
REPORT FG-
09-20-72

AIR CUSHION RESTRAINT SYSTEM-HUMAN RUN
LEFT FOOT

HSG724 SLED IMPACT TEST
90-115-016
HOLLOWMAN AIR FORCE BASE
4-D DATA SHE CLEGS GCU



H6575A SLED IMPACT TEST
 90-116-016
 HOLLOWMAN AIR FORCE BASE
 A-D DATA SAE CLASS 600

AIR CUSHION RESTRAINT SYSTEM-HUMAN RUN
 LEFT FOOT
 LEFT FOOT RESULTANT

FIGURE
 REPORT PG-
 09-20-72

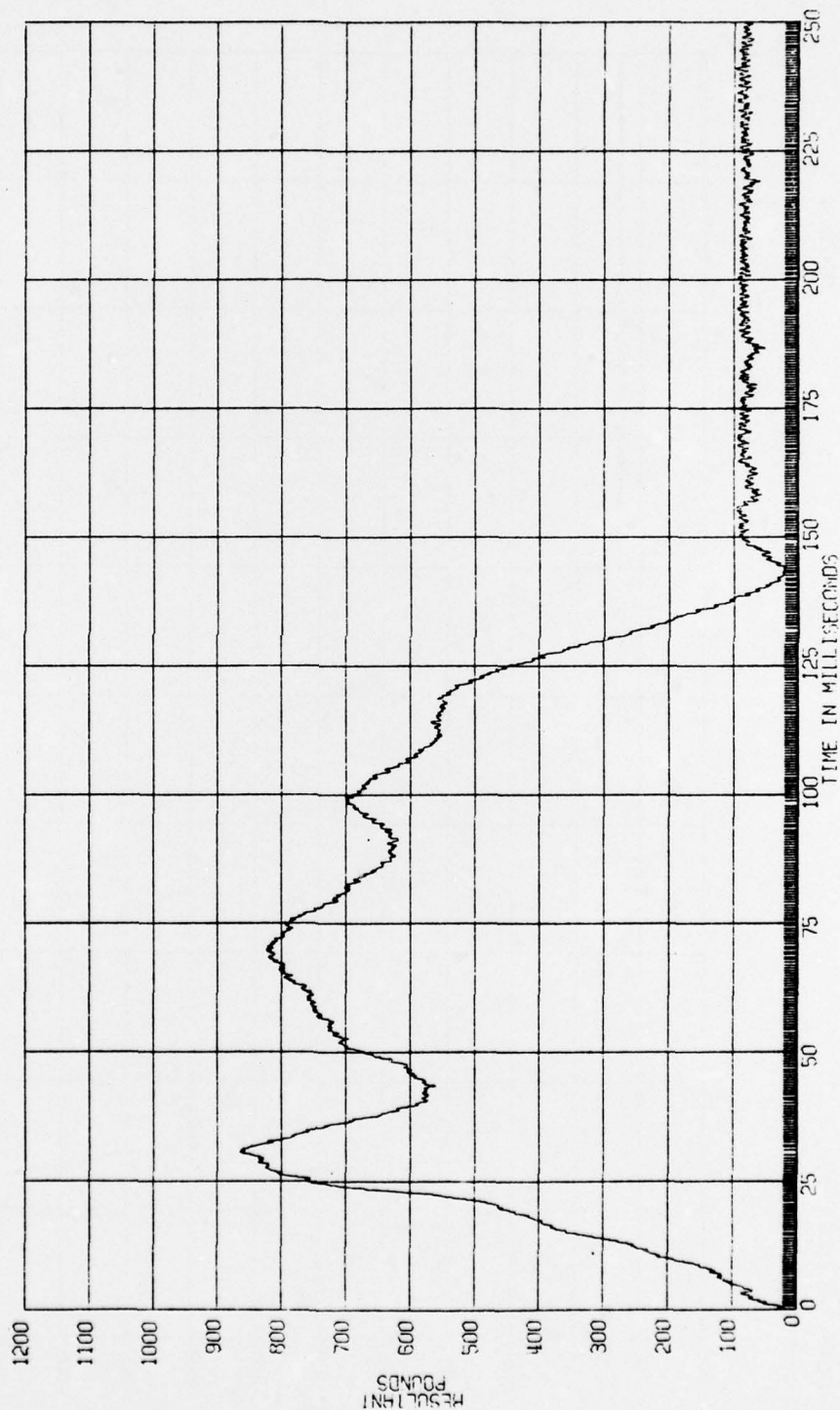
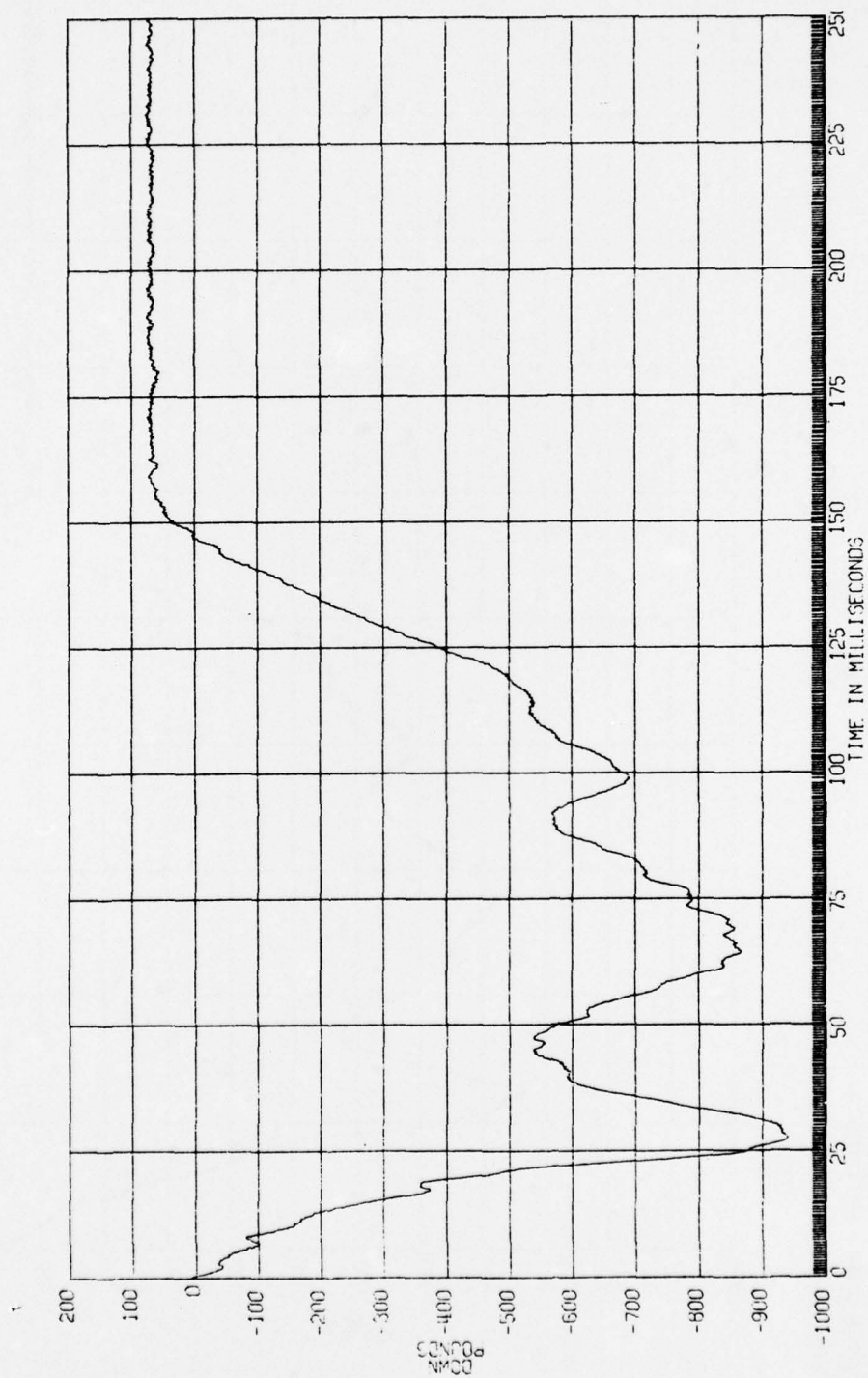


FIGURE
REPORT PG-
09-20-72

AIR CUSHION RESTRAINT SYSTEM-HUMAN RUN
RIGHT FOOT

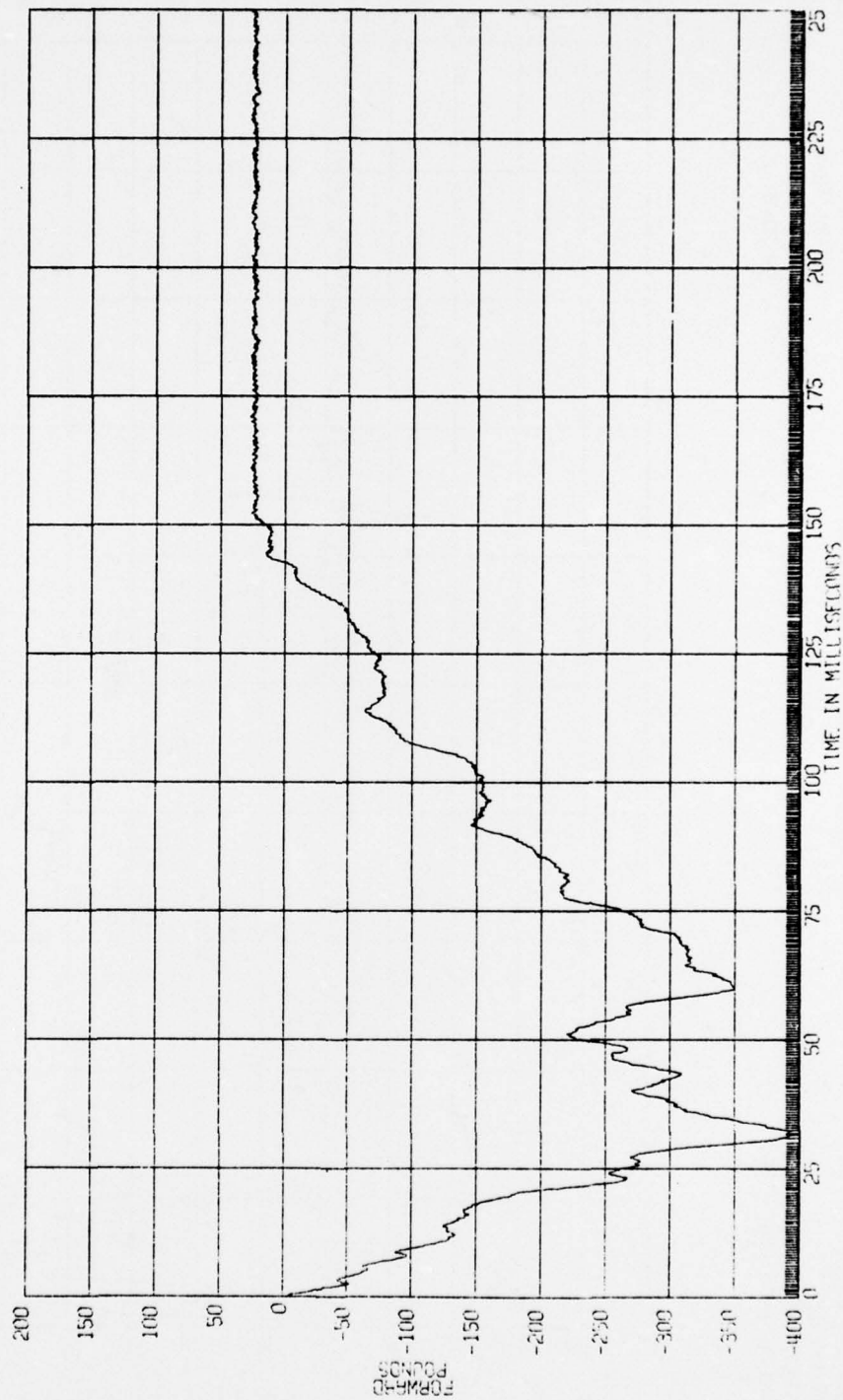
H6575A SLED IMPACT TEST
90-116-016
HOLLAND AIR FORCE BASE
A-D DATA SAE CLASS 000



H6575A SLED IMPACT TEST
90-116-016
HOLLOWIN AIR FORCE BASE
H-D DATA SHE CLASS 600

AIR CUSHION RESTRAINT SYSTEM-HUMAN RUN
RIGHT FOOT

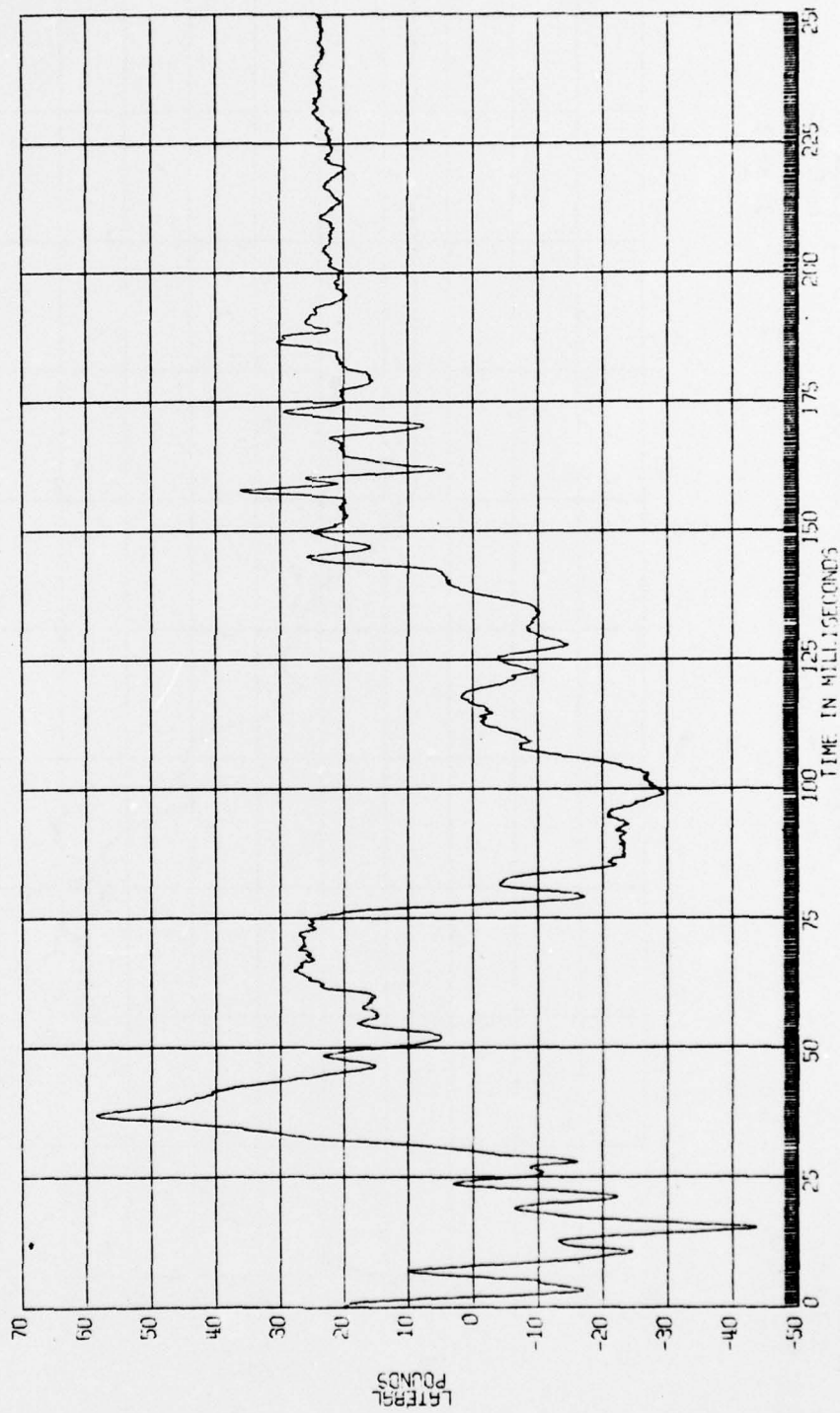
FIGURE
REPORT PC-
09-20-72



H6575A SLID IMPACT TEST
90-116-016
HOLLOWMAN AIR FORCE BASE
A-D DATA SHE CLASS 600

AIR CUSHION RESTRAINT SYSTEM-HUMAN RUN
RIGHT

FIGURE
REPORT PG--
09-20-72



H6575A SLED IMPACT TEST
 90-118-016
 HOLLOWMAN AIR FORCE BASE
 A-D DATA SAE CLASS 600

AIR CUSHION RESTRAINT SYSTEM-HUMAN RUN
 RIGHT FOOT RESULTANT

FIGURE
 REPORT PG-
 09-20-72

